An underwater photograph of a rocky seabed with various marine life, including a large mushroom-shaped coral on the left and several yellowish-orange sponges in the center. The water is dark blue, and the scene is illuminated from above, creating a dramatic effect. The bottom of the image features a decorative pattern of horizontal wavy lines in shades of blue.

THE PRESENT STATE OF MARINE ECOSYSTEMS IN THE SPANISH MEDITERRANEAN IN A CLIMATE CHANGE CONTEXT

Main authors: Manuel Vargas Yáñez, M^a Carmen García Martínez, Francina Moya Ruiz, José Luis López-Jurado Marqués, Mariano Serra Tur, Rocío Santiago Domenech, Rosa Balbín Chamorro.

Other authors: Jordi Salat, Josep Pascual, Teodoro Ramírez Cárdenas, Elena Tel, Francisco Fernández Corregidor, M^a Paz Jiménez Gómez, Andreas Reul, Gregorio Parrilla Barrera.



*To the memory of Argeo Rodríguez de León,
who promoted and defended the RADMED project
and the monitoring and study of the
Spanish Mediterranean ecosystems.*



Acknowledgements

We would like to thank very sincerely the crews of all the research vessels and the technicians from such vessels and from the Instituto Español de Oceanografía who have taken part in more than 25 years of oceanographic campaigns in the Spanish Mediterranean. This work would have not been possible without their excellent and enthusiastic work.

Abstract

Multidisciplinary time series generated by the monitoring programs supported by the Spanish Institute for Oceanography (IEO, Instituto Español de Oceanografía) in the Spanish Mediterranean Waters are analyzed. These time series extend from 1992 in some cases, whereas in others they started in 2007 when the different monitoring programs funded by IEO were merged in the current project RADMED. These time series are used to describe the average values and ranges of variability of different variables that could be useful for describing the environmental state of the Spanish Mediterranean waters. Such analyses and statistics are provided as tables that could be used as a reference for future research work or for management purposes.

Data from the IEO monitoring programs are complemented with meteorological information from the Spanish Meteorological Agency (AEMET, Agencia Estatal de Meteorología), satellite data from the NOAA (National Oceanic and Atmospheric Agency) and l'Estartit oceanographic and meteorological station, operated by Institut de Ciències del Mar (ICM/CSIC).

Besides the description of the current environmental state of the Spanish Mediterranean marine ecosystems, an analysis of long term trends is carried out, assessing the possible changes associated to Climate Change.

CONTENTS

Preface	9
Main results and summary for policymakers.....	10
Before we start.....	14
Chapter 1. Introduction.....	15
1.1. Geographical framework	15
1.2. Climatic forcing and thermohaline circulation.....	15
1.3. Water masses and circulation in the Western Mediterranean	17
1.4. Chemical and biological properties of the Western Mediterranean.....	19
Chapter 2. The environmental monitoring Project RADMED	21
The environmental state of the Spanish Mediterranean.....	33
Chapter 3. The Alboran Sea: From Cape Pino to Cape Gata.....	33
3.1 Meteorological conditions.....	35
3.2 Water masses.....	36
3.3 Dissolved oxygen, nutrient and chlorophyll-a distributions	39
3.4 Phytoplanktonic distributions	45
3.4.1 Micro-phytoplankton.....	45
3.4.2 Nano and picoplankton	48
3.5 Meso-zooplanktonic abundance and biomass.....	49
3.6 Tables. Seasonal statistics for the Alboran Sea.....	51
Chapter 4. Cape Palos and Balearic Islands	73
4.1 Meteorological conditions	75

4.2 Water masses	77
4.3 Dissolved oxygen, nutrient and chlorophyll-a distributions	79
4.4 Phytoplanktonic distributions	84
4.4.1 Micro-phytoplankton.....	84
4.4.2 Nano and picoplankton	88
4.5 Meso-zooplanktonic abundance and biomass.....	85
4.6 Tables. Seasonal statistics for Cape Palos and Balearic Islands.....	90
Chapter 5. Tarragona and Barcelona	133
5.1 Meteorological conditions.....	134
5.2 Water masses	135
5.3 Dissolved oxygen, nutrient and chlorophyll-a distributions	136
5.4 Phytoplanktonic distributions	140
5.4.1 Micro-phytoplankton	140
5.4.2 Nano and picoplankton.....	142
5.5. Tables. Seasonal statistics for Tarragona and Barcelona.....	143
Chapter 6. Climate Change. Main trends	165
6.1 Description of time series.....	165
6.2 Analysis of trends for temperature, salinity and mean sea level	166
6.3 Analysis of trends for chemical and biological variables.....	172
References	179



Preface

The monitoring of the marine environment is the surveillance and observation of its environmental conditions. This objective is achieved by measuring certain variables that can be considered as proxies of the state of marine ecosystems. These measurements have to be systematic, periodic and permanent, with no time limitation.

But, why should we carry out this activity which is expensive and requires many human and material means? Which are the objectives pursued? Is it really important?

This book is not intended to give an answer for those already convinced, including oceanographers involved in monitoring activities, but for a general public and those people not involved in the marine observation.

An easy explanation could be provided by means of a comparison. Let's change the initial question. Instead of asking why marine monitoring is important, let's ask: why do we visit the doctor? We all know the answer. There are two reasons. One of them would be the appearance of a symptom which indicates that there is a problem. The other reason would be a periodic checking to confirm that everything is all right or to detect any possible anomaly before it worsens. In both cases the doctor will carry out some tests and will measure some variables that could be good indicators of our health state: cholesterol and sugar concentration in blood, arterial pressure, etc. Let's consider a blood analysis and suppose that the cholesterol concentration is 236 mg/dl. This value does not provide complete information. Is it too high?, too low?, should we worry about it and have any drug to correct it? We usually find the answer to these questions in the analysis report. Close to the figure 236 mg/dl, it can be read: reference values: 108 - 268 mg/dl. If our cholesterol level is within the specified range, we can consider that it is "normal".

Hitherto everything seems familiar to us. Nevertheless, it is possible that not all of us have considered the following question: How do we know that these are the normal values for the cholesterol concentration? The same question could be posed for any other variable within the blood analysis. The answer is that it is the result of a statistical work. Researchers have carried out many measurements along the time. The statistical analyses of these data have allowed us to establish which the average values are, and the variability ranges for healthy individuals and for the cholesterol concentration or for any other variable. In this way, the reference values are established. Besides the visits to the doctor caused by the appearance of any symptom, we will make periodic reviews for checking that the levels of all the health indicators are within the expected ranges.

It is exactly the same for the observation of the sea. We could go to any geographical point at the sea for two reasons: There is any problem (symptom, illness), such as an oil leak, the mortality of a certain species, etc. and we desire to find out the origin and consequences of the problem. Or we could visit that geographical point simply because we want to check the "health" of that region of the sea. In both cases the procedure is similar to the one followed by the doctor. We will measure several variables that could be considered as good indicators of the health state of the sea: temperature, salinity, dissolved oxygen and chlorophyll concentrations, etc. Consider the case that the chlorophyll concentration at the sea surface is 5 mg/m³. Once again the next question is: Is this a normal value? We could answer this question only if many measurements had been previously carried out and the average values and ranges of variability had been established. Once the mean values and variability ranges have been established, we should visit the same geographical location to check the health state of that particular region.

Finally, some considerations should be taken into account before deciding the methodology for establishing the average values and variability ranges for the environmental variables. When considering the human health, some indicators can take different values and vary within a different range when considering different age or sex groups. In such cases, the studies should be differentiated for each group. For the case of the sea, most of the variables analysed will take different values for different regions and for different seasons. Therefore our studies should be differentiated for the different seasons and geographical regions on which we are interested.

In summary, marine monitoring is to the sea what medical analyses and checks are to the human health. It is a question of environmental health.

Main results and summary for policymakers

Detecting alterations of the physical, chemical and biological properties of the marine ecosystems (including phyto and zooplanktonic communities) requires that mean values and variability ranges have been previously established.

The knowledge of the mean values and variability ranges of environmental variables that could be used as indicators of the ecosystem state, cannot be achieved by means of one single oceanographic campaign. Neither a reduced number of them, covering one or a few seasonal cycles would be enough. This goal requires the permanent monitoring of such environmental variables.

The Instituto Español de Oceanografía (IEO, Spanish Institute for Oceanography) has funded several monitoring programs within the Mediterranean Sea since 1992. Since 2007, all these programs have been merged into the RADMED project (Time Series of Oceanographic Data in the Mediterranean Sea). This program is devoted to the multidisciplinary monitoring of Spanish Mediterranean waters from Malaga to Barcelona, including the waters surrounding the Balearic Islands.

This report is a first attempt to analyze all the information available up to the moment, trying to establish for the different regions studied in RADMED Project the mean values and ranges of variability for variables such as: sea temperature and salinity, sea level, chlorophyll-a concentration, nutrient concentrations (nitrate, nitrite, phosphate and silicate), dissolved oxygen concentration, Secchi disk depth, the abundance of micro, nano and pico-phytoplanktonic cells, and the abundance and biomass of broad zooplanktonic groups.

In addition to the statistical analyses that characterize the current environmental state of the Spanish Mediterranean waters, long-term trends were analyzed in the cases where the length of the time series allowed us to do so. Therefore, possible alterations associated to climate change were considered. For the long-term studies, time series obtained from the IEO monitoring programs were completed with data from other institutions: Agencia Estatal de Meteorología (AEMET, Statal Meteorological Agency) and l'Estartit Oceanographic and meteorological station, operated by Institut de Ciències del Mar (ICM/CSIC). Satellite sea surface temperature data were obtained from NOAA (National Oceanic and Atmospheric Agency, USA). Temperature and salinity data from the MEDAR/MEDATLAS (Mediterranean Data Archeology and Recue) data base were also compiled.

The main result is to note the potentiality of the RADMED monitoring Project for generating long time series that can be analyzed for establishing the current environmental state of the Spanish Mediterranean. These statistics could be used as a reference for future works and could be useful for determining the importance of possible alterations such as those caused by climate change or any other anthropogenic stressor (oil spills, coastal infrastructures, etc.). For the first time, since the lunch of the monitoring programs in the Spanish Mediterranean, the statistics that help to define the current state of its ecosystems have been tabulated. Mean values and variability ranges are provided on a seasonal basis for the variables already mentioned: chlorophyll-a, nutrients, oxygen, etc. The maintenance of a monitoring system based on in situ sampling, i.e., based on the sampling from oceanographic vessels, is expensive and has many difficulties. As a consequence of it, the present time series have many gaps and in some cases they do not have the needed length. Nevertheless, in this work the corresponding statistics are presented even in those cases where the time series do not have the desired length. In such cases the objective of this work is to show the kind of products that a monitoring system such as the RADMED one could provide in the future. Improving the length and quality of oceanographic time series and the corresponding statistics is just a question of perseverance. The results presented in this report, mainly in form of tables, will periodically be updated and made accessible to the scientific community, environmental policy-makers and general public.

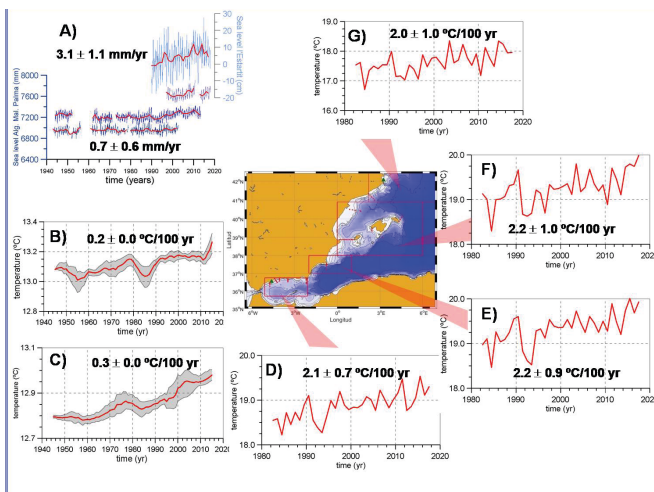
Long-term trends have been estimated in the case of the longest time series. These analyses update

previous works already published by the IEO, such as *Cambio Climático en el Mediterráneo Español*, 1ª y 2ª edición (*Climate change in the Spanish Mediterranean*, first and second edition). The results in the present report show a clear warming and salinity increase of the Spanish Mediterranean waters. These trends have been estimated for the period 1945-2016 for the intermediate and deep waters. Data from both the RADMED project and the MEDAR/MEDATLAS data base have been used for such estimations. Intermediate waters have been considered as those extending from a depth of 150 m to 600 m. Deep waters are considered as those extending from 600 m to the sea bottom. If temperature and salinity values for these layers are averaged for the whole geographical area covered by RADMED project, it can be established that intermediate and deep waters have increased its temperature at a rate ranging between 0.2 and 0.3 °C/100 years (Figure 1). It should be noted that an increase of 0.3 °C for a 100 year period could look like a small one. Nevertheless, this warming is affecting a very large volume of water, much larger than the one corresponding to the surface water (which can increase its temperature more easily). The intermediate and deep water warming requires a huge amount of heat.

The surface layer in the Mediterranean Sea is usually considered as that extending from the surface to 150 m depth. This layer experiences very large fluctuations due to its contact with the atmosphere and the consequent heat and fresh water exchange. Its monitoring requires a sampling frequency higher than the one used in RADMED project. For this reason, satellite sea surface temperature data have been analyzed. These time series extend from 1982 to 2017 and show very clear trends at the four geographical areas considered for this type of data: Alboran, Murcia, Levante and Baleares, and Cataluña. In all the cases, temperature trends are close to 2 °C/100 years. Figure 1 shows a summary of such trends.

Mean sea level has been measured by means of the IEO tide gauge network. Time series from tide gauges in Algeciras, Malaga and Palma de Mallorca have been analyzed. These data have been completed with those from the tide gauge in l'Estartit station (ICM/CSIC). All of these time series showed positive trends. The Málaga sea level time series extends from 1944 to 2013 and showed a sea level trend of 0.7 mm/yr. This positive trend has increased from the beginning of the 1990s. The l'Estartit sea level time series extends from 1990 to 2017, and has a strong and positive trend of 3.1 mm/yr.

The salinity increased along the whole water column (not shown in figure 1, see chapter 6). The salinity trends ranged between 0.1 and 0.3 psu/100 years (although salinity is dimensionless in the practical salinity scale, hereafter "psu" will be used for salinity. Its meaning is practical salinity unit and is very close to grams of salt per kg of sea water).



As already commented, the time series obtained in RADMED Project have allowed us to perform a statistical analysis of some chemical and biological variables that could be considered as good indicators of the current state of marine ecosystems. This analysis has revealed the existence of geographical areas with differentiated properties along the seasonal cycle within the Spanish Mediterranean.

Figure 1. Figure 1A shows from the bottom to the top, monthly sea level time series in Algeciras, Málaga, Palma de Mallorca and l'Estartit (blue lines). Red lines are the corresponding annual time series. Figures 1B and C show the temperature evolution of the intermediate (B) and deep (C) layers for the whole study area in the RADMED project. Red lines show the annual time series and the grey shaded zones are the

uncertainty associated to the calculation of annual temperatures. Figures D, E, F and G show the evolution of the sea surface temperature measured by means of satellite radiometers in four regions: Alboran Sea, Murcia region, Balearic Islands and Catalonia.

Two different periods can be distinguished throughout the year in most of the Spanish Mediterranean waters. A first period could be named as “mixed water column period” (affecting the upper tens or hundreds of meters). During this period the autumn and winter storms homogenize the upper part of the water column, injecting nutrients at the upper well illuminated layer (photic layer). From spring and mainly during summer, the heating of the surface layer produces a density contrast with the colder deep waters. This period is named as “the stratified period”.

Figures 2 and 3 show a scheme with the statistical values of some of the biochemical variables monitored in RADMED Project along the water column within the frame of RADMED Project. Figure 2 is for the “mixed water column period” corresponding to autumn and winter, and figure 3 is for the “stratified period”. According to these figures, there is a trophic gradient from southwest to northeast with a reduction of the concentrations of chlorophyll, nutrients and the abundance of large phytoplanktonic cells such as diatoms. Three main areas could be distinguished. The first one is the most productive one and corresponds to the Alboran Sea. Nevertheless, it can already be appreciated an increase of the oligotrophy of the waters from west to east within the Alboran Sea. This could suggest a further division between the Western and Eastern Alboran Sea. A second region could be considered as that corresponding to the waters around Cape Palos and surrounding the Balearic Islands, both in the insular and peninsular sides. This area is characterized by very low nutrient and chlorophyll concentrations. Finally, the waters in the northern sector, within Catalonia region show an intermediate situation between the most productive waters in the Alboran Sea, and the most oligotrophic ones in the Balearic Islands and Cape Palos area.

The highest nutrient concentrations at the surface layer and the highest chlorophyll concentrations are observed during the mixed water column period, when the stormy activity injects nutrients into the photic layer, producing a phytoplanktonic bloom. This bloom is observed in winter or early spring in most of the areas, but in some cases it is anticipated to autumn, when the intensity of the wind and the frequency of storms start to increase.

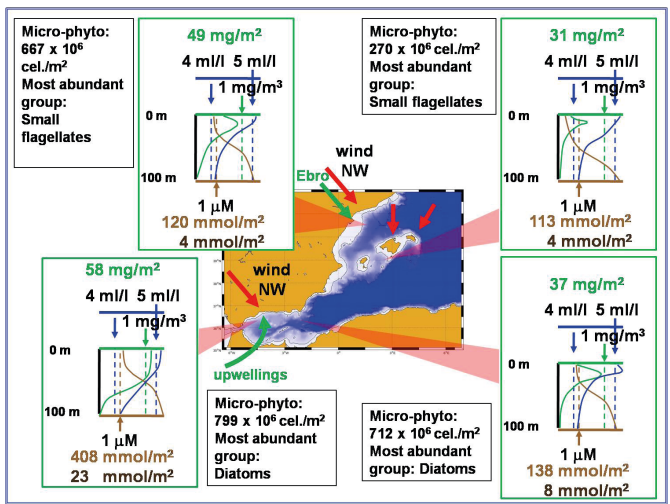


Figure 2. Mixed water column period, from the end of autumn to the end of winter or early spring. The study area is divided into four regions, differentiated by their physical and biochemical properties: The Western Alboran Sea, The Eastern Alboran Sea, Cape Palos and Balearic Islands, and Catalan waters. For each region there is a scheme showing the main features of the vertical chlorophyll-a (green line), dissolved oxygen (blue line), and nitrate (light brown line) profiles. Some values are marked in the axes: the 1 mg/m³ value for the chlorophyll-a, the values 4 and 5 ml/l for the dissolved oxygen and the value 1 μM for nitrate. These reference values facilitate the interpretation of these schemes and help to show more clearly the differences between different areas. Values for the integrated chlorophyll (green numbers) and integrated phosphate (dark brown numbers) have been inserted. It has also been included a legend indicating the most abundant micro-phytoplanktonic group and the total micro-phytoplanktonic cell abundance. Red lines indicate the predominant wind directions and the green lines show the position of the frequent upwelling areas and the mouth of the river Ebro.

The maximum chlorophyll concentrations in the Western Alboran Sea are observed at the sea surface during this period. Such concentrations are higher than 1 mg/m³. Dissolved oxygen is also maximum at the sea surface, indicating that the causes are both the higher solubility of gases at cool winter waters and the photosynthetic activity. Surface nitrate concentrations are over 1 μM. These values indicate an important nutrient supply to the upper layers which would be associated to the north-westerly winds prevailing during this time of the year, and to the upwelling processes which are frequent in the Western Alboran Sea. The highest chlorophyll concentrations in the eastern sector of the Alboran Sea during this mixing period are not observed at the sea surface, but at 20 m depth. These maximum values are lower than 1 mg/m³. The dissolved oxygen maximum is at the same depth

or slightly shallower. Chlorophyll, nitrate and phosphate concentrations integrated along the water column, show a decrease when compared with the western sector of the Alboran Sea (see green, light and dark Brown numbers in figure 2). Diatoms are the most abundant micro-phytoplanktonic group during this period of the year both in the Western and Eastern Alboran Sea. Nevertheless, the total micro-phytoplankton abundance (diatoms plus dinoflagellates and small flagellates) descend from the western (799×10^6 cel./m²) to the eastern (712×10^6 cel./m²) sector. The zooplanktonic biomass shows a similar gradient within the Alboran Sea.

Both in the insular and peninsular sectors of the Balearic Sea, the maximum chlorophyll concentrations are observed in winter at the sea surface and at 20 m depth. Such values are close to 0.4 mg/m³. Surface nitrate concentrations reach the highest values of the year, but these concentrations are below 1 μM. The most abundant micro-phytoplanktonic group is small flagellates, although it should be noticed that diatoms experience an important increase with respect to other periods of the year. The total abundance of micro-phytoplanktonic cells is the lowest one of the whole Spanish Mediterranean, with 277×10^6 cel./m². To the north of the Balearic Islands, in the Catalan waters, surface nitrate concentrations are also higher during this mixing period, but once again they are below the 1 μM value. The chlorophyll maximum is around 20 m depth, being this value higher than those from Cape Palos and Balearic Islands, and close to those from the eastern sector of the Alboran Sea (0.6 mg/m³). The most abundant micro-phytoplanktonic group is small flagellates, being its abundance higher than the one from the Balearic Islands, but lower than the abundance from the Eastern Alboran Sea (677×10^6 cel./m²). Vertically integrated chlorophyll, nitrate and phosphate concentrations are included in figure 2 and show the impoverishment of the waters from the Western Alboran Sea to the Balearic Islands and the slight recovery towards Catalan waters.

Figure 3 shows the decrease of the surface nitrate and chlorophyll concentrations in the Western Alboran Sea for the stratified period (when compared with the mixing one). Nevertheless, these concentrations grow rapidly with depth and they are over 1 μM and 1 mg/m³ at 20 m depth. These values decrease towards the east and the chlorophyll maximum deepens to 50 m. This feature is usually known as the Deep Chlorophyll Maximum (DCM). The chlorophyll concentration at the DCM in the Eastern Alboran Sea is around 0.5 mg/m³. The west-east oligotrophic gradient can be more clearly observed if vertically integrated concentrations are compared. These concentrations for chlorophyll, nitrate and phosphate decrease from 47 mg/m², 351 and 20 mmol/m² respectively in the western sector, to 14 mg/m², 17 and 4 mmol/m² in the eastern one. Another difference between both sides of the Alboran Sea is observed in the micro-phytoplanktonic abundances. Diatoms are the most abundant group in the western sector and the total abundance (diatoms, plus dinoflagellates and small flagellates) is 335×10^6 cel./m² during this stratified period. At the Eastern Alboran Sea the most abundant group is small flagellates and the total abundance is 233×10^6 cel./m².

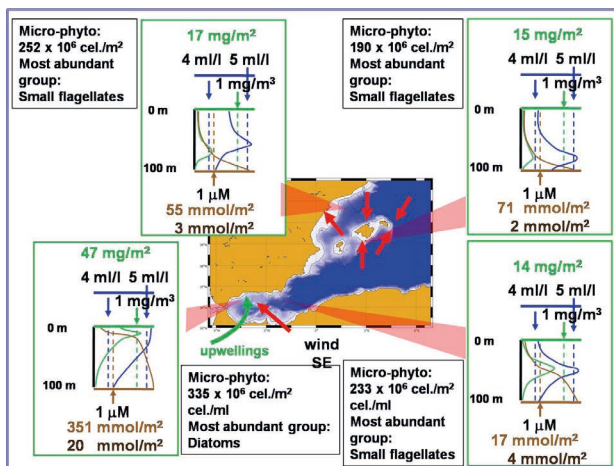



Figure 3. Stratified water column period, from the beginning of spring to the end of autumn. The study area is divided into four regions, differentiated by their physical and biochemical properties: The Western Alboran Sea, The Eastern Alboran Sea, Cape Palos and Balearic Islands, and Catalan waters. For each region there is a scheme showing the main features of the vertical chlorophyll-a (green line), dissolved oxygen (blue line), and nitrate (light brown line) profiles. Some values are marked in the axes: the 1 mg/m³ value for the chlorophyll-a, the values 4 and 5 ml/l for the dissolved oxygen and the value 1 μM for nitrate. These reference values facilitate the interpretation of these schemes and help to show more clearly the differences between different areas. Values for the integrated chlorophyll (green numbers), integrated nitrate (light brown numbers) and integrated phosphate (dark brown numbers) have been inserted. It has also been included a legend indicating the most abundant micro-phytoplanktonic group and the total micro-phytoplanktonic cell abundance. Red lines indicate the predominant wind directions and the green line shows the position of the frequent upwelling areas.



This trend accents towards Cape Palos and the Balearic Islands where the DCM is at 75 m depth during the stratified period, with concentrations around 0.2 mg/m³. Nitrate are depleted at the sea surface and concentrations keep below 1 μM until 75 or 100 m. Small flagellates is the most abundant group and the total micro-phytoplanktonic abundance is the lowest one from the whole area analyzed in RADMED project (190 x 10⁶ cel./m²). The zooplanktonic biomass is significantly lower than the one from the Alboran Sea. Finally, the conditions in the Catalan Sea are similar to those already described for Cape Palos and Balearic Islands, but surface nutrient concentrations, chlorophyll concentrations and micro-phytoplanktonic abundances are slightly higher.

Before we start

Before starting the reading of this report, we would like to make some considerations which hopefully will facilitate its reading.

The structure of this work is the following one: Chapter 1 is an introduction where main geographical features of the study area are presented. This chapter includes a revision of the main water masses, their circulation and biochemical properties in the Western Mediterranean, as this is the basin where the Spanish Mediterranean is located. Chapter 2 describes the monitoring program RADMED (Oceanographic time series in the Mediterranean Sea), funded by the Instituto Español de Oceanografía.

Following this introductory chapters, there are three chapters (chapters 3, 4 and 5) devoted to the analysis of certain variables that could be used as indicators of the state of the Spanish Mediterranean marine ecosystems. The study area is divided into three main regions: The Alboran Sea (chapter 3), Cape Palos and Balearic Islands, both the peninsular side, around Cape San Antonio, and the insular area (chapter 4), and finally the Catalan waters (chapter 5).

Chapters 3, 4 and 5 have the same structure. Each one is initiated with an introduction for the corresponding region. This introduction could be somehow repetitive as it contains some of the information presented in chapter 1. The reason for its inclusion is twofold. On one hand it includes specific information for the region considered in each chapter that was not included in the more general chapter 1. On the other hand, each chapter could be read independently. In this way, the reader interested in a particular region could read the corresponding chapter without reading the rest of the book. After this introduction, there is a section dealing with the average meteorological conditions for each geographical area. Then, temperature and salinity for the main water masses are described. The next section is devoted to the average chlorophyll, dissolved oxygen and nutrient concentrations. Then, the abundances of the main micro-phytoplanktonic groups and the abundances of the nano and pico-phytoplankton (both eukaryote and prokaryote) are analyzed. Each chapter finalizes with the analysis of the abundances of the main meso-zooplanktonic groups in those cases where this information is available.

The analysis of all the variables described above is made by means of the description and discussion of the corresponding graphics. Besides this, one of the main goals of the present work is to provide tables with the statistics that allow us to describe the present state of the Spanish Mediterranean. These tables are a material that could be consulted by other researchers, managers or general public. Nevertheless, the volume of this information is such that could make the reading of this work very cumbersome. For this reason, these tables can be found at the end of each chapter. In this way, they can be consulted by the interested reader, while those who prefer a more direct and light reading can omit it. It is also important to note that not all the tables corresponding to all the oceanographic stations sampled in RADMED project have been included. Such an amount of information would make this report too extensive. Nevertheless, these statistics have been calculated and could be made available in the case it was needed.

This work ends with chapter 6, which includes a long-term analysis of those time series with a sufficient length. This chapter could be considered as an update of previous reports dealing with climate change

and published by Instituto Español de Oceanografía in 2008 and 2010. This chapter evidences some of the changes which the Western Mediterranean is currently undergoing, very likely as a consequence of climate change.

1. INTRODUCTION.

1.1 The geographical framework.

First of all, the main geographical accidents that will be frequently referred to in the present report, will be described. The objective is to facilitate the reading to those readers not familiarized with the Mediterranean Sea.

Spanish Mediterranean waters extend from the eastern limit of the Strait of Gibraltar to the frontier with France in Portbou (Girona province), including the waters that surround the Balearic Islands. These waters are within the Western Mediterranean or Western Basin, which is one of the two main basins that form the Mediterranean Sea (the other one would be the Eastern Mediterranean or Eastern Basin). If the Strait of Gibraltar is not considered, the Western Basin extends from the imaginary line connecting Point Europa and Point Almina (Fig. 1.1) to the line connecting Cape Bon (Tunisia) and Cape Lilibeo (Sicily Island).

If the Mediterranean is considered as a whole, it is a semi-enclosed sea, whose only natural connection to the world ocean is the Strait of Gibraltar. This connection and the climatic conditions in the Mediterranean Sea, determine its physical and biochemical characteristics.

Some of the main sub-basins and seas that form the Western Mediterranean are presented in figure 1.1. One of the main basins is the Algero-Provençal one. According to the limits defined by the International Hydrographic Organization, the main seas within the Spanish waters are the Alboran and Balearic Seas. The first one extends from the eastern limit of the Strait of Gibraltar to the line that connects Cape Gata (Almería province) with Cape Figalo (Algeria). The limits of the Balearic Sea are: the line from Cape San Antonio to the south of Formentera Island (Cape Berbería). The line from Cape Berbería to Cabrera Island, and from here to “del Aire” Island, to the south of Menorca Island. Finally, a line from Cape Favaritx, to the north of Menorca Island, to Cape San Sebastián, in Girona province.

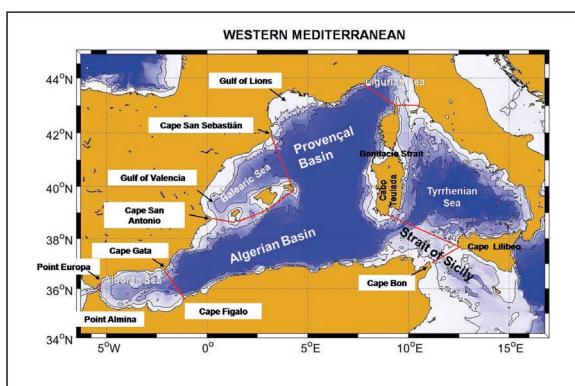


Figure 1.1. Main basins in the Western Mediterranean.

1.2. Climatic forcing and thermohaline circulation.

In this section the oceanographic framework of the Spanish Mediterranean waters is described. That is, the physical and biochemical properties of its waters, its circulation and the factors that determine such properties. This description will help to understand the main results presented in this work,

based on the data collected under the umbrella of the monitoring programs funded by the Instituto Español de Oceanografía (IEO, other reviews of the Mediterranean Sea circulation and variability can be consulted in Schroeder et al., 2012 or Millot et al., 1999, for instance).

In a summarized way, it could be established that the circulation of the Mediterranean Sea and the properties of its water masses, are the result of the freshwater deficit in the Mediterranean, the net heat loss through its surface, and the water exchange with the Atlantic Ocean through the Strait of Gibraltar.

The Mediterranean Sea is a concentration basin, i.e., the evaporation exceeds the fresh water supply due to rainfall and river runoff (see, for instance, Skliris et al., 2018; Jordà et al., 2017; Criado-Aldeanueva et al., 2012; Ludwig et al., 2009; Struglia et al., 2004; Boukthir and Barnier, 2000; Tixeront, 1970, for a revision of precipitation, evaporation and river runoff values). Because of this hydric deficit, the Mediterranean should lose around one meter height per year. This does not happen because of its connection with the Atlantic Ocean. Nevertheless, the situation is much more complex. Because of the net evaporation (evaporation excess over precipitation and river runoff), the waters flowing into the Mediterranean through the Strait of Gibraltar, gradually increase their salinity. In summer, the heating of the surface waters compensates for the effect of salinity on the water density. However, the winter cold and dry winds that blow from the continent, mainly in the northern sector of the Mediterranean Sea (Gulf of Lions, Adriatic Sea, Northern Aegean Sea, Rhode Island), cool the surface waters. Both the salinity increase and the temperature decrease contribute to the density increase of the upper part of the water column. These dense waters mix with those below and sink until they find their equilibrium depth (waters with the same density). This process produces the mixing of the water column and the homogenization of the physical and chemical properties of the water column. If this violent mixing affects the upper 150 or 300 m of the water column, it is named as intermediate convection or formation of intermediate waters (Juza et al., 2019; Lacombe and Tchernia, 1972). If it affects the whole water column, to a depth of 2000 or 2500 m, it is named as deep convection or formation of deep waters (Fig. 1.2, Mihanovic et al., 2018; Léger et al., 2017; Stommel, 1972; Anati and Stommel, 1970; MEDOC Group, 1970).

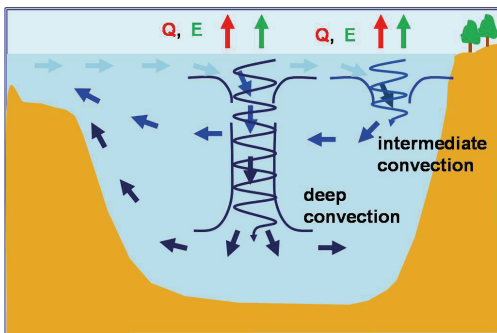


Figure 1.2. Scheme for the intermediate and deep water formation.

These intermediate and deep waters formed in winter, are saltier and colder, and therefore denser, than the waters flowing into the Mediterranean Sea from the Atlantic Ocean. This density difference generates a deep counter current of Mediterranean waters that finally flow out of the Mediterranean through the Strait of Gibraltar.

If heat fluxes are averaged for the whole Mediterranean surface and a complete year, the Mediterranean Sea experiences a net heat loss of

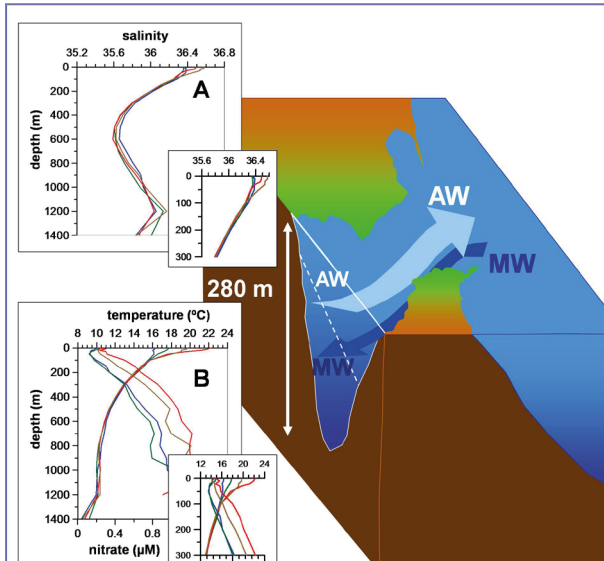
around 5 W/m^2 (see Jordà et al., 2017; Criado-Aldeanueva et al., 2012; Ruiz et al., 2008 for a revision of the heat fluxes in the Mediterranean Sea). If it is considered that, on the average and for a long period of time, the Mediterranean is in an equilibrium state, there has to be a balance between the net evaporation, the net heat loss through its surface, and the salt, water and heat fluxes through the Strait of Gibraltar. This balance can be summarized as follows:

The water volume that flows at the surface from the Atlantic Ocean must be equal to the water volume that flows out of the Mediterranean beneath the Atlantic Water, plus the net evaporation in the Mediterranean Sea. In this way, a water or volume balance is established. The water from the Atlantic has a lower salinity than the one flowing out from the Mediterranean. Nevertheless, as the Atlantic flow is larger than the Mediterranean one, there is a balance for the salt transport through Gibraltar, with a net salt transport equal to zero. Finally, the Atlantic current is warmer than the Mediterranean deep water and therefore there is a net heat transport into the Mediterranean Sea. This net heat transport compensates for the 5 W/m^2 heat losses through the sea surface (Bethoux, 1979).

This circulation of water flowing into the Mediterranean Sea from the Atlantic, its transformation into saltier, colder and denser deep and intermediate waters, and their circulation back to the Atlantic, is known as the Mediterranean thermohaline circulation. This is very similar to the thermohaline circulation that occurs on a planetary scale over the world oceans. For this reason, the Mediterranean Sea has frequently been considered as a natural laboratory (Bethoux et al., 1999).

1.3. Water masses and circulation in the Western Mediterranean.

As already commented, Atlantic waters flow at the sea surface through the Strait of Gibraltar. The first factor which conditions the properties of the waters flowing into the Mediterranean Sea is the depth of the Strait. The Camarinal Sill, between Point Camarinal (Bologna, Cádiz province) and Point Malabata (Tanger, Morocco) has a maximum depth close to 300 m. Therefore, the properties of the water flowing into the Mediterranean would be those of the waters that occupy the upper 300 m of the Atlantic Ocean in the Gulf of Cádiz (Fig. 1.3). This water mass that forms the surface layer of the Mediterranean Sea is named as Atlantic Water (AW).



The first basin receiving this water mass is the Alboran Sea. The Atlantic Current, leaves the Strait of Gibraltar in a northeast direction approaching the Spanish coast close to Point Calaburras, to the west of Fuengirola (Fig. 1.4). This current describes an anticyclonic gyre (clockwise) in the western part of the Alboran Sea, and a second anticyclonic gyre in the eastern sector, to the east of Cape Tres Forcas (Fig. 1.4, Renault et al., 2012; Viúdez et al., 1996; Parrilla and Kinder, 1987; Parrilla, 1984).

Figure 1.3. Circulation scheme through the Strait of Gibraltar. Fig. 1.3A: Seasonal climatological profiles for the salinity in the Gulf of Cadiz. The zoom corresponds to the upper 300 m of the water column. Figure 1.3B: Seasonal climatological profiles for potential temperature and nitrate concentrations in the Gulf of Cadiz. The zoom corresponds to the upper 300 m of the water column.

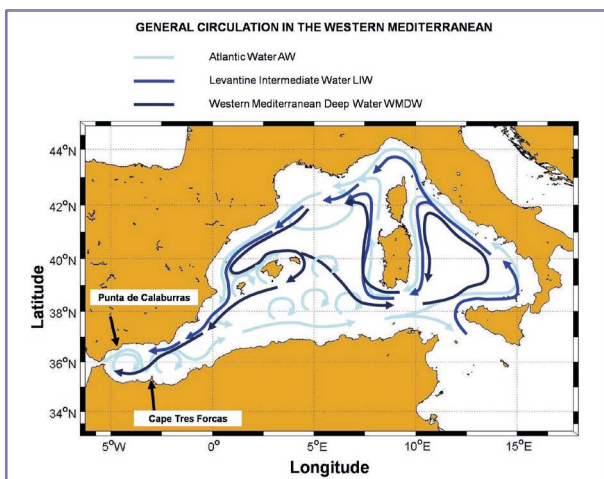



Figure 1.4. Schematic general circulation in the Western Mediterranean.

After describing the second anticyclonic gyre, the current progresses along the Algerian continental slope and receives the name of Algerian Current. This current is unstable and cyclonic and anticyclonic gyres frequently detach from the main current. Anticyclonic gyres usually have a larger size and longer duration and constitute an efficient mechanism for the AW transport towards the north, through the Balearic Channels: The Ibiza Channel (between the peninsula and the Ibiza Island), and the Mallorca Channel (between Ibiza and Mallorca Island, Millot, 1999). The Algerian Current bifurcates to the south of Sardinia. One branch flows



to the east through the Sicily Channel to finally get into the Eastern Mediterranean, whereas the other branch flows into the Tyrrhenian Sea where it describes a cyclonic gyre. Part of this branch finally gets out of the Tyrrhenian Sea through the Corsica Channel, while another part flows to the south of Sardinia, then turns to the north along the western coast of Sardinia, and finally merges with the current that flows to the north of Corsica. Once both currents merge, they receive the name of Northern Current (initially it was known as the Ligurian Current). The Northern Current flows along the continental slope of the French coast and then turns to the south along the Spanish continental slope (Millot, 1999). When this current reaches the Ibiza Channel, it is divided once more into two branches. One of them flows to the south through the Ibiza Channel, and the other one turns to the northeast, to the north of the Balearic Islands, forming the Balearic Current (Ruiz et al., 2009, Pinot and Ganachaud, 1999; Pinot et al., 1995).

Although our interest is in the Spanish waters which are located at the Western Mediterranean, their dynamics cannot be fully understood without the knowledge of the processes and dynamics of the Eastern Basin, to the east of the Sicily Channel.

The branch of AW which flows into the Eastern Mediterranean becomes saltier as it progresses to the east, because of the intense evaporation. In summer, to the south of Rhodes Island and in front of the Syria and Israel coasts, the salinity of the AW has increased from 36.2 or 36.3 at Gibraltar, to 39.2 psu. This salinity increase would also produce a density increase were it not compensated by the intense summer warming. In winter, cold and dry continental winds cool the surface waters. As the temperature of these salty waters decreases, the situation becomes unstable and finally the surface waters mix with those waters below. The upper 200 or 300 m of the water column are mixed with temperature and salinity values of 15 °C and 38.9 psu, receiving the name of Levantine Intermediate Water (LIW, Malanotte-Rizzoli et al., 2003; Nittis and Lascaratos, 1999, Wüst, 1961).

Once the severe winter conditions relax, these waters sink and are replaced at the sea surface by new AW flowing from the west. The LIW sinks and spreads along the Eastern Basin and finally flows into the western one.

The LIW flows to the west decreasing its temperature and salinity by mixing with the AW that flows eastwards above it. In the Sicily Channel its temperature and salinity are close to 14 °C and 38.75 psu. These values continue to descend in the Western Basin and they are around 13.2 °C and 38.5 psu in the Alboran Sea. Nevertheless, before crossing the Sicily Channel, the LIW is involved in a new process of water formation. Part of the LIW flows into the Adriatic Sea where the intensity of winter winds is higher than the one in the Levantine Basin and the winter cooling of surface waters is more intense. Although the process is more complex and involves the northern sector of the Adriatic Sea, with shallower waters and a strong influence of continental ones, here we simply state that the final result is the mixing of the whole water column to a maximum depth of 1200 m, (maximum depth in the Southern Adriatic), with values close to 13 °C and 38.5 psu. This new water mass receives the name of Adriatic Deep Water (ADW). After flowing through the Strait of Otranto, it sinks and mixes with LIW, filling the deep layers of the Eastern Mediterranean and reaching its final properties of 13.3 °C y 38.63 psu.

In the Western Mediterranean the LIW flows between 150 and 400 or even 500 m. It crosses the Sicily Channel and follows a circulation pattern similar to the one described by the AW (see dark blue line in Fig. 1.4). It flows into the Alboran Sea, and finally gets out of the Mediterranean through the Strait of Gibraltar. Nevertheless, before out-flowing, this water mass takes part in another deep water formation process.

The Ligurian Sea region, and mainly the area to the south of the Gulf of Lions, is characterized by a cyclonic circulation. This kind of circulation induces the divergence of surface waters and the upward movement of intermediate waters. In this way, LIW is closer to the sea surface at the centre of the gyre. Frequent and intense winter storms with cold and dry continental winds produce the salinity increase and the cooling of surface waters. When these waters reach the density of the LIW, they are mixed and a layer of 400 or 500 m becomes homogenized. This process is usually referred to as the pre-conditioning phase. During the end of winter, the persistence of stormy conditions produce a further

cooling of the surface waters which eventually reach the deep water density. The whole water column to a maximum depth of 2000 or 2500 m is mixed with temperature and salinity values around 12.7-12.9 °C and 38.4 psu (Mihanovic et al., 2018; Léger et al., 2017; Smith et al., 2008; Leaman and Schott, 1991; MEDOC Group, 1970). This new water mass is named as Western Mediterranean Deep Water (WMDW). It sinks and spreads along the Western Mediterranean. WMDW partially flows into the Tyrrhenian Sea where Tyrrhenian Dense Water (TDW) is formed by mixing of this water mass with the waters that overflow from the Eastern Mediterranean.

If the winter convection occurs in the continental shelf waters which have lower salinity because of the influence of continental waters, this process produces the formation of intermediate waters which receive the name of Western Intermediate Water (WIW), which flows beneath the AW and above the LIW with temperature values lower than 13 °C and salinity values ranging from 37.7 to 38.3 psu (Juza et al., 2019; Pinot and Ganachaud, 1999; Pinot et al., 1995; López-Jurado et al., 1995).

Finally, all these water masses, WMDW, TDW, LIW and WIW, overflow through the Strait of Gibraltar (García-Lafuente et al., 2017; Naranjo et al., 2015, black line in Figure 1.4). It should be noticed that, once in Gibraltar, it undergoes severe mixing and it is difficult to distinguish them at the westernmost side of the Strait.


More details about the properties of the water masses and the circulation within the different regions of the Spanish Mediterranean will be offered in the following chapters. For the moment, and according to the brief description presented above, it could be stated that the Western Mediterranean is mainly formed by three layers: The upper layer which extends from the sea surface to 150 m and is occupied by AW from the nearby Atlantic Ocean, the intermediate layer, from 150 to 600 m, occupied by LIW from the Eastern Mediterranean and WIW from the Western Basin, and the deep layer, from 600 m to the sea bottom, occupied by WMDW and TDW.

1.4. Chemical and biological properties of the Western Mediterranean.

The Mediterranean Sea has an oligotrophic character which increases from west to east and also from north to south (Powley et al., 2017; Siokou-Frangou et al., 2010; D'Ortenzio and Ribera D'Alcalá, 2009; Bethoux et al., 2002, 1998). The origin of the Mediterranean oligotrophy is associated to its thermohaline circulation. The surface waters flowing into the Mediterranean from the Atlantic Ocean have low nutrient (nitrate, phosphate and silicate) concentrations because of the phytoplankton uptake. On the contrary, the Mediterranean waters that outflow to the Atlantic Ocean, as a deep current, are nutrient rich. As a result of this water exchange, the nutrient net transport for the Mediterranean Sea is negative with a net nutrient loss. If, in a first approach, we accept that the Mediterranean is in an equilibrium state, there must be other external nutrient sources that close this balance. Such sources seem to be the river runoff, the depositions of atmospheric dust and the nitrogen fixation by autotrophic bacteria (Bethoux et al., 1998; Macías et al., 2018; 2014).

The Mediterranean Sea is characterized by the existence of two clearly differentiated periods: A stratified period, from mid-spring to the end of autumn, and a second period during winter when the upper part of the water column is well mixed. During the first of these periods, nutrients are scarce or are depleted in the upper layer and phytoplanktonic communities are dominated by the small-size fraction, that is, the picoplankton, (Siokou-Frangou et al., 2010; Arin et al., 2005; Estrada, 1985) both eukaryote and prokaryote (photo-autotrophic bacteria of the genus *Synechococcus* and *Prochlorococcus*). During this stratified period, the presence of a Deep Chlorophyll Maximum (DCM) is almost ubiquitous over the thermocline (Segura-Noguera et al., 2016; Lavigne et al., 2015; Estrada, 1996, 1985). The intensity of this maximum decreases and its position deepens towards the east and south. Although the DCM is partially caused by the photo-acclimatization of photo-autotrophic cells, and even by the sinking of cells and detritus from the layers above, it has been observed that this maximum coincides with higher phytoplanktonic abundances and it is the result of in situ growth and higher primary production (Estrada, 1985). This chlorophyll maximum is frequently accompanied by an oxygen maximum located at the same depth or slightly above it.

During the stratified period, nutrients increase with depth from the sea surface, where they are



almost depleted. This is caused by oxidation processes carried out by nitrifying bacteria. Maximum concentrations are around 9 μM for nitrate and 0,45 μM for phosphate, coinciding with the depth of the LIW core (between 200 and 400 m, depending on the region within the Mediterranean Sea). Nutrients smoothly decrease below this maximum until values close to 8-8.5 μM and 0.4 μM for nitrate and phosphate respectively (Schroeder et al., 2010). The maximum nutrient concentrations and the corresponding oxygen minimum are associated to the LIW and are caused by the remineralization of organic matter sunk during the LIW formation process or during its pathway from the Levantine Basin to the western Mediterranean (Balbin et al., 2014). Silicate do not show this maximum at intermediate depths, and simply increase with depth from the sea surface. This has been linked to lower remineralization rates for silicate (García-Martínez et al., 2018a, Minas et al., 1991).

From the end of autumn, and mainly during winter, storms produce the mixing of the upper part of the water column, injecting nutrients to the photic layer. As a result of this mixing, there is a phytoplanktonic bloom in autumn or early spring, while deep mixing could limit cell growth because of the lack of light. This bloom is characterized by an increase of the proportion of large cells such as diatoms. At the same time, high chlorophyll concentrations can be observed at the sea surface. The vertical distribution of nutrients and chlorophyll are quite homogeneous and the DCM can disappear. As the spring season progresses the thermocline is developed, and the intensity and frequency of storms decrease. The nutrient supply to the upper layers is inhibited and, as the nutrients are consumed, the stratified situation is re-established. Once again the abundance of small size cells increases and the regenerated production, based on ammonium consumption, prevails over the new one, based on nitrate consumption.

Nevertheless, several works have shown that this pattern, generally accepted, can present important variations, depending on the region of the Mediterranean that is considered (D'Ortenzio and Ribera d'Alcalá, 2009). Despite its oligotrophic character, the Mediterranean Sea has production rates higher than those expected. This fact has been named as "the Mediterranean paradox" (Estrada, 1996; Sournia, 1973). The explanation to this paradox seems to be the existence of high regenerated production rates and the existence of fertilizing mechanisms able to reduce the general oligotrophic character of the Mediterranean Sea at some particular areas. Some of these mechanisms would be the intermediate and deep water formation processes, which could inject large amounts of nutrients into the upper layers. These processes would occur at the Northwestern Mediterranean Sea, in the Gulf of Lions and Ligurian Sea, in the southern Adriatic Sea, in the Aegean Sea, and to the south of the Rhodes Island, in the Levantine Basin. Another factor capable of fertilizing certain geographical areas would be the existence of oceanic fronts and mesoscale structures such as cyclonic gyres that favour the vertical circulation and the injection of nutrients to the photic layer. Some of these structures would be located at the Northwestern Alboran Sea, at the Almeria-Oran frontal system, over the continental slope of the Catalan Sea, and along the northern slope of the Balearic Islands. These two latter frontal systems would be associated to the southward extension of the Northern Current that flows along the Ligurian Sea and the Gulf of Lions, and to its northeastward deflection along the Balearic Current. Another frontal zone is found at the Aegean Sea, and is caused by the convergence of the low salinity waters from the Black Sea with the salty waters of the Levantine Basin. Finally, another factor that can enrich the Mediterranean waters is the nutrient supply associated to rivers such as the Rhone, in the Gulf of Lions, the Po, in the Adriatic Sea, The river Ebro, in Catalonia, or the Nile in the Egypt coast. These nutrient supplies can even produce eutrophication episodes (Macías et al., 2018) and the hypoxia in those areas close to the river estuaries. Another eutrophic area is that in the Gulf of Gabes. Nevertheless, in this case it is not clear whether the high chlorophyll values are caused by urban and industrial effluents or they are simply a problem of calibration of chlorophyll satellite data in very shallow waters.

This great variety of processes has led to some authors to establish different regions within the Mediterranean Sea, according to the moment and intensity of the spring bloom and to the shape of the chlorophyll vertical profiles. There exist areas with a strong winter or early spring bloom, followed by a stratified period, whereas in other regions high chlorophyll concentrations are observed during the whole year, etc.

Spanish Mediterranean waters spread over a wide area of the Western Mediterranean, covering almost the complete latitude range, from the Alboran Sea, in the southern part of it, to the Catalan waters, to the north and close to the deep water formation areas. The Balearic Islands are located between these two extremes and constitute a transition zone between the southern waters, with a higher Atlantic influence, and the northern waters with AW severely modified after recirculation in the Western Mediterranean. The exchange between these two water masses would occur through the Balearic Channels, between the peninsular coast and the Ibiza, Mallorca and Menorca Islands. In summary, it can be expected that the Mediterranean waters that surround both the peninsular and insular Spanish coasts will be affected by a high diversity of phenomena which modulate their physical, chemical and biological properties in a similar way to that described for the whole Western Mediterranean (García-Martínez et al., 2019).

2. THE MULTIDISCIPLINARY MONITORING PROJECT RADMED.

The RADMED Project “Oceanographic time series in the Mediterranean Sea” was launched in 2007 with the objective of unifying and extending previous monitoring programs funded by the Instituto Español de Oceanografía (IEO) within the Spanish Mediterranean waters.

ECOMALAGA project was initiated in 1992, and it was devoted to the monitoring of the physical, chemical and biological properties of the waters around the Malaga Bay. Sampling was initially limited to the continental shelf, with maximum sampling depths of 200 m. In 2000, some oceanographic stations were included over the continental slope. Campaigns were quarterly, once per season, and included CTD profiles and water samples for the determination of nutrient (nitrate, nitrite, phosphate and silicate), chlorophyll-a and oxygen concentrations as well as the abundance of micro-phytoplanktonic cells. Oblique trawls with BONGO nets with 250 μm mesh size were carried out for the analysis of the meso-zooplanktonic abundance and biomass.

In 1994 a similar Project was launched in the continental shelf waters around Cape Palos, in the Murcia region: ECOMURCIA. In this case it was not included the micro-phytoplankton and the meso-zooplankton sampling.

It was also in 1994 when the ECOBALEARES Project was initiated. In this project a transect made of three oceanographic stations was sampled to the south of Mallorca Island. The sampling was monthly initially and then quarterly from 2000. In this case, samples for the analysis of micro-phytoplanktonic cells and meso-zooplanktonic abundance and biomass were included.

Finally, CIRBAL Project was launched in 1996. This project was oriented to physical oceanography and the study of the water masses and their circulation within the Balearic Channels. The sampling included mainly CTD profiles, although in some cases, samples for the determination of nutrient and chlorophyll-a concentrations were also obtained.

In 2007 all these projects were merged into a single one devoted to the multidisciplinary monitoring of the continental shelf and slope of the Spanish Mediterranean waters. The current sampling includes some deep stations. RADMED oceanographic stations are approximately distributed along transects normal to the coast. These transects include those stations already sampled in the previous projects and some new stations which extend the monitoring to deeper waters. Two new transects have also been included in the Catalan waters, in front of the Ebro Delta and in front of Barcelona. Another transect has been included to the northeast of Menorca Island and a deep station to the south of Cabrera Island. Figure 2.1 shows the position of the RADMED oceanographic stations.

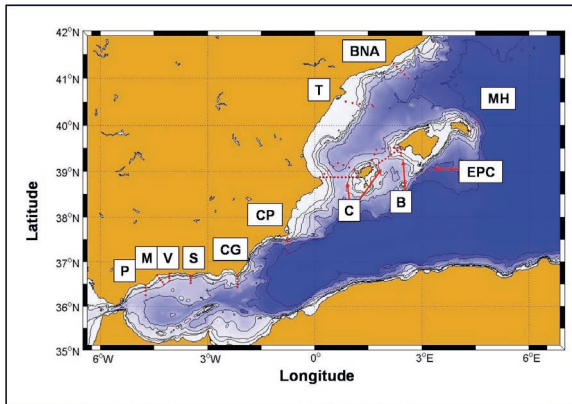


Figure 2.1. Map of the RADMED oceanographic stations.

All the stations are visited on a quarterly basis, once per season. Stations are named by a letter corresponding to each transect and a number increasing from the coast to the open sea. For instance, stations in the Cape Pino transect are named with the letter P, in Málaga transect with the letter M, Vélez, V, Cape Sacratif, S and Cape Gata, CG. The station closest to the coast in Cape Pino transect is P1, and the most offshore one is P4. Stations from Cape Palos transect are labelled as CP. These stations go from CP1 to CP5. 37 stations, forming two triangles, are located in the Ibiza and Mallorca Channels.

These stations were previously sampled in the CIRBAL Project. Stations C1 to C10 form the base of the triangle in the Mallorca Channel (between Mallorca and Ibiza Islands). Stations C11 to C21 are the base of the second triangle, in the Ibiza Channel (between Ibiza Island and Cape San Antonio, in the peninsular coast). Stations C22 to C29 are the northern part of the Ibiza Channel triangle, and stations C30 to C37 correspond to the Mallorca Channel. Stations B1 to B3 form the transect B, to the south of Mallorca Island. This transect was previously included in ECOBALEARES project. EPC station (from the Spanish “Estación Profunda de Cabrera”, Cabrera Deep station), has been included in the RADMED project. This station allows us to monitor deep Mediterranean waters to a maximum depth of 2300 m. The Mahon transect (MH) has also been included in the frame of RADMED project. It is made of four stations extending in a northeast direction from Menorca Island. Finally, transects T and BNA are in front of the river Ebro estuary (Tarragona province) and in front of Barcelona, and they are made of 4 and 5 stations respectively.

CTD profiles are obtained in all the stations. The hydrographic sampling is done using CTDs, mainly model SBE 911 and as spare instruments the models SBE 25 or SBE 19+, installed in a carousel water sampler SBE 32. CTDs are equipped with a Dissolved Oxygen SBE 43 sensor. Dissolved Oxygen and conductivity sensors are calibrated using water samples for selected depths of the water column at least once per campaign, when it lasts less than a week, and at least at the beginning and the end of the campaign, when it is longer. The Dissolved Oxygen determinations to calibrate the SBE 43 sensor are performed by the Winkler titration method (Strickland and Parsons, 1972). The salinity calibrations are done using a Gildline 8400 Autosal.

Water samples for the determination of nutrients and chlorophyll-a are taken at all the stations. Water samples for nutrient determinations are taken at 0, 10, 20, 50, 75, 100, 200, 300, 500, 700, 1000 and sea bottom for deep stations, while sampling is limited to the station depth for the shallower ones. Nutrient samples are collected using 12 mL vials that are kept frozen at -20 °C until they are analyzed in the laboratory. Nitrate, nitrite and silicate concentrations are determined according to the method of Armstrong et al. (1967), modified by Grasshof (1969). Phosphate concentrations are determined by the method of Treguer and Le Corre (1975). All these methods are adapted to oligotrophic waters and analyses are performed with a Technicon Autoanalyzer AAIII and QuAatro Marine of SEAL 25 Analytical. Samples for chlorophyll-a determination are limited to the upper 100m of the water column (0, 10, 20, 50, 75 and 100m) or to the maximum depth for shallower stations. 1 L samples are filtered and kept frozen at -20 °C until they are analyzed by fluorometry (Holm-Hansen et al., 1965) using a Turner 10AU spectro-fluorometer, previously calibrated with pure chlorophyll-a.

Stations labelled as “2” are considered as representative of the continental shelf conditions. In such stations water samples are taken at 0, 10, 20, 50, 75 and 100 m for the analysis of the micro-phytoplankton (> 20 µm). Micro-phytoplankton samples are preserved in 150 mL bottles and fixed with 2 mL of acid lugol solution and stored in darkness until they are analyzed. Cell counts are performed using an inverted microscope after sedimentation of variable volumes of seawater (25-100

mL), depending on cell concentration (Utermöhl, 1958). First, cells from subsamples are counted over the whole bottom of the sedimentation chamber scanned at 50X magnification. Secondly, on two transects of the whole bottom area of the sedimentation chamber at 100X magnification, and finally, on one transect of the whole bottom area of the sedimentation chamber at 200X magnification. Determinations are done to genera level in most of the cases and to species level when possible. Finally, results are aggregated into three main groups. Diatoms, dinoflagellates and small flagellates. Coccolithophores are not analyzed in the present sampling. The reason is that coccolithophores suffer rapid dissolution in acid lugol. Good preservation of coccolithophore cells has been obtained with very weak formaldehyde solutions buffered with hexamethylenetetramine (Sournia, 1978; Thomas, 1997). This means having to store twice the volume of samples and double the examination work, which cannot be achieved due to the lack of space and qualified personnel during the campaigns and at the laboratory. It would also be desirable to sample the other micro-phytoplanktonic groups both at the continental shelf and the slope stations. These analyses demand much time, and the lack of qualified personnel do not allow us to accomplish the continental slope sampling for the moment.

Pico and nanophytoplankton samples are preserved in 5 mL cryotubes fixed with 200 μ l of 50% glutaraldehyde solution and frozen at -80 °C until they are analyzed using a FACSCalibur (Becton Dickinson) flow cytometer. The pico-phytoplankton (*Prochlorococcus*, *Synechococcus* and picophytoeukaryotes) and nanophytoeukaryote groups are described and enumerated according to their specific auto-fluorescence properties and side scatter differences (Gasol, 1999).

Zooplankton sampling is carried out at stations 2 and 4 for each transect. These samples are obtained by means of oblique hauls from 100 m to the surface (or from the sea bottom for shallower stations). Hauls are made with BONGO-nets equipped with 100 and 250 μ m mesh size nets, equipped with flowmeters to determine the filtered volume, at a vessel speed of 2 knots. Immediately after collection, the zooplankton samples are split in two subsamples for biomass and taxonomic analysis with a Folsom plankton splitter. Subsamples for taxonomic studies are preserved with 4% neutralized formaldehyde buffered with hexamethylenetetramine. Representative aliquots for taxonomic analysis are analyzed and the organisms identified to the level of main taxonomic groups: Copepods, appendicularians, cladocerans, doliolids, chaetognaths, siphonophores, ostracods and scyphozoans. Abundance is calculated as individuals/m³. Subsamples for biomass are frozen (-20 °C) for subsequent estimation of the biomass as dry weight (Harris et al., 2000; Lovegrove, 1966). Samples for biomass measurements are concentrated on Whatman GF/C filters previously weighted. These filters are then dried in a drying oven at 60 °C for about 24 h and stored in a desiccator for approximately 1 h. Then, biomass values are estimated by subtracting the initial weight of the filter from the final weight. Biomass is calculated as mg/m³.

Sampling protocols can be consulted in López-Jurado et al., 2015 or in www.repositorio.ieo.es/e-ieo/handle/10508/1762.

Table 2.1 shows the position and depth for all the RADMED oceanographic stations and the type of sampling carried out at each station. This table is included for the completeness of the present work and to provide information to the reader about the available data at each region of the Spanish Mediterranean in the case it could be required.

It is important to note that the maintenance of a monitoring program with a seasonal periodicity and the spatial coverage of RADMED Project is a difficult task. These difficulties include bad weather conditions that do not allow the development of the campaigns at the scheduled time, the occasional lack of oceanographic vessels at the established times, instrument failures or the lack of qualified personnel. Besides this, RADMED has been developed step by step from 1992, when ECOMALAGA project was initiated, to 2007, when all the previous monitoring programs were unified. New stations have been added along the time to complete the spatial coverage, and new variables have been included to achieve a better description of the ecosystem state. For all these reasons, each of the RADMED variables has a different time and spatial coverage and time series present frequent gaps. Although the RADMED team works for correcting these deficiencies, the data scarcity is a problem in some cases and it will be referred to along the present report. Tables 2.2 to 2.9 show the data availability for each variable and for each year and season.

Table 21. Position of RADMED stations. Last column is the type of sampling carried out at each station. N, nutrients, C, chlorophyll, FM, micro-phytoplankton (microscopy), FC, nano and pico-phytoplankton (flow cytometry), Z, zooplankton hauls.

Transect	Long. (deg.)	Lon. (min.)	Lat. (deg.)	Lat. (min.)	Station	Depth	Sampling depths	Sampling
P	-4	-44.3580	36	28.2000	P1	30	0-10-20	N-C
	-4	-44.4960	36	25.4280	P2	130	0-10-20-50-75-	N-C-FM-FC-Z
	-4	-44.5320	36	21.0960	P3	530	0-10-20-50-75-100-200-300-bottom	N-C
M	-4	-44.4960	36	15.0000	P4	870	0-10-20-50-75-100-200-300-500-bottom	N-C-FC-Z
	-4	-24.3480	36	41.7600	M1	20	0-10-20	N-C
	-4	-21.2160	36	38.3160	M2	75	0-10-20-50-75	N-C-FM-FC-Z
	-4	-18.6180	36	35.5980	M3	200	0-10-20-50-75-100-200	N-C
V	-4	-15.8280	36	32.5380	M4	350	0-10-20-50-75-100-200-bottom	N-C-FC-Z
	-4	-13.1220	36	29.4900	M5	500	0-10-20-50-75-100-200-300-500	N-C
	-4	-3.9900	36	44.1180	V1	20	0-10-20	N-C
	-4	-3.8460	36	41.2500	V2	75	0-10-20-50-75	N-C-FM-FC-Z
	-4	-3.9000	36	38.2800	V3	300	0-10-20-50-75-100-200-300	N-C
S	-4	-3.9000	36	34.2000	V4	490	0-10-20-50-75-100-200-300-bottom	N-C-FC-Z
	-3	-28.0920	36	40.7460	S1	200	0-10-20-50-75-100-200	N-C
	-3	-28.0920	36	39.3480	S2	300	0-10-20-50-75-100-200-300	N-C-FM-FC-Z
	-3	-28.0920	36	37.4220	S3	500	0-10-20-50-75-100-200-300-500	N-C
	-3	-28.0920	36	34.6140	S4	650	0-10-20-50-75-100-200-300-500-bottom	N-C-FC-Z
CG	-3	-28.0920	36	31.7220	S5	750	0-10-20-50-75-100-200-300-500-bottom	N-C
	-2	-9.9120	36	42.1800	CG1	50	0-10-20-50	N-C
	-2	-9.9120	36	40.6500	CG2	75	0-10-20-50-75	N-C-FM-FC-Z
	-2	-9.9120	36	37.1520	CG3	100	0-10-20-50-75-100	N-C
CP	-2	-9.9120	36	29.8260	CG4	700	0-10-20-50-75-100-200-300-500-700	N-C-FC-Z
	-2	-9.9120	36	25.3320	CG5	1130	0-10-20-50-75-100-200-300-500-700-1000-bottom	N-C
	0	-45.4500	37	33.0120	CP1	50	0-10-20-50	N-C
	0	-45.4500	37	29.7900	CP2	75	0-10-20-50-75	N-C-FM-FC-Z
	0	-45.4500	37	27.3660	CP3	600	0-10-20-50-75-100-200-300-500-bottom	N-C
B	0	-45.4500	37	22.3680	CP4	2100	0-10-20-50-75-100-200-300-500-700-1000-bottom	N-C-FC-Z
	2	25.6020	39	28.6020	B1	75	0-25-50-75	N-C-FM-FC-Z
	2	25.6020	39	24.1020	B2	100	0-25-50-75-100	N-C-FM-FC-Z
	2	25.6020	39	20.5020	B3	200	0-25-50-75-100-200	N-C-FM-FC-Z

Transect	Long. (deg.)	Lon.(min.)	Lat. (deg.)	Lat. (min.)	Station	Depth	Sampling depths	Sampling
C	2	24.0000	39	30.0000	1	78		
	2	19.0020	39	27.1980	2	95	0-25-50-75-bottom	N-C
	2	13.9980	39	24.7980	3	117		
	2	9.0000	39	22.0020	4	130	0-25-50-75-100-bottom	N-C
	2	4.0020	39	19.3980	5	479		
	1	58.8000	39	16.6020	6	585	0-25-50-75-100-200-300-500-bottom	N-C
	1	53.5980	39	13.8000	7	638		
	1	48.4980	39	11.2020	8	500	0-25-50-75-100-200-300-500	N-C
	1	43.2000	39	8.2020	9	290		
	1	37.9020	39	5.4000	10	78	0-25-50-75	N-C
	1	10.2000	38	52.2000	11	106	0-25-50	N-C
	1	4.0020	38	52.2000	12	125	0-25-50-75-100-bottom	N-C
	0	58.8000	38	52.2000	13	450		
	0	52.2000	38	52.2000	14	660	0-25-50-75-100-200-300-500-bottom	N-C
	0	45.4020	38	52.2000	15	840		
	0	39.4020	38	52.2000	16	750	0-25-50-75-100-200-300-500-bottom	N-C
	0	33.3000	38	52.2000	17	670		
	0	27.0000	38	52.2000	18	300	0-25-50-75-100-200-300	N-C-FC-Z
	0	20.5980	38	52.2000	19	120	0-25-50-75-100-bottom	N-C
	0	14.5980	38	52.2000	20	95	0-25-50-75-bottom	N-C-FM-FC-Z
	0	8.8020	38	52.2000	21	30	0-25	N-C
	0	16.2000	38	56.7000	22	123		
	0	23.8020	39	1.3980	23	500		
	0	31.5000	39	6.0000	24	1070	1000-bottom	S
	0	39.1020	39	10.6980	25	1260	1000-1100-1200-bottom	S
	0	48.4020	39	7.9980	26	1120	1000-bottom	S
	0	57.4980	39	5.2020	27	817		
	1	6.4980	39	2.4000	28	285		
	1	12.1980	39	0.5400	29	110	0-25-50	N-C
	1	32.8020	39	8.2020	30	89		

Transect	Long. (deg.)	Lon.(min.)	Lat. (deg.)	Lat. (min.)	Station	Depth	Sampling depths	Sampling
	1	36.4980	39	15.0000	31	525		
	1	40.2000	39	21.7980	32	915		
	1	43.9980	39	28.6020	33	1373	1000-1100-1200-bottom	S
	1	53.8020	39	29.5020	34	1231	1000-1100-1200	S
	2	3.4020	39	30.0000	35	557		
	2	13.0020	39	30.7980	36	108		
	2	19.6980	39	31.2000	37	89		
MH	4	21.4980	39	52.0020	Mh1	70	0-25-50-bottom	N-C
	4	25.0020	39	57.0000	Mh2	180	0-25-50-75-100-bottom	N-C-FM-FC-Z
	4	30.0000	40	3.4980	Mh3	1500	0-25-50-75-100-200-300-500-700-1000-bottom	N-C
	4	34.9620	40	10.0020	Mh4	2500	0-25-50-75-100-200-300-500-700-1000-1500-bottom	N-C-FC-Z-S
EPC	3	10.2600	39	0.0000	317	2315	0-25-50-75-100-200-300-500-700-1000-1500-bottom	N-C
T	0	52.2480	40	30.1980	T1	50	0-10-20-50	N-C
	1	3.8820	40	28.7700	T2	75	0-10-20-50-75	N-C-FM-FC-Z
	1	15.8280	40	27.3900	T3	100	0-10-20-50-75-100	N-C
	1	36.0000	40	25.9020	T4	950	0-10-20-50-75-100-200-300-500-700-bottom	N-C-FC-Z
BNA	2	12.6000	41	19.2420	BNA1	75	0-10-20-50-75	N-C
	2	18.1320	41	15.0000	BNA2	295	0-10-20-50-75-100-200-bottom	N-C-FM-FC-Z
	2	24.6480	41	10.0000	BNA3	700	0-10-20-50-75-100-200-300-500-700	N-C
	2	31.1700	41	4.9980	BNA4	1320	0-10-20-50-75-100-200-300-500-700-1000-bottom	N-C-FC-Z
	2	37.6800	41	0.0000	BNA5	1670	0-10-20-50-75-100-200-300-500-700-1000-bottom	N-C

Stations 2		1992	1993	1994	1995	1996	1997	1998	1999	2000	2001	2002	2003
TS													
N													
O													
Cl													
M													
CYT													
Z.A.													
Z.B.													

Stations 2		2004	2005	2006	2007	2008	2009	2010	2011	2012	2013	2014	2015	2016
TS														
N														
O														
Cl														
M														
CYT														
Z.A.														
Z.B.														

Table 2.2 Available data for the stations 2 (continental shelf) for the Cape Pino (P), Málaga (M) and Vélez (V) transects. Each year is divided into four squares corresponding to the four theoretical campaigns: winter, spring, summer and autumn. For each variable the square is shaded if data are available. Gaps in white can be caused by instrument failures, lack of personnel for the sampling or the works at the laboratory or lost of the samples. TS is for temperature and salinity (obtained with CTD probes), N for inorganic nutrients (nitrate, nitrite, phosphate and silicate), O is for oxygen, Cl, chlorophyll-a, M microphytoplanktonic abundance determined by means of inverted optic microscopy, CYT is for nano and pico-phytoplanktonic abundances determined by means of flow cytometry, Z.A. is for meso-zooplanktonic abundance and Z.B. for meso-zooplanktonic biomass (dry weight).

Stations 2 and 4		2004	2005	2006	2007	2008	2009	2010	2011	2012	2013	2014	2015	2016
TS														
N														
O														
CI														
M														
CYT														
Z.A.														
Z.B.														

Stations CP2 and CP4		2003	2004	2005	2006	2007	2008	2009	2010	2011	2012	2013	2014	2015	2016
TS															
N															
O															
CI															
M															
CYT															
Z.A.															
Z.B.															

Table 2.3 Available data at stations 4 for the transects P, M and V, and at stations 2 and 4 for the Cape Sacratif (S) and Cape Gata (CG) transects.

Table 2.4. Available data at stations 2 and 4 for the Cape Palos (CP) transect.

Stations C20 and C18		1996	1997	1998	1999	2000	2001	2002	2003	2004	2005	2006
TS												
N												
O												
Cl												
M												
CYT												
Z.A.												
Z.B.												

Stations C20 and C18		2007	2008	2009	2010	2011	2012	2013	2014	2015	2016
TS											
N											
O											
Cl											
M											
CYT											
Z.A.											
Z.B.											

Table 2.5. Available data for stations C20 and C18 at the southern part of the Ibiza Channel triangle.

	1994	1995	1996	1997	1998	1999	2000	2001	2002	2003	2004
TS	■	■	■	■	■	■	■	■	■	■	■
N											
O											
CI											
M											
CYT											
Z.A.											
Z.B.											

	2005	2006	2007	2008	2009	2010	2011	2012	2013	2014	2015	2016
TS	■		■	■	■	■	■	■	■	■	■	■
N												
O												
CI												
M												
CYT												
Z.A.												
Z.B.												

Table 2.6. Available data for the station 2 at Mallorca (B) transect.

	2007	2008	2009	2010	2011	2012	2013	2014	2015	2016
TS	█									
Z		█								
O										
CI										
M										
CYT										
Z.A.										
Z.B.										

Table 2.7. Available data for the stations 2 and 4 at the Mahon (MH) transect.

	2007	2008	2009	2010	2011	2012	2013	2014	2015	2016
TS										
Z										
O										
CI										
M										
CYT										
Z.A.										
Z.B.										

Table 2.8 Available data for the stations 2 and 4 at Tarragona transect.

Stations BNA2 and BNA4		2007	2008	2009	2010	2011	2012	2013	2014	2015	2016
TS											
Z											
O											
Cl											
M											
CYT											
Z.A.											
Z.B.											

Table 2.9. Available data for stations 2 and 4 at Barcelona transect.

The Environmental State Of The Spanish Mediterranean

The following chapters present the description of the spatial distributions of certain variables that could be used to determine the current state of the marine ecosystems in the Spanish Mediterranean waters. One of the main objectives of these chapters and of the RADMED project, is to establish the mean values corresponding to each variable at each region of the Spanish Mediterranean throughout the seasonal cycle, and to provide variability ranges for such variables. For this purpose, the figures presented and the corresponding discussions will be completed with tables including the statistics that describe the environmental state of the Mediterranean waters. Such tables could be used for consultation and as a reference for future works. The oceanographic information obtained from in situ sampling, has been completed with meteorological information obtained from the Agencia Estatal de Meteorología (AEMET, Meteorological State agency).

The description of the different regions that form the Spanish Mediterranean will be addressed from the south to the north. The first chapter will be focused on the Alboran Sea, then, the waters surrounding Cape Palos (Murcia region) and the Balearic Islands will be analyzed. Finally, chapter 5 will study the waters in the Catalonia region. In this latter case, the RADMED data will be completed with those from l'Estartit Oceanographic Station, in Girona province, operated by the Institut de Ciències del Mar (ICM/CSIC).

3. THE ALBORAN SEA: FROM CAPE PINO TO CAPE GATA.

The first region analyzed is the Alboran Sea, which extends from the eastern limit of the Strait of Gibraltar (line connecting Point Europa, to the north, with Point Almina, to the south) to the line that connects Cape Gata, in the Almeria province, with Cape Figalo, in Algiers. Figure 3.1 shows the stations from the westernmost RADMED stations within the Alboran Sea: Cape Pino transect (P), to the west of Calaburras Point, Malaga transect (M) and Velez transect (V). Figure 3.2 shows the position of the stations from the Cape Sacratif transect (S), and Cape Gata transect (CG).

A schematic of the surface circulation in the Alboran Sea has been included in figure 3.1 (see for instance Viudez et al., 1996; Parrilla and Kinder, 1987; Parrilla, 1984). This scheme shows the inflow of the Atlantic Current through the Strait of Gibraltar (blue line). This current flows in a northeast direction after leaving the Strait. Then, it turns to the southeast describing a large anticyclonic gyre (clockwise) which occupies the western sub-basin of the Alboran Sea. The Atlantic Current impinges on the African coast and once again turns to the northeast at Cape Tres Forcas, and finally describes a new anticyclonic gyre in the eastern sub-basin of the Alboran Sea (blue circles in Fig. 3.1). The Atlantic Water (AW) feeds the Atlantic Current and both anticyclonic gyres described above, and it occupies the upper part of the water column. This water mass has a low degree of modification, that is, its properties are similar to those of the AW in the Gulf of Cadiz. The thickness of the AW layer is variable depending on the dynamics of each area. Surface waters sink and accumulate at the inner part of the anticyclonic gyres and its depth can reach 200 m. Colder and saltier Mediterranean waters flow below the AW. These water masses are the Levantine Intermediate Water (LIW), The Western Intermediate Water (WIW) and the Western Mediterranean Deep Water (WMDW, see Vargas-Yáñez et al., 2017 for a more extensive revision of the water masses in the Western Mediterranean). Over the northern contour of the Atlantic Current, or, to its left, according to the sense of the movement, there is an elevation of the deep water masses. As a consequence of it, a strong thermohaline front is generated and the interface separating Atlantic and Mediterranean waters becomes close to the sea surface.

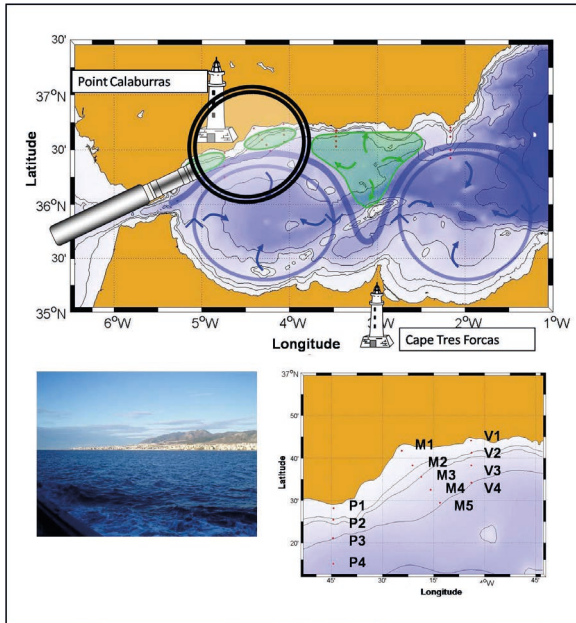


Figure 3.1. Alboran Sea map including the main features of its surface circulation. Picture of the Malaga coast during a RADMED campaign. Detail of the oceanographic stations at the westernmost RADMED transects: Cape Pino, Malaga and Velez.

This frontal system is usually named at the Western Alboran Sea as the Alboran Sea frontal system (Viudez et al., 1996; Tintoré et al., 1991). It is continued at the Eastern Alboran Sea, and its eastern contour receives the name of the Almeria-Oran front (Tintoré et al., 1988). The thickness of the AW layer at these frontal areas is around 75 m depth, or even 50 m (Cano and Gil, 1984; Parrilla, 1984).

Another factor affecting the vertical distribution of Atlantic and Mediterranean waters is the presence of cyclonic circulation areas (anticlockwise). Such areas are frequently found between Point Europa and Calaburras, in front of Malaga Bay, and at the northeastern sector of the Alboran Sea. These areas have been colored in green in figure 3.1 (García-Lafuente et al., 1998; Cano, 1978).

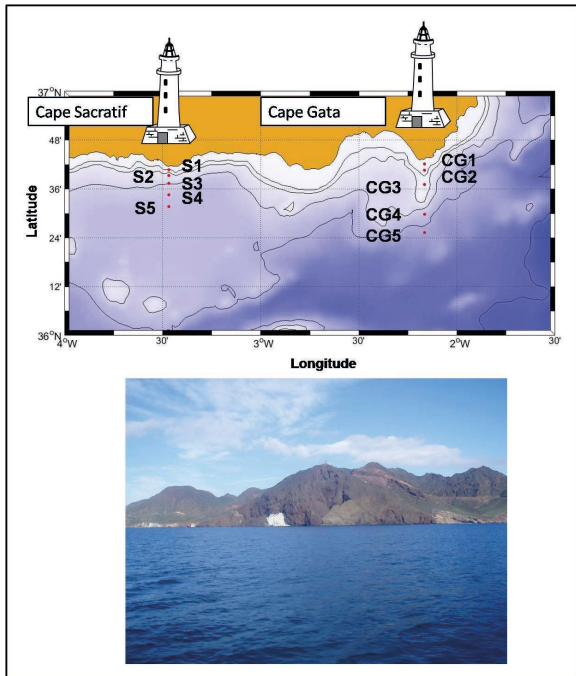


Figure 3.2. Oceanographic stations at Cape Sacratif and Cape Gata transects. Picture of Cape Gata coast during a RADMED cruise.

The inner parts of the cyclonic structures behave contrary to the anticyclonic gyres. There is a divergence of surface waters and the upwelling of sub-surface and deep waters. The interface separating Atlantic and Mediterranean waters becomes close to the sea surface as in the case of the Alboran and Almeria-Oran fronts.

waters which prevents the nutrient supply to the upper well illuminated waters (photic layer). These areas usually show low chlorophyll concentrations, reflecting a low primary production, and the phytoplankton assemblages are dominated by the small-size fraction (picoplankton, < 2 μm Equivalent Spherical Diameter, ESD, Reul et al., 2005; Rodríguez et al., 1998). The low primary production is mainly regenerated and sustains a low zooplanktonic biomass. On the contrary, there is an upwelling of deep

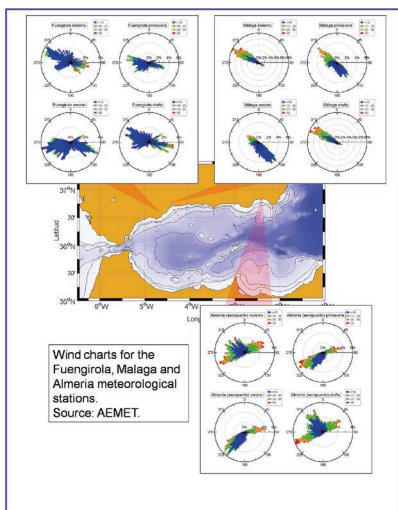
waters at the frontal zones and the inner part of cyclonic gyres producing an important supply of nutrients to the photic layer. These areas have high rates of primary production, a higher importance of the new production, and a larger percentage of large phytoplanktonic cells (microplankton > 20 µm ESD). Diatoms are more abundant and the zooplanktonic biomass is higher.

Finally, the wind influence should be considered. Besides the fertilizing effect of mixing caused by the stormy winter activity, frequent episodes of westerly winds can produce the upwelling of deep waters (Vargas-Yáñez et al., 2010a).

3.1 Meteorological conditions.

Air temperature, and intensity and wind direction on an hourly basis was obtained from the AEMET (State Meteorological Agency) at the Fuengirola, Malaga and Almeria meteorological stations. Wind data were averaged and a daily wind vector was estimated. Then, it was estimated the direction of origin and intensity (km/h) of the wind. Hereafter winter is considered as January to March, spring is April to June, summer is from July to September, and autumn from October to December. For each season it was estimated the relative frequency for the daily wind direction and the corresponding wind intensity. Figure 3.3 shows the seasonal wind charts for Fuengirola, Malaga and Almeria, expressing the wind direction for daily winds as percentages. The color scale indicates the wind intensity in km/h.

In Fuengirola, the westernmost location in our study area, westerly winds are more frequent in winter, spring and autumn. Nevertheless, the strongest storms, with wind intensities higher than 30 km/h (red color) correspond to southeast winds. In spring, winds from the east and from the west (both northwest and southwest) alternate and the wind intensity decreases (mean velocity lower than 10 km/h in most of the cases). Finally, the relative frequency of easterly winds increases in summer. A similar situation is observed in Malaga, where westerly winds dominate in winter and autumn. Spring is a transition period with similar frequencies for westerly and easterly winds, and easterly winds are the most frequent ones in summer. In the case of Malaga, it should be noticed that the wind direction is polarized in the southeast-northwest axis. This is a result of the topography of this area. The strongest winds (> 30 km/h) in Malaga are mainly from the northwest, usually named in this region as “terrales”. Finally, in Almeria, the wind directions are mainly the southwest, northeast and northwest during winter and autumn. In summer and spring the wind is polarized in the southwest-northeast axis. High intensity winds (>30 km/h) occur at all the directions with similar probabilities and are more frequent than in Fuengirola and Malaga. Generally speaking, it can be said that westerly winds are the predominant ones in the Alboran Sea throughout the year, with the only exception of summer when the frequency of easterly winds increases.



For each month of the year the average daily maximum, daily minimum and daily mean air temperatures were obtained. Figure 3.4 shows the air temperature climatological values for Fuengirola, Malaga and Almeria. Such values are quite similar for the three locations. The lowest ones are observed in January, with minimum temperatures ranging from 8.3 °C in Málaga to 11.4 °C in Fuengirola. Maximum temperatures for January are close to 16.3 or 16.5 °C in Almeria and Malaga, and around 16.9 °C in Fuengirola. The highest temperatures correspond to August at the three locations. Minimum daily temperatures are between 22.2 °C in Malaga and 23.6 °C in Almeria, and maximum ones range between 28.6 °C in Fuengirola and 30.4-30.6 °C in Malaga and Almeria.

Figure 3.3. Wind charts for the meteorological stations in Fuengirola, Malaga and Almeria. These charts show the percentages for the direction for the daily winds. The percentage of winds with a intensity lower than 10 km/h is indicated in blue, the percentage of winds with intensities between 10 and 20 km/h is in green, between 20 and 30 km/h in orange, and the percentage of winds with intensities higher than 30 km/h are indicated in red. These charts are presented for the four seasons at each location. The upper left corner is for winter, spring is at the upper right, summer at the lower left, and autumn at the lower right corner.

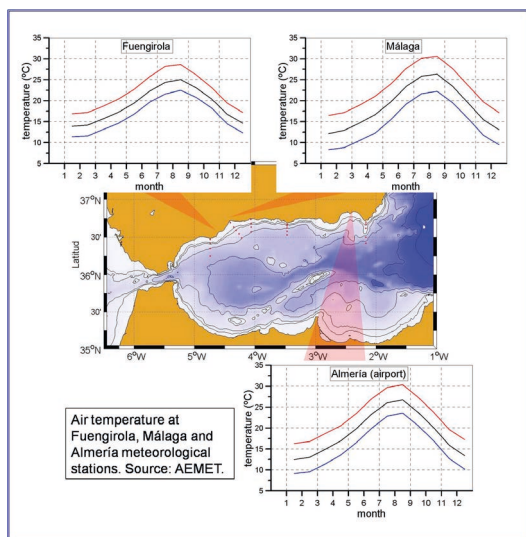


Figure 3.4. Average monthly values for the daily minimum (blue), daily maximum (red) and daily mean air temperatures (black) in Fuengirola, Málaga and Almería meteorological stations.

3.2 Water masses.

The upper layer of the Mediterranean Sea is occupied by the AW that flows into the Mediterranean Sea through the Strait of Gibraltar. Those water masses formed in the Mediterranean Sea flow beneath the AW. Such water masses are mainly the Levantine Intermediate Water (LIW), formed in the Levantine Basin, close to Rhodes Island, the Western Mediterranean Deep Water (WMDW), formed in the Gulf of Lions, and the Tyrrhenian Dense Water (TDW), formed in the Tyrrhenian Sea. A fourth Mediterranean water mass is the Western Intermediate Water (WIW). This water mass has a more elusive and intermittent character than those already mentioned. The properties of the AW are modified because of the effect of evaporation and mixing with resident waters as they progress into the Mediterranean Sea. Figure 3.5 shows a TS diagram (potential temperature-salinity) for the waters in the Gulf of Cadiz.

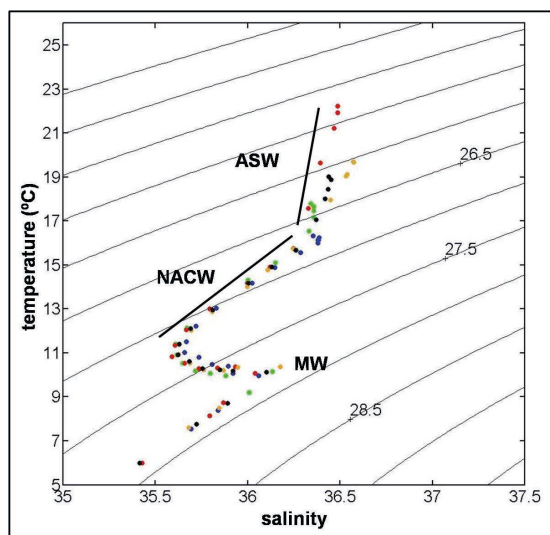


Figure 3.5. TS diagram presenting potential temperature versus salinity for the Gulf of Cadiz. Blue dots correspond to winter climatological values, green dots are for spring, red dots for summer and light brown ones for autumn. Black dots represent annual mean values. ASW: Atlantic Surface Water, NACW: North Atlantic Central Water, MW: Mediterranean Water.

Blue dots correspond to the winter climatological TS diagram, obtained using all the available TS profiles from 1945 to 2000 in MEDAR/MEDATLAS data base (MEDAR Group, 2002). The temperature and salinity decreases from the sea surface to 600 m depth where TS values are close to 11 °C and 35.66 ups. This is a characteristic of North Atlantic Central Waters (NACW). Before continuing, it should be clarified that the salinity measurements presented in this work are expressed in the practical salinity scale. In this scale, salinity should be expressed as a dimensionless number as it is obtained as a quotient of conductivities. Nevertheless, it is frequent to use practical salinity units (psu) and it will be used in the present work.

From 600 m depth, the salinity increases as a result of the influence of the Mediterranean water that outflows through the Strait of Gibraltar. The water that flows into the Mediterranean Sea is limited by the maximum depth at the Camarinal Sill, which is around 300 m. Taking into account the existence of a counter current of Mediterranean water, the maximum depth of the AW inflow is lower. According to Minas et al. (1991) the thickness of this current is between 150 and 200 m at Gibraltar. Therefore, the properties of the surface layer at the westernmost sector of the Mediterranean Sea will be those of the segment marked in figure 3.5 as NACW and ASW (Atlantic Surface Water), or more precisely, a mixing of both of them. From spring (green dots in figure 3.5) and mainly in summer (red dots), the surface waters get warmer and slightly saltier, producing an almost vertical segment in the TS diagram.

Figure 3.6 shows an average TS diagrams for winter (blue), spring (green), summer (red) and autumn (light brown) obtained using all the data from ECOMALAGA and RADMED projects from 1992 to 2015. Let's consider that, if WMDW (black dot in figure 3.6) was beneath the NACW, the temperature and salinity values along the water column would be those of the mixing line connecting the AW values with those of the WMDW. Those dots closer to the NACW have a higher proportion of this water mass, while those ones closer to the WMDW have a higher proportion of Mediterranean water. The 37.5 psu value is approximately at the midpoint between the AW and the WMDW and is usually considered as the salinity corresponding to the interface separating the Atlantic waters flowing to the east, and Mediterranean waters flowing to the west. Those dots above the mixing line at the Mediterranean side of the diagram correspond to the presence of the LIW. Those points below the mixing line, with temperature values lower than 13 °C, indicate the presence of the WIW. This latter water mass is a very cold water formed in winter over the continental shelf of the Gulf of Lions or the Balearic Sea. As these waters are over the continental shelf, they are not affected by LIW, which flows at greater depths over the continental slope. The influence of continental waters is also another factor contributing to the low salinity of these waters. The final result is a water mass colder and fresher than the LIW which is located below the AW and over the LIW.

If the AW values within the Alboran Sea are displaced to the right, it indicates a higher degree of modification caused by mixing with Mediterranean waters.

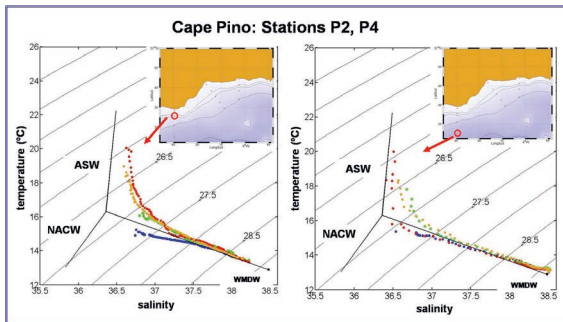


Figure 3.6. Average TS diagrams for winter (blue), spring (green), summer (red) and autumn (light brown) obtained from all the available potential temperature and salinity profiles from RADMED project in stations P2 and P4 from Cape Pino transect.

Figure 3.6 shows clearly the influence of the Atlantic waters at station P4. This oceanographic station is close to the position of the Atlantic Current which surrounds the Western Alboran Anticyclonic Gyre (see fig. 3.1). The stronger influence of Mediterranean waters towards the coast can be observed at station P2. This is the result of the elevation of Mediterranean waters to the left of the

Atlantic Current (according to the sense of the flow), and the formation of the Alboran Sea Front.

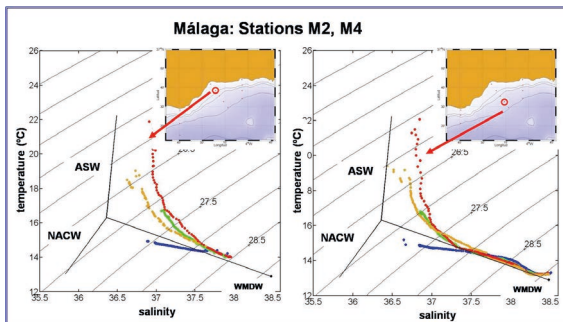


Figure 3.7. The same as in figure 3.6, but for the Málaga transect.

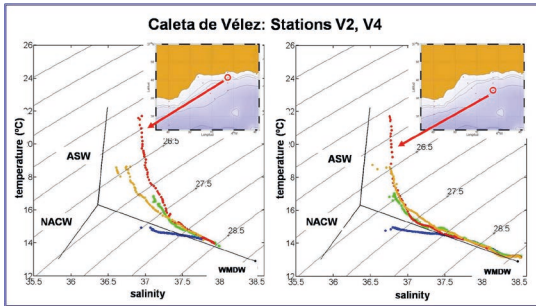


Figure 3.8. The same as in figure 3.6, but for the Velez transect.

Figures 3.7 and 3.8 show the average TS diagrams obtained from the ECOMALAGA and RADMED complete time series at stations M2 and M4 in the Malaga transect (Figure 3.7) and at stations V2 and V4 in Velez transect (Figure 3.8). An increase of the Mediterranean influence is observed at the surface waters in both cases, being such influence higher towards the east (transect V, figure 3.8). The difference between these transects and the Cape Pino one, despite

of the short distance between these transects, is explained by the dynamics of this area of the Alboran Sea. Transect P is exposed to the direct influence of the Atlantic Current, being this influence stronger towards the open sea (P4). Transects M and V are within a cyclonic circulation area that produces the upwelling of Mediterranean waters to the sea surface.

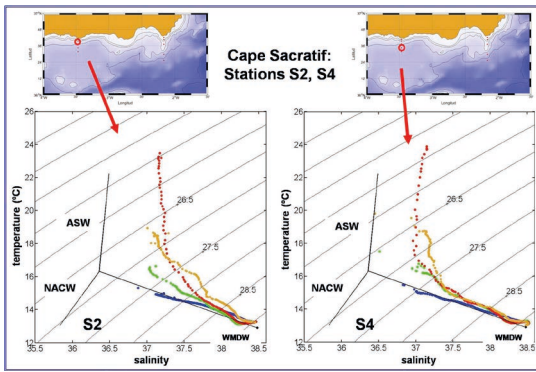


Figure 3.9. The same as in figure 3.6, but for the Cape Sacratif transect.

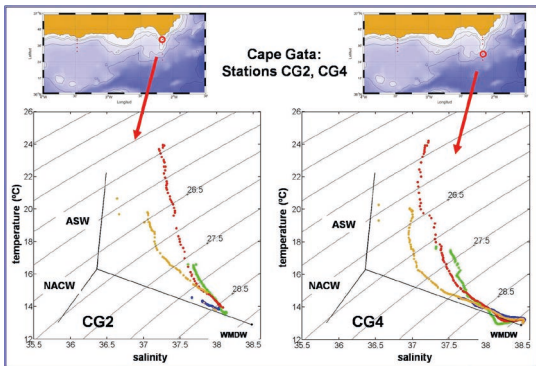


Figure 3.10. The same as in figure 3.6, but for Cape Gata transect.

Figures 3.9 and 3.10 show the eastward increase of the Mediterranean water influence. This influence is even higher at the continental shelf stations S2 and CG2 than at the continental slope ones: S4 and CG4. The Mediterranean character of the inshore stations could be explained, once again, by the position of the Atlantic Current and the associated frontal system, and the frequent cyclonic circulation areas that usually occupy this part of the Alboran Sea (see figure 3.1). On the other hand, the previous section showed that westerly winds prevail during most of the year.

These winds and the west-east orientation of the coast would favor the upwelling processes by Ekman transport. This phenomenon would have a stronger intensity at the coastal zone.

Another feature observed in all the TS diagrams, is the existence of a salinity seasonal cycle, with maximum salinity values in spring that decrease in summer, reaching minimum values in autumn. Two explanations can be invoked to explain the summer and autumn salinity decrease. First, as already commented, summer is the only season when easterly winds prevail. Easterly winds would accumulate surface Atlantic waters against the coast. Nevertheless, westerly winds are recovered during autumn, in contradiction with the salinity minimum during this season. The salinity decrease in summer could

be caused by the influence of easterly winds, and the low salinity values during autumn, despite of the westerly wind recovery, could be caused by certain inertia in the dynamics of the Alboran Sea. High surface salinity values would not be observed until winter, after the prevalence of westerly winds during the whole autumn season. Another explanation is that the salinity seasonal cycle could be linked to the variability of the Alboran Sea circulation. The circulation scheme depicted in figure 3.1 is the one most frequently described in the literature, but it is far from being a permanent feature. On the contrary, many works have shown that the anticyclonic gyres that occupy both sub-basins of the Alboran Sea, to the west and east of Cape Tres Forcas, can increase their size, reaching the Spanish coasts, or shrink, being constrained to the southern sector of the Alboran Sea, leaving the northern coasts filled with Mediterranean waters. These two gyres could even disappear, being substituted by an Atlantic Current flowing close to the Moroccan coast (Renault et al., 2012; Vargas-Yáñez et al., 2002). The low salinity values at the Spanish coast during autumn, (higher Atlantic influence), could indicate a maximum development of the Alboran Sea anticyclonic gyres.

The figures shown above and the corresponding explanations have not been derived from a single oceanographic survey or from a limited set of them covering just one seasonal cycle, but from time series that in some cases extend along more than 20 years. Therefore, the results obtained could be considered as representative of the average or most frequent behavior in this region of the Mediterranean Sea. Furthermore, one of the main objectives of the present work is to provide statistical values that could be used for consultation for future works, model initialization or simply to check possible alterations in the Mediterranean Sea. With this purpose, tables 3.1 to 3.4 are presented at the end of this chapter. These tables include mean values, standard deviations and the number of data used to estimate such statistics along the seasonal cycle. This information is presented for the potential temperature and salinity along the water column at stations P2 and P4 (tables 3.1 and 3.2), and for the stations CG2 and CG4, in Cape Gata transect (tables 3.3 and 3.4). These two oceanographic stations represent the west-east gradient existent in the Alboran Sea. The inclusion of both stations 2 and 4 also account for the inshore-offshore gradients. In the case of Cape Gata transect, statistics have been calculated using only RADMED data, from 2007, while in the case of transects P, M and V, data from ECOMALAGA (from 1992) are available. Finally, it is important to note that similar statistics and tables have been obtained for all the transects and stations in RADMED project. However, only some selected stations are presented in this work for the sake of brevity. The complete information will be presented somewhere else.

3.3 Dissolved oxygen, nutrient and chlorophyll-a distributions.

Figures 3.11 and 3.12 show the average vertical profiles in winter (A), spring (B), summer (C) and autumn (D) for the concentrations of nitrate (light brown line), nitrite (dark brown line), dissolved oxygen (blue line) and chlorophyll-a (green line) at the oceanographic stations P2 and P4 (Cape Pino transect). Station 2 is representative of the conditions over the continental shelf, whereas station 4 is over the continental slope. Figures 3.13 and 3.14 show the same results, but for the CG2 and CG4 stations, in Cape Gata transect, the easternmost section of the Alboran Sea. Dots within the profiles correspond to the average values obtained at discrete depths from the RADMED sampling (table 2.1). These values are estimated from time series that in some cases extend from 1992 to 2016. To facilitate the visualization of the profiles and the way the concentrations change with depth, continuous lines obtained by means of Statistical Optimal Interpolation (Vargas-Yáñez et al., 2005; Gomis et al., 2001) have been included.

Besides these figures, tables 3.5 and 3.6 show the statistics for the mean values, standard deviations and number of data used, for the stations 2 and 4 in Cape Pino transect (P). Table 3.7 shows the average Secchi disk depth for the P, M and V transects. Tables 3.8 and 3.9 present the same information, but for the easternmost transect in the Alboran Sea: Cape Gata. Table 3.10 shows the Secchi disk depths for the Cape Sacratif (S) and Cape Gata (CG) transects. Once again we repeat that the goal of presenting all this information, maybe too extensive and a little bit tedious, is to offer the reader a reference material for consultation in future Works.

Figure 3.11 shows that at P2 station, in winter and spring, the highest chlorophyll-a concentrations are observed at the sea surface and at 10 m depth respectively, coinciding with the highest oxygen concentrations at the sea surface (> 5.5 ml/l), and with nitrate and nitrite concentrations higher than 1 μM and 0.2 μM respectively. This chlorophyll maximum deepens to 20 m in summer when nitrate and nitrite concentrations are almost depleted at the sea surface. Nevertheless, nutrient concentrations increase rapidly with depth and, at 20 m depth, yet in the photic layer, reach values close to those found at the sea surface during winter and spring. In autumn, the maximum chlorophyll concentration is observed at the sea surface. It is important to note that the concentration at the chlorophyll maximum is always over 1 mg/m^3 . Surface chlorophyll concentrations are also over this value throughout the whole year, with the only exception of summer when they are slightly over 0.5 mg/m^3 .

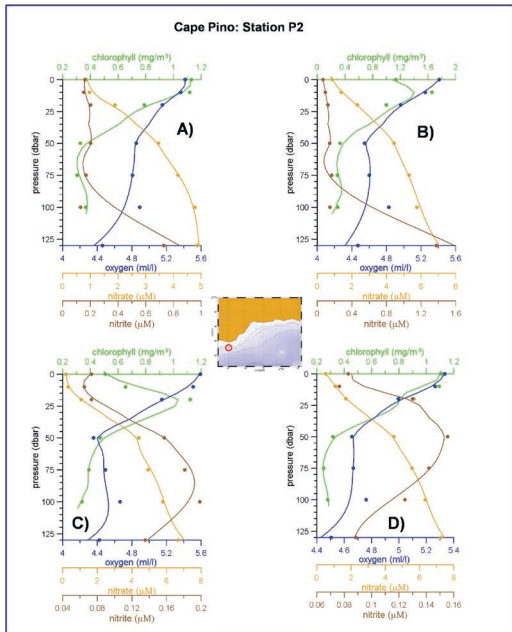


Figure 3.11. Average vertical profiles for the station P2 obtained using all the available profiles from RADMED Project. Green line corresponds to chlorophyll-a, blue line to dissolved oxygen, light brown line to nitrate and dark brown line to nitrite. Figure 3.11A corresponds to winter, B to spring, C to summer and D to autumn.

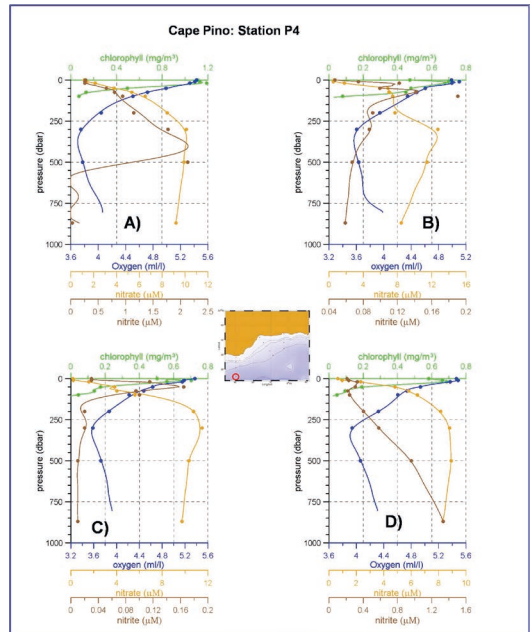


Figure 3.12. The same as in figure 3.11, but for station P4.

Surface phosphate concentrations are maxima in winter (0.16 μM), decreasing to 0.06 and 0.07 μM in spring and summer (table 3.5). However, its concentration increases to 0.12 and 0.13 μM at 20 m depth during spring and autumn. During summer, concentrations over 0.1 μM are not reached until 50 m depth. Surface silicate concentrations are high in winter and minimum in summer, similarly to what was observed for nitrate and phosphate. Nevertheless, at 20 m of depth, silicate concentrations are over 1 μM throughout the whole year. The dissolved oxygen at this shelf station decreases continuously with depth up to the sea bottom (130 m), whereas nitrate, phosphate and silicate increase towards the bottom where the concentrations range, depending on the season, between 5.16 and 6.71 μM (nitrate), 0.24 and 0.32 μM (phosphate) and 1.89 and 3.82 μM (silicate). Notice that both in summer and autumn (Fig. 3.11C, D) there is a relative nitrite maximum between 50 and 100 m depth. This maximum coincides with an oxygen relative minimum (oxygen increases again below this minimum up to the bottom). The nitrite maximum is usually referred to as Primary Nitrite Maximum (PNM) and is associated to an incomplete nitrate reduction by the phytoplankton (Lomas and Lipschultz, 2006). Nevertheless, Rodríguez (1982) already observed it in the Malaga waters and considered that it could be caused by the remineralization of organic matter. This latter hypothesis could be supported by the oxygen decrease at the nitrite maximum.

Station P4, over the continental slope, with a depth of 870 m, is close to the most frequent position of the Atlantic Jet that flows into the Alboran Sea through the Strait of Gibraltar. Chlorophyll-a, nutrient and dissolved oxygen distributions are similar to those described for station P2, but some differences can be observed (Fig. 3.12 and table 3.6). The surface chlorophyll concentrations are close to or higher than 0.5 mg/m^3 throughout the whole year. The highest value is observed in winter (1.1 mg/m^3). Considering the water column, the highest values are reached at 20 m depth in winter and autumn and at 10 m in spring and summer. Comparing the maximum values found along the water column for the different seasons, the highest one corresponds to winter (1.2 mg/m^3). These chlorophyll maximums are not so intense for the rest of the year (0.7 mg/m^3 for spring, summer and autumn). The dissolved oxygen maximum is observed at the upper part of the water column, slightly shallower than the chlorophyll one, (0 to 10 m), and its concentration ranges from 5.1 to 5.5 ml/l.

Station P4 is deeper than station P2. Therefore, some properties of the nutrient vertical distributions can be observed more clearly. During winter, spring and summer, nitrate concentrations increase with depth up to 300 m, reaching values over $10 \text{ }\mu\text{M}$. In autumn, the nitrate maximum is at 500 m, with a value of $8.9 \text{ }\mu\text{M}$. Then, the concentration slightly decreases below this maximum up to the sea bottom where it ranges between 8.3 and $9.7 \text{ }\mu\text{M}$. This behavior is similar to that of phosphate concentrations that reach maximum values between 0.35 and $0.48 \text{ }\mu\text{M}$ from 300 to 500 m. Silicate concentrations do not show this maximum and simply increase continuously from the sea surface to the bottom where it is between 7.1 and $9.9 \text{ }\mu\text{M}$. The nitrate and phosphate maxima coincide with the minimum oxygen concentration (3.61 - 3.94 ml/l), at 500 m depth. These nutrient maxima and oxygen minima are associated to the core of the LIW, characterized by an absolute salinity maximum of 38.5 psu, between 400 and 500 m depth. The lack of a silicate maximum has been explained by a lower remineralization rate.

Once again, nitrite concentrations show a maximum between 20 and 75 m with values ranging between $0.16 \text{ }\mu\text{M}$ and $0.33 \text{ }\mu\text{M}$ during spring, summer and autumn. The winter nitrite maximum is somehow different being located at the same depth as the nitrate and phosphate one. During autumn, nitrite concentrations increase beneath the maximum located at 20 m depth. This PNM coincides with a change in the slope of the vertical distribution of dissolved oxygen.

The statistics for the westernmost Alboran Sea stations (P2 and P4), can be consulted in tables 3.5 and 3.6 (at the end of the chapter). The nutrient, oxygen and chlorophyll vertical profiles for the M and V transects, close to Cape Pino one, are similar to those already described and are not presented for brevity. In summary, chlorophyll concentrations at the upper part of the water column are high throughout the whole year at the western sector of the Alboran Sea. Furthermore, the highest value is observed at the sea surface during some seasons, whereas during other seasons it is located at 10 or 20 m depth. The maximum of dissolved oxygen is also at shallow depths. It is usually at the same depth of the chlorophyll maximum or above it. This suggests that it is associated to the photosynthetic activity and a high primary production. This high productivity masks the oxygen decrease that should be observed in summer because of the lower solubility of gases at warm waters. Many works devoted to the analysis of chlorophyll concentrations along the water column in the Mediterranean Sea have described the chlorophyll bloom at surface waters during winter or early spring. This bloom is a consequence of the mixing of the upper water column and the nutrient supply to the photic layer during winter storms. As nutrients are consumed at the surface layer by phytoplankton uptake, a Deep Chlorophyll Maximum (DCM) is developed. Its depth and intensity increase and decrease respectively as spring and summer progresses and the nutrients become depleted. Similarly, the DCM deepens and weakens towards the east and south where the oligotrophy of the Mediterranean Sea is more pronounced (Lavigne et al., 2015; Bethoux et al., 1998; Estrada, 1996). The figures corresponding to Cape Pino transect (Fig. 3.11 and 3.12), and tables 3.5 and 3.6, show that the chlorophyll maximum in this sector of the Alboran Sea cannot be considered a DCM, as this maxima are frequently at the sea surface or at depths between 10 and 20 m. This difference with regard to other Mediterranean regions could be explained by the high nutrient concentrations at the surface layer throughout the whole year. The highest nitrate and phosphate concentrations are observed at the sea surface in winter, as a consequence of mixing and winter stormy activity. Then, such concentrations decrease reaching a minimum value in summer. Nevertheless, nitrate and phosphate concentrations as high as $1 \text{ }\mu\text{M}$ and 0.1

μM respectively can be found at 20 m depth.

The high chlorophyll and nutrient concentrations observed in the western sector of the Alboran Sea, relax towards the east (Cape Gata transect, Fig. 3.13 and 3.14). At station CG2, the surface chlorophyll concentrations reach the maximum value in winter, but such value is only 0.59 mg/m^3 . Also during winter, the highest concentration along the water column is found at 10 m depth (0.63 mg/m^3). From spring and along the summer, the chlorophyll surface concentrations decrease, being about 0.1 mg/m^3 , and a DCM is developed at depths close to 50 m. Chlorophyll concentrations at the DCM are between 0.3 and 0.5 mg/m^3 . The DCM becomes shallower in autumn (20 m of depth) and its concentration increases to 0.76 mg/m^3 . Surface chlorophyll concentration increases during autumn, (0.3 mg/m^3). The chlorophyll concentration at the DCM during autumn is the highest value recorded along the seasonal cycle at the oceanographic station CG2. Such an autumn increase has frequently been described in the Mediterranean Sea and at other temperate regions, and is caused by the beginning of the stormy season. Dissolved oxygen concentrations reach maximum values above the position of the DCM. In this case, a clear seasonal cycle is observed for the surface concentrations. Surface oxygen values are maxima in winter, (5.68 ml/l), when cold waters favor the solubility of gases, and minimum in summer (4.61 ml/l). The summer decrease for the surface oxygen concentration is caused by the low solubility of gases in warm waters. This thermal effect is not compensated by a high primary productivity, as in the Cape Pino transect. On the contrary, chlorophyll and nutrient concentrations decrease during summer, suggesting a decrease of the primary production.

At station CG2, the highest surface nitrate concentrations are observed in autumn ($0.85 \mu\text{M}$), whereas they are very low for the rest of the year (between 0.08 and $0.12 \mu\text{M}$). Surface phosphate concentrations reach a maximum value in spring ($0.1 \mu\text{M}$), being very low for the other seasons (0.01 - $0.03 \mu\text{M}$). The vertical distribution of nitrite does not follow a clear pattern, and the PNM is not clearly identified. It should be noted that, because of the problems in the maintenance of the monitoring program, the mean values estimated for some of the seasons are based only on 2 or 4 data points. If time series have strong time variability (as expected for continental shelf areas), the estimated mean values could not be fully representative of the true mean conditions.

Despite the scarcity of available data, the oceanographic station over the continental slope (CG4) presents smoother vertical profiles (Fig. 3.14 and table 3.9). The highest surface chlorophyll concentrations are obtained in winter (0.4 mg/m^3), being very low in spring and summer (0.1 and 0.08 mg/m^3 respectively). Surface chlorophyll values increase again in autumn (0.24 mg/m^3). Such low values are coincident with the depletion of nitrate and phosphate at the sea surface during most of the year. Nitrate ranges between 0.08 and $0.13 \mu\text{M}$ (maximum value in autumn). Phosphate ranges between 0.03 and $0.09 \mu\text{M}$. The DCM is clearly observed throughout the year at 50 m depth and with a concentration that changes between 0.45 and 0.51 mg/m^3 . The dissolved oxygen concentration reaches a maximum value above the DCM and there is a clear seasonal cycle at the sea surface associated to the temperature cycle. As in the case of Cape Pino transect (and for most of the Mediterranean Sea), there are nitrate and phosphate maxima between 300 and 500 m, coinciding with a minimum of dissolved oxygen and with the core of the LIW. Nitrate concentrations change between 7.65 and $10.39 \mu\text{M}$ and phosphate concentrations range between 0.47 and $0.55 \mu\text{M}$ at the position of the nutrient maximum. The values of the dissolved oxygen minimum are between 3.72 and 4.3 ml/l . The PNM is at 75 m depth during the whole year.

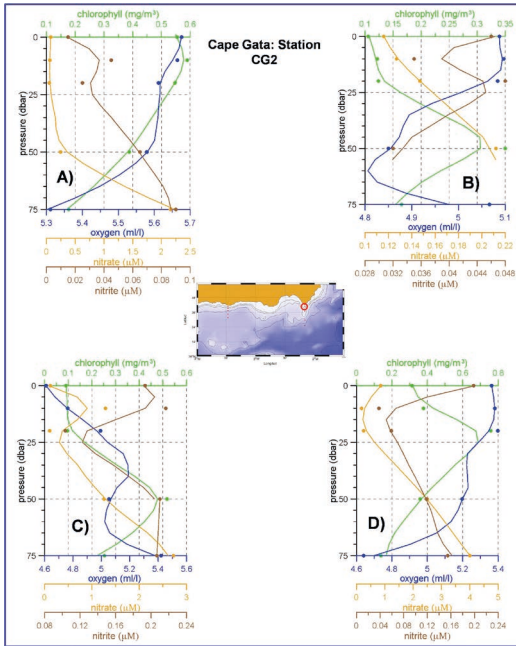


Figure 3.13. The same as in figure 3.11, but for station CG2.

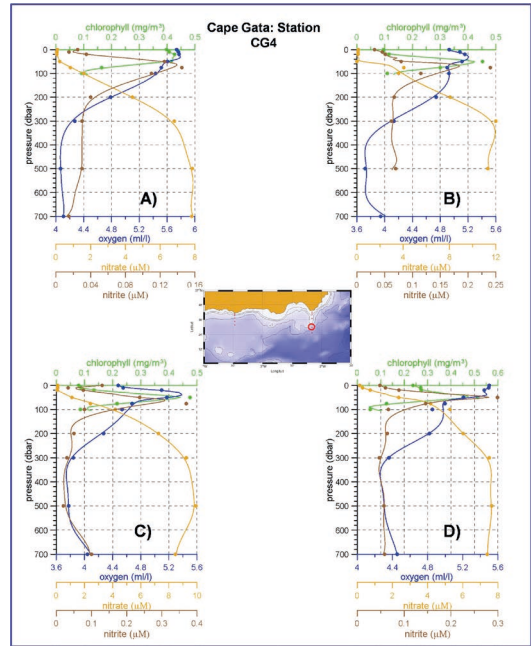


Figure 3.14. The same as in figure 3.11, but for station CG4.

In order to have a more clear idea about the productivity of the whole water column at the different regions of the Alboran Sea, chlorophyll, nutrient and oxygen concentrations were vertically integrated. To facilitate comparison, both continental shelf and slope stations were integrated up to 100 m or to the maximum depth in the case of shallower stations. Integrated chlorophyll concentrations are expressed in mg/m^2 , integrated nutrient concentrations in mmol/m^2 , and the oxygen ones in l/m^2 .

Besides the integrated concentrations, the mixed layer depth (MLD) was estimated by means of the threshold method (De Boyer Montégut et al., 2004). This depth is estimated as that where the temperature difference respect of a reference value, (temperature at 10 m depth) exceeds $0.3\text{ }^\circ\text{C}$. MLD is an important variable as it offers information about the intensity of the processes that supply nutrients to the photic layer, causing the latter phytoplanktonic bloom. The nutricline depth is closely related to the MLD. It has been considered as the depth where nitrogen (nitrate plus nitrite) overcomes the value $1\text{ }\mu\text{M}$ (Macías et al., 2008).

Dashed black line in figures 3.15A and B show the position of the MLD at Cape Pino stations (P2 and P4). The thickness of this layer is maximum (maximum depth) in winter, with a value of 60 m at station P2 and 80 m at P4. The shallowest position of the MLD occurs in summer, being at 10 m depth in both stations. The seasonal cycle of the nutricline was estimated from the vertical profiles presented in figures 3.11 and 3.12 (not shown for the clarity of the plots). This cycle shows an inverse pattern to that of the MLD. Its depth reaches a minimum value in winter (between 5 and 12 m) and a maximum value in summer (28 m at station P2 and 22 m at P4). Anyway, these values are low and indicate that the nutricline is always located at shallow waters.

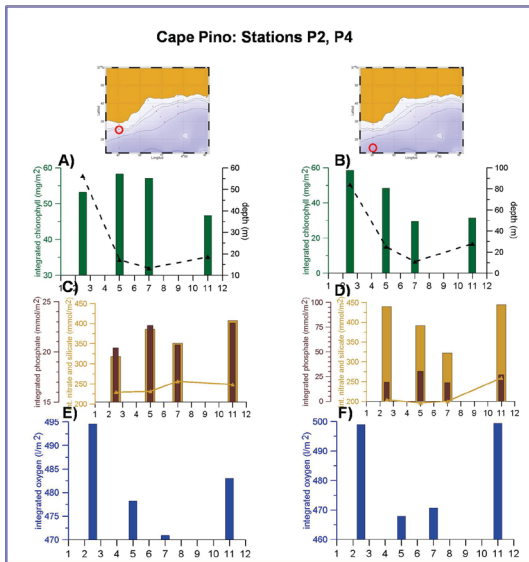


Figure 3.15. Figures 3.15A and B. Integrated chlorophyll-a concentrations for the upper 100 m of the water column expressed in mg/m² (green bars) and mixed layer depth (black dashed line). Figure A corresponds to station P2, and figure B to station P4. Figures C (station P2) and D (station P4) are the integrated nitrate plus nitrite concentrations for the upper 100 m of the water column, expressed in mmol/m² (light brown bars). Dark brown bars show the integrated phosphate concentrations, also in mmol/m². Light brown lines are the integrated silicate concentrations in mmol/m². Figures E (station P2) and F (station P4) show the integrated dissolved oxygen concentrations for the upper 100 m of the water column, expressed in l/m².

The maximum values of integrated chlorophyll are observed in spring at station P2 and in winter at station P4. These values are close to 60 mg/m². As already commented, there is usually a chlorophyll maximum along the water column. This maximum is shallower in winter and spring, when there is a higher nutrient supply to the photic layer, and deeper during the stratified seasons. The chlorophyll concentration at the depth of such a maximum is always above 1 mg/m³ at station P2 and over 0.7 mg/m³ at station P4 (tables 3.5 and 3.6). The depth of this maximum, ranges in both oceanographic stations between 0 and 20 m. This result is consistent with the

shallow position of the nutricline, even during the stratified period of the year. According to these results, the chlorophyll maximum in the western sector of the Alboran Sea, cannot be considered as a DCM, but a sub-surface maximum.

The preceding information, mainly the shallow depth of the nutricline, the high chlorophyll concentrations and the position of the chlorophyll maximum, close to the sea surface, suggests an important nutrient supply to the photic layer throughout the year. Another factor supporting this hypothesis is the absence of a clear seasonal cycle at station P2 for the integrated concentrations of nitrogen (nitrate plus nitrite, light Brown bars in figures 3.15C and D), phosphate (dark brown bars) and silicate (continuous light brown line). On the contrary, at station P4, integrated nitrogen changes during the year following the evolution of the mixed layer depth and the nutricline, showing maximum values in winter (< 450 mmol/m²) and decreasing in summer (> 300 mmol/m²), and increasing again in autumn. Integrated concentrations of phosphate and silicate do not show a clear seasonality, with values that range between 20 and 25 mmol/m² in the case of phosphate, and between 200 and 250 mmol/m², for the case of silicate.

Finally, figures 3.15E and F show the integrated concentration of dissolved oxygen (blue bars). It should be noticed that there is not a seasonal cycle for the surface oxygen concentrations (as should be expected because of the changes in the gas solubility), but there is a seasonal cycle for the integrated concentrations. This latter seasonality is very likely linked to the cycle of primary production depicted from the integrated chlorophyll evolution. Nevertheless, the abrupt decrease of the integrated oxygen concentration in spring is not consistent with the high chlorophyll values during this season. The explanation could be linked to oxidation processes for the high rates of primary production in this region of the Alboran Sea, or the advection of waters from the nearby Strait of Gibraltar. These oxidation processes would produce the formation of an oxygen extra-minimum (Minas et al., 1991). Advection and mixing processes cannot be resolved with the available information.

Figure 3.16 shows the integrated concentrations of chlorophyll, nitrogen, phosphate and oxygen, and the mixed layer depth for the stations CG2 and CG4. The integrated chlorophyll reaches maximum values in winter, decreasing during spring and summer and increasing again in autumn. This pattern is reflected in the evolution of the integrated concentrations of dissolved oxygen. Surprisingly, chlorophyll and oxygen concentrations are lower in spring than in summer at CG2.

The mixed layer depth shows the expected behavior, with maximum values in winter, caused by the

stormy activity, a decrease in spring, and minimum values (maximum stratification) in summer. During autumn, as the storms become more frequent, the mixed layer depth starts increasing again. Although this behavior seems similar to that described for the Western Alboran Sea, it should be noticed that the integrated chlorophyll concentrations are lower. The winter maximum is lower than 40 mg/m² at station CG2, and is only slightly over 30 mg/m² at station CG4. The lowest values reached during spring at CG2 are close to 15 mg/m². At CG4 the lowest values are observed during summer and are close to 20 mg/m². On the contrary, the highest concentrations at Cape Pino transect were about 60 mg/m², and the lowest ones were 35 mg/m² at station P4. If integrated nutrient concentrations are compared in figures 3.15 and 3.16, values corresponding to Cape Gata transect are also lower than those observed at Cape Pino. The decrease of nutrient and chlorophyll concentrations indicates an increase of the oligotrophy of the Alboran Sea towards the east. One of the consequences of this west-east gradient is the existence of a DCM at Cape Gata. This DCM is developed during spring and summer at station CG2 and is located at 50 m depth. It is also observed at the same depth (50 m) during the whole year at station CG4. This depth is similar to that found at other areas of the Mediterranean Sea such as the Balearic Sea (Arin et al., 2005; Estrada, 1996). Contrary to what was observed at cape Pino, the low productivity of the waters cannot mask the seasonal cycle of the dissolved oxygen concentration at the sea surface. This cycle is caused by changes in the solubility of gases with temperature. Dissolved oxygen concentrations reach maximum values at the sea surface in winter (5.68 and 5.74 ml/l) at CG2 and CG4 respectively) and minimum ones in summer (4.61 and 4.48 ml/l).

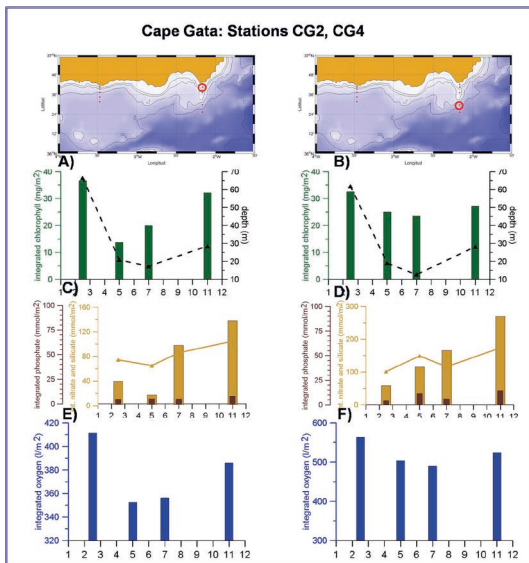


Figure 3.16. The same as in figure 3.15, but for stations CG2 and CG4 in Cape Gata transect.

3.4 Phytoplankton distribution.

3.4.1 Micro-phytoplankton.

As already explained in chapter 2, the largest size fraction (micro-phytoplankton, > 20 µm Equivalent Spherical Diameter, ESD), is sampled along the upper 100 m of the water column at the continental shelf stations. Three broad groups, with distinctive trophic characteristics: diatoms, dinoflagellates and small flagellates, (Latasa et al., 2016, 2010) are analyzed. Coccolithophores are not studied as they need different conservation techniques and this would considerably increase the number of samples, already very high in the case of micro-phytoplankton sampling.

Station P2, at the westernmost sector of the Alboran Sea, and station CG2, at its eastern limit,

will once again be used for the description of the vertical distribution of micro-phytoplankton. The corresponding statistics are presented in tables 3.11 and 3.12.

Figures 3.17 and 3.18 show the average distributions for the micro, nano and pico-phytoplankton. Here we describe these figures, including the plots corresponding to the smallest size fraction (nano and pico-plankton). However, this size fraction will be addressed in the following section.

Figure 3.17A, shows the winter average profiles for the abundances of the following micro-phytoplanktonic groups: diatoms (green line), dinoflagellates (red line) and small flagellates (light Brown line). Figure 3.17B shows the average vertical profiles for the abundances of nanoeukaryote cells (2-20 µm ESD, black line), picoeukaryote cells (0.2-2 µm ESD, grey line), and pico-prokaryote cells from the genera Prochlorococcus (blue) and Synechococcus (red). The analysis of nano and pico-plankton cells is done by means of flow cytometry (see chapter 2), therefore the time needed to complete the analysis is minor than the one required for the micro-phytoplankton analysis. This fact, allows us to

sample a station at the continental shelf, and another one at the continental slope (stations 2 and 4 respectively within each transect). Continuous lines in figure 3.17B, correspond to station P2, over the shelf, whereas dashed lines correspond to station P4, over the slope. Figures 3.17C and D show the average vertical profiles for the micro-phytoplankton abundances (3.17C) and for the pico and nanoplankton abundances (3.17D) for the spring season. Figures 3.17E, F correspond to summer and figures 3.17G, H to autumn. The upper axis in figures B, D, F and H corresponds to *Prochlorococcus* and *Synechococcus*, while the lower axis is for pico and nano eukaryotes.

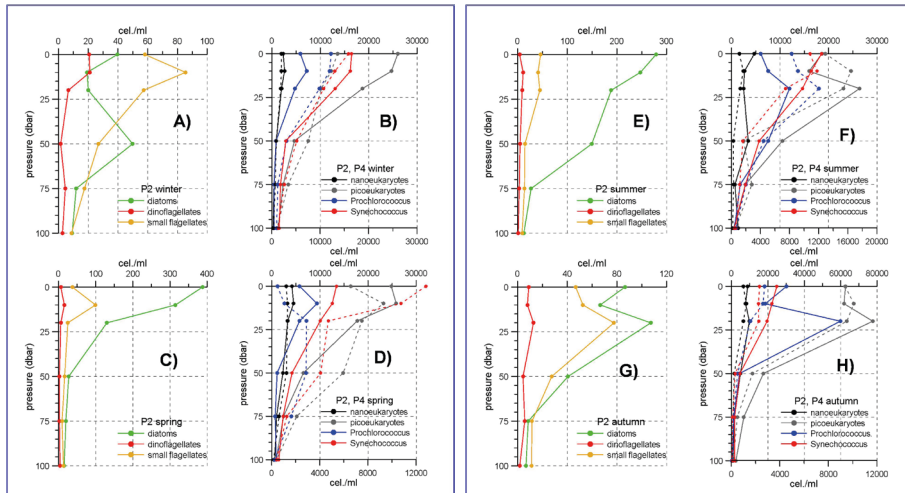


Figure 3.17. Figure 3.17A shows the winter average profiles for the abundances of diatoms (green), dinoflagellates (red) and small flagellates (light brown) obtained using all the available profiles from RADMED Project at station P2. Figure 3.17B shows the winter average profiles for the abundance of nanoplankton cells (continuous black line), picoplanktonic eukaryote cells (continuous grey line), and bacteria from the genera *Prochlorococcus* (continuous blue line) and *Synechococcus* (continuous red line) at station P2. Dashed lines correspond to station P4. All the abundances are expressed in cells per milliliter (cel./ml). Figures C, D are the same, but for spring, figures E, F correspond to summer and figures G, H to autumn. The upper axis in figures B, D, F and H corresponds to *Prochlorococcus* and *Synechococcus*, and the lower axis to pico and nano eukaryotes.

At station P2, diatoms are the most abundant group in spring, summer and autumn within the micro-phytoplankton group. Small flagellates are more abundant than diatoms just in winter at the upper 30 m. Diatom abundances are again the highest ones at 50 m depth. During winter, the abundance of both groups are below 100 cel./ml. The abundance of diatoms shows a bloom in spring with values at the sea surface and at 10 m depth close to 400 cel./ml. Then, the abundance decreases with depth. The abundance of small flagellates also shows a slight increase in spring at 10 m depth. According to the most frequently described behavior in the Mediterranean Sea, summer time is characterized by a strong thermal stratification, oligotrophic conditions, low phytoplanktonic abundances, the development of a DCM and the dominance of the smallest size fraction of the phytoplankton community. Nevertheless, station P2 shows important diatom abundances at the sea surface (250 cel./ml) during summer. Finally, during autumn, the highest abundances occur at 20 m depth. As in the case of the chlorophyll concentrations, this cannot be considered a deep maximum, but a sub-surface one (see section 3.3). The autumn diatom maximum is around 100 cel./ml. Small flagellates also show a maximum at 20 m depth, although their abundance is slightly lower than the diatom one (Fig. 3.17G). Dinoflagellates have low abundances throughout the whole year and along the whole water column. The highest average values reach 21 cel./ml at the sea surface during winter, and the lowest ones are around 1 cel./ml at 100 m depth in autumn (table 3.11). It should be noticed, that this range, between 1 and 21 cel./ml, is referred to the vertical distributions averaged for each season of the year. Table 3.11 shows mean values, standard deviations and ranges of variability. In this case the ranges of variability are made of the lowest and highest values recorded for the complete time series, instead of the range of variability for the seasonal mean values.

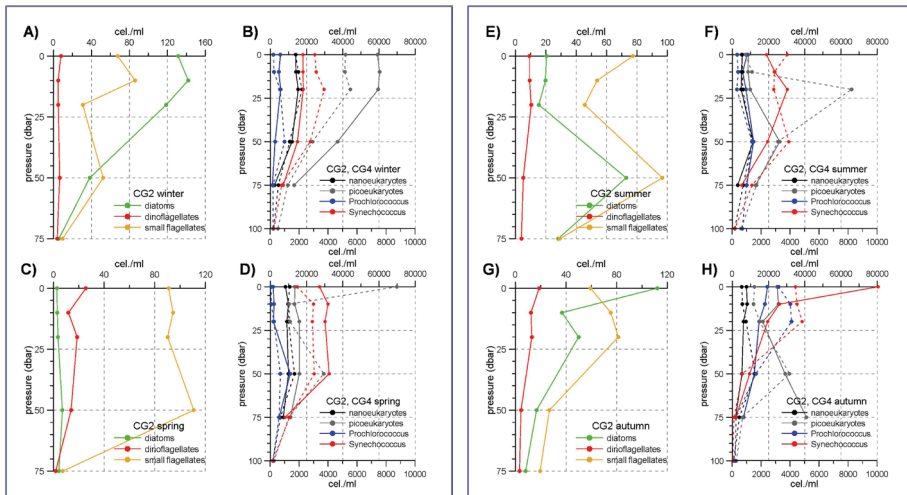


Figure 3.18. The same as in figure 3.17, but for stations CG2 and CG4 in Cape Gata transect.

The stations M2 and V2, located at the continental shelf, close to the P transect, in the western sector of the Alboran Sea, show a similar behavior to the one described for station P2 (results are not shown for the sake of brevity). The abundance of micro-phytoplanktonic cells and the diatom dominance during most of the year, decrease towards the east. This situation affects both Cape Sacratif (not shown) and Cape Gata transects, and it is illustrated in fig. 3.18 which shows the average vertical profiles for the abundances of micro, nano and pico-phytoplanktonic cells at stations CG2 and CG4. This figure follows the same organization and color criteria used in figure 3.17. First, it should be noticed that the highest micro-phytoplanktonic abundances occur in winter, and this is the only season when diatoms are the most abundant group. This winter maximum is observed at 10 m depth and its value is under 150 cel./ml, lower than the 300 cel./ml reached in spring at station P2. For the rest of the year, small flagellates are the most abundant group, with maximum abundances at 50 m depth in spring and summer and at 20 m depth in autumn and winter. Notice that the DCM is usually found at 50 m depth during the stratified period in other areas of the Mediterranean Sea (Estrada et al., 2014, Estrada, 1996).

The differences in the micro-phytoplankton relative composition between the westernmost Alboran Sea transects (Cape Pino, Malaga and Velez) and the easternmost transects (Sacratif and Cape Gata) are more clearly observed in figures 3.19 to 3.22. These figures show the relative abundances for the three analyzed groups, vertically integrated for the upper 100 m of the water column (or to the maximum depth for shallower stations). Figure 3.19 corresponds to winter, figure 3.20 to spring, 3.21 to summer and 3.22 to autumn. The vertically integrated abundances are expressed in cel./m² and figures 3.19 to 3.22 show the percentage corresponding to each group. Light green corresponds to diatoms, green is used for dinoflagellates, and dark green is for small flagellates.

Diatoms are the most abundant group during the four seasons at station M2, in front of Malaga. This group is also the most abundant one at station P2 during spring, summer and autumn, being overcome by small flagellates in winter. Diatoms are also the most abundant group during most of the year at station V2 (winter, spring, summer) being small flagellates the most abundant group in autumn.

The dominance of diatoms is not observed at stations S2 and CG2. Small flagellates are the most abundant group from spring to autumn and diatoms are the main group only in winter. Dinoflagellates show low abundances throughout the year for the whole Alboran Sea continental shelf.

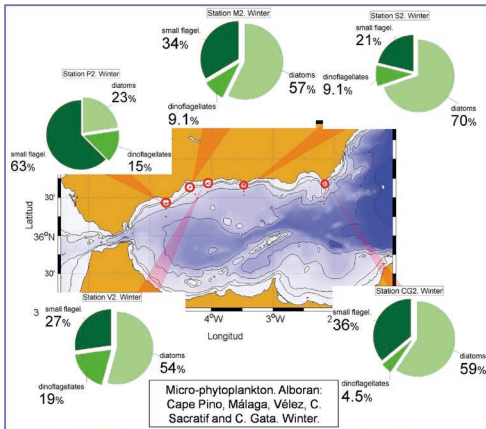


Figure 3.19. Winter relative abundance for the following micro-phytoplanktonic groups: diatoms (light green), dinoflagellates (green) and small flagellates (dark green) for the stations in the continental shelf of the Alboran Sea: P2, M2, V2, S2 and CG2.

Figure 3.20. The same as in figure 3.19, but for spring.

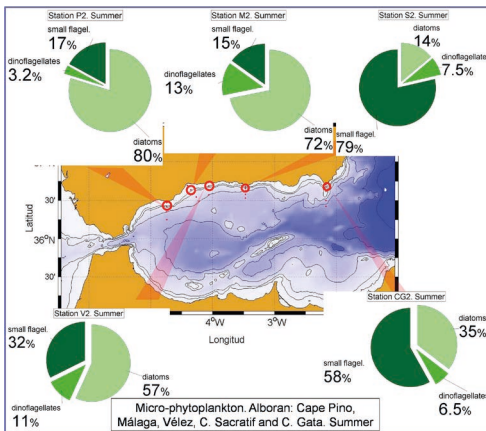
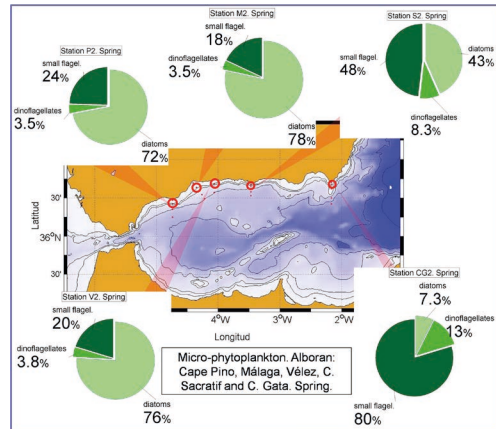


Figure 3.21. The same as in figure 3.19, but for summer.

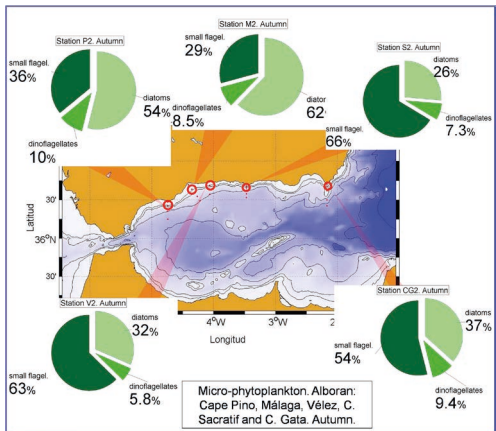


Figure 3.22. The same as in figure 3.19, but for autumn.

Besides the changes in the relative abundances among the different micro-phytoplanktonic groups, there are seasonal and geographical differences in the total number of phytoplanktonic cells. The total number of cells, vertically integrated and adding the three groups at station P2, reaches a minimum value in winter (335×10^6 cel./m²) and a maximum value in summer (890×10^6 cel./m²). High values are also observed during spring: 799×10^6 cel./m². If the four seasonal values are averaged, the value obtained is 627×10^6 cel./m². At station CG2, the minimum value is observed in summer (333×10^6 cel./m²), and the maximum abundance corresponds to winter (712×10^6 cel./m²). The annual mean value is 480×10^6 cel./m², indicating an important decrease for micro-phytoplanktonic cells from west to east.

3.4.2 Nano and picoplankton.

The smallest size fraction in the phytoplankton is made of nano and picoplankton. Within this size fraction, the lowest abundances during the whole year at stations P2 and P4 correspond to the eukaryote nanoplankton group, with average values ranging between 1000 and 3000 cel./ml along the whole year. Once again, it should be noticed that this is the range for the seasonally averaged values.

Abundances from the complete set of oceanographic campaigns show a much higher variability range (see tables 3.13 to 3.16). The prokaryote pico-phytoplankton (photoautotroph bacteria from genera *Prochlorococcus* and *Synechococcus*) show higher abundances that can reach 30 000 cel./ml. The eukaryote picoplankton has abundances similar to those of the prokaryote group. At stations P2 and P4, *Synechococcus* has the highest abundances at the sea surface, decreasing with depth. The only exception is observed in the summer average profile at station P4 where the maximum value is observed at 10 m depth, a shallow position within the water column.

At stations CG2 and CG4 the observed pattern is similar to the one described for the stations P2 and P4. Abundances are of the order of 10^3 cel./ml for the eukaryote nanoplankton, and of the order of 10^4 cel./ml for the picoplankton, both the eukaryote and prokaryote. The highest abundances for the *Synechococcus* group are usually observed at the sea surface, although in some cases, as in spring, such abundances are quite homogeneous from the surface to 50 m depth. *Prochlorococcus* and the eukaryote picoplankton can show maxima at 50 m depth, for instance, in spring and summer. Notice that the scale used in the plots corresponding to P and CG transects are different, in order to show more clearly the vertical profiles. The axis for the CG abundances reaches 80 000 cel./ml. Nevertheless, this large value is caused by the autumn surface abundance for the *Synechococcus* at station CG2. During the rest of the year, maximum values are around 30 000 cel./ml, similarly to the abundances observed at Cape Pino transect.

3.5 Meso-zooplanktonic abundance and biomass.

The abundance of broad meso-zooplanktonic groups has been determined using samples obtained with BONGO nets equipped with a 250 μm mesh, in the ECOMALAGA surveys (P, M and V transects) and in the RADMED ones (from 2007). The groups considered are: copepods, appendicularians, cladocerans, doliolids, chaetognaths, siphonophores, ostracods and scyphozoans. Abundances, expressed in individuals per cubic meter, standard deviations, variability ranges (minimum and maximum values recorded along the complete time series), and the number of campaigns used for the estimation of the statistics are presented in tables 3.17 and 3.18 for the stations P2 and CG2. Tables corresponding to the stations M2 and V2 are not presented to avoid an excessive length of this chapter. Station P2 has been chosen as representative of the conditions in the western Alboran Sea, and CG2 is used to illustrate the oligotrophic conditions in the eastern sector. It is important to notice that the statistics for the stations S2 and CG2 (Cape Sacratif and Cape Gata transects) cannot be considered as robust ones. The reason is that these stations have been sampled from 2007 in the frame of RADMED project. Frequent technical problems and the lack of ship and personnel availability have produced numerous gaps in the time series and some seasons are represented by just two or even one sample. Some previous works have analyzed the phyto and zooplanktonic distributions along wide geographical areas using data from just one seasonal cycle (Latasa et al., 2016, 2010; Ramírez et al., 2005; Reul et al., 2005; Salat et al., 2002; L'Helguen et al., 2002). Nevertheless, in such cases, the obtained statistics do not have the same validity than those estimated from the stations P2, M2, and V2. The latter have been sampled from 1992 in the frame of ECOMALAGA project and the available time series are longer. Despite this shortcoming, CG2 statistics have been included in table 3.18, and the relative abundances for the main zoo-planktonic groups for stations P2, M2, V2, S2 and CG2 have been presented for the whole northern Alboran Sea (figures 3.23, 3.24, 3.25 and 3.26). These data have been included for the completeness of the present work. However, the corresponding discussions should be taken with caution.

Figure 3.23 shows the relative composition of the meso-zooplanktonic community (> 250 μm) at the northern Alboran Sea continental shelf during winter.

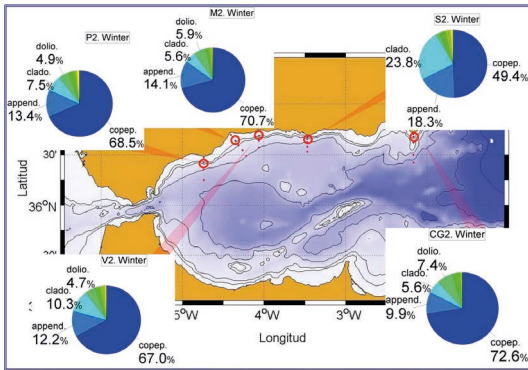


Figure 3.23. Relative importance of the abundances of the main mesozooplanktonic groups during winter at the northern continental shelf of the Alboran Sea (P2, M2, V2, S2 and CG2 stations). The groups analyzed are: copepods, appendicularians, cladocerans, doliolids, chaetognaths, ostracods, siphonophores and scyphozoans. Only groups with relative abundances higher than 5 % have been included for the clarity of the plot.

Copepods are the most abundant group during winter. Their relative abundance is higher than 50 % in all the oceanographic stations, with the only exception of station CG2 where this group represents the 49.4 %. Other groups with significant abundances are appendicularians, cladocerans and doliolids. The rest of the groups have relative abundances lower than 5 %.

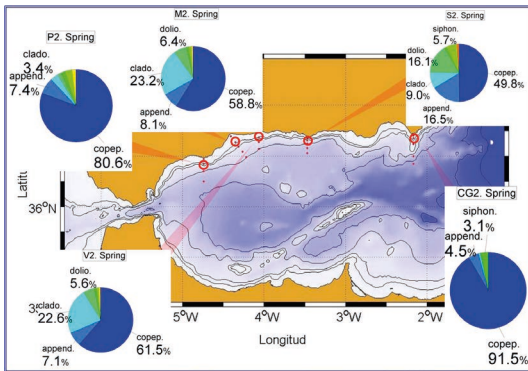


Figure 3.24. The same as in figure 3.23, but for spring.

During spring (Figure 3.24) copepods are the most abundant group with percentages over 50 %, except in station S2 in Cape Sacratif transect, where the copepod abundance is close to 50 %. The other groups with important abundances are appendicularians, cladocerans and doliolids. Notice the increase of the relative abundance of cladocerans in Malaga and Velez.

During summer (Fig. 3.25), there is a significant increase of cladocerans in all the Alboran Sea stations. This group is more abundant than copepods at stations P2 and S2, and it is the second in importance at the rest of the stations. Other groups with abundances higher than 5 % are appendicularians and doliolids, and also chaetognaths at station CG2. Finally, during autumn (Fig. 3.26) copepods is again the most abundant group at all the stations, although their abundance is not as high as in winter and spring. Cladocerans are the second most abundant group, except at station CG2, where this second position corresponds to chaetognaths.

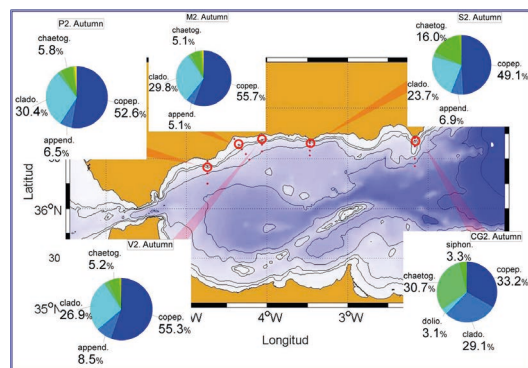


Figure 3.25. The same as in figure 3.23, but for the summer.

If the total number of individuals is considered, that is, the sum of all the groups, the highest abundances are always observed during summer. At station P2 (Cape Pino), the winter, spring, summer and autumn abundances are 527, 509, 1217 and 790 ind./m³ respectively. At station M2 (Malaga), total abundances for the four seasons are 1094, 760, 1547 and 1315 ind./m³. At station V2, in Velez transect, the four seasonal values are: 1111, 1119, 2172 and 1252 ind./m³. Finally, at the easternmost transects, Cape Sacratif and Cape Gata, the total abundances are: 765, 1364, 2241 and 728 ind./m³ for station S2 and 1140, 1028, 1497 and 935 ind./m³ for station CG2.

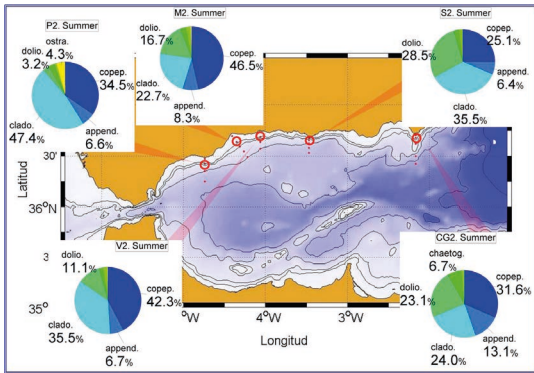


Figure 3.26. The same as in figure 3.23, but for the autumn.

At stations P2, M2 and V2, where the time series are longer, the highest number of individuals per cubic meter during summer coincides with the highest biomasses that reach the values 18.8, 30.2 and 31.5 mg/m³ respectively. At station CG2, the highest value of meso-zooplanktonic biomass is observed during Winter. Nevertheless, these values at this station are quite similar throughout the whole year with a minimum value of 4.5 mg/m³ in spring, and a maximum one of 7.5 mg/m³ in winter. Once again, it is observed a decrease of the zooplanktonic biomass with respect to the western transects (Cape Pino, Malaga and Velez).

3.6 Tables. Seasonal statistics for the Alboran Sea.

Table 3.1. Seasonal mean values for the potential temperature and salinity along the water column at station P2. Three columns with mean values, standard deviations and number of data used, are presented for each season and depth level.

Station P2. Potential temperature standard deviation number of data												
Depth	Winter			Spring			Summer			Autumn		
5	15.04	0.49	19	15.93	0.60	16	19.27	2.06	17	18.17	1.83	21
10	14.97	0.48	20	15.90	0.95	18	17.94	1.77	17	17.70	1.66	21
15	14.93	0.48	20	15.61	0.85	18	17.35	1.42	18	17.17	1.49	21
20	14.85	0.48	20	15.30	0.61	18	16.64	1.15	18	16.86	1.37	21
25	14.81	0.50	20	15.12	0.52	18	16.28	1.01	18	16.59	1.34	20
30	14.75	0.52	20	14.93	0.59	18	16.00	0.92	18	16.19	1.31	21
35	14.69	0.53	19	14.71	0.61	18	15.70	0.95	18	15.90	1.26	21
40	14.66	0.55	18	14.57	0.55	18	15.24	0.77	18	15.72	1.27	20
45	14.61	0.54	20	14.39	0.56	18	14.85	0.51	17	15.46	1.21	21
50	14.55	0.54	20	14.29	0.58	18	14.81	0.60	18	15.27	1.12	20
75	14.18	0.49	20	13.90	0.50	18	14.01	0.40	18	14.30	0.58	20
100	13.83	0.48	15	13.62	0.30	15	13.59	0.22	17	13.80	0.45	20

Station P2. Salinity standard deviation number of data												
Depth	Winter			Spring			Summer			Autumn		
5	36.82	0.23	18	36.87	0.21	17	36.67	0.24	17	36.66	0.23	21
10	36.85	0.23	19	36.95	0.20	18	36.71	0.26	17	36.69	0.24	21
15	36.93	0.34	20	37.06	0.20	18	36.76	0.27	18	36.72	0.25	21
20	36.98	0.37	20	37.18	0.22	18	36.84	0.26	18	36.75	0.26	21
25	37.03	0.41	20	37.25	0.24	18	36.95	0.27	18	36.80	0.28	20

Station P2. Salinity standard deviation number of data												
Depth	Winter			Spring			Summer			Autumn		
30	37.10	0.45	20	37.34	0.22	18	36.98	0.26	18	36.90	0.31	21
35	37.19	0.46	19	37.42	0.24	18	37.11	0.24	18	36.97	0.32	21
40	37.26	0.48	18	37.49	0.24	18	37.17	0.28	18	37.03	0.35	20
45	37.29	0.47	20	37.63	0.28	18	37.29	0.30	18	37.15	0.35	21
50	37.35	0.47	20	37.77	0.19	17	37.40	0.28	18	37.22	0.35	20
75	37.69	0.39	20	38.00	0.18	17	37.89	0.19	18	37.69	0.27	20
100	37.92	0.29	15	38.08	0.15	15	38.09	0.09	17	37.97	0.19	20

Table 3.2. The same as in table 3.1, but for station P4.

Station P4. Potential temperature standard deviation number of data												
Depth	Winter			Spring			Summer			Autumn		
5	15.31	0.75	6	17.25	1.15	4	19.99	1.87	5	18.34	1.05	7
10	15.23	0.77	6	16.83	0.92	4	19.42	1.69	5	18.21	0.95	7
15	15.18	0.75	6	16.54	0.74	4	18.68	1.49	5	17.87	0.93	7
20	15.16	0.73	6	16.26	0.48	4	18.29	1.43	5	17.52	1.05	7
25	15.14	0.74	6	15.97	0.38	4	17.86	1.32	5	17.23	1.19	7
30	15.13	0.74	6	15.67	0.30	4	16.70	1.01	5	16.80	1.32	7
35	15.13	0.73	6	15.53	0.40	4	15.80	0.91	5	16.57	1.31	7
40	15.12	0.72	6	15.20	0.55	4	15.79	0.78	5	16.28	1.27	7
45	15.08	0.72	6	15.11	0.54	4	15.60	0.72	5	16.05	1.18	7
50	14.97	0.59	6	15.06	0.51	4	15.43	0.66	5	15.74	0.96	7
75	14.56	0.56	6	14.49	0.31	4	14.73	0.35	5	14.79	0.60	7
100	14.22	0.61	6	13.86	0.16	4	14.00	0.25	5	14.22	0.72	7
150	13.53	0.29	6	13.41	0.11	4	13.38	0.25	5	13.44	0.39	7
200	13.27	0.14	6	13.29	0.09	4	13.22	0.09	5	13.28	0.19	7
300	13.21	0.03	6	13.26	0.12	4	13.21	0.04	5	13.21	0.03	7
400	13.19	0.02	6	13.22	0.09	4	13.16	0.02	5	13.16	0.02	7
500	13.14	0.01	6	13.16	0.09	4	13.11	0.02	5	13.12	0.01	7
600	13.09	0.01	6	13.10	0.06	4	13.06	0.02	5	13.07	0.01	7
700	13.04	0.01	5	13.04	0.04	4	13.03	0.01	5	13.03	0.01	7
800	12.98	0.02	5	13.01	0.04	3	12.99	0.01	5	12.98	0.02	7

Station P4. Salinity standard deviation number of data												
Depth	Winter			Spring			Summer			Autumn		
5	36.80	0.45	6	36.74	0.22	4	36.51	0.07	5	36.57	0.13	7
10	36.81	0.44	6	36.73	0.24	4	36.52	0.08	5	36.57	0.14	7
15	36.82	0.44	6	36.77	0.24	4	36.50	0.12	5	36.59	0.16	7
20	36.82	0.44	6	36.80	0.22	4	36.49	0.15	5	36.60	0.18	7
25	36.84	0.43	6	36.84	0.24	4	36.48	0.16	5	36.62	0.21	7

Station P4. Salinity standard deviation number of data												
Depth	Winter			Spring			Summer			Autumn		
30	36.88	0.45	6	36.91	0.23	4	36.50	0.23	5	36.64	0.24	7
35	36.93	0.49	6	36.98	0.30	4	36.49	0.22	5	36.71	0.28	7
40	36.97	0.50	6	37.08	0.32	4	36.61	0.18	5	36.79	0.31	7
45	37.02	0.53	6	37.12	0.33	4	36.64	0.21	5	36.88	0.32	7
50	37.05	0.56	6	37.18	0.39	4	36.70	0.18	5	36.96	0.34	7
75	37.36	0.59	6	37.58	0.29	4	37.22	0.31	5	37.35	0.33	7
100	37.67	0.46	6	37.96	0.20	4	37.76	0.21	5	37.77	0.21	7
150	38.20	0.13	6	38.25	0.07	4	38.21	0.12	5	38.24	0.09	7
200	38.36	0.04	6	38.35	0.10	4	38.37	0.05	5	38.35	0.07	7
300	38.47	0.01	6	38.46	0.04	4	38.49	0.01	5	38.48	0.03	7
400	38.51	0.01	6	38.50	0.02	4	38.51	0.00	5	38.51	0.01	7
500	38.52	0.00	6	38.51	0.01	4	38.51	0.00	5	38.51	0.00	7
600	38.51	0.00	6	38.51	0.01	4	38.51	0.00	5	38.51	0.00	7
700	38.50	0.00	5	38.50	0.01	4	38.50	0.00	5	38.50	0.00	7
800	38.49	0.00	5	38.49	0.01	3	38.49	0.01	5	38.49	0.01	7

Table 3.3. The same as in table 3.1, but for station CG2.

Station CG2.Potential temperature standard deviation number of data												
Depth	Winter			Spring			Summer			Autumn		
5	14.35	0.53	4	16.44	1.30	5	23.71	1.55	6	19.81	2.38	7
10	14.33	0.53	4	16.30	1.25	5	22.98	1.96	6	19.79	2.39	7
15	14.28	0.56	4	16.00	1.31	5	22.21	2.43	6	19.72	2.41	7
20	14.27	0.56	4	15.72	1.41	5	21.31	3.23	6	19.14	2.67	7
25	14.25	0.56	4	15.41	1.56	5	20.53	3.73	6	18.70	2.66	7
30	14.23	0.58	4	15.03	1.71	5	19.78	3.63	6	18.01	2.48	7
35	14.21	0.58	4	14.79	1.57	5	17.99	3.18	6	17.29	2.25	7
40	14.19	0.58	4	14.54	1.47	5	16.44	2.02	6	16.89	2.05	7
45	14.16	0.57	4	14.35	1.36	5	15.57	1.36	6	16.57	1.92	7
50	14.10	0.56	4	14.20	1.26	5	14.92	0.86	6	16.23	1.80	7
75	13.90	0.55	3	13.62	0.43	3	13.94	0.20	3	13.79	0.17	4

Station CG2.Salinity standard deviation number of data												
Depth	Winter			Spring			Summer			Autumn		
5	37.80	0.31	4	37.68	0.25	5	37.21	0.26	6	37.05	0.50	7
10	37.80	0.30	4	37.69	0.24	5	37.28	0.21	6	37.06	0.50	7
15	37.81	0.31	4	37.72	0.22	5	37.28	0.17	6	37.06	0.50	7
20	37.82	0.31	4	37.76	0.22	5	37.31	0.22	6	37.09	0.48	7
25	37.83	0.30	4	37.80	0.21	5	37.38	0.22	6	37.11	0.44	7

Station CG2.Salinity standard deviation number of data												
Depth	Winter			Spring			Summer			Autumn		
30	37.84	0.30	4	37.87	0.24	5	37.43	0.20	6	37.15	0.43	7
35	37.84	0.30	4	37.91	0.22	5	37.50	0.22	6	37.23	0.42	7
40	37.85	0.30	4	37.96	0.21	5	37.61	0.21	6	37.31	0.47	7
45	37.86	0.29	4	38.00	0.20	5	37.70	0.21	6	37.36	0.48	7
50	37.88	0.27	4	38.02	0.20	5	37.82	0.16	6	37.49	0.38	7
75	38.05	0.14	3	38.13	0.15	3	38.08	0.08	3	37.99	0.08	4

Table 3.4. The same as in 3.1, but for station CG4.

Station CG4.Potential temperature standard deviation number of data												
Depth	Winter			Spring			Summer			Autumn		
5	14.59	0.54	3	17.34	0.59	4	23.80	1.22	6	20.05	1.98	6
10	14.57	0.52	3	17.24	0.63	4	23.23	1.90	6	20.02	1.99	6
15	14.55	0.50	3	17.07	0.70	4	21.68	2.28	6	19.97	2.01	6
20	14.52	0.47	3	16.82	0.69	4	20.21	1.74	6	19.89	2.00	6
25	14.45	0.50	3	16.25	0.92	4	19.14	1.32	6	19.31	2.04	6
30	14.33	0.52	3	15.87	0.74	4	17.85	0.94	6	18.58	1.75	6
35	14.17	0.59	3	15.46	0.70	4	17.22	0.96	6	18.08	1.75	6
40	14.12	0.62	3	15.06	0.53	4	16.76	0.94	6	17.54	1.48	6
45	14.09	0.63	3	14.71	0.41	4	16.06	0.59	6	16.81	0.84	6
50	14.08	0.67	3	14.52	0.48	4	15.61	0.51	6	16.21	0.81	6
75	14.01	0.69	3	13.57	0.32	4	14.11	0.43	6	14.77	0.50	6
100	13.98	0.75	3	13.17	0.23	4	13.64	0.25	6	14.22	0.44	6
150	13.62	0.31	3	12.99	0.15	4	13.21	0.18	6	13.40	0.15	6
200	13.46	0.09	3	12.97	0.14	4	13.13	0.17	6	13.25	0.18	6
300	13.34	0.10	3	13.09	0.18	4	13.22	0.09	6	13.25	0.12	6
400	13.28	0.06	3	13.25	0.08	4	13.19	0.06	6	13.22	0.06	6
500	13.22	0.04	3	13.20	0.05	4	13.13	0.05	6	13.17	0.06	6
600	13.18	0.05	3	13.14	0.04	4	13.07	0.04	6	13.13	0.07	6
700	13.13	0.06	3	13.07	0.04	3	13.03	0.04	5	13.03	0.01	4

Station CG4. Salinity standard deviation number of data												
Depth	Winter			Spring			Summer			Autumn		
5	37.63	0.40	3	37.52	0.24	4	37.17	0.32	6	36.96	0.56	6
10	37.64	0.39	3	37.54	0.22	4	37.14	0.33	6	36.96	0.56	6
15	37.65	0.36	3	37.56	0.20	4	37.08	0.34	6	36.98	0.57	6
20	37.70	0.29	3	37.58	0.21	4	37.10	0.39	6	37.00	0.57	6
25	37.74	0.29	3	37.65	0.27	4	37.31	0.38	6	36.98	0.58	6
30	37.80	0.31	3	37.62	0.26	4	37.38	0.41	6	36.95	0.58	6
35	37.84	0.32	3	37.69	0.25	4	37.41	0.41	6	36.97	0.58	6
40	37.85	0.32	3	37.73	0.25	4	37.44	0.40	6	37.01	0.57	6

Station CG4. Salinity standard deviation number of data												
Depth	Winter			Spring			Summer			Autumn		
45	37.87	0.30	3	37.74	0.29	4	37.51	0.39	6	37.04	0.56	6
50	37.89	0.28	3	37.81	0.22	4	37.56	0.36	6	37.10	0.55	6
75	37.92	0.28	3	38.07	0.08	4	37.97	0.24	6	37.54	0.46	6
100	37.99	0.21	3	38.12	0.03	4	38.12	0.06	6	37.85	0.37	6
150	38.17	0.01	3	38.15	0.03	4	38.22	0.06	6	38.23	0.07	6
200	38.26	0.04	3	38.20	0.04	4	38.29	0.08	6	38.33	0.07	6
300	38.45	0.06	3	38.33	0.08	4	38.46	0.04	6	38.47	0.02	6
400	38.52	0.02	3	38.48	0.05	4	38.52	0.01	6	38.52	0.01	6
500	38.53	0.01	3	38.52	0.01	4	38.52	0.01	6	38.52	0.01	6
600	38.53	0.01	3	38.52	0.01	4	38.51	0.01	6	38.51	0.01	6
700	38.52	0.01	3	38.51	0.01	3	38.50	0.01	5	38.50	0.00	4

Table 3.5. Seasonal mean values for chlorophyll-a, dissolved oxygen, nitrate, nitrite, phosphate and silicate concentrations along the water column for the station P2. Three columns with mean values, standard deviation and number of data are presented for each season and depth level.

Station P2. Chlorophyll-a (mg/m ³) standard deviation number of data												
Depth	Winter			Spring			Summer			Autumn		
0	1.13	0.97	18	1.13	0.93	20	0.51	0.33	16	1.11	1.50	20
10	1.12	0.83	18	1.66	1.49	21	0.66	0.44	17	1.09	1.21	20
20	0.79	0.67	18	1.00	0.82	20	1.12	0.93	18	0.91	0.95	20
50	0.33	0.30	17	0.33	0.23	20	0.47	0.35	18	0.32	0.25	20
75	0.31	0.26	16	0.29	0.16	19	0.39	0.24	17	0.25	0.21	18
100	0.37	0.42	16	0.30	0.29	20	0.34	0.41	17	0.28	0.33	18

Station P2. Oxygen (ml/l) standard deviation number of data												
Depth	Winter			Spring			Summer			Autumn		
0	5.41	0.42	17	5.41	0.44	16	5.59	0.58	14	5.34	0.42	19
10	5.36	0.51	17	5.25	0.49	16	5.51	0.69	14	5.27	0.46	19
20	5.15	0.47	17	4.97	0.64	16	5.15	0.62	15	5.00	0.56	19
50	4.85	0.45	17	4.55	0.44	16	4.36	0.39	15	4.66	0.51	19
75	4.81	0.50	16	4.60	0.52	16	4.50	0.55	15	4.67	0.32	19
100	4.89	0.61	14	4.83	0.72	16	4.66	0.68	15	4.76	0.52	19
130	4.46	0.28	4	4.47	0.58	4	4.43	0.47	7	4.50	0.31	9

Station P2. Nitrate (µM) standard deviation number of data												
Depth	Winter			Spring			Summer			Autumn		
0	0.89	0.69	16	0.86	0.95	16	0.20	0.26	17	0.62	0.76	18
10	1.59	1.76	17	1.32	1.25	16	0.33	0.60	16	1.16	1.43	18
20	2.15	2.06	17	2.19	1.63	16	1.08	1.65	17	1.83	1.71	18
50	3.61	1.92	17	4.23	1.93	17	4.40	2.45	17	4.50	2.51	18

Station P2. Nitrate (μM) standard deviation number of data												
Depth	Winter			Spring			Summer			Autumn		
75	4.29	1.86	17	5.09	1.97	17	4.94	2.22	17	5.42	1.93	18
100	4.89	1.82	17	5.54	2.03	17	5.80	1.93	17	6.12	1.76	18
130	5.16	2.27	10	6.15	2.17	7	6.67	1.72	9	6.71	2.18	11

Station P2. Nitrite (μM) standard deviation number of data												
Depth	Winter			Spring			Summer			Autumn		
0	0.16	0.08	16	0.06	0.03	16	0.07	0.06	16	0.08	0.06	17
10	0.16	0.07	16	0.09	0.06	16	0.07	0.05	17	0.08	0.07	16
20	0.20	0.17	16	0.12	0.08	16	0.07	0.04	17	0.13	0.11	17
50	0.20	0.07	15	0.15	0.08	16	0.16	0.06	16	0.15	0.11	17
75	0.17	0.05	14	0.17	0.11	16	0.18	0.07	17	0.14	0.08	17
100	0.13	0.05	14	0.15	0.10	16	0.20	0.14	17	0.12	0.08	17
130	0.67	1.73	10	1.19	2.68	7	0.14	0.08	9	0.08	0.05	10

Station P2. Phosphate (μM) standard deviation number of data												
Depth	Winter			Spring			Summer			Autumn		
0	0.13	0.06	17	0.11	0.06	17	0.08	0.04	17	0.10	0.09	18
10	0.14	0.08	17	0.15	0.13	17	0.09	0.06	17	0.11	0.08	18
20	0.17	0.09	17	0.16	0.09	17	0.12	0.07	17	0.15	0.11	18
50	0.21	0.09	17	0.25	0.12	17	0.25	0.11	17	0.29	0.16	18
75	0.23	0.09	17	0.27	0.12	17	0.26	0.11	17	0.30	0.10	17
100	0.25	0.09	17	0.28	0.13	17	0.28	0.10	17	0.29	0.08	17
130	0.24	0.11	10	0.28	0.15	7	0.32	0.09	9	0.28	0.10	11

Station P2. Silicate (μM) standard deviation number of data												
Depth	Winter			Spring			Summer			Autumn		
0	1.30	0.72	17	0.92	0.66	17	0.51	0.22	16	1.12	0.74	18
10	1.54	1.07	17	1.16	0.72	17	0.78	0.52	16	1.36	0.90	18
20	1.79	1.32	17	1.49	0.92	17	1.43	1.18	17	1.52	0.81	18
50	2.42	1.32	17	2.57	1.36	17	3.21	1.15	17	2.75	1.37	18
75	2.74	1.37	17	3.00	1.33	17	3.39	1.13	17	3.19	1.18	18
100	2.97	1.45	17	3.21	1.43	17	3.73	1.01	17	3.50	1.16	18
130	2.96	1.48	10	3.28	1.89	7	3.96	1.11	9	3.82	1.35	11

Table 3.6. The same as in table 3.5, but for station P4.

Station P4. Chlorophyll-a (mg/m^3) standard deviation number of data												
Depth	Winter			Spring			Summer			Autumn		
0	1.11	1.04	5	0.47	0.54	6	0.50	0.26	3	0.58	0.42	6
10	1.13	1.25	5	0.70	0.74	6	0.70	0.20	3	0.66	0.33	6

Station P4. Chlorophyll-a (mg/m ³) standard deviation number of data												
Depth	Winter			Spring			Summer			Autumn		
20	1.19	1.45	5	0.68	0.47	6	0.56	0.08	3	0.69	0.49	6
50	0.50	0.45	5	0.48	0.28	6	0.17	0.07	3	0.19	0.14	6
75	0.13	0.10	5	0.45	0.61	6	0.14	0.02	3	0.10	0.11	6
100	0.07	0.04	5	0.08	0.04	6	0.04	0.02	3	0.05	0.04	6

Station P4. Oxygen (ml/l) standard deviation number of data												
Depth	Winter			Spring			Summer			Autumn		
0	5.44	0.42	6	4.99	0.84	4	5.37	0.67	4	5.46	0.48	7
10	5.41	0.42	6	5.10	0.55	4	5.18	0.59	4	5.48	0.51	7
20	5.34	0.37	6	5.00	0.58	4	5.15	0.65	4	5.37	0.40	7
50	4.99	0.32	6	4.61	0.57	4	4.63	0.36	4	4.94	0.42	7
75	4.72	0.25	6	4.48	0.68	4	4.48	0.36	4	4.74	0.39	7
100	4.51	0.23	6	4.35	0.81	4	4.22	0.33	4	4.61	0.33	7
200	4.05	0.27	6	3.94	0.84	4	3.87	0.27	4	4.32	0.31	7
300	3.75	0.24	6	3.61	0.57	4	3.59	0.35	4	3.94	0.20	7
500	3.77	0.23	6	3.63	0.35	4	3.73	0.40	4	4.06	0.28	7
870												

Station P4. Nitrate (µM) standard deviation number of data												
Depth	Winter			Spring			Summer			Autumn		
0	1.19	0.88	4	0.41	0.58	3	0.19	0.08	2	0.65	0.71	6
10	1.41	0.87	4	0.34	0.39	3	0.21	0.10	2	0.96	0.77	6
20	2.14	1.21	4	1.21	1.32	3	1.60	1.02	2	2.32	1.93	6
50	3.78	0.89	4	5.38	2.60	3	3.83	1.98	2	4.82	2.30	6
75	5.33	1.25	4	5.28	2.49	3	4.05	1.92	2	5.83	2.47	6
100	6.51	1.44	4	5.54	2.71	3	5.62	2.55	2	6.45	2.82	6
200	8.45	0.69	4	5.45	2.26	2	10.75		1	8.16	2.93	6
300	10.11	0.47	4	10.00	2.72	2	11.48		1	8.79	2.21	6
500	9.92	0.22	4	10.26	1.18	2	10.34		1	8.93	2.18	6
870	9.20	0.22	3	9.03	0.58	2	9.73		1	8.32	1.97	6

Station P4. Nitrite (µM) standard deviation number of data												
Depth	Winter			Spring			Summer			Autumn		
0	0.27	0.19	4	0.04	0.03	3	0.03	0.02	2	0.21	0.30	6
10	0.26	0.15	4	0.06	0.03	3	0.03	0.00	2	0.23	0.38	6
20	0.26	0.15	4	0.09	0.06	3	0.12	0.05	2	0.33	0.41	6
50	0.65	0.78	4	0.16	0.08	3	0.17	0.05	2	0.31	0.47	6
75	0.80	1.18	4	0.16	0.03	3	0.10	0.05	2	0.22	0.31	6
100	0.94	1.49	4	0.14	0.11	3	0.10	0.08	2	0.24	0.41	6
200	1.15	1.93	4	0.06	0.03	2	0.02		1	0.40	0.77	6
300	1.77	2.86	4	0.05	0.03	2	0.02		1	0.58	1.22	6

Station P4. Nitrite (μM) standard deviation number of data												
Depth	Winter			Spring			Summer			Autumn		
500	2.13	3.53	4	0.04	0.03	2	0.01		1	0.96	2.09	6
870	0.03	0.00	2	0.04	0.02	2	0.01		1	1.34	2.90	6

Station P4. Phosphate (μM) standard deviation number of data												
Depth	Winter			Spring			Summer			Autumn		
0	0.11	0.04	4	0.12	0.08	3	0.03	0.01	2	0.08	0.05	6
10	0.11	0.05	4	0.17	0.13	3	0.04	0.02	2	0.10	0.06	6
20	0.13	0.06	4	0.18	0.14	3	0.10	0.01	2	0.17	0.13	6
50	0.21	0.04	4	0.35	0.16	3	0.22	0.05	2	0.30	0.11	6
75	0.24	0.08	4	0.39	0.25	3	0.26	0.02	2	0.37	0.11	6
100	0.27	0.13	4	0.40	0.28	3	0.33	0.01	2	0.38	0.16	6
200	0.28	0.16	4	0.24	0.13	2	0.29		1	0.41	0.21	6
300	0.33	0.19	4	0.40	0.10	2	0.33		1	0.48	0.26	6
500	0.35	0.21	4	0.46	0.05	2	0.44		1	0.44	0.25	6
870	0.30	0.22	3	0.43	0.03	2	0.37		1	0.41	0.24	6

Station P4. Silicate (μM) standard deviation number of data												
Depth	Winter			Spring			Summer			Autumn		
0	0.92	0.55	4	0.59	0.43	3	0.57	0.07	2	0.86	0.48	6
10	1.02	0.61	4	0.55	0.36	3	0.67	0.06	2	1.01	0.64	6
20	1.37	0.83	4	0.90	0.75	3	1.30	0.32	2	1.77	1.07	6
50	2.02	1.24	4	2.26	0.65	3	2.11	0.77	2	2.88	1.62	6
75	2.60	1.54	4	2.82	1.11	3	2.42	0.34	2	3.32	1.57	6
100	3.33	1.94	4	2.95	1.08	3	3.72	0.28	2	3.78	1.92	6
200	3.84	2.06	4	2.63	0.38	2	5.79		1	4.80	2.32	6
300	4.92	2.59	4	5.16	0.65	2	6.76		1	6.03	2.68	6
500	6.31	3.39	4	6.75	0.28	2	8.06		1	7.16	3.06	6
870	7.10	4.70	3	8.59	1.64	2	9.91		1	9.25	4.04	6

Table 3.7. Seasonally averaged Secchi disk depths for the westernmost transects in the Alboran Sea: P, M and V. Three columns with mean values, standard deviations and number of data used, are presented for each season.

Secchi disk depth (m) standard deviation number of data												
	Winter			Spring			Summer			Autumn		
P2	14.1	4.7	17	13.1	4.1	20	15.4	5.7	18	16.1	5.2	21
P4	16.4	3.3	5	18.0	5.5	6	18.5	6.5	6	17.7	6.8	9
M2	12.6	5.7	18	12.7	5.6	22	16.7	9.9	18	16.9	5.6	21
M4	13.1	3.3	7	16.0	6.4	7	20.4	8.2	7	18.4	6.8	9
V2	13.2	4.7	20	14.4	6.5	22	20.2	6.7	18	18.4	5.0	20
V4	15.7	5.3	7	16.1	6.4	7	24.6	4.7	5	18.0	6.5	8

Table 3.8. Seasonal mean values for chlorophyll-a, dissolved oxygen, nitrate, nitrite, phosphate and silicate concentrations along the water column for the station CG2. Three columns with mean values, standard deviation and number of data are presented for each season and depth level.

Station CG2. Chlorophyll-a (mg/m ³) standard deviation number of data												
Depth	Winter			Spring			Summer			Autumn		
0	0.59	0.36	3	0.11	0.02	5	0.09	0.01	6	0.31	0.28	5
10	0.63	0.39	3	0.12	0.03	5	0.11	0.02	6	0.38	0.31	5
20	0.62	0.32	3	0.12	0.03	5	0.10	0.02	6	0.76	0.70	5
50	0.45	0.15	3	0.35	0.21	5	0.49	0.36	6	0.36	0.15	5
75	0.21	0.21	3	0.17	0.09	4	0.23	0.16	6	0.14	0.09	5

Station CG2. Oxygen (ml/l) standard deviation number of data												
Depth	Winter			Spring			Summer			Autumn		
0	5.68	0.24	4	5.09	0.46	4	4.61	0.49	5	5.36	0.47	5
10	5.66	0.26	4	5.10	0.49	4	4.76	0.53	5	5.38	0.49	5
20	5.61	0.26	4	5.08	0.48	4	4.99	0.68	5	5.40	0.43	5
50	5.58	0.23	4	4.85	0.63	4	5.05	0.65	5	5.20	0.92	5
75	5.31	0.27	3	5.07	0.62	2	5.42	0.03	2	4.64	0.23	4

Station CG2. Nitrate (µM) standard deviation number of data												
Depth	Winter			Spring			Summer			Autumn		
0	0.08	0.05	2	0.06	0.06	2	0.12	0.03	3	0.85	1.30	4
10	0.06	0.03	2	0.06	0.06	2	1.29	1.58	3	0.18	0.09	4
20	0.05	0.02	2	0.07	0.07	2	0.11	0.05	3	0.25	0.19	4
50	0.25	0.07	2	0.25	0.03	2	1.26	0.95	3	2.50	3.00	4
75	2.16	0.01	2	0.99		1	2.73	0.39	3	4.00	2.65	4

Station CG2. Nitrite (µM) standard deviation number of data												
Depth	Winter			Spring			Summer			Autumn		
0	0.02	0.01	2	0.03	0.02	2	0.19	0.25	3	0.20	0.26	4
10	0.05	0.02	2	0.03	0.01	2	0.22	0.15	3	0.04	0.02	4
20	0.03	0.01	2	0.03	0.02	2	0.10	0.11	3	0.06	0.05	4
50	0.07	0.03	2	0.06	0.02	2	0.21	0.18	3	0.12	0.08	4
75	0.09	0.00	2	0.16		1	0.21	0.16	3	0.15	0.09	4

Station CG2. Phosphate (µM) standard deviation number of data												
Depth	Winter			Spring			Summer			Autumn		
0	0.01	0.01	2	0.10	0.06	2	0.03	0.03	3	0.03	0.00	4
10	0.04	0.02	2	0.09	0.07	2	0.06	0.04	3	0.02	0.00	4
20	0.07	0.02	2	0.09	0.07	2	0.03	0.02	3	0.07	0.04	4
50	0.05	0.01	2	0.10	0.07	2	0.06	0.05	3	0.13	0.15	4
75	0.11	0.01	2	0.04		1	0.12	0.03	3	0.19	0.12	4

Station CG2. Silicate (μM) standard deviation number of data												
Depth	Winter			Spring			Summer			Autumn		
0	0.72	0.13	2	0.89	0.24	2	0.60	0.09	3	0.68	0.15	4
10	0.75	0.17	2	0.82	0.12	2	1.21	0.74	3	0.66	0.20	4
20	0.76	0.19	2	0.86	0.04	2	0.66	0.09	3	0.78	0.38	4
50	0.93	0.11	2	1.22	0.01	2	1.21	0.35	3	1.80	1.31	4
75	1.82	0.04	2	1.49		1	1.94	0.21	3	2.36	1.09	4

Table 3.9. The same as in table 3.8, but for station CG4.

Station CG4. Chlorophyll-a (mg/m^3) standard deviation number of data												
Depth	Winter			Spring			Summer			Autumn		
0	0.40	0.19	3	0.10	0.03	5	0.08	0.02	5	0.24	0.17	4
10	0.41	0.18	3	0.10	0.03	5	0.09	0.03	5	0.27	0.17	4
20	0.43	0.20	3	0.12	0.03	5	0.13	0.11	5	0.27	0.07	4
50	0.47	0.31	3	0.45	0.25	5	0.48	0.31	5	0.51	0.25	4
75	0.16	0.02	3	0.30	0.15	5	0.22	0.09	5	0.13	0.06	4
100	0.07	0.02	3	0.11	0.06	5	0.09	0.04	5	0.06	0.02	4

Station CG4. Oxygen (ml/l) standard deviation number of data												
Depth	Winter			Spring			Summer			Autumn		
0	5.74	0.27	3	4.93	0.78	3	4.48	0.53	4	5.50	0.48	4
10	5.76	0.28	3	5.08	0.58	3	4.55	0.54	4	5.50	0.46	4
20	5.77	0.28	3	5.16	0.57	3	5.10	0.80	4	5.45	0.44	4
50	5.60	0.19	3	5.11	0.62	3	5.17	0.44	4	5.21	0.70	4
75	5.52	0.17	3	4.90	0.59	3	4.68	0.62	4	5.00	0.66	4
100	5.44	0.21	3	4.93	0.61	3	4.53	0.68	4	4.85	0.60	4
200	4.79	0.43	3	4.74	0.54	3	4.27	0.54	4	4.82	0.28	4
300	4.27	0.38	3	4.13	0.51	3	3.84	0.51	4	4.36	0.31	4
500	4.07	0.14	3	3.72	0.39	3	3.78	0.49	4	4.30	0.34	4
700	4.11	0.15	2	3.94		1	4.04	0.53	2	4.46	0.38	4

Station CG4. Nitrate (μM) standard deviation number of data												
Depth	Winter			Spring			Summer			Autumn		
0	0.08	0.01	2	0.07	0.06	2	0.11	0.04	3	0.13	0.08	4
10	0.06	0.01	2	0.06	0.06	2	0.09	0.07	3	0.31	0.35	4
20	0.06	0.02	2	0.06	0.05	2	0.07	0.05	3	0.74	1.06	4
50	0.22	0.17	2	0.06	0.06	2	1.12	1.10	3	2.35	1.38	4
75	0.84	0.69	2	2.49	1.58	2	2.42	0.42	3	4.18	1.97	4
100	1.60	0.47	2	3.17	0.43	2	4.19	1.49	3	5.27	2.68	4
200	4.40	1.09	2	6.27	1.78	2	7.26		1	6.03	2.61	3
300	6.82	1.30	2	10.39	1.59	2	9.25		1	7.51	3.29	3

Station CG4. Nitrate (μM) standard deviation number of data												
Depth	Winter			Spring			Summer			Autumn		
500	7.86	0.47	2	10.19	1.10	2	9.92		1	7.65	3.32	3
700	7.82	0.48	2	8.32		1	8.46		1	7.39	3.25	3

Station CG4. Nitrite (μM) standard deviation number of data												
Depth	Winter			Spring			Summer			Autumn		
0	0.03	0.02	2	0.03	0.00	2	0.13	0.08	3	0.05	0.04	4
10	0.02	0.01	2	0.03	0.02	2	0.03	0.02	3	0.06	0.06	4
20	0.04	0.02	2	0.03	0.02	2	0.08	0.04	3	0.09	0.10	4
50	0.13	0.10	2	0.07	0.01	2	0.24	0.14	3	0.30	0.04	4
75	0.15	0.04	2	0.21	0.03	2	0.37	0.22	3	0.15	0.07	4
100	0.11	0.06	2	0.07	0.04	2	0.08	0.01	3	0.07	0.03	4
200	0.04	0.01	2	0.04	0.02	2	0.05		1	0.06	0.03	3
300	0.03	0.01	2	0.04	0.02	2	0.03		1	0.05	0.02	3
500	0.03	0.00	2	0.05	0.02	2	0.02		1	0.06	0.02	3
700	0.02	0.01	2	0.03		1	0.10		1	0.06	0.02	3

Station CG4. Phosphate (μM) standard deviation number of data												
Depth	Winter			Spring			Summer			Autumn		
0	0.03	0.02	2	0.09	0.07	2	0.09	0.09	3	0.04	0.01	4
10	0.04	0.02	2	0.08	0.06	2	0.03	0.02	3	0.04	0.02	4
20	0.04	0.01	2	0.08	0.06	2	0.03	0.02	3	0.07	0.06	4
50	0.04	0.02	2	0.10	0.07	2	0.07	0.07	3	0.13	0.09	4
75	0.04	0.00	2	0.15	0.12	2	0.06	0.04	3	0.22	0.09	4
100	0.06	0.01	2	0.16	0.07	2	0.08	0.04	3	0.26	0.12	4
200	0.19	0.01	2	0.27	0.10	2	0.25		1	0.28	0.01	3
300	0.38	0.00	2	0.47	0.09	2	0.55		1	0.40	0.01	3
500	0.51	0.08	2	0.46	0.05	2	0.49		1	0.44	0.02	3
700	0.56	0.12	2	0.39		1	0.48		1	0.44	0.02	3

Station CG4. Silicate (μM) standard deviation number of data												
Depth	Winter			Spring			Summer			Autumn		
0	0.83	0.06	2	0.85	0.01	2	0.58	0.13	3	0.69	0.23	4
10	0.80	0.03	2	0.84	0.02	2	0.54	0.07	3	0.71	0.27	4
20	0.88	0.01	2	0.97	0.09	2	0.59	0.07	3	0.80	0.38	4
50	0.86	0.01	2	1.37	0.18	2	0.99	0.30	3	1.62	0.70	4
75	1.19	0.30	2	2.09	0.55	2	1.60	0.21	3	2.53	0.63	4
100	1.46	0.29	2	2.16	0.20	2	2.27	0.22	3	3.13	1.08	4
200	2.78	0.33	2	3.44	0.64	2	3.40		1	3.94	0.42	3
300	4.67	0.82	2	5.82	0.78	2	4.98		1	5.81	0.55	3
500	7.10	0.11	2	7.99	0.74	2	6.75		1	7.79	0.40	3
700	7.91	0.21	2	7.54		1	6.53		1	8.68	0.50	3

Table 3.10. Seasonally averaged Secchi disk depths for the easternmost transects in the Alboran Sea: S and CG. Three columns with mean values, standard deviations and number of data used, are presented for each season.

Secchi disk depth (m) standard deviation number of data												
	Winter			Spring			Summer			Autumn		
S2	17.7	4.1	7	17.0	6.4	6	25.6	3.8	7	20.1	7.7	8
S4	15.7	5.5	7	16.8	6.0	6	26.6	3.8	7	20.8	7.7	8
CG2	14.0	0.0	3	15.2	5.7	6	24.2	5.4	6	21.3	5.7	9
CG4	15.7	1.5	3	22.8	5.0	6	25.4	4.0	7	23.1	5.9	8

Table 3.11. Average abundances expressed as cells per milliliter (cel./ml), along the water column for the station P2 for the following micro-phytoplanktonic groups: diatoms, dinoflagellates and small flagellates. For each season five columns are presented: Seasonal mean value, standard deviation, number of data used, minimum and maximum values recorded for each group and season along the complete time series.

		Station P2. Diatoms (cells/ml)																		
		Winter					Spring					Summer					Autumn			
Depth	Mean	σ	n	Min.	Max.	Mean	σ	n	Min.	Max.	Mean	σ	n	Min.	Max.	Mean	σ	n	Min.	Max.
0	25	17	9	6	54	237	298	15	0	1037	165	187	10	30	692	60	85	11	2	307
10	19	18	10	3	52	252	281	10	0	747	247	200	10	2	566	67	103	14	0	397
20	20	21	13	1	71	99	92	15	0	273	146	101	10	2	310	85	116	16	1	411
50	22	37	11	3	135	24	37	15	0	146	62	59	8	3	193	41	54	15	0	198
75	10	5	6	2	16	15	19	8	0	58	27	27	6	1	83	9	7	9	1	19
100	9	8	7	2	26	12	14	8	0	38	13	12	6	3	37	4	3	8	0	7

		Station P2. Dinoflagellates (cells/ml)																		
		Winter					Spring					Summer					Autumn			
Depth	Mean	σ	n	Min.	Max.	Mean	σ	n	Min.	Max.	Mean	σ	n	Min.	Max.	Mean	σ	n	Min.	Max.
0	21	18	10	1	50	6	4	15	0	18	3	2	10	0	7	7	4	11	2	16
10	13	18	9	0	60	13	12	10	0	37	11	8	10	0	25	6	6	14	0	20
20	5	5	13	0	15	6	5	15	0	19	9	6	10	1	19	10	10	16	0	34
50	2	1	11	0	4	2	2	15	0	5	3	2	8	1	7	4	3	15	0	12
75	5	9	7	0	26	2	2	8	0	6	3	3	6	1	10	3	3	8	0	8
100	3	5	7	0	15	3	3	8	0	8	2	1	6	0	4	1	1	8	0	3

Station P2. Small flagellates (cells/ml)																				
Depth	Winter					Spring					Summer					Autumn				
	Mean	σ	n	Min.	Max.	Mean	σ	n	Min.	Max.	Mean	σ	n	Min.	Max.	Mean	σ	n	Min.	Max.
0	58	60	10	0	170	26	31	15	0	82	46	38	11	1	116	31	30	11	4	94
10	41	53	9	0	151	58	52	9	0	153	32	23	9	0	67	54	57	14	0	209
20	37	67	13	0	239	18	22	15	0	76	45	38	11	0	109	59	70	16	0	225
50	18	20	11	0	59	14	19	15	0	69	15	11	9	0	34	20	26	15	0	90
75	18	19	7	0	62	7	10	8	0	32	14	10	6	2	29	12	12	9	0	36
100	9	11	7	0	33	5	5	7	0	15	7	3	5	4	11	10	11	9	0	35

Table 3.12. The same as in table 3.11, but for station CG2.

CG2. Diatoms (cells/ml)																				
Depth	Winter					Spring					Summer					Autumn				
	Mean	σ	n	Min.	Max.	Mean	σ	n	Min.	Max.	Mean	σ	n	Min.	Max.	Mean	σ	n	Min.	Max.
0	131	174	5	1	464	2	3	6	0	8	14	17	6	0	44	112	224	6	3	613
10	142	191	5	3	510	2	2	6	0	4	13	16	6	0	43	37	64	6	1	180
20	119	156	5	13	427	3	3	5	0	9	10	15	6	0	41	50	83	6	3	234
50	38	35	5	2	82	5	9	6	0	25	49	73	6	0	207	17	18	6	3	55
75	6	5	5	1	12	3	4	5	0	9	19	27	6	0	76	8	7	6	0	18

CG2. Dinoflagellates (cells/ml)																				
Depth	Winter					Spring					Summer					Autumn				
	Mean	σ	n	Min.	Max.	Mean	σ	n	Min.	Max.	Mean	σ	n	Min.	Max.	Mean	σ	n	Min.	Max.
0	8	9	5	0	22	17	26	6	0	73	6	5	6	0	13	19	21	6	3	64
10	5	5	5	1	15	8	8	6	0	21	6	5	6	0	14	10	4	5	3	15
20	5	5	5	1	14	15	11	5	0	32	7	7	6	0	19	13	10	6	5	32
50	7	6	5	0	17	9	11	6	0	29	3	3	6	0	9	4	2	5	1	5
75	4	4	5	0	12	1	1	5	0	2	3	3	6	0	9	3	1	4	2	3

CG2. Small flagellates (cells/ml)																				
Depth	Winter					Spring					Summer					Autumn				
	Mean	σ	n	Min.	Max.	Mean	σ	n	Min.	Max.	Mean	σ	n	Min.	Max.	Mean	σ	n	Min.	Max.
0	68	76	5	4	171	61	74	6	0	217	52	45	6	0	111	59	45	6	12	129
10	86	115	5	17	315	63	58	6	0	136	36	33	6	0	97	75	74	6	7	226
20	31	45	5	2	119	72	66	5	0	155	30	31	6	0	92	81	84	6	6	259
50	52	46	5	10	136	74	100	6	0	249	65	100	6	0	281	27	13	6	5	37
75	10	8	5	0	23	4	7	5	0	17	20	25	6	0	67	20	12	6	4	36

Tabla 3.13. Average abundances expressed in cells per milliliter (cel./ml), along the water column for the station P2 for the nanoeukaryote and picoeukaryote cells and for the photoautotroph bacteria of the genera Prochlorococcus and Synechococcus. For each season and depth level five columns are presented: seasonal mean value, standard deviation, number of data used and minimum and maximum values recorded along the complete time series.

P2. Nanoeukaryotes (cells/ml)																				
Depth	Winter					Spring					Summer					Autumn				
	Mean	σ	n	Min.	Max.	Mean	σ	n	Min.	Max.	Mean	σ	n	Min.	Max.	Mean	σ	n	Min.	Max.
0	2378	1042	6	1264	4346	1700	665	8	723	2856	3162	2743	6	765	9105	1340	352	6	1003	2096
10	2633	1424	6	1060	4993	1821	1255	8	785	4262	1804	924	6	801	3727	1172	507	7	259	1921
20	2008	985	6	1006	4100	1342	754	8	335	2847	1679	1035	6	609	3228	1481	763	7	185	2543
50	936	586	6	312	1743	938	975	8	114	2990	2323	2476	6	320	7418	742	495	7	112	1575
75	459	353	6	156	1222	413	306	8	93	994	493	304	6	138	1036	259	215	7	6	647
100	255	135	6	91	485	268	128	8	72	547	925	1587	6	78	4436	122	88	7	15	263

P2. Picoeukaryotes (cells/ml)																				
Depth	Winter				Spring				Summer				Autumn							
	Mean	σ	n	Min.	Max.	Mean	σ	n	Min.	Max.	Mean	σ	n	Min.	Max.	Mean	σ	n	Min.	Max.
0	26041	10179	6	12452	40165	9943	5030	8	1550	15014	12446	5905	6	5348	24257	9407	5305	6	3755	18189
10	24713	10230	6	9668	37045	10354	7809	8	1527	27271	10672	4391	6	5308	19115	9295	4942	7	3692	18579
20	18721	10538	6	6916	36642	7114	3584	8	2171	12412	17614	10419	6	7694	32371	11658	9970	7	2673	34176
50	4683	3571	6	1743	9916	2643	2467	8	90	7084	7015	7950	6	668	23858	2642	1358	7	1281	4761
75	2351	1979	6	581	5886	993	838	8	302	2849	1928	2511	6	302	7458	1025	939	7	48	2796
100	1316	1231	6	236	3647	381	384	8	45	1336	303	236	6	96	796	376	365	7	33	1159

P2. Synechococcus (cells/ml)																				
Depth	Winter				Spring				Summer				Autumn							
	Mean	σ	n	Min.	Max.	Mean	σ	n	Min.	Max.	Mean	σ	n	Min.	Max.	Mean	σ	n	Min.	Max.
0	16474	11032	6	5305	38878	13431	8931	8	1145	29658	18557	16220	6	7282	54164	24886	14704	6	7151	53088
10	16179	11964	6	5575	41934	12567	11763	8	199	38471	16422	17493	6	5217	55090	22215	13729	7	4421	49336
20	13085	11183	6	3494	36951	10071	6398	8	2391	22472	14605	14762	6	1187	44902	19577	11388	7	3862	38415
50	2861	1875	6	1100	6033	4209	4123	8	668	13286	5708	6789	6	743	20362	4610	2543	7	955	8567
75	1778	1344	6	614	4072	2363	2544	8	766	8804	2871	4795	6	257	13569	1731	1158	7	90	4183
100	1501	1252	6	127	3341	1482	1372	8	249	3752	586	486	6	141	1611	1729	2044	7	66	6545

P2. Prochlorococcus (cells/ml)																				
Depth	Winter				Spring				Summer				Autumn							
	Mean	σ	n	Min.	Max.	Mean	σ	n	Min.	Max.	Mean	σ	n	Min.	Max.	Mean	σ	n	Min.	Max.
0	5879	7959	6	602	23208	5786	10500	8	0	33250	6038	6841	6	947	21061	30248	47034	6	4466	135156
10	7185	10592	6	581	30309	9409	12280	8	0	30119	7555	4900	6	947	16379	18532	23795	7	0	75147
20	4769	6271	6	560	17716	5785	9435	8	0	29929	11943	9188	6	947	28753	59798	120915	7	0	355560
50	848	491	6	234	1701	1131	1180	8	84	3702	7575	9597	6	0	24608	4415	3140	7	1380	10629
75	444	326	6	0	833	706	894	8	39	2980	1789	1517	6	72	4725	1264	1516	7	0	4743
100	433	212	6	156	772	951	1240	8	39	3326	620	650	6	0	1650	478	522	7	0	1608

Table 3.14. The same as in table 3.13, but for station P4.

		P4. Nanoeukaryotes (cells/ml)																			
		Winter			Spring			Summer			Autumn										
Prof	Depth	Mean	σ	n	Min.	Max.	Mean	σ	n	Min.	Max.	Mean	σ	n	Min.	Max.					
0	0	2006	617	4	1010	2573	1221	483	6	589	1899	1103	633	3	638	1998	978	420	5	185	1362
10	10	1985	676	4	1000	2898	1310	464	6	596	2032	1642	791	3	842	2719	1236	601	5	437	2246
20	20	1856	612	3	1054	2539	1323	739	6	213	2645	1223	399	3	712	1686	989	522	4	156	1596
50	50	922	509	4	222	1509	1231	782	6	111	2057	258	54	3	189	320	232	155	5	51	479
75	75	720	596	4	102	1704	619	404	6	72	1384	304	182	3	120	551	145	103	5	24	290
100	100	377	198	4	42	545	172	150	6	30	461	155	65	3	99	246	74	94	5	9	260

		P4. Picoeukaryotes (cells/ml)																			
		Winter			Spring			Summer			Autumn										
Depth	Prof	Mean	σ	n	Min.	Max.	Mean	σ	n	Min.	Max.	Mean	σ	n	Min.	Max.					
0	0	13613	4188	4	8427	18954	6574	4839	6	1536	16383	12900	5401	3	6317	19546	9386	3695	5	2700	13073
10	10	12279	3500	4	8422	15978	9285	5993	6	1605	17621	16420	6061	3	8511	23236	10097	5792	5	2749	16336
20	20	10205	3092	3	7721	14563	7496	6371	6	1112	19706	15402	5964	3	7041	20542	9522	8159	4	823	19938
50	50	7545	6121	4	665	16809	5953	5793	6	177	15665	1677	411	3	1377	2258	1738	1605	5	278	4788
75	75	3392	3358	4	237	8925	2088	2967	6	156	8602	2806	2909	3	153	6856	484	350	5	36	895
100	100	1085	855	4	78	2443	410	461	6	9	1228	590	311	3	266	1009	171	186	5	36	515

P4. Prochlorococcus (cells/ml)																				
Depth	Winter				Spring				Summer				Autumn							
	Mean	σ	n	Min.	Max.	Mean	σ	n	Min.	Max.	Mean	σ	n	Min.	Max.	Mean	σ	n	Min.	Max.
0	12208	18745	4	557	44649	1174	1479	6	12	431	12362	5121	3	5239	17060	18123	15498	5	2719	47656
10	11938	16825	4	1016	41034	2632	3415	6	44	9803	13693	5615	3	6018	19293	17331	12845	5	5608	42099
20	9824	12629	3	838	27685	7222	10731	6	47	30057	18017	4312	3	14163	24037	10311	7129	4	3350	21896
50	2996	3960	4	323	9830	7154	7378	6	90	19646	6629	4818	3	1542	13099	3352	2110	5	362	6695
75	1223	1446	4	198	3695	4058	3965	6	21	9072	2948	2895	3	485	7012	919	620	5	69	1635
100	958	1417	4	0	3407	607	591	6	21	1689	947	780	3	0	1910	257	223	5	36	557

P4. Synechococcus (cells/ml)																				
Depth	Winter				Spring				Summer				Autumn							
	Mean	σ	n	Min.	Max.	Mean	σ	n	Min.	Max.	Mean	σ	n	Min.	Max.	Mean	σ	n	Min.	Max.
0	15796	11486	4	3437	34153	32020	36001	6	160	109558	16167	9901	3	7875	30084	15411	7857	5	6467	25327
10	13024	8518	4	3096	25568	26838	30283	6	65	92040	17610	11011	3	8829	33138	14840	8918	5	1943	26448
20	10700	5521	3	2916	15128	11764	7181	6	415	22547	11130	2445	3	7774	13532	14958	10780	4	404	30634
50	5113	4238	4	611	11342	10166	11182	6	1066	33953	2349	826	3	1249	3240	2025	2339	5	311	6632
75	2554	1522	4	278	4515	3132	2215	6	817	7485	1704	1115	3	395	3120	570	412	5	129	1287
100	1290	898	4	201	2536	1004	676	6	50	1856	852	361	3	515	1353	316	169	5	201	653

Table 3.15. The same as in table 3.13, but for the station CG2.

CG2. Nanoeukaryotes (cells/ml)																				
Depth	Winter					Spring					Summer					Autumn				
	Mean	σ	n	Min.	Max.	Mean	σ	n	Min.	Max.	Mean	σ	n	Min.	Max.	Mean	σ	n	Min.	Max.
0	1755	533	4	850	2222	1059	645	5	161	2013	698	164	6	509	1000	987	489	5	269	1729
10	1777	495	4	925	2156	1260	512	5	588	1805	643	186	6	458	994	1036	585	5	229	1876
20	1931	649	4	814	2425	1154	495	4	605	1853	621	101	6	486	740	778	301	5	458	1161
50	1505	478	4	785	2018	1261	640	5	192	1980	1449	1349	6	410	4324	677	509	5	60	1601
75	302	143	4	195	548	907	802	4	54	2207	380	279	6	132	785	232	141	5	69	416

CG2. Picoeukaryotes (cells/ml)																				
Depth	Winter					Spring					Summer					Autumn				
	Mean	σ	n	Min.	Max.	Mean	σ	n	Min.	Max.	Mean	σ	n	Min.	Max.	Mean	σ	n	Min.	Max.
0	7409	6817	4	934	18799	1696	1700	5	593	5019	1117	463	6	668	1922	3104	3347	5	557	9581
10	7547	6549	4	946	18346	1687	1387	5	646	4381	1096	532	6	734	2144	3192	2730	5	592	7647
20	7457	5761	4	1066	16747	2018	1393	4	728	4340	1241	817	6	548	2949	2107	1061	5	814	3575
50	4662	2290	4	988	7240	2007	1240	5	894	4192	3279	4155	6	729	12528	3648	2162	5	1099	6900
75	1653	2190	4	204	5435	1399	1260	4	162	3273	1614	1320	6	299	4081	5124	7945	5	257	20960

CG2. Prochlorococcus (cells/ml)																				
Depth	Winter					Spring					Summer					Autumn				
	Mean	σ	n	Min.	Max.	Mean	σ	n	Min.	Max.	Mean	σ	n	Min.	Max.	Mean	σ	n	Min.	Max.
0	5592	6211	4	488	16222	1535	1627	5	0	4167	8178	10895	6	389	29072	19365	12754	5	0	35296
10	4701	3047	4	293	8287	2086	2300	5	120	6418	5676	5609	6	1835	18100	18003	13101	5	0	40482
20	5664	3336	4	335	8856	1711	734	4	775	2762	7541	5438	6	2068	16934	14809	12668	5	0	37052
50	2612	2735	4	701	7314	11003	15898	5	614	42484	11726	6006	6	3337	20123	12126	10292	5	1207	30637
75	1121	644	4	135	1838	4870	7810	4	0	18383	7957	7567	6	1512	21959	6123	3438	5	2308	12360

CG2. <i>Synechococcus</i> (cells/ml)																							
Depth	Winter						Spring						Summer						Autumn				
	Mean	σ	n	Min.	Max.	Mean	σ	n	Min.	Max.	Mean	σ	n	Min.	Max.	Mean	σ	n	Min.	Max.			
0	18052	9461	4	11602	34359	27198	30480	5	26	83516	18842	8412	6	280	25135	80574	111735	5	9921	303352			
10	17944	6908	4	12638	29776	31817	26806	5	408	81720	23512	16015	6	116	54483	26016	9832	5	8718	36531			
20	18192	3953	4	14968	24904	30195	13116	4	16270	51758	30373	21186	6	11096	75162	19509	10078	5	5853	34616			
50	14973	5390	4	7743	22926	32470	14880	5	5967	48046	19453	13683	6	5054	43937	9582	8570	5	755	25812			
75	7165	9431	4	985	23479	8108	8889	4	880	23146	5191	5345	6	665	15553	1945	1350	5	425	4102			

Table 3.16. The same as in table 3.13, but for station CG4.

CG4. Nanoeukaryotes (cells/ml)																							
Depth	Winter						Spring						Summer						Autumn				
	Mean	σ	n	Min.	Max.	Mean	σ	n	Min.	Max.	Mean	σ	n	Min.	Max.	Mean	σ	n	Min.	Max.			
0	1754	423	3	1158	2087	1347	678	5	469	2335	658	365	5	266	1274	668	272	4	401	1119			
10	1941	606	3	1125	2577	1232	704	5	498	2450	713	490	5	347	1674	701	341	4	302	1240			
20	2197	522	3	1465	2646	1262	582	5	490	2211	733	349	5	359	1299	956	342	4	494	1410			
50	1347	716	3	500	2251	1681	1320	5	488	4248	1367	683	5	474	2389	1584	1583	4	120	4123			
75	566	132	3	380	677	704	419	5	117	1207	765	332	5	305	1147	499	524	4	165	1404			
100	240	71	3	159	332	186	115	5	39	359	175	56	5	102	274	101	18	4	72	120			

CG4. Picoeukaryotes (cells/ml)																							
Depth	Winter						Spring						Summer						Autumn				
	Mean	σ	n	Min.	Max.	Mean	σ	n	Min.	Max.	Mean	σ	n	Min.	Max.	Mean	σ	n	Min.	Max.			
0	5199	3579	3	2126	10219	8747	15510	5	596	39762	922	290	5	611	1357	1531	568	4	859	2230			
10	5150	3935	3	2014	10699	1307	726	5	620	2690	1361	613	5	602	2332	1466	556	4	725	2203			
20	5525	3935	3	2287	11063	1366	694	5	665	2592	8235	14391	5	416	37008	1896	558	4	1019	2515			
50	2924	1499	3	1263	4895	3700	2392	5	838	7883	3157	1931	5	1141	6072	3955	2069	4	1269	7087			
75	1211	524	3	778	1949	1293	764	5	512	2643	1677	1008	5	596	3524	714	567	4	216	1596			
100	534	263	3	174	793	260	154	5	78	473	613	345	5	290	1238	281	272	4	15	737			

CG4. Prochlorococcus (cells/ml)																				
Depth	Winter				Spring				Summer				Autumn							
	Mean	σ	n	Min.	Max.	Mean	σ	n	Min.	Max.	Mean	σ	n	Min.	Max.	Mean	σ	n	Min.	Max.
0	1712	1305	3	631	3547	513	446	5	57	1311	2709	2757	5	347	8075	25480	19225	4	0	47520
10	1996	1933	3	577	4729	558	569	5	0	1309	3194	3040	5	700	9126	32044	21243	4	0	57854
20	5430	6433	3	741	14526	1956	2561	5	0	6906	2532	966	5	857	3497	32728	22874	4	0	59438
50	7890	9759	3	195	21659	5551	4980	5	487	14140	10837	6264	5	4566	22661	12993	5951	4	2904	17531
75	1445	1360	3	347	3362	4853	2500	5	407	7381	7791	7189	5	766	20939	2044	911	4	1099	3000
100	1544	1855	3	147	4165	1378	1598	5	117	4180	5471	7725	5	928	20874	1558	1400	4	266	3907

CG4. Synechococcus (cells/ml)																				
Depth	Winter				Spring				Summer				Autumn							
	Mean	σ	n	Min.	Max.	Mean	σ	n	Min.	Max.	Mean	σ	n	Min.	Max.	Mean	σ	n	Min.	Max.
0	24509	13212	3	6729	38373	14804	11993	5	434	29678	30319	12034	5	13539	49665	34775	6920	4	23479	42023
10	25273	15005	3	5077	41010	23792	14039	5	368	43266	23207	12246	5	7892	43167	35753	7558	4	22832	41801
20	29733	18237	3	5615	49704	23267	14425	5	70	43173	22928	8300	5	14012	34688	38499	11394	4	21048	52522
50	22020	12414	3	6419	36792	24203	17204	5	13649	58454	31204	19251	5	5033	55074	5582	4335	4	793	12605
75	6230	2635	3	3814	9895	10640	16310	5	1179	43228	10905	16130	5	1925	43100	913	593	4	296	1605
100	1996	612	3	1467	2853	1354	475	5	689	2174	1407	1138	5	332	3465	289	82	4	174	401

Table 3.17. Average abundances, expressed as individuals per cubic meter, for the main meso-zooplanktonic groups for station P2. For each season five columns are presented: mean seasonal value, standard deviation, number of data used and minimum and maximum values recorded along the complete time series.

Group	P2. Meso-zooplanktonic abundance (individuals/m ³).																			
	Winter					Spring					Summer					Autumn				
	Mean	σ	n	Min.	Max.	Mean	σ	n	Min.	Max.	Mean	σ	n	Min.	Max.	Mean	σ	n	Min.	Max.
Copepods	366	229	8	37	783	401	408	10	53	1120	420	265	9	101	872	416	312	10	41	1146
Appendicularians	74	58	8	0	162	37	54	10	1	172	80	87	9	3	266	51	35	10	8	108
Cladocerans	22	18	8	0	51	17	15	10	0	40	577	883	9	7	2538	240	465	10	2	1601
Doliolids	32	54	8	0	170	26	61	10	0	204	39	60	9	0	202	17	20	10	0	69
Chaetognaths	19	16	8	2	47	9	11	10	0	32	35	47	9	3	165	46	85	10	0	296
siphonophores	6	4	8	1	15	10	15	10	2	53	13	9	9	2	35	9	15	10	1	52
Ostracods	8	9	8	1	32	8	7	10	2	20	52	99	9	0	327	11	8	10	3	32
Scyphozoans	0	1	8	0	3	1	2	10	0	6	1	4	9	0	12	0	1	10	0	3
Biomass (mg/m ³)	16.1	12.0	12	1.7	38.1	12.0	10.9	13	0.2	35.8	18.8	28.4	12	0.4	100.6	10.7	6.0	11	0.9	21.6

Table 3.18. The same as in table 3.17, but for the station CG2.

Group	CG2. Abundancia zooplanctónica (individuos/m ³).																			
	Winter					Spring					Summer					Autumn				
	Mean	σ	n	Min.	Max.	Mean	σ	n	Min.	Max.	Mean	σ	n	Min.	Max.	Mean	σ	n	Min.	Max.
Copepods	825	38	2	787	862	941	426	1	426	825	38	2	787	862	941	310	310	1	1	1146
Appendicularians	112	60	2	52	172	46	177	1	177	112	60	2	52	172	46	0	0	1	1	108
Cladocerans	64	9	2	55	72	6	324	1	324	64	9	2	55	72	6	272	272	1	1	1601
Doliolids	84	84	2	0	167	3	312	1	312	84	84	2	0	167	3	29	29	1	1	296
Chaetognaths	37	34	2	3	71	0	90	1	90	37	34	2	3	71	0	287	287	1	1	296
siphonophores	14	3	2	11	16	32	21	1	21	14	3	2	11	16	32	31	31	1	1	52
Ostracods	2	2	2	0	3	0	3	1	3	2	2	2	0	3	0	0	0	1	1	32
Scyphozoans	2	2	2	0	3	0	144	1	144	2	2	2	0	3	0	6	6	2	0	12
Biomass (mg/m ³)	7.5	2.9	2	4.6	10.4	4.5	6.2	2	3.1	5.9	6.2	4.0	2	2.2	10.2	6.0	0.4	2	5.6	6.4

4. CAPE PALOS AND BALEARIC ISLANDS.

The following geographical area monitored in the frame of RADMED Project is Cape Palos, located to the northeast of Cape Gata and the Alboran Sea. (Fig. 4.1).

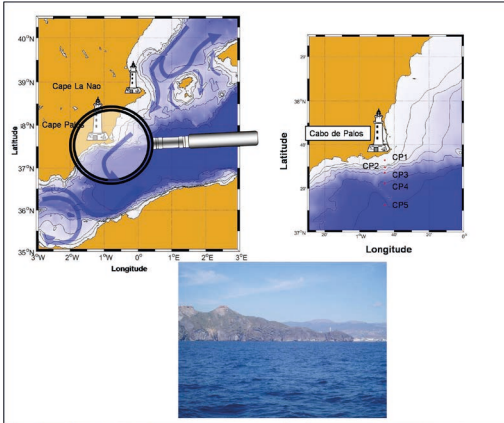


Figure 4.1. Geographical location of Cape Palos. On the right, position of the oceanographic stations sampled in Cape Palos transect. Picture obtained during the sampling of Cape Palos transect during a RADMED campaign.

Cape Palos transect extends southwards from the Cape of the same name. This transect includes some stations already sampled in the frame of the former Project ECOMURCIA, and some new stations added in RADMED project. To the north of Cape Palos, the main geographical features are the capes San Antonio and La Nao, in Alicante province. This part of the Spanish eastern coast is separated from Ibiza (Balearic Islands) by the Ibiza Channel. The Mallorca Channel separates Ibiza and Mallorca Islands, and finally, the Menorca Island is at the easternmost sector of the Balearic Archipelago (Fig. 4.2).

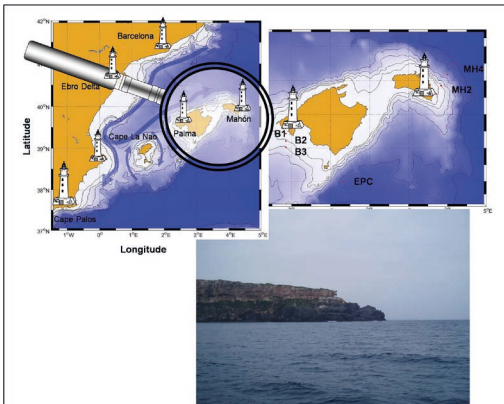


Figure 4.2. Balearic Archipelago map. To the right, position of the oceanographic stations sampled in the Mallorca and Mahon transects and the Cabrera Deep Station. Picture of the Menorca coast during a RADMED campaign.

The RADMED Project includes several transects within the Balearic Sea. Stations B1, B2 and B3 extend southwards from Mallorca Island. This transect is named as Mallorca transect (B), and it belonged to the former ECOBALEARES project initiated in 1994 (fig. 4.2). Deep Cabrera Station (EPC, from Spanish Estación Profunda de Cabrera, fig. 4.2) is located to the south of Cabrera Island. Only CTD profiles are carried out at this station. This station has a depth of 2300 m, being appropriate for monitoring the temperature and salinity of deep Mediterranean waters. Mahon transect extends

northeastwards from the Menorca Island. This transect is fully multidisciplinary.

As already shown in chapter 2, there are 37 oceanographic stations in the Ibiza and Mallorca Channels, forming two triangles. These stations belonged to the former CIRBAL project, oriented to the study of the circulation and thermohaline properties of the water masses within the Balearic Channels. Initially, this project was oriented towards the physical oceanography. In order to complete a multidisciplinary monitoring along the peninsula continental shelf and slope, a multidisciplinary sampling was implemented at stations C20 and C18, within the base of the triangle of the Ibiza Channel (Fig. 4.3). The sampling at these stations includes CTD profiles and samples for the determination of the concentrations of chlorophyll-a, dissolved oxygen, inorganic nutrients and the abundance of phyto and zooplanktonic communities.

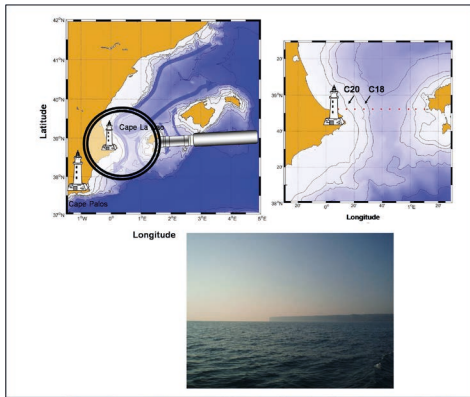


Figure 4.3. Map of the Ibiza Channel. To the right, position of the multidisciplinary stations from the Ibiza Channel (C20 and C18). Picture of San Antonio Cape during a RADMED campaign.

All this area, including Cape Palos and Balearic Islands, could be considered as a transition area between the waters located to the south, in the Alboran Sea and the Algerian basin, and those waters located to the north, in front of the Catalan coast and close to the Gulf of Lions. The former zone would be characterized by the influence of the Atlantic Water that flows through the Strait of Gibraltar. The latter area is filled by waters with a much higher degree of modification caused by a longer residence time within the Mediterranean Sea. In order to clarify these differences, the following paragraphs include a review of the main features of the circulation in this area.

As already described in the previous chapter, the Atlantic Water (AW) usually forms two anticyclonic gyres within the western and eastern sub-basins of the Alboran Sea. After surrounding the eastern one, the Atlantic Current continues along the Algerian continental slope forming the so called Algerian Current. This current is unstable and both cyclonic and anticyclonic gyres detach from it. The anticyclonic ones are usually larger and have a longer life time being an efficient means for the northward transport of AW (Millot, 1999). These gyres can reach the Balearic Channels.

The Algerian Current splits in two branches at the Sicily Channel. One branch flows into the Eastern Mediterranean where it will finally be transformed into Levantine Intermediate Water (LIW). The other branch gets into the Tyrrhenian Sea where it describes a cyclonic circuit. When the AW reaches the Corsica Channel, it partially flows through it. Another part of the AW completes a cyclonic circuit in the Tyrrhenian Sea and finally exits to the south of Sardinia, then turns northwards and flows along the western coasts of Sardinia and Corsica, and finally merges with the AW that flows through the Corsica Channel. When both branches merge, they receive the name of Northern Current (Fig. 1.4 in the introduction chapter).

The Northern Current flows along the Ligurian Sea, the continental slope in front of the Gulf of Lions and finally turns southwards along the continental slope of Catalonia. This current continues its pathway southwards until the Gulf of Valencia. Here, a branch of it crosses southwards the Ibiza Channel, while a second branch turns northeastwards flowing along the northern slope of the Balearic Islands, forming the Balearic Current. According to this circulation scheme, the RADMED C20 and C18 oceanographic stations would be affected by the current that flows through the Ibiza Channel, whereas those stations in the Mahon transect (MH) would be affected by the Balearic Current. In both cases, these Atlantic waters would be severely modified because of the long residence time in the Western Mediterranean and the effect of evaporation and mixing with the Mediterranean waters that flow beneath the AW. Furthermore, the Northern Current describes a cyclonic gyre in front of the Gulf of Lions. This cyclonic circulation upwells the LIW towards the sea surface reducing the stability of the water column. This fact and the intense cold and dry winds that blow in winter in this region of the Mediterranean Sea are responsible of the formation of deep waters. The centre of the deep water formation area is around 42 °N, 5 °E (Leaman and Schott, 1991; Anati and Stommel, 1970; MEDOC Group, 1970). All these factors contribute to the high salinity of surface waters in winter in the Balearic Sea. Such salinity values are over 38 psu, while the temperature at the sea surface is close to 13 °C.

The continental shelf of the regions close to the Gulf of Lions, such as the Catalan coast, receives fresh water inputs from rivers such as Rhone and Ebro. This fresh water supply reduces the salinity of coastal waters that do not reach the high values of the open sea waters. On the other hand, the continental shelf waters have a maximum depth of 200 m and therefore are out of the influence of the LIW that flows between 200 and 600 m depth. Consequently, the continental shelf waters increase their salinity because of the action of the cold and dry winds that blow from the continent, but not

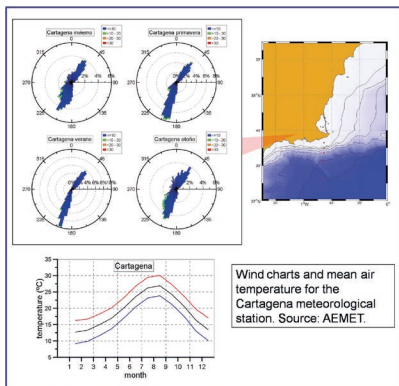
as much as those at the open sea. The temperature of shelf waters decreases considerably in winter because of the action of winter storms. This cooling could be even more intense than the one affecting the open sea because it affects to a smaller water volume. Continental shelf water temperature can decrease below 13 °C and reach values as low as 11 °C. The final result is the formation of a new water mass, called Western Intermediate Water (WIW) which salinity is in the range 37.7-38.3 psu and its temperature is below 13 °C. This water mass is denser than the AW and sinks below it, but its density is lower than the LIW one, and consequently it flows over it occupying approximately the 100-200 m layer. (Juza et al., 2019; Vargas-Yáñez et al., 2012a; Pinot y Ganachaud, 1999; López-Jurado et al., 1995; López-Jurado, 1990; Salat and Font, 1987).

According to the previous description, it could be expected that those waters to the north of the Balearic Islands would have a higher salinity and lower temperature in winter than those to the south of the islands (transect B, Mallorca transect), being the latter affected by the AW transported by the anticyclonic gyres detached from the Algerian Current. However, the actual situation is not as simple, as there is an important water exchange through the Balearic Channels (figures 4.2 and 4.3). This water exchange produces fluctuations in the position of the transition zone between the waters with a higher influence of the AW and those waters with a higher degree of modification.

The circulation of the surface layer and the processes of deep and intermediate water formation, have other consequences, besides the modification of the temperature and salinity of the water masses. Deep and intermediate water formation leads to the homogenization of the water column. In this way, deep nutrient-rich waters are mixed with surface waters having a fertilizing effect during winter. Such processes generate vertically homogeneous distributions of nutrients, chlorophyll and oxygen. When stormy conditions cease during spring, a phytoplanktonic bloom is observed. This bloom is characterized by the dominance of diatoms and high primary production rates. Besides this, the Rhone and Ebro runoff supplies nutrients to surface waters also contributing to the enhancement of the primary production.

The southward extension of the Northern Current along the Catalan continental slope and the Balearic Current generate two frontal zones with upwelling of water masses that favors the injection of nutrients into the photic layer and the increase of primary production. These fronts are known as the Catalan and Balearic fronts. Such oceanographic structures would not affect the waters located to the south of the islands. Cape Palos is located further to the south. The main current flowing southwards along the Spanish continental slope is not named as the Northern Current at this latitude. This current turns to the east at some place close to Cape Palos in order to complete a cyclonic circuit in the Western Mediterranean. This region is neither affected by the Almeria-Oran front, further to the south, nor by the effects of the Catalan and Balearic fronts and the intense northerly storms. It could be expected that this region will be more oligotrophic than those regions to the north of the islands. In fact, the oligotrophy of the Mediterranean Sea increases both eastwards and southwards (Lavigne et al., 2015; Siokou-Frangou et al., 2010).

4.1 Meteorological conditions.



Hourly data of wind intensity and direction were obtained from the Cartagena meteorological station (AEMET). Daily average intensity and direction were then calculated. Daily minimum, mean and maximum temperatures were also obtained. Figure 4.4 shows the seasonal wind charts for this station, expressing the direction for daily winds as percentages. The color scale indicates the wind intensity in km/h. Also in figure 4.4 are included the daily minimum, mean and maximum temperatures averaged for each month of the year.

Figure 4.4. Wind charts and air temperature for the Cartagena meteorological station. The direction of origin of winds is expressed as percentages and the color scale indicates their intensity: lower than 10 km/h in blue, between 10 and 20 km/h in green, between 20 and 30 km/h in orange, and higher than 30 km/h in red. The wind chart in the upper left corner corresponds to winter, at the upper right one to spring, lower left corner is for summer and the lower right corner is for autumn. The lower plot is for the daily minimum (blue), mean (black) and maximum (red) temperatures averaged for each month of the year.

The lowest air temperatures are recorded in January when the daily minimum is 9.2 °C and the maximum is 16.3 °C. The daily mean temperature averaged for January is 12.7 °C. The highest values are reached in August. Daily minimum, maximum and mean values for this month are 23.9 °C, 30.1 °C and 26.9 °C respectively.

Wind direction is polarized in the southwest-northeast direction. Notice that wind intensity is not very high, especially during spring and summer when it is lower than 10 km/h.

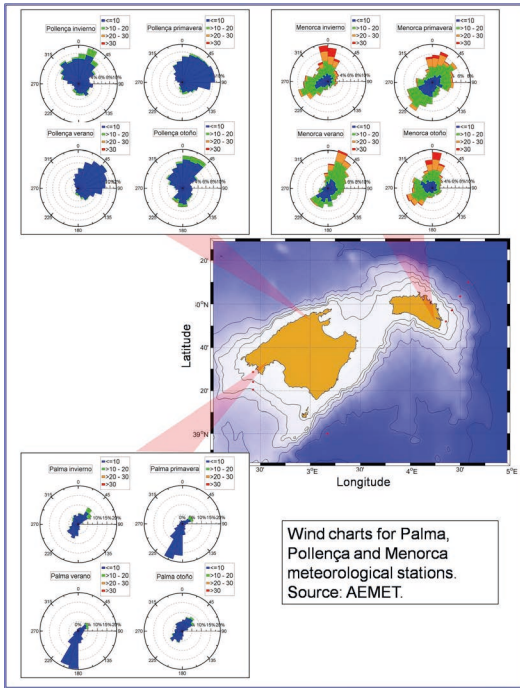


Figure 4.5. Wind charts for the Pollença, Menorca and Palma (Porto Pi) meteorological stations. The direction of the origin of the winds is expressed as percentages and the color scale indicates the intensity (see figure 4.4 legend).

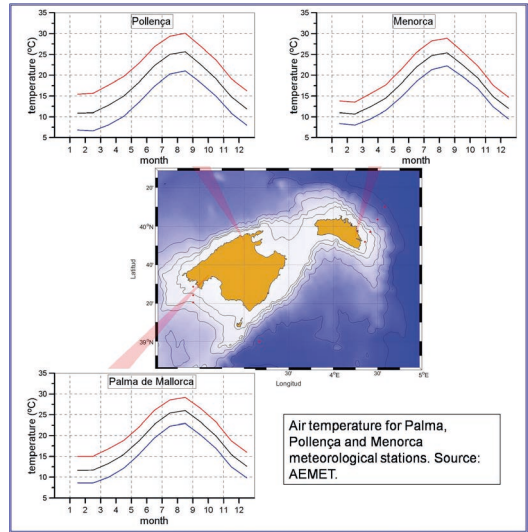


Figure 4.6. Daily minimum (blue), mean (black) and maximum (red) temperatures averaged for each month of the year at Pollença, Menorca and Palma (Porto Pi) stations.

Figures 4.5 and 4.6 show the wind charts for each season and the air temperatures averaged for each month for Palma de Mallorca (Porto Pi), Pollença and Menorca (source AEMET).

Figure 4.5 shows that at the northern part of Mallorca Island, the prevailing wind direction is north. Only in autumn there is an increase of the southerly winds. In Menorca, northeast and southwest winds alternate throughout the year with the only exception of winter, when the wind blows from the north and southwest. It should be noticed that the wind intensity in Menorca is higher than the one at the other locations, being frequent wind intensities higher than 30 km/h. Storms are mainly from the north. At the southern part of Mallorca Island (Porto Pi, Palma), the prevailing direction is southwest, although winds from the northeast are also recorded, mainly in winter. The wind intensity at this location is much lower than in Menorca, being in most of the cases lower than 10 km/h.

Minimum temperatures are observed in January and February. Daily mean values for these months range between 10.7 °C in Menorca and 11.7 °C in Palma. The lowest daily minimum temperatures are recorded in Pollença, 6.8 °C, and the highest ones in Palma, 8.6 °C. Finally, the highest temperatures correspond to August, with daily maximum values of 28.9 °C, 30.1 °C and 29.2 °C in Menorca, Pollença and Palma respectively.

4.2 Water masses.

Figure 4.7 shows the average TS diagrams for the stations CP2 and CP4 at the Cape Palos continental shelf and slope. These diagrams show a salinity increase with respect to the Alboran Sea stations, as expected because of their longer distance to the Strait of Gibraltar. The surface salinity reaches maximum values in winter and spring, 37.7 psu and 37.8 psu respectively, it descends in summer and has the minimum values in autumn: 37.28 psu. At 75 m depth, the salinity values range between 38.15 and 38.0 psu, corresponding the minimum values, once more, to autumn. Salinity decreases seawards. At station CP4, the salinity has the lowest values in autumn along the upper 100 m of the water column (the only exception is observed at the sea surface). It is important to note that the surface salinity at station CP4 is lower than 37.5 psu. Such value is frequently considered as the interface between Atlantic and Mediterranean waters. This result would indicate that the Cape Palos area is not affected by surface waters that have recirculated along the Western Mediterranean. On the contrary, this region would be affected by Atlantic waters recently advected from the Strait of Gibraltar.

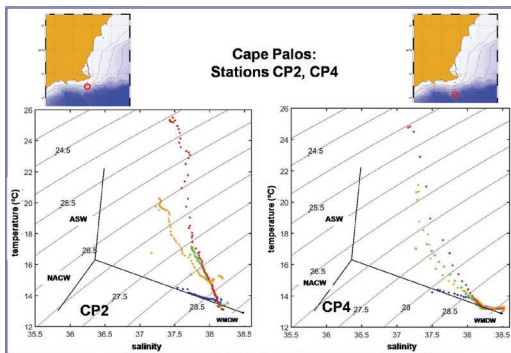


Figure 4.7. Average TS diagrams for winter (blue), spring (green) and summer (red) and autumn (light brown) obtained from all the available potential temperature and salinity profiles from RADMED project in stations CP2 and CP4 from Cape Palos transect.

The summer salinity decrease and the following minimum during autumn, were already described for the Alboran Sea in the previous chapter. In the case of the Alboran Sea, there is a change in the wind direction during the summer months, when the prevailing direction shifts from west to east. This would explain the accumulation of AW against the coast and the salinity decrease. The other hypothesis proposed is a larger development of the two anticyclonic gyres that occupy most of

this basin. The prevailing winds during summer and autumn in Cartagena meteorological station (very close to Cape Palos, Fig. 4.4) alternate the southwest and northeast direction, being this behavior similar to that observed throughout the rest of the year. This fact would support the hypothesis that the progressive increase of the AW influence at the coasts of the northern Alboran Sea and Cape Palos, during summer and autumn, is not caused by the wind, but associated to a change in the surface circulation. The Atlantic Current would be displaced northwards, with a larger size of the Alboran Sea anticyclonic gyres and also with a larger transport of AW from the Algerian Current by means of the gyres detached from such a current.

The depth of station CP4 allows us to observe the presence of the LIW, with TS values of 13.23-13.31 °C and 38.52-38.53 psu, and the Western Mediterranean Deep Water (WMDW) at the bottom of this station with values of 12.88-12.90 °C and 38.48-38.49 psu. The temperature relative minimum, above the maximum associated to the LIW, indicates the presence of WIW (Fig. 4.7).

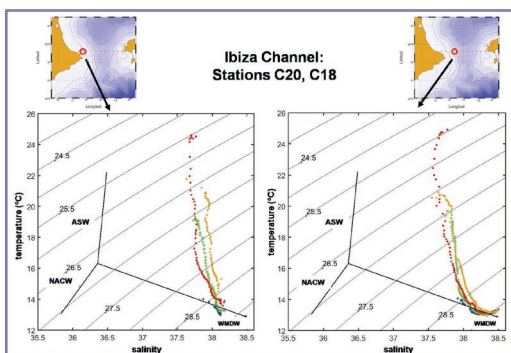


Figure 4.8. The same as in figure 4.7, but for stations C20 and C18 in the Ibiza Channel.

Figure 4.8 shows the average TS diagrams for the stations C20 and C18 at the peninsular continental shelf and slope of the Ibiza Channel. The salinity at the sea surface shows the gradient that exists at the region covered by the RADMED project. At station C20, the salinity ranges between 38.06 psu in winter and 37.71 psu in summer. Salinity decreases seawards, as in the case of Cape Palos and oscillates between 37.98 psu in winter and 37.68 psu in summer. A first difference between the Ibiza Channel stations and those already analyzed,

is that the lowest salinity is observed in summer. The other difference is that the salinity is over 37.5 psu during all the seasons. These differences evidence the higher Mediterranean influence to the north. Another important feature in the water masses of the Ibiza Channel is the presence of very cold waters with temperatures lower than 13 °C in winter at 80 m depth and with salinity values around 38.1 psu. Such values are found at 50 m depth at station C18. These salinity and temperature values suggest the formation of WIW in the continental shelf in areas close to the Ibiza Channel.

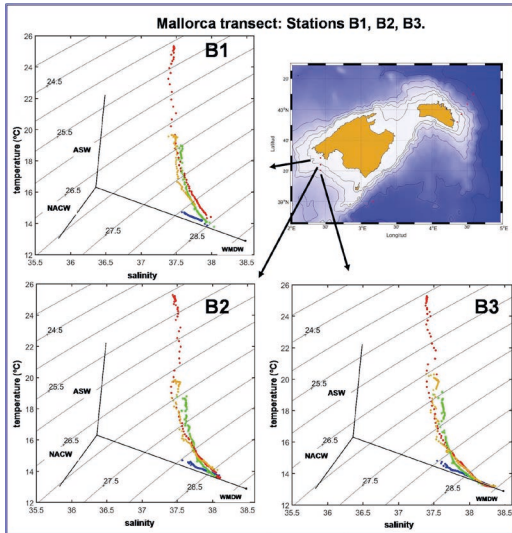


Figure 4.9. The same as in figure 4.7, but for the stations B1, B2 and B3 in the Mallorca transect.

In Mallorca transect (B), to the south of Mallorca Island, the salinity is lower than in the peninsular part of the Ibiza Channel, and quite similar to that found in Cape Palos transect. The lowest values are observed in summer. During summer and also during autumn, the surface salinity is lower than 37.5 psu. The lower salinity values in the eastern sector of the Ibiza Channel (B1, B2 and B3 stations) when compared with those at the western part of it (C20 and C18), could be related to the circulation through the Channels that has been depicted in the schemes of figures 4.1, 4.2 and 4.3 (Pinot and Ganachaud, 1999; Pinot et al., 1995). According to this scheme, the southward extension of the Northern Current would flow along the peninsular side of the Ibiza Channel, whereas the AW intrusions would occur along the eastern side of it, close to Mallorca Island.

The salinity increases at the Mahon transect (Fig. 4.10), evidencing the presence of AW with a higher degree of modification. Its seasonal cycle is similar to that already described for the other transects and it shows a decrease during summer and autumn. There is a sharp decrease of the temperature during winter, above the position of the LIW, indicating the presence of WIW. The temperature and salinity values for the LIW at station MH4 are 13.17-13.23 °C and 38.52-38.55 psu, whereas at the bottom, the TS values, corresponding to the WMDW, are 12.89-12.9 °C and 38.49 psu.

Cabrera Deep Station (Fig. 4.11) shows the influence of WIW in spring (green dots) and LIW and WMDW values similar to those found at stations CP4 and MH4: 13.2 °C and 38.52-38.53 psu (LIW) and 12.88-12.89 °C and 38.48-38.49 psu (WMDW).

As in the case of the Alboran Sea (chapter 3) and as it will be done for the Catalan waters (chapter 5), the average values obtained for each station are presented in tables 4.1 to 4.10 at the end of this chapter.

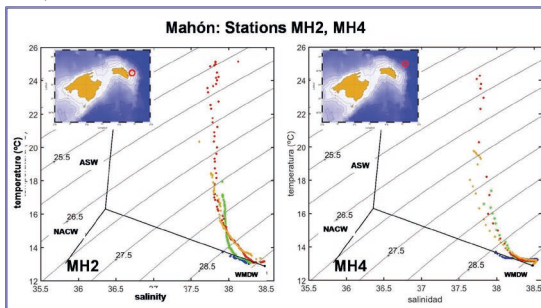


Figure 4.10. The same as in figure 4.7, but for the stations MH2 and MH4 at the Mahon transect.

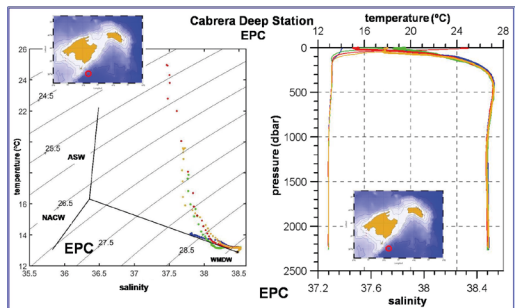


Figure 4.11. TS Diagram (left) and average vertical profiles of potential temperature and salinity (right) at the Cabrera Deep Station (EPC from the Spanish acronym) for the four seasons: winter (blue), spring (green), summer (red) and autumn (light brown).

4.3 Dissolved oxygen, nutrient and chlorophyll-a distributions.

Figures 4.12 and 4.13 show the seasonally averaged vertical profiles for the concentrations of chlorophyll-a, dissolved oxygen, nitrate and nitrite for the stations CP2 and CP4 in Cape Palos transect. Figures 4.14 and 4.15 correspond to stations C20 and C18 in the peninsular side of the Ibiza Channel. Both areas are occupied by waters poorer than those described in the Alboran Sea. At station CP2, over the Cape Palos continental shelf, surface nitrate concentrations are very low from winter to summer. Such concentrations only experience a significant increase in autumn, when they are over 1 μM (Fig. 4.12). Phosphate concentrations are also quite low throughout the year and along the whole water column (up to 75 m depth), with the only exception of autumn, when concentrations are as high as 0.16 μM for depths greater than 50 m (table 4.11). Nitrite shows a Primary Nitrite Maximum (PNM) throughout the year. Its depth ranges between 50 and 75 m (see figure 4.12 and table 4.11).

The chlorophyll vertical distribution reflects the nutrient scarcity. A Deep Chlorophyll Maximum (DCM) is present from winter to summer at 50 or 75 m depth. The chlorophyll concentrations at the DCM range between 0.28 and 0.5 mg/m^3 , being these values much lower than those estimated for the Alboran Sea. During autumn, the highest chlorophyll concentrations are observed at the sea surface, coinciding with the nutrient increase at the surface layer. In this case the surface chlorophyll concentration is 0.5 mg/m^3 . The vertical distributions of dissolved oxygen are rather erratic and there is not a clear relation between the DCM position and the position of the oxygen maximum. This behavior could be related to the high time variability of coastal waters and the short length of the available time series.

Nutrient, chlorophyll and dissolved oxygen vertical profiles at station CP4 have a more regular shape (Fig. 4.13). The highest nitrate values are observed in winter, when the highest chlorophyll and dissolved oxygen concentrations are also observed on the sea surface. However, such values are relatively low (0.4 mg/m^3). During spring, summer and autumn, the surface nitrate concentrations decrease and a DCM is developed at 50, 75 and 20 m depth, respectively. The maximum dissolved oxygen concentration is located over the chlorophyll maximum (20, 50 and 0 m). Phosphate concentrations are quite similar at the sea surface throughout the year (table 4.12). Nitrite concentrations show a PNM during all the seasons between 50 and 75 m depth. During some seasons, as in the case of summer, a second nitrite maximum is observed at 500 m depth, associated to the presence of the LIW (Fig. 4.13).

The depth of station CP4 allows us to observe the increase of nitrate, nitrite, phosphate and silicate with depth. These concentrations reach maximum values between 300 and 700 m. Nitrate concentrations can be over 10 μM and phosphate ones over 0.75 μM . Silicate concentrations increase continuously to the sea bottom where they reach values between 8.55 and 10 μM .

At both stations CP2 and CP4, the concentration of dissolved oxygen at the sea surface follows a seasonal cycle with minimum values in summer and maximum ones in winter and spring. This indicates that this cycle is strongly influenced by the sea temperature and its influence on the solubility of gasses.

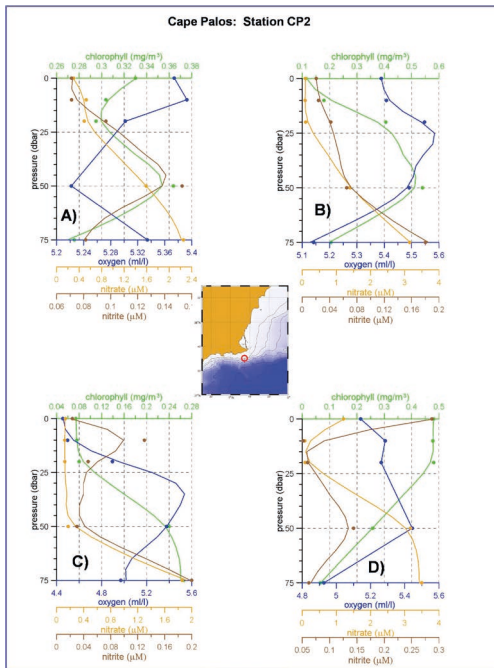


Figure 4.12. Average vertical profiles for the station CP2 obtained using all the available profiles from RADMED Project. Green line corresponds to chlorophyll-a, blue line to dissolved oxygen, light brown line to nitrate and dark brown line to nitrite. Figure 4.12A corresponds to winter, B to spring, C to summer and D to autumn.

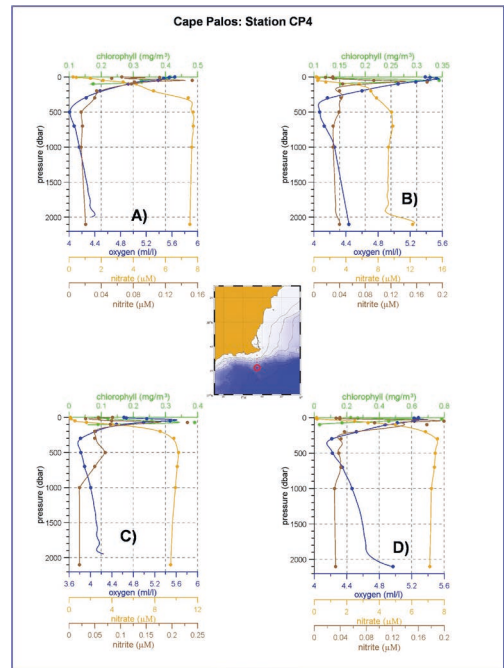


Figure 4.13. The same as in figure 4.12, but for station CP4.

Vertical profiles for the concentrations of nutrients, chlorophyll-a and dissolved oxygen at stations C20 and C18, from the Ibiza Channel, show very similar conditions to those described for the Cape Palos transect (Fig. 4.14 and 4.15), with very slight differences. One of such differences is that the highest concentrations of surface nitrate are observed in winter instead of autumn. Another difference is that the chlorophyll maximum is never at the sea surface. During winter, the nutrient supply to the surface layer is higher and the chlorophyll maximum is at 20 m depth, descending to 50 and 75 m depth for the rest of the year. The highest values are around 0.4 mg/m^3 . The dissolved oxygen shows a clear seasonal cycle at the sea surface linked to the sea temperature, with a minimum value in summer and a maximum one in winter. Its position is at the same depth or over the depth of the DCM. Once again, the phosphate concentrations along the upper 75 m of the water are low, ranging between 0.03 and $0.08 \text{ }\mu\text{M}$ and showing a quite homogeneous distribution (tables 4.14 and 4.15). Station C18 is deeper than C20 and therefore an increase of nutrient concentrations can be observed below the upper 100 m of the water column.

It is not worth extending in the description of the distributions at the B transect, to the south of Mallorca Island, as they are quite similar to those in the Ibiza Channel. As an example, figure 4.16 shows such distributions at station B2, at the central position of the B transect. Conditions within the waters of this transect are very oligotrophic. They are characterized by very low nitrate concentrations at the sea surface and chlorophyll-a values around 0.4 mg/m^3 . The highest concentrations for all these variables are recorded in winter, when the DCM is around 25 m depth. It sinks to 50, 75 and even 100 m depth during the following seasons (Fig. 4.16).

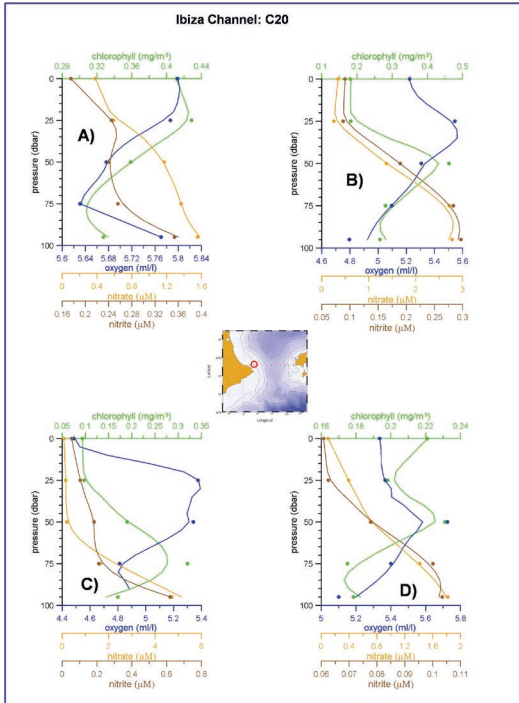


Figure 4.14. The same as in figure 4.12, but for station C20.

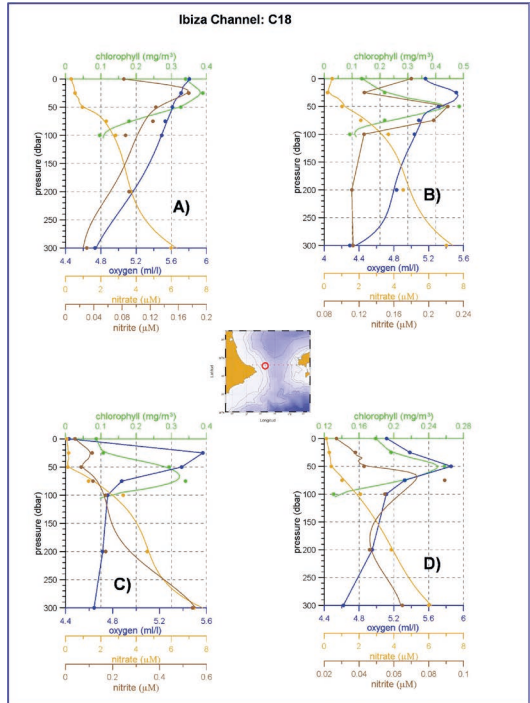


Figure 4.15. The same as in figure 4.12, but for station C18.

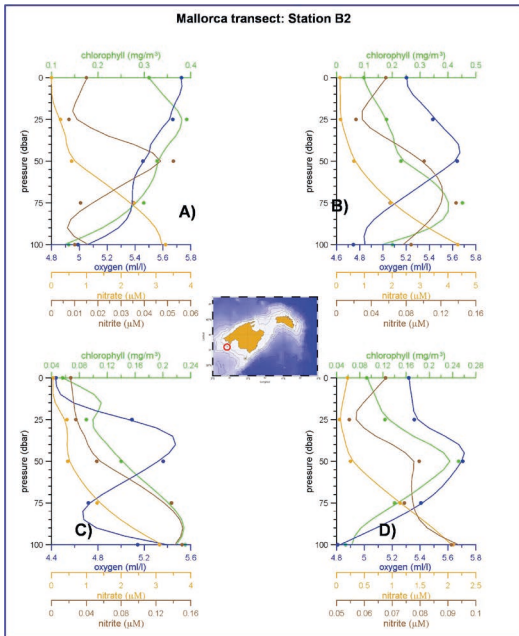


Figure 4.16. The same as in figure 4.12, but for station B2.

The Mahon transect shows some common features with the Cape Palos, Ibiza Channel and Mallorca transects, but also some distinctive characteristics (Fig. 4.17 and 4.18). As in most of the oceanographic stations within the Balearic Sea, there is a clear seasonal cycle with maximum surface nitrate concentrations in winter which decrease throughout the year. Phosphate concentrations are low and quite regular along the whole year. Chlorophyll concentrations follow those of nitrate, and the highest values are observed in winter, being such values at the upper layer of the water column. Nitrite concentrations present a PNM at depths ranging between 25 and 75 m and the dissolved oxygen concentration also has a deep maximum over the DCM.

The main difference found at stations MH2 and MH4 is that the intensity of the winter chlorophyll maximum is around 0.6 mg/m^3 , being higher than those observed in Cape Palos, Ibiza Channel and Mallorca transects. According to this result, the nutrient supply at the sea surface is also higher, the nutrient supply at the sea surface is also higher,

with nitrate concentrations during winter of $0.89 \text{ } \mu\text{M}$ at 25 m depth at MH2, and $1.06 \text{ } \mu\text{M}$ at the sea surface at MH4 (see tables 4.21 and 4.22).

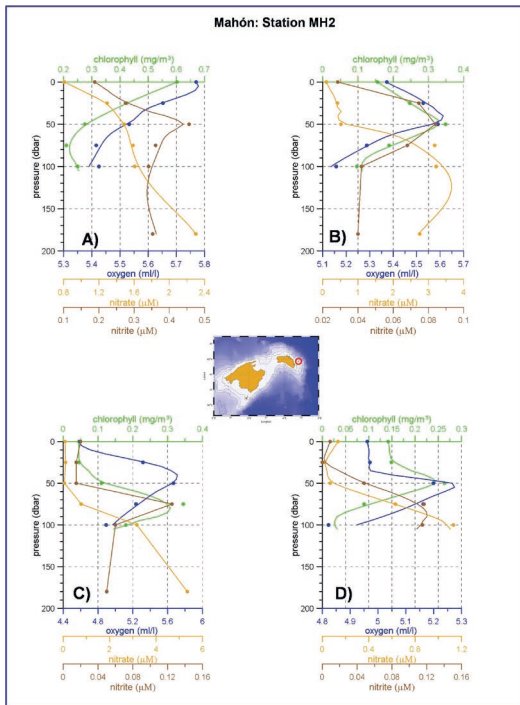


Figure 4.17. The same as in figure 4.12, but for station MH2.

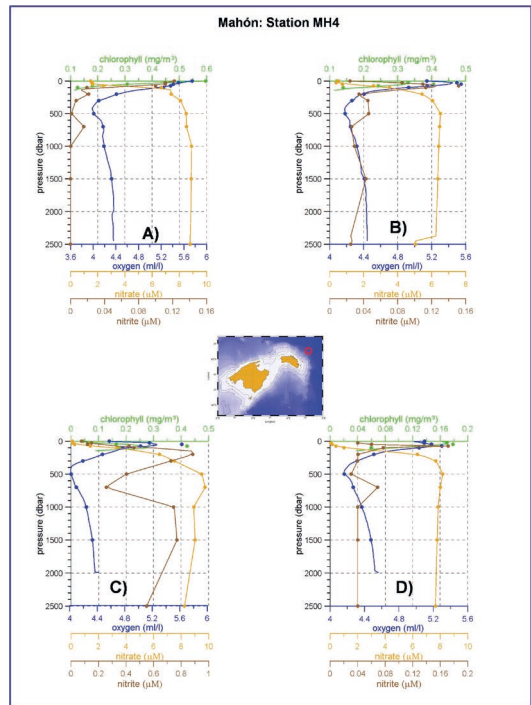


Figure 4.18. The same as in figure 4.12, but for station MH4.

Figures 4.19 to 4.22 show the mixed layer depth and the concentrations of chlorophyll, nitrogen (nitrate plus nitrite), phosphate, silicate and dissolved oxygen integrated for the upper 100 m of the water column. These figures support the increase of the oligotrophic character of the Spanish Mediterranean waters from the Alboran Sea (see previous chapter) towards the area of Cape Palos and the Balearic Sea.

It should be noticed that the differences already described between the Mahon transect and those to the south, concerning the intensity of the DCM and the winter concentrations of chlorophyll at the sea surface, are not observed when the integrated chlorophyll is analyzed. In most of the oceanographic stations analyzed within this geographical area (Cape Palos and Balearic Sea), the highest values occur in winter, ranging between 23 and 35 mg/m². After this winter maximum, the integrated chlorophyll decreases reaching minimum values during summer and autumn, between 14 and 18 mg/m².

The nutricline, estimated from figures 4.12 to 4.18, is deeper than at the Alboran Sea, being frequent values around 50 m or even 80 and 90 m during autumn in the Mahon transect. The only exceptions to this behavior would be the station CP2, during autumn, and the stations in the Mahon transect during winter. This result is in agreement with the development of a DCM. Nutrient integrated concentrations are much lower than in the Alboran Sea. This decrease is especially important in the case of phosphate integrated concentrations which in most of the oceanographic stations are around or lower than 5 mmol/m².

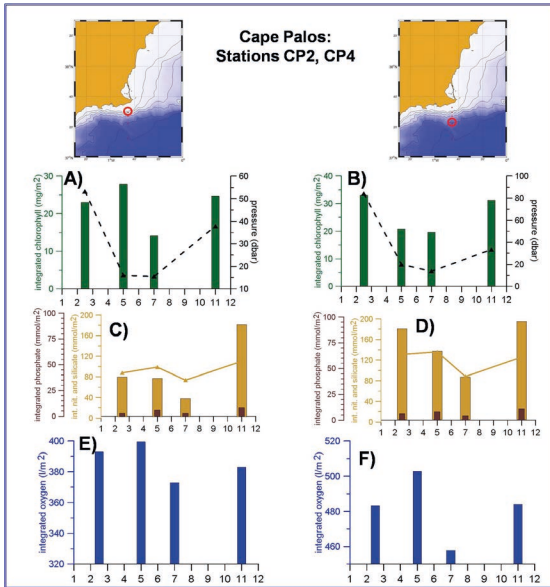


Figure 4.19. Figures 4.19A and B. Integrated chlorophyll-a concentrations for the upper 100 m of the water column expressed in mg/m^2 (green bars), mixed layer depth (black dashed line). Figure A corresponds to station CP2, and figure B to station CP4. Figures C (station CP2) and D (station CP4) are the integrated nitrate plus nitrite concentrations for the upper 100 m of the water column, expressed in mmol/m^2 (light brown bars). Dark brown bars show the integrated phosphate concentrations, also in mmol/m^2 and the light brown lines are the integrated silicate concentrations in mmol/m^2 . Figures E (station CP2) and F (station CP4) show the integrated dissolved oxygen concentrations for the upper 100 m of the water column, expressed in l/m^2 .

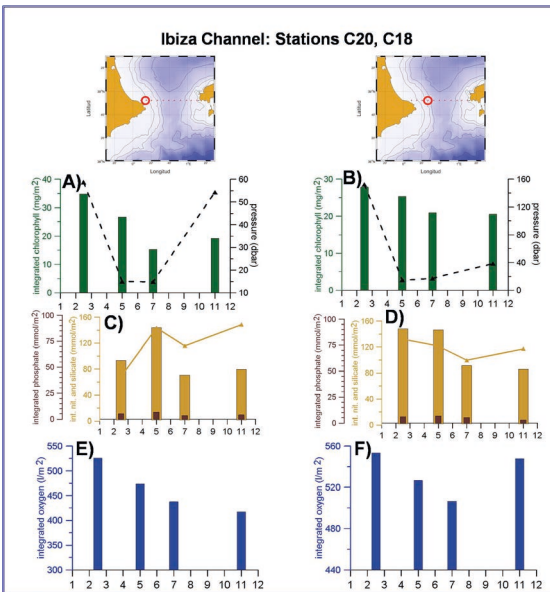


Figure 4.20. The same as in figure 4.19, but for stations C20 and C18.

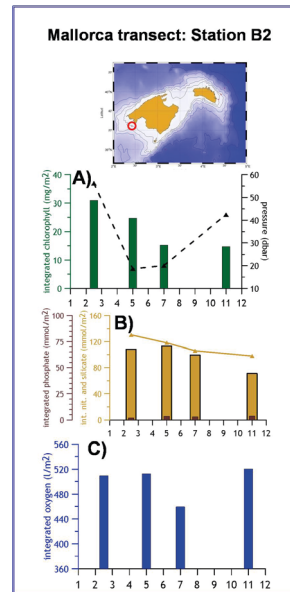


Figure 4.21. The same as in figure 4.19, but for station B2.

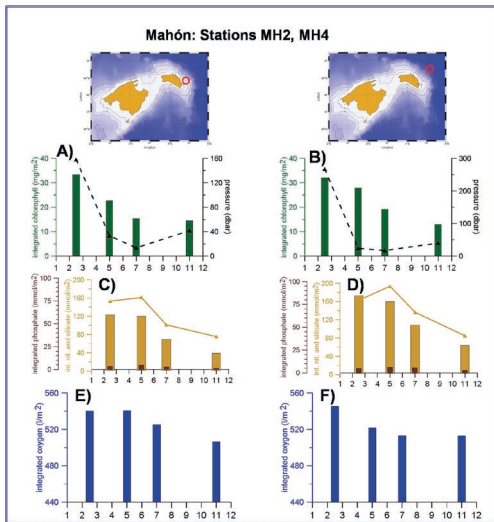


Figure 4.22. The same as in figure 4.19, but for stations MH2 and MH4.

4.4 Phytoplankton distribution.

4.4.1 Micro-phytoplankton.

Figures 4.23A, C, E and G show the vertical distributions for diatoms (green line), dinoflagellates (red line) and small flagellates (light brown line) at station CP2 in the Cape Palos continental shelf during winter, spring, summer and autumn. Throughout the year, and for most of the depth levels, small flagellates seem to be the prevailing group. Maximum abundances for this group seem to occur at the surface layer, decreasing with depth.

From winter to summer, the highest abundances of this group are observed at the upper 25 m of the water column, with values ranging between 60 and 80 cel./ml. Diatoms are more abundant at the sea surface and at 10 m depth during winter and autumn, when the nutrient supply to the upper layer is higher (70 and 40 cel./ml; nutricline at 35 m and at the sea surface respectively). On the contrary, diatoms develop a deep maximum at 50 m depth in spring, whereas in summer their abundance has a minimum value at the surface and increases slightly towards the sea bottom. Dinoflagellates show low abundances during the whole year and along the whole water column with values lower than 18 cel./ml. The statistics corresponding to the average micro-phytoplankton distributions can be seen in table 4.24.

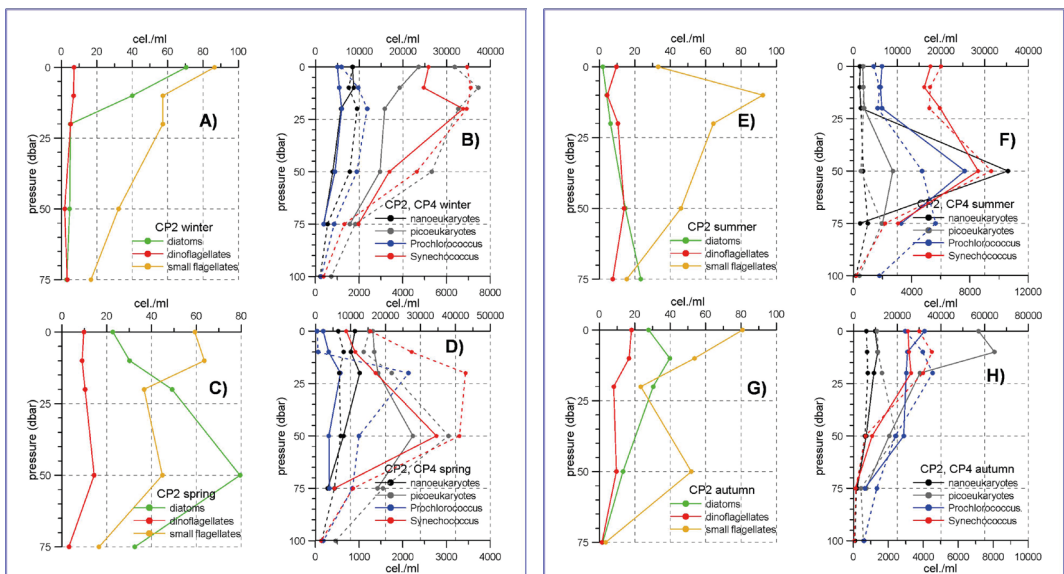


Figure 4.23. Figure 4.23A shows the winter average profiles for the abundances of diatoms (green), dinoflagellates (red) and small flagellates (light brown) obtained using all the available profiles from RADMED Project at station CP2. Figure 4.23B shows the winter average profiles for the abundance of nanoplanktonic cells (continuous black line), picoplanktonic eukaryote cells (continuous grey line), and bacteria from the genera *Prochlorococcus* (continuous blue line) and *Synechococcus* (continuous red line) at station CP2. Dashed lines correspond to station CP4. All the abundances are expressed in cells per milliliter (cel./ml). Figures C, D are the same, but for spring, figures E, F correspond to summer and figures G, H to autumn. The upper axis in figures B, D, F and H corresponds to *Prochlorococcus* and *Synechococcus*, and the lower axis to pico and nano eukaryotes.

Figures 4.24 A, C, E and G present the vertical micro-phytoplanktonic distributions for station C20, in the Ibiza Channel (see table 4.25). Once again the prevailing group throughout the year and along the whole water column is the small flagellates group. This group is more abundant at the upper part of the water column, at the sea surface or at 25 m depth, as already observed at station CP2. The highest abundances for this group are between 60 and 100 cel./ml. The highest abundances for the diatom group are recorded during spring with values close to 60 cel./ml, whereas in winter the vertical distribution is more homogeneous with abundances around 35 cel./ml. During summer, this group develops a deep maximum at 75 m depth, while during autumn the distribution returns to be vertically homogeneous with very low values that range between 5 and 10 cel./ml. Dinoflagellates are the least abundant group. Only during summer this group experiences a slight increase reaching abundances close to 20 cel./ml.

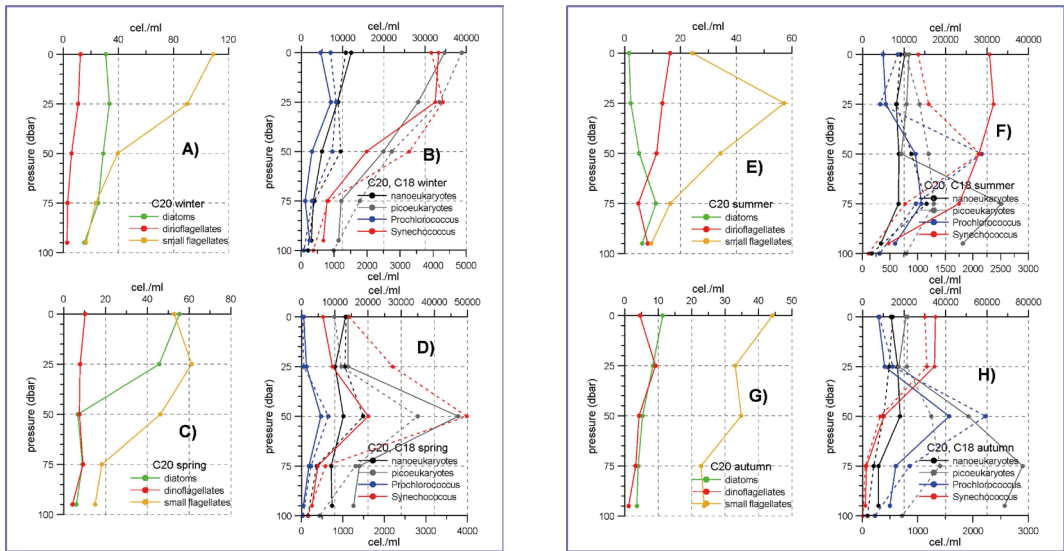


Figure 4.24. The same as in figure 4.23, but for the stations C20 and C18.

The micro-phytoplanktonic distributions for station B2, to the south of Mallorca Island, are presented in figure 4.25. The main features for these distributions are similar to those observed at Cape Palos and Ibiza Channel transects with a clear domain of small flagellates. The highest abundances for this group are observed at the upper 25 m of the water column with values ranging between 40 and 80 cel./ml. Diatoms are very scarce at these very oligotrophic waters, and develop deep maxima at 75 m depth during winter and spring, 100 m during summer, and between 50 and 75 m in autumn. Nevertheless, such maxima are just a slight increase that does not exceed 10 or 20 cel./ml. Dinoflagellates are more abundant than diatoms during some seasons and at several depth levels. It should be noticed the summer dinoflagellate increase, with values over 20 cel./ml. Tables 4.26, 4.27 and 4.28 show the statistics corresponding to the average seasonal distributions for the micro-phytoplankton at stations B1, B2 and B3 in the Mallorca transect.

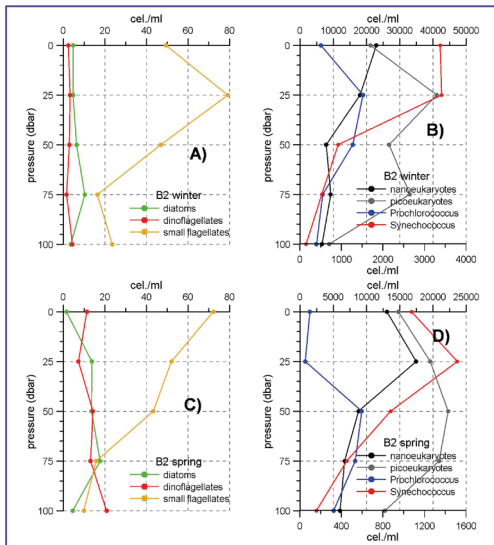
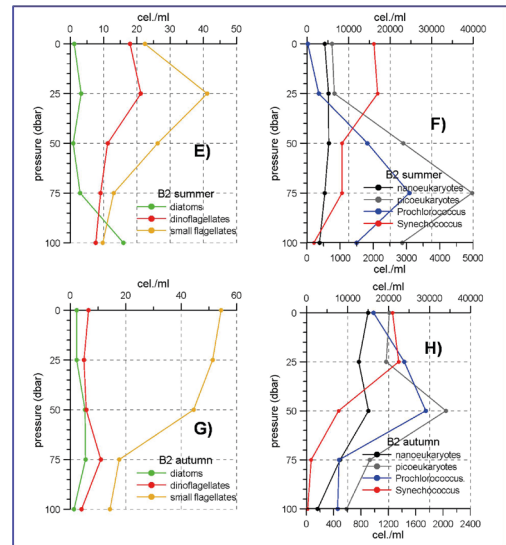


Figure 4.25. The same as in figure 4.23, but for station B2.



Finally, station MH2 shows again the domain of small flagellates throughout the year for all the analyzed depth levels (Fig. 4.26 and table 4.28). However, the abundances for this group, especially in winter and spring, are higher than for the rest of the oceanographic stations analyzed in this chapter. Such abundances reach 120 cel./ml at the sea surface. Diatoms are very scarce at this oceanographic station during the whole year, and dinoflagellates experience a slight increase during summer and autumn.

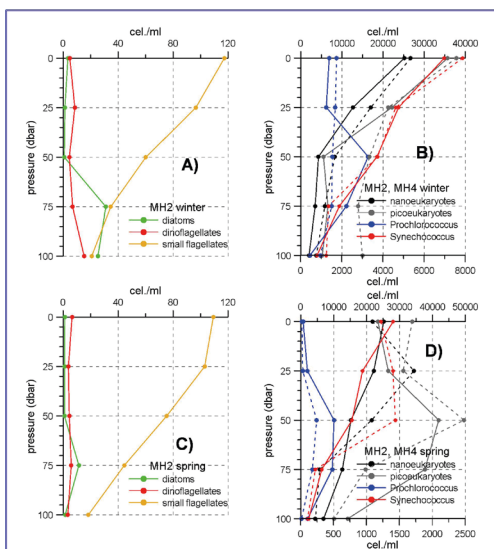
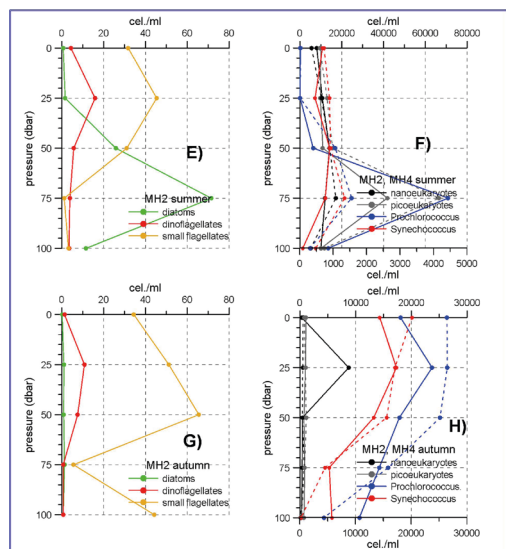


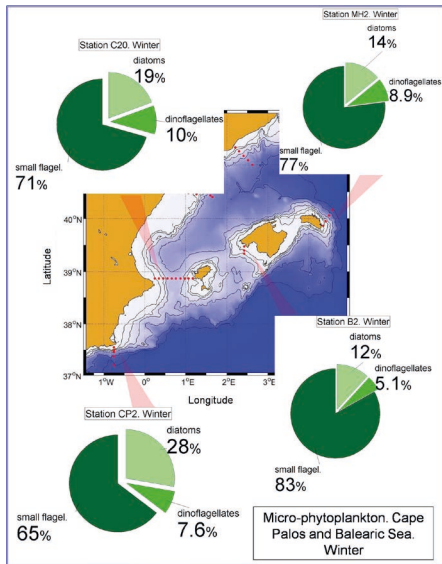
Figure 4.26. The same as in figure 4.23, but for stations MH2 and MH4.



In order to illustrate the relative importance of the different taxonomic groups, the abundances of diatoms, dinoflagellates and small flagellates have been vertically integrated and expressed as percentages in figures 4.27 to 4.30.

During winter, the most abundant group at all the oceanographic stations is the small flagellate one,

followed by diatoms. Cape Palos is the transect where diatoms have a higher relative abundance during this season, decreasing their importance northwards. During spring, diatoms become the most important group at Cape Palos. This group also increases considerably at station C20, in the Ibiza Channel, although small flagellates are still the most abundant one, and the same is observed at station B2 in the Mallorca transect and at station MH2. Notice the increase of dinoflagellates at station B2. During summer, diatoms are the most abundant group at station MH2, whereas the small flagellates dominate the rest of the zone of study. Once again, dinoflagellates experience an increase at station B2 to the south of Mallorca. Finally, diatoms return to be the most important group at Cape Palos in autumn, being the small flagellates group the dominant one at the rest of the oceanographic stations.



Besides the changes in the relative importance of the different micro-phytoplanktonic groups throughout the year, there are also changes in the total abundance of micro-phytoplanktonic cells. The total number of cells is minimum in summer, ranging, depending on the oceanographic station, between 85×10^6 cel./m² (MH2) and 198×10^6 cel./m² (CP2). The highest total abundances are observed in winter, being station B2 the only exception, where the total number of cells reaches the maximum value in spring. Such values range between 247×10^6 cel./m² at station B2 and 388×10^6 cel./m² at station MH2.

Figure 4.27. Winter relative abundances for the following micro-phytoplanktonic groups: diatoms (light green), dinoflagellates (green) and small flagellates (dark green) for the stations in the continental shelf of Cape Palos and the Balearic Sea: CP2, C20, B2 and MH2.

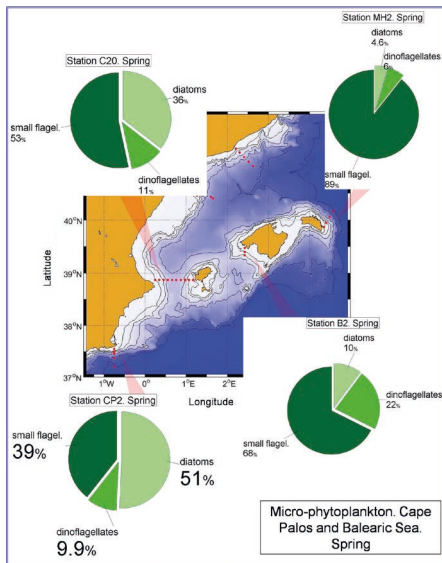


Figure 4.28. The same as in figure 4.27, but for spring.

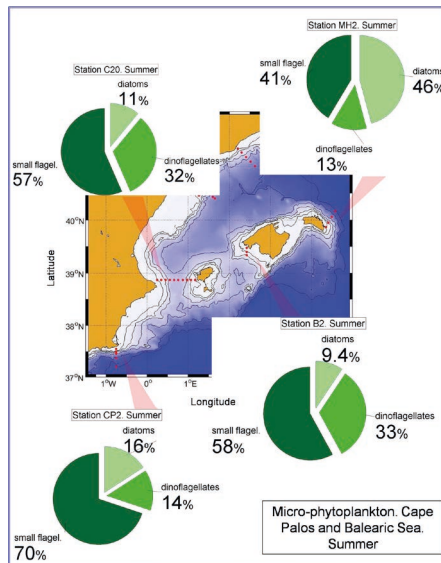


Figure 4.29. The same as in figure 4.27, but for summer.

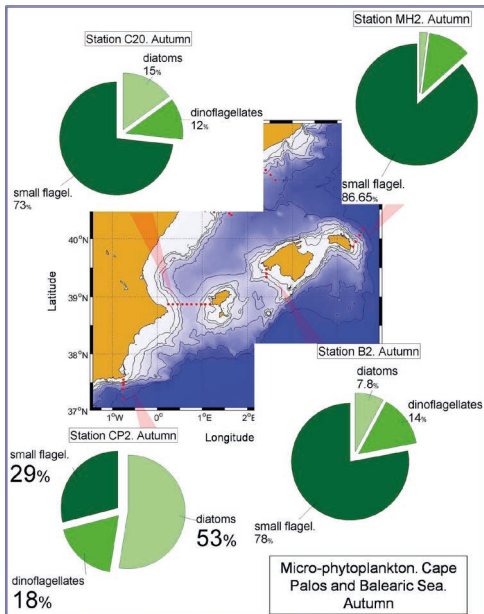


Figure 4.30. The same as in figure 4.27, but for autumn.

4.4.2 Nano and picoplankton.

The abundance of nanoeukaryote (2 to 20 μm ESD) and picoeukaryote and picoprokaryote (0.2 to 2 μm ESD) cells, are analyzed by means of flow cytometry in both the continental shelf stations: CP2, C20, B2 and MH2, and the continental slope ones: CP4, C18 and MH4. The three stations in the Mallorca transect (B) are over the continental shelf.

Figures 4.23 B, D, F and H show the vertical distributions for the nano and picoplankton at stations CP2 (solid line) and CP4 (dashed lines). The upper axis in figures B, D, F and H corresponds to *Prochlorococcus* and *Synechococcus*, while the lower axis is for pico and nano eukaryotes. The corresponding statistics are presented in tables 4.30 and 4.31. At these stations, the least abundant group are the nanoeukaryotes that hardly exceed 5 000 cel./ml. The following group would be that form by picoeukaryotes, but abundances are still of the

order of 10^3 cel./ml. Photoautotrophic bacteria of the genus *Prochlorococcus* have abundances around 10 000 cel./ml, and finally, the most abundant group is *Synechococcus*, with maximum abundances that can reach 40 000 cel./ml. at this stations. At Cape Palos transect, *Prochlorococcus* has a deeper distribution (Moore et al., 1995), and usually forms a deep maximum around 50 or even 75 m depth, whereas *Synechococcus* shows a preference for shallow waters (0-25 m). However, such a preference is not completely clear at this transect, as *Synechococcus* vertical profile has a deep maximum at 50 m during summer. There are not very clear differences between the continental shelf and slope stations.

Figures 4.24 B, D, F and H show the vertical distributions for the nano and picoplanktonic groups at stations C20 (solid lines) and C18 (dashed lines) in the Ibiza Channel transect. Statistics are in tables 4.32 and 4.33.

Main features of the Ibiza Channel transect are similar to those described for the Cape Palos transect. Eukaryote cells, both nano and picoplanktonic ones, have abundances one order of magnitude lower than the abundances of prokaryote cells. It cannot be established which of the photo-autotrophic bacteria are the most abundant ones. In some cases *Prochlorococcus* is the most abundant group, whereas in other cases the highest abundances correspond to *Synechococcus*. Neither can be established a clear difference between station C20 (continental shelf) and station C18 (continental slope). Results in this transect seem to confirm that *Prochlorococcus* has a deeper distribution than that of *Synechococcus*. For instance, *Synechococcus* has maximum abundances, around 30 000 cel./ml in summer at the sea surface and at 50 m (depending on where station C20 or C18 is considered). *Prochlorococcus* has maximum abundances between 10 000 and 30 000 cel./ml at 50 and 75 m. During autumn, *Synechococcus* is again more abundant from the sea surface to 25 m depth (30 000-35 000 cel./ml), and the highest abundances for *Prochlorococcus* are observed at 50 m of depth.

At station B2 (fig. 4.25 B, D, F y H and table 4.34), to the south of Mallorca Island, the differences among groups are clearer. Eukaryote pico and nanoplankton shows abundances much lower than those from the prokaryote picoplankton, and rarely exceed 3000 cel./ml. The highest *Prochlorococcus* and *Synechococcus* abundances are between 20 000 and 30 000 cel./ml. In the case of *Synechococcus*, such values are observed at the sea surface in winter and at 25 m depth during spring, and between the surface and 25 m during summer and autumn. *Prochlorococcus* is more abundant between 25 and 50 m in winter, between 50 and 75 m in spring, and at 75 and 50 m depth in summer and autumn respectively. These results from station B2, confirm that this group is more abundant at waters deeper

than those occupied by *Synechococcus*.

At the Mahon transect (fig. 4.26 B, D, F and H, MH2 solid lines and MH4 dashed lines) the nano and picoeukaryote cells show higher abundances during winter than at the other oceanographic stations, reaching values around 5 000 cel./ml or higher. On the contrary, for the rest of the year the abundances are low and similar to those of this geographical area, with very homogeneous values along the water column, around 1 000 cel./ml. The only exception would be a strong increase of the eukaryote nanoplankton at station MH2 during autumn at 25 m depth. The abundances of *Prochlorococcus* and *Synechococcus* show maximum values ranging between 15 000 and 25 000 cel./ml. As already said, the *Synechococcus* distribution is shallower than the *Prochlorococcus* one, with the only exception of autumn when both groups reach the highest values at the sea surface and decrease towards the sea bottom. The statistics corresponding to these stations are presented in tables 4.35 and 4.36.

4.5 Meso-zooplanktonic abundance and biomass.

Long time series of meso-zooplanktonic biomass from the preceding project ECOMALAGA are available for the Alboran Sea and such time series have been continued under the umbrella of the RADMED project. On the contrary, all the available information for the peninsular shelf of the eastern Spanish coast comes from RADMED. Furthermore, these time series have very numerous gaps because of frequent problems and the lack of qualified personal. The same situation stands for the Mahon transect. Consequently, it is difficult to obtain seasonal average values for the biomass and abundance of the main meso-zooplanktonic groups.

In order to complete the information about this geographical area and to establish some sort of comparison with the Alboran Sea, we have considered the table 1 from Fernández de Puellas et al. (2007) where the abundances of broad taxonomic groups are presented (table 4.37 in the present work). Figure 4.31 has been made with data from this table. This figure shows the relative importance of the main meso-zooplanktonic groups in station B1 in the Mallorca transect for the four seasons. Figure 4.31 shows that copepods are the most abundant group all the year round, with relative abundances higher than 50 %. The other groups with relative abundances higher than 5 % are appendicularians, doliolids and cladocerans. As for the Alboran Sea, there is an important increase of cladocerans in spring and mainly in summer when this group becomes the second most abundant one. According to Fernández de Puellas et al. (2007) the zooplanktonic biomass has an annual mean value of 5.4 mg/m³, reaching a maximum value in April (6.4 mg/m³) and a minimum one in August (4 mg/m³).

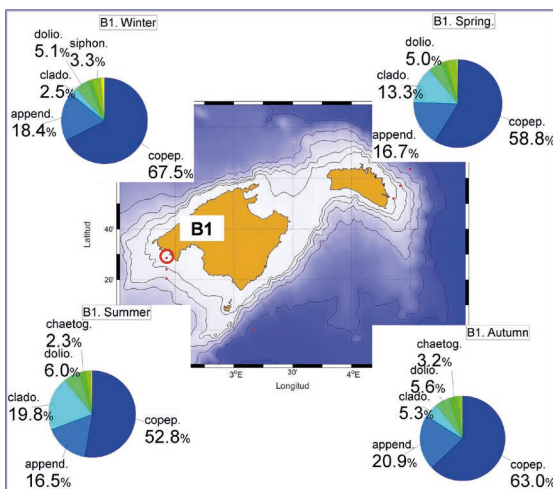


Figure 4.31. Relative importance of the main meso-zooplanktonic groups during the four seasons at station B1 in the Mallorca transect. The upper left corner plot corresponds to winter, the upper right to spring, the lower left to summer and the lower right to autumn. The groups represented in this figure are: copepods, appendicularians, cladocerans, doliolids, chaetognaths, ostracods, siphonophores and scyphozoans. For the clarity of the plot, only percentages over 5 % have been represented. This figure has been made from data in table 1 in Fernández de Puellas et al., 2007.

4.6 Tables. Seasonal statistics for Cape Palos and the Balearic Sea.

Table 4.1. Seasonal mean values for the potential temperature and salinity along the water column at station CP2. Three columns with mean values, standard deviations and number of data, are presented for each season and depth level.

Station CP2 (Potential temperature standard deviation number of data)												
Depth	Winter			Spring			Summer			Autumn		
5	14.18	0.73	6	17.09	1.58	6	25.34	0.61	6	20.30	2.29	7
10	14.09	0.67	6	16.92	1.54	6	25.19	0.72	6	20.23	2.41	7
15	14.00	0.63	6	16.48	1.51	6	23.89	1.46	6	20.20	2.44	7
20	13.90	0.61	6	16.11	1.53	6	22.89	1.55	6	19.84	2.69	7
25	13.82	0.62	6	15.79	1.45	6	20.26	1.74	6	19.75	2.78	7
30	13.80	0.63	6	15.25	1.47	6	18.07	2.20	6	19.62	2.90	7
35	13.78	0.63	6	14.89	1.36	6	16.81	1.57	6	19.33	3.01	7
40	13.78	0.66	6	14.64	1.31	6	16.25	1.18	6	18.59	2.85	7
45	13.73	0.59	6	14.31	1.05	6	15.64	0.74	6	17.70	2.26	7
50	13.69	0.56	6	14.07	0.90	6	15.11	0.55	6	16.98	1.95	7
75	13.49	0.46	5	13.30	0.13	5	13.69	0.28	4	14.77	1.31	6

Station CP2 (Salinity standard deviation number of data)												
Depth	Winter			Spring			Summer			Autumn		
5	37.70	0.33	6	37.74	0.24	6	37.43	0.20	6	37.28	0.50	7
10	37.76	0.31	6	37.77	0.21	6	37.48	0.20	6	37.29	0.49	7
15	37.82	0.28	6	37.82	0.18	6	37.57	0.37	6	37.29	0.49	7
20	37.89	0.25	6	37.87	0.17	6	37.70	0.25	6	37.28	0.51	7
25	37.96	0.23	6	37.92	0.15	6	37.69	0.27	6	37.31	0.50	7
30	37.99	0.22	6	37.96	0.14	6	37.75	0.27	6	37.33	0.49	7
35	38.01	0.20	6	38.00	0.13	6	37.86	0.15	6	37.43	0.44	7
40	38.05	0.14	6	38.04	0.13	6	37.89	0.13	6	37.43	0.44	7
45	38.08	0.11	6	38.05	0.12	6	37.92	0.11	6	37.49	0.42	7
50	38.09	0.09	6	38.08	0.11	6	37.99	0.08	6	37.60	0.37	7
75	38.15	0.06	5	38.16	0.08	5	38.11	0.04	4	38.02	0.11	6

Table 4.2. The same as in table 4.1, but for station CP4.

Station CP4. (Potential temperature standard deviation number of data)												
Depth	Winter			Spring			Summer			Autumn		
5	14.41	0.46	7	17.32	1.15	6	24.84	1.20	6	21.09	2.09	6
10	14.37	0.45	7	16.89	1.03	6	24.50	0.94	6	20.64	2.23	7
15	14.29	0.46	7	16.61	0.98	6	22.90	0.90	6	20.66	2.20	7

Station CP4. (Potential temperature standard deviation number of data)												
Depth	Winter			Spring			Summer			Autumn		
20	14.23	0.49	7	16.18	1.17	6	21.01	0.91	6	20.68	2.16	7
25	14.14	0.53	7	15.88	1.30	6	18.96	0.92	6	20.16	2.51	7
30	14.08	0.51	7	15.39	1.03	6	17.58	0.47	6	18.75	2.93	7
35	14.02	0.51	7	14.97	0.78	6	16.73	0.51	6	18.21	3.27	7
40	13.95	0.50	7	14.54	0.66	6	15.97	0.50	6	17.93	3.44	7
45	13.92	0.50	7	14.31	0.56	6	15.40	0.43	6	17.29	2.89	7
50	13.91	0.53	7	14.13	0.45	6	14.96	0.34	6	16.40	1.93	7
75	13.67	0.44	7	13.61	0.37	6	13.89	0.28	6	14.54	0.54	7
100	13.48	0.41	6	13.34	0.24	6	13.48	0.25	6	13.83	0.26	7
150	13.30	0.31	6	13.20	0.15	6	13.21	0.22	6	13.33	0.27	7
200	13.24	0.26	6	13.20	0.11	6	13.19	0.18	6	13.25	0.17	7
300	13.20	0.16	6	13.30	0.06	6	13.23	0.03	6	13.31	0.09	7
400	13.23	0.04	6	13.25	0.02	6	13.22	0.03	6	13.25	0.06	7
500	13.18	0.03	6	13.20	0.03	6	13.15	0.04	6	13.18	0.05	7
600	13.12	0.03	6	13.14	0.03	6	13.09	0.03	6	13.11	0.04	7
700	13.08	0.03	6	13.08	0.03	6	13.05	0.02	6	13.06	0.05	7
800	13.04	0.03	6	13.04	0.02	6	13.02	0.02	6	13.02	0.04	7
900	13.02	0.03	6	13.00	0.02	6	12.98	0.02	6	12.98	0.02	7
1000	13.00	0.03	6	12.97	0.02	6	12.95	0.02	6	12.95	0.02	7
1200	12.95	0.03	6	12.93	0.01	6	12.91	0.02	6	12.91	0.02	7
1400	12.92	0.03	6	12.90	0.02	5	12.89	0.03	6	12.89	0.02	7
1600	12.90	0.02	6	12.89	0.02	5	12.88	0.03	6	12.88	0.02	7
1800	12.89	0.02	6	12.89	0.01	5	12.88	0.02	6	12.89	0.02	7
2000	12.89	0.01	4	12.88	0.01	3	12.86	0.01	2	12.89	0.01	5

Station CP4 (Salinity standard deviation number of data)												
Depth	Winter			Spring			Summer			Autumn		
5	37.58	0.30	7	37.43	0.25	6	37.19	0.21	6	37.31	0.55	6
10	37.61	0.28	7	37.49	0.23	6	37.24	0.24	6	37.27	0.51	7
15	37.66	0.25	7	37.54	0.23	6	37.33	0.23	6	37.29	0.51	7
20	37.74	0.22	7	37.60	0.22	6	37.42	0.24	6	37.31	0.51	7
25	37.82	0.25	7	37.67	0.22	6	37.47	0.32	6	37.29	0.53	7
30	37.86	0.25	7	37.75	0.22	6	37.66	0.24	6	37.32	0.51	7
35	37.91	0.24	7	37.82	0.19	6	37.75	0.20	6	37.38	0.45	7
40	37.95	0.22	7	37.92	0.17	6	37.79	0.17	6	37.45	0.41	7
45	37.98	0.20	7	37.96	0.16	6	37.87	0.16	6	37.47	0.34	7
50	38.02	0.17	7	37.98	0.15	6	37.93	0.12	6	37.48	0.30	7

Station CP4 (Salinity standard deviation number of data)												
Depth	Winter			Spring			Summer			Autumn		
75	38.15	0.09	7	38.13	0.05	6	38.09	0.06	6	37.86	0.17	7
100	38.18	0.05	6	38.17	0.03	6	38.16	0.04	6	38.12	0.07	7
150	38.28	0.06	6	38.26	0.06	6	38.26	0.04	6	38.25	0.06	7
200	38.35	0.08	6	38.34	0.05	6	38.36	0.05	6	38.35	0.05	7
300	38.45	0.07	6	38.49	0.02	6	38.48	0.02	6	38.50	0.02	7
400	38.51	0.01	6	38.52	0.01	6	38.52	0.01	6	38.53	0.01	7
500	38.52	0.01	6	38.53	0.01	6	38.52	0.01	6	38.53	0.01	7
600	38.52	0.01	6	38.52	0.01	6	38.51	0.01	6	38.52	0.01	7
700	38.51	0.01	6	38.51	0.01	6	38.51	0.01	6	38.51	0.01	7
800	38.51	0.01	6	38.50	0.01	6	38.50	0.01	6	38.50	0.01	7
900	38.50	0.01	6	38.50	0.01	6	38.49	0.00	6	38.49	0.01	7
1000	38.50	0.01	6	38.49	0.01	6	38.49	0.01	6	38.49	0.01	7
1200	38.49	0.01	6	38.48	0.00	6	38.48	0.01	6	38.48	0.01	7
1400	38.48	0.01	6	38.48	0.00	5	38.47	0.01	6	38.47	0.01	7
1600	38.48	0.01	6	38.48	0.00	5	38.47	0.01	6	38.47	0.01	7
1800	38.48	0.01	6	38.48	0.00	5	38.47	0.01	6	38.48	0.01	7
2000	38.48	0.00	4	38.48	0.00	3	38.47	0.00	2	38.48	0.01	5

Table 4.3. The same as in table 4.1, but for station C20.

Station C20 (Potential temperature standard deviation number of data)												
Depth	Winter			Spring			Summer			Autumn		
5	13.65	0.76	13	19.04	2.25	20	24.60	0.87	8	20.85	2.19	9
10	13.60	0.72	13	18.32	2.07	20	24.41	0.91	8	20.87	2.06	10
15	13.54	0.69	13	17.50	1.92	20	21.54	1.72	8	20.88	2.07	10
20	13.46	0.65	13	16.35	1.76	20	20.09	2.04	8	20.55	2.01	10
25	13.39	0.62	13	15.49	1.64	20	18.49	2.07	8	20.38	2.10	10
30	13.36	0.60	13	14.77	1.06	20	17.28	1.49	8	20.02	2.15	10
35	13.32	0.58	13	14.46	1.00	20	16.38	1.24	8	19.11	2.00	9
40	13.24	0.56	13	14.19	0.89	20	15.81	1.08	8	18.57	2.01	9
45	13.22	0.56	13	13.80	0.56	19	15.39	0.85	8	17.96	2.22	9
50	13.20	0.52	13	13.67	0.50	20	15.08	0.76	8	17.06	1.61	9
75	13.05	0.50	13	13.30	0.30	20	14.01	0.64	8	15.44	1.86	9

Station C20 (Salinity standard deviation number of data)												
Depth	Winter			Spring			Summer			Autumn		
5	38.06	0.11	12	37.78	0.24	20	37.71	0.39	8	37.91	0.28	9
10	38.07	0.10	12	37.83	0.25	20	37.70	0.39	8	37.91	0.26	10

Station C20 (Salinity standard deviation number of data)												
Depth	Winter			Spring			Summer			Autumn		
15	38.08	0.09	12	37.88	0.16	19	37.69	0.30	8	37.91	0.26	10
20	38.06	0.11	13	37.91	0.14	19	37.76	0.25	8	37.91	0.26	10
25	38.07	0.10	13	37.95	0.14	19	37.77	0.25	8	37.95	0.24	10
30	38.08	0.09	13	38.01	0.11	19	37.74	0.26	8	37.96	0.21	10
35	38.08	0.08	13	38.03	0.11	20	37.79	0.26	8	37.90	0.34	9
40	38.09	0.08	13	38.05	0.10	20	37.85	0.26	8	37.93	0.22	9
45	38.10	0.07	13	38.06	0.10	20	37.89	0.24	8	37.97	0.13	9
50	38.11	0.07	13	38.06	0.14	20	37.95	0.22	8	37.97	0.10	9
75	38.12	0.07	13	38.11	0.11	20	38.10	0.07	8	38.06	0.04	9

Table 4.4. The same as in table 4.1, but for station C18

Station C18 (Potential temperature standard deviation number of data)												
Depth	Winter			Spring			Summer			Autumn		
5	13.93	0.67	11	18.96	2.26	20	24.77	0.95	8	20.72	2.31	11
10	13.69	0.74	13	18.27	1.88	20	24.69	0.93	8	20.71	2.30	11
15	13.66	0.71	13	17.46	1.55	20	22.45	1.91	8	20.70	2.31	11
20	13.59	0.68	13	16.46	1.46	20	20.45	2.43	8	20.62	2.23	11
25	13.54	0.65	13	15.68	1.42	20	18.76	2.03	8	20.29	2.12	11
30	13.43	0.61	13	14.78	0.92	20	17.74	2.28	8	20.03	2.19	11
35	13.41	0.61	13	14.41	0.82	20	16.68	1.69	8	19.43	2.22	11
40	13.38	0.60	13	14.16	0.72	20	15.88	1.21	8	18.16	1.38	11
45	13.32	0.54	13	13.98	0.61	20	15.27	0.92	8	17.17	1.30	11
50	13.29	0.53	13	13.85	0.55	20	14.92	0.77	8	16.51	1.30	11
75	13.18	0.43	13	13.47	0.39	20	13.81	0.31	8	14.41	0.80	10
100	13.13	0.38	13	13.28	0.30	20	13.46	0.16	8	13.90	0.85	10
150	13.08	0.30	13	13.14	0.23	20	13.24	0.13	7	13.39	0.22	10
200	13.09	0.30	13	13.06	0.21	20	13.14	0.15	7	13.26	0.20	10
300	13.16	0.26	12	13.08	0.16	17	13.17	0.12	5	13.22	0.12	10

Station C18 (Salinity standard deviation number of data)												
Depth	Winter			Spring			Summer			Autumn		
5	37.98	0.26	11	37.84	0.18	19	37.68	0.39	8	37.71	0.32	11
10	38.01	0.26	13	37.85	0.19	19	37.67	0.38	8	37.71	0.31	11
15	38.09	0.12	12	37.89	0.20	19	37.57	0.33	8	37.72	0.31	11
20	38.10	0.10	12	37.89	0.19	19	37.66	0.36	8	37.74	0.29	11
25	38.10	0.10	12	37.92	0.18	19	37.71	0.34	8	37.78	0.26	11
30	38.10	0.09	12	37.93	0.14	19	37.77	0.29	8	37.82	0.24	11

Station C18 (Salinity standard deviation number of data)												
Depth	Winter			Spring			Summer			Autumn		
35	38.11	0.09	12	37.95	0.12	19	37.82	0.29	8	37.84	0.20	11
40	38.12	0.08	12	37.99	0.11	19	37.87	0.29	8	37.84	0.23	11
45	38.11	0.09	13	38.02	0.13	19	37.89	0.27	8	37.89	0.19	11
50	38.12	0.08	13	38.05	0.11	19	37.95	0.22	8	37.93	0.16	11
75	38.14	0.07	13	38.12	0.08	19	38.07	0.10	8	38.09	0.05	10
100	38.16	0.07	13	38.14	0.09	20	38.16	0.04	8	38.16	0.05	10
150	38.20	0.05	13	38.21	0.09	20	38.21	0.03	7	38.25	0.06	10
200	38.26	0.07	13	38.26	0.09	20	38.27	0.04	7	38.31	0.06	10
300	38.38	0.10	12	38.38	0.08	17	38.44	0.04	5	38.46	0.04	10

Table 4.5. The same as in table 4.1, but for station B1.

Station B1 (Potential temperature standard deviation number of data)												
Depth	Winter			Spring			Summer			Autumn		
5	14.66	0.63	49	18.81	2.73	52	25.28	1.24	49	19.65	2.35	47
10	14.62	0.63	44	18.47	2.66	47	25.19	1.25	46	19.60	2.40	45
15	14.61	0.66	49	18.11	2.56	53	25.05	1.32	50	19.62	2.38	47
20	14.55	0.64	44	17.39	2.22	47	24.39	1.86	46	19.57	2.42	45
25	14.52	0.63	49	16.82	1.88	53	22.91	2.30	50	19.51	2.34	47
30	14.48	0.65	44	16.19	1.51	47	20.66	2.23	46	19.27	2.36	45
35	14.45	0.66	44	15.71	1.18	47	18.81	1.62	46	18.84	2.16	45
40	14.42	0.67	44	15.38	0.99	47	17.52	1.21	46	18.07	1.77	45
45	14.38	0.65	44	15.12	0.91	47	16.79	1.05	46	17.40	1.42	45
50	14.33	0.61	49	14.92	0.80	53	16.08	0.90	50	16.67	0.94	46
75	13.88	0.31	12	14.05	0.52	13	14.35	0.41	15	15.12	0.70	13

Station B1 (Salinity standard deviation number of data)												
Depth	Winter			Spring			Summer			Autumn		
5	37.62	0.25	49	37.55	0.27	52	37.46	0.18	50	37.46	0.18	47
10	37.63	0.26	44	37.57	0.26	47	37.47	0.19	46	37.47	0.18	45
15	37.64	0.23	49	37.54	0.28	53	37.45	0.20	50	37.48	0.17	47
20	37.67	0.24	44	37.59	0.25	46	37.44	0.18	46	37.50	0.18	45
25	37.67	0.23	49	37.60	0.25	53	37.41	0.29	50	37.50	0.19	46
30	37.70	0.23	44	37.65	0.24	47	37.44	0.30	46	37.49	0.20	44
35	37.71	0.22	44	37.69	0.23	47	37.48	0.32	46	37.48	0.23	45
40	37.73	0.21	44	37.73	0.21	47	37.56	0.26	46	37.50	0.23	44
45	37.75	0.21	44	37.76	0.21	47	37.65	0.21	45	37.52	0.24	45
50	37.77	0.18	49	37.76	0.22	53	37.69	0.17	50	37.51	0.27	47

Station B1 (Salinity standard deviation number of data)												
Depth	Winter			Spring			Summer			Autumn		
75	37.94	0.17	12	37.92	0.21	13	37.94	0.21	15	37.76	0.19	13

Table 4.6. The same as in table 4.1, but for station B2.

Station B2 (Potential temperature standard deviation number of data)												
Depth	Winter			Spring			Summer			Autumn		
5	14.59	0.62	27	18.67	2.74	30	25.20	1.28	24	19.81	2.37	25
10	14.51	0.60	22	18.25	2.63	25	25.06	1.32	20	19.76	2.45	23
15	14.51	0.62	27	17.88	2.34	31	24.72	1.44	24	19.79	2.38	25
20	14.42	0.63	22	17.20	2.00	25	24.10	1.58	20	19.75	2.48	23
25	14.40	0.63	27	16.94	2.03	31	22.54	1.78	23	19.74	2.39	25
30	14.30	0.64	22	16.14	1.38	25	20.95	2.24	19	19.65	2.41	23
35	14.26	0.63	22	15.65	1.21	25	19.04	1.95	20	19.10	1.95	23
40	14.23	0.64	22	15.18	1.01	25	17.51	1.27	20	18.29	1.52	23
45	14.20	0.64	22	14.83	0.91	25	16.56	1.00	20	17.60	1.44	23
50	14.20	0.60	27	14.65	0.72	31	15.86	0.85	24	16.68	1.08	24
75	14.00	0.50	27	13.95	0.59	30	14.37	0.55	24	14.67	0.60	24
100	13.86	0.46	10	13.69	0.24	10	13.64	0.21	9	14.10	0.70	9

Station B2 (Salinity standard deviation number of data)												
Depth	Winter			Spring			Summer			Autumn		
5	37.66	0.27	27	37.58	0.28	30	37.45	0.15	24	37.47	0.24	25
10	37.71	0.28	22	37.62	0.30	25	37.47	0.18	20	37.48	0.25	23
15	37.67	0.26	28	37.57	0.34	31	37.45	0.20	24	37.48	0.24	25
20	37.73	0.28	22	37.63	0.28	24	37.51	0.24	20	37.50	0.25	23
25	37.70	0.26	28	37.61	0.29	31	37.50	0.26	23	37.50	0.25	25
30	37.76	0.27	22	37.69	0.26	25	37.54	0.24	19	37.54	0.27	23
35	37.77	0.26	22	37.74	0.24	25	37.42	0.38	20	37.51	0.32	22
40	37.79	0.26	22	37.76	0.24	25	37.53	0.29	20	37.49	0.31	23
45	37.81	0.25	22	37.79	0.23	25	37.59	0.26	20	37.53	0.31	23
50	37.80	0.22	28	37.78	0.24	31	37.66	0.22	24	37.53	0.28	25
75	37.94	0.17	28	37.93	0.20	30	37.92	0.14	24	37.85	0.20	25
100	37.99	0.18	11	37.99	0.16	10	38.06	0.10	9	38.07	0.09	9

Table 4.7. The same as in table 4.1, but for station B3.

Station B3 (Potential temperature standard deviation number of data)												
Depth	Winter			Spring			Summer			Autumn		
5	14.65	0.63	26	18.80	2.81	30	25.11	1.23	23	20.09	2.38	23
10	14.50	0.58	22	18.23	2.54	25	25.01	1.25	20	20.02	2.46	21
15	14.50	0.59	27	17.84	2.26	31	24.55	1.38	23	20.03	2.37	23
20	14.39	0.58	22	17.34	2.02	25	23.74	1.68	19	19.97	2.47	21
25	14.40	0.58	27	16.63	1.52	31	22.27	1.83	23	19.94	2.37	23
30	14.30	0.58	22	15.94	1.23	25	20.56	2.00	20	19.59	2.26	21
35	14.25	0.59	22	15.51	1.00	25	18.83	1.81	20	19.02	2.02	20
40	14.22	0.60	22	15.17	0.92	25	17.51	1.27	20	18.36	1.72	21
45	14.21	0.62	22	14.85	0.83	25	16.53	0.86	20	17.66	1.56	21
50	14.20	0.60	27	14.68	0.75	31	15.85	0.71	23	17.04	1.48	23
75	13.98	0.56	27	13.97	0.57	31	14.37	0.63	23	14.78	0.62	23
100	13.78	0.41	27	13.62	0.46	31	13.63	0.34	23	13.86	0.31	22
150	13.42	0.24	27	13.28	0.25	30	13.26	0.14	22	13.34	0.17	23
200	13.23	0.07	9	13.20	0.05	11	13.15	0.10	8	13.21	0.07	9

Station B3 (Salinity standard deviation number of data)												
Depth	Winter			Spring			Summer			Autumn		
5	37.60	0.28	26	37.57	0.28	30	37.39	0.21	23	37.50	0.29	23
10	37.68	0.28	22	37.63	0.27	25	37.40	0.22	20	37.53	0.31	21
15	37.64	0.26	28	37.61	0.28	31	37.40	0.25	23	37.53	0.30	23
20	37.70	0.28	22	37.61	0.35	25	37.41	0.22	19	37.54	0.30	21
25	37.67	0.27	28	37.62	0.30	31	37.47	0.26	22	37.54	0.29	23
30	37.73	0.28	22	37.68	0.27	25	37.40	0.44	20	37.55	0.36	21
35	37.75	0.28	22	37.72	0.26	25	37.44	0.39	20	37.51	0.41	20
40	37.76	0.28	22	37.75	0.26	25	37.51	0.34	20	37.49	0.43	21
45	37.79	0.26	22	37.77	0.27	25	37.58	0.34	20	37.51	0.43	21
50	37.79	0.24	28	37.76	0.26	31	37.65	0.32	23	37.53	0.37	23
75	37.93	0.18	28	37.95	0.21	31	37.93	0.18	23	37.82	0.21	23
100	38.06	0.13	27	38.04	0.17	31	38.09	0.10	23	38.03	0.12	23
150	38.18	0.11	28	38.19	0.13	31	38.21	0.07	23	38.20	0.08	23
200	38.34	0.08	9	38.35	0.12	11	38.32	0.07	8	38.37	0.03	9

Table 4.8. The same as in table 4.1, but for station MH2.

Station MH2 (Potential temperature standard deviation number of data)												
Depth	Winter			Spring			Summer			Autumn		
5	13.48	0.30	4	17.13	3.05	6	25.11	1.60	3	18.47	2.75	3
10	13.42	0.25	5	16.51	2.67	6	24.24	1.41	3	18.46	2.76	3
15	13.37	0.27	5	16.11	2.43	6	23.31	1.74	3	18.43	2.81	3
20	13.37	0.28	5	15.75	2.15	6	21.51	2.39	3	18.40	2.85	3
25	13.36	0.30	5	15.45	1.89	6	20.01	2.62	3	18.37	2.89	3
30	13.35	0.33	5	15.00	1.46	6	18.46	2.29	3	18.36	2.90	3
35	13.37	0.36	5	14.62	1.13	6	17.20	1.53	3	18.36	2.90	3
40	13.40	0.39	5	14.38	0.88	6	16.45	1.49	3	18.36	2.90	3
45	13.40	0.39	5	14.13	0.58	6	15.63	1.45	3	17.86	2.77	3
50	13.38	0.37	5	13.97	0.47	6	15.15	1.26	3	17.36	2.74	3
75	13.29	0.24	5	13.55	0.31	6	13.93	0.60	3	14.81	0.31	3
100	13.22	0.23	5	13.36	0.27	6	13.40	0.23	3	13.95	0.29	3
150	13.08	0.26	5	13.14	0.11	5	13.11	0.06	3	13.61	0.38	3

Station MH2 (Salinity standard deviation number of data)												
Depth	Winter			Spring			Summer			Autumn		
5	38.03	0.16	4	37.92	0.21	6	37.83	0.24	3	37.76	0.28	3
10	38.07	0.16	5	37.95	0.23	6	37.87	0.25	3	37.76	0.28	3
15	38.07	0.16	5	37.95	0.24	6	37.73	0.14	3	37.77	0.28	3
20	38.08	0.16	5	37.95	0.26	6	37.79	0.15	3	37.77	0.29	3
25	38.09	0.16	5	37.96	0.26	6	37.85	0.18	3	37.78	0.29	3
30	38.10	0.15	5	37.97	0.25	6	37.84	0.17	3	37.78	0.30	3
35	38.11	0.14	5	37.98	0.25	6	37.81	0.15	3	37.78	0.30	3
40	38.12	0.14	5	37.99	0.24	6	37.85	0.12	3	37.79	0.31	3
45	38.13	0.13	5	38.01	0.24	6	37.91	0.12	3	37.81	0.28	3
50	38.14	0.13	5	38.01	0.23	6	37.97	0.12	3	37.80	0.29	3
75	38.16	0.14	5	38.09	0.20	6	38.16	0.13	3	38.00	0.11	3
100	38.19	0.14	5	38.16	0.15	6	38.24	0.15	3	38.15	0.05	3
150	38.23	0.14	5	38.27	0.08	5	38.36	0.13	3	38.29	0.09	3

Table 4.9. The same as in table 4.1, but for station MH4.

Station MH4 (Potential temperature standard deviation number of data)												
Depth	Winter			Spring			Summer			Autumn		
5	13.71	0.24	6	17.38	2.84	7	24.29	1.67	4	19.77	2.92	5
10	13.66	0.25	6	16.36	2.27	8	24.08	1.51	4	19.74	2.88	5

Station MH4 (Potential temperature standard deviation number of data)												
Depth	Winter			Spring			Summer			Autumn		
15	13.60	0.29	6	16.04	2.15	8	23.52	1.42	4	19.70	2.87	5
20	13.50	0.35	6	15.72	1.85	8	22.96	1.45	4	19.66	2.87	5
25	13.42	0.31	6	15.43	1.67	8	22.29	1.30	4	19.58	2.79	5
30	13.41	0.30	6	15.02	1.38	8	20.29	1.61	4	19.50	2.74	5
35	13.39	0.30	6	14.71	1.14	8	18.21	1.47	4	19.39	2.72	5
40	13.37	0.28	6	14.31	0.81	8	17.12	1.35	4	19.30	2.63	5
45	13.37	0.29	6	14.10	0.75	8	16.00	1.12	4	18.95	2.40	5
50	13.34	0.26	6	13.91	0.59	8	15.41	0.95	4	18.03	2.24	5
75	13.33	0.25	6	13.35	0.20	8	13.82	0.51	4	15.33	0.72	5
100	13.32	0.22	6	13.23	0.11	8	13.43	0.20	4	14.13	0.54	5
150	13.31	0.12	6	13.12	0.14	8	13.20	0.05	4	13.36	0.16	5
200	13.23	0.08	6	13.12	0.11	8	13.18	0.03	4	13.24	0.07	5
300	13.29	0.11	6	13.17	0.08	8	13.18	0.04	4	13.21	0.04	5
400	13.25	0.12	6	13.14	0.09	8	13.16	0.06	4	13.20	0.05	5
500	13.20	0.11	6	13.10	0.08	8	13.13	0.06	4	13.14	0.06	5
600	13.12	0.08	6	13.04	0.07	8	13.09	0.05	4	13.09	0.06	5
700	13.06	0.06	6	13.00	0.06	8	13.03	0.04	4	13.04	0.05	5
800	13.02	0.06	6	12.98	0.05	8	12.98	0.04	4	12.99	0.05	5
900	12.97	0.05	6	12.94	0.03	8	12.95	0.03	4	12.96	0.04	5
1000	12.94	0.04	6	12.93	0.02	8	12.93	0.02	4	12.93	0.04	5
1200	12.91	0.02	6	12.91	0.02	8	12.90	0.02	4	12.90	0.02	5
1400	12.89	0.02	6	12.90	0.02	8	12.89	0.03	4	12.90	0.01	5
1600	12.90	0.01	6	12.91	0.02	7	12.91	0.01	4	12.91	0.01	5
1800	12.90	0.01	6	12.91	0.01	7	12.91	0.01	4	12.90	0.00	5
2000	12.90	0.01	6	12.91	0.00	7	12.90	0.01	4	12.90	0.01	4
2200	12.90	0.01	5	12.90	0.01	7	12.89	0.01	3	12.90	0.01	4
2400	12.90	0.01	5	12.90	0.01	7	12.89	0.02	2	12.90	0.01	4

Station MH4 (Salinity standard deviation number of data)												
Depth	Winter			Spring			Summer			Autumn		
5	37.99	0.18	6	37.93	0.29	7	37.78	0.10	4	37.70	0.18	5
10	37.98	0.14	6	37.92	0.24	8	37.74	0.07	4	37.71	0.17	5
15	38.01	0.12	6	37.95	0.26	8	37.79	0.10	4	37.72	0.18	5
20	38.05	0.12	6	37.98	0.26	8	37.83	0.11	4	37.72	0.18	5
25	38.07	0.13	6	37.99	0.26	8	37.79	0.16	4	37.74	0.18	5
30	38.08	0.13	6	38.00	0.27	8	37.77	0.18	4	37.76	0.17	5
35	38.09	0.13	6	38.04	0.23	8	37.87	0.15	4	37.78	0.15	5

Station MH4 (Salinity standard deviation number of data)												
Depth	Winter			Spring			Summer			Autumn		
40	38.10	0.12	6	38.12	0.18	8	37.91	0.10	4	37.79	0.15	5
45	38.12	0.12	6	38.14	0.18	8	37.89	0.12	4	37.75	0.18	5
50	38.12	0.12	6	38.16	0.16	8	37.96	0.09	4	37.65	0.33	5
75	38.17	0.13	6	38.25	0.10	8	38.15	0.06	4	37.86	0.18	5
100	38.21	0.13	6	38.32	0.09	8	38.25	0.04	4	38.09	0.12	5
150	38.35	0.13	6	38.39	0.04	8	38.35	0.06	4	38.31	0.07	5
200	38.43	0.06	6	38.45	0.03	8	38.43	0.04	4	38.42	0.03	5
300	38.53	0.02	6	38.51	0.02	8	38.50	0.01	4	38.50	0.01	5
400	38.55	0.03	6	38.52	0.02	8	38.52	0.01	4	38.53	0.01	5
500	38.54	0.03	6	38.52	0.02	8	38.52	0.01	4	38.53	0.01	5
600	38.53	0.02	6	38.51	0.02	8	38.52	0.01	4	38.52	0.01	5
700	38.51	0.02	6	38.50	0.02	8	38.50	0.01	4	38.51	0.01	5
800	38.50	0.01	6	38.49	0.01	8	38.49	0.01	4	38.50	0.01	5
900	38.49	0.01	6	38.49	0.01	8	38.49	0.00	4	38.49	0.01	5
1000	38.48	0.01	6	38.48	0.01	8	38.48	0.00	4	38.48	0.01	5
1200	38.48	0.01	6	38.48	0.01	8	38.47	0.01	4	38.48	0.00	5
1400	38.48	0.01	6	38.48	0.01	8	38.48	0.01	4	38.48	0.00	5
1600	38.48	0.01	6	38.48	0.01	7	38.48	0.01	4	38.48	0.00	5
1800	38.48	0.00	6	38.49	0.00	7	38.48	0.00	4	38.49	0.00	5
2000	38.49	0.00	6	38.49	0.00	7	38.48	0.00	4	38.49	0.00	4
2200	38.49	0.00	5	38.49	0.01	7	38.48	0.00	3	38.49	0.00	4
2400	38.49	0.01	5	38.49	0.01	7	38.49	0.01	2	38.49	0.00	4

Table 4.10. The same as in table 4.1, but for station EPC.

Station EPC (Potential temperature standard deviation number of data)												
Depth	Winter			Spring			Summer			Autumn		
5	14.11	0.43	7	17.89	2.51	5	24.98	1.16	4	19.62	2.78	5
10	14.08	0.42	7	17.64	2.49	5	24.93	1.14	4	19.61	2.53	6
15	14.04	0.42	7	16.84	2.33	5	23.82	1.31	4	19.59	2.53	6
20	13.99	0.43	7	15.97	1.89	5	22.79	2.42	4	19.58	2.53	6
25	13.98	0.43	7	15.67	1.79	5	22.01	2.69	4	19.56	2.53	6
30	13.99	0.42	7	15.22	1.79	5	20.06	2.14	4	19.51	2.51	6
35	13.98	0.44	7	14.70	1.16	5	18.08	1.17	4	19.34	2.46	6
40	13.97	0.46	7	14.22	0.66	5	16.70	0.69	4	18.90	2.37	6
45	13.97	0.47	7	14.03	0.54	5	15.84	0.67	4	18.18	2.27	6
50	13.93	0.42	7	13.91	0.51	5	15.26	0.61	4	17.47	1.71	6
75	13.77	0.24	7	13.47	0.30	5	13.91	0.30	4	15.14	0.97	6

Station EPC (Potential temperature standard deviation number of data)												
Depth	Winter			Spring			Summer			Autumn		
100	13.57	0.20	7	13.23	0.19	5	13.47	0.23	4	13.94	0.27	6
150	13.28	0.06	7	13.19	0.15	5	13.23	0.14	4	13.31	0.10	6
200	13.20	0.06	7	13.21	0.14	5	13.21	0.06	4	13.18	0.07	6
300	13.19	0.05	7	13.22	0.06	5	13.21	0.07	4	13.18	0.06	6
400	13.18	0.02	7	13.20	0.02	5	13.18	0.06	4	13.18	0.05	6
500	13.13	0.01	7	13.15	0.03	5	13.13	0.06	4	13.15	0.04	6
600	13.08	0.02	7	13.10	0.02	5	13.08	0.05	4	13.09	0.03	6
700	13.02	0.01	7	13.05	0.03	5	13.02	0.04	4	13.04	0.03	6
800	12.97	0.01	7	13.01	0.02	5	12.98	0.03	4	12.99	0.02	6
900	12.94	0.01	7	12.96	0.02	5	12.95	0.03	4	12.95	0.02	6
1000	12.92	0.01	7	12.94	0.02	5	12.92	0.03	4	12.93	0.01	6
1200	12.90	0.02	7	12.91	0.02	5	12.89	0.02	4	12.90	0.02	6
1400	12.90	0.01	7	12.90	0.02	5	12.88	0.02	4	12.89	0.02	6
1600	12.90	0.00	7	12.90	0.01	5	12.89	0.01	4	12.90	0.01	6
1800	12.90	0.01	7	12.90	0.01	5	12.89	0.01	4	12.90	0.01	6
2000	12.90	0.01	6	12.90	0.01	5	12.89	0.01	4	12.90	0.01	5
2200	12.90	0.01	6	12.90	0.01	4	12.88	0.02	3	12.88	0.02	3

Station EPC (Salinity standard deviation number of data)												
Depth	Winter			Spring			Summer			Autumn		
5	37.82	0.16	7	37.78	0.16	5	37.47	0.29	4	37.73	0.13	5
10	37.81	0.14	7	37.77	0.16	5	37.48	0.30	4	37.70	0.14	6
15	37.81	0.14	7	37.78	0.20	5	37.51	0.32	4	37.70	0.14	6
20	37.82	0.14	7	37.81	0.23	5	37.48	0.26	4	37.70	0.14	6
25	37.82	0.14	7	37.88	0.22	5	37.61	0.26	4	37.70	0.14	6
30	37.84	0.13	7	37.90	0.22	5	37.67	0.25	4	37.71	0.15	6
35	37.86	0.13	7	37.92	0.23	5	37.77	0.24	4	37.70	0.16	6
40	37.88	0.12	7	37.96	0.21	5	37.84	0.19	4	37.71	0.19	6
45	37.89	0.11	7	37.98	0.19	5	37.85	0.15	4	37.68	0.21	6
50	37.91	0.10	7	38.02	0.16	5	37.90	0.13	4	37.69	0.22	6
75	38.01	0.14	7	38.10	0.12	5	38.07	0.09	4	37.94	0.11	6
100	38.22	0.07	7	38.15	0.10	5	38.17	0.05	4	38.13	0.06	6
150	38.34	0.05	7	38.28	0.06	5	38.31	0.06	4	38.30	0.06	6
200	38.42	0.04	7	38.39	0.05	5	38.39	0.06	4	38.39	0.05	6
300	38.50	0.02	7	38.49	0.03	5	38.50	0.02	4	38.49	0.02	6
400	38.53	0.01	7	38.52	0.00	5	38.52	0.02	4	38.52	0.01	6
500	38.52	0.00	7	38.52	0.01	5	38.52	0.02	4	38.53	0.01	6

Station EPC (Salinity standard deviation number of data)												
Depth	Winter			Spring			Summer			Autumn		
600	38.51	0.00	7	38.52	0.01	5	38.51	0.01	4	38.52	0.01	6
700	38.50	0.00	7	38.51	0.01	5	38.50	0.01	4	38.51	0.01	6
800	38.49	0.00	7	38.50	0.01	5	38.49	0.01	4	38.50	0.00	6
900	38.48	0.00	7	38.49	0.01	5	38.49	0.00	4	38.49	0.00	6
1000	38.48	0.00	7	38.48	0.01	5	38.48	0.00	4	38.48	0.00	6
1200	38.48	0.01	7	38.48	0.01	5	38.47	0.00	4	38.47	0.01	6
1400	38.48	0.00	7	38.48	0.01	5	38.47	0.01	4	38.47	0.01	6
1600	38.48	0.00	7	38.48	0.00	5	38.48	0.00	4	38.48	0.01	6
1800	38.48	0.00	7	38.48	0.00	5	38.48	0.00	4	38.48	0.01	6
2000	38.49	0.00	6	38.48	0.00	5	38.48	0.00	4	38.49	0.00	5
2200	38.49	0.00	6	38.48	0.00	4	38.48	0.00	3	38.48	0.00	3

Table 4.11. Seasonal mean values for chlorophyll-a, dissolved oxygen, nitrate, nitrite, phosphate and silicate concentrations along the water column for the station CP2. Three columns with mean values, standard deviations and number of data are presented for each season and depth level.

Station CP2 (Chlorophyll-a (mg/m ³) standard deviation number of data)												
Depth	Winter			Spring			Summer			Autumn		
0	0.33	0.18	8	0.11	0.07	6	0.08	0.01	6	0.48	0.62	5
10	0.30	0.12	8	0.18	0.09	6	0.08	0.01	6	0.48	0.60	5
20	0.30	0.13	8	0.41	0.37	6	0.10	0.04	6	0.48	0.31	5
50	0.36	0.10	8	0.54	0.47	6	0.28	0.11	6	0.26	0.15	5
75	0.28	0.19	7	0.21	0.11	6	0.26	0.08	6	0.07	0.05	5

Station CP2 (Oxygen (ml/l) standard deviation number of data)												
Depth	Winter			Spring			Summer			Autumn		
0	5.37	0.39	6	5.39	0.38	6	4.46	0.47	5	5.14	0.30	6
10	5.39	0.37	6	5.41	0.43	6	4.50	0.49	5	5.29	0.42	7
20	5.30	0.41	6	5.55	0.54	6	4.90	0.66	5	5.26	0.50	7
50	5.22	0.46	6	5.49	0.63	6	5.38	0.66	5	5.44	0.70	7
75	5.33	0.29	5	5.14	0.50	5	4.97	0.72	3	4.93	0.28	6

Station CP2 (Nitrate (µM) standard deviation number of data)												
Depth	Winter			Spring			Summer			Autumn		
0	0.39	0.36	4	0.08	0.05	4	0.13	0.07	3	1.11	1.43	4
10	0.56	0.57	4	0.07	0.06	4	0.12	0.01	3	0.60	0.91	4
20	0.53	0.56	4	0.11	0.02	4	0.12	0.03	3	0.78	1.21	4
50	1.40	0.47	4	1.16	1.55	4	0.17	0.08	3	3.63	2.05	4
75	1.82	0.73	3	2.95	1.16	4	1.86	0.46	3	3.80	1.75	4

Station CP2 (Nitrite (µM) standard deviation number of data)												
Depth	Winter			Spring			Summer			Autumn		
0	0.12	0.09	4	0.02	0.01	4	0.02	0.02	3	0.22	0.31	4
10	0.12	0.11	4	0.02	0.01	4	0.13	0.11	3	0.06	0.04	4
20	0.14	0.09	4	0.04	0.01	4	0.05	0.03	3	0.06	0.04	4
50	0.19	0.07	4	0.07	0.02	4	0.03	0.01	3	0.11	0.06	4
75	0.16	0.11	3	0.15	0.10	4	0.20	0.08	3	0.05	0.02	4

Station CP2 (Phosphate (µM) standard deviation number of data)												
Depth	Winter			Spring			Summer			Autumn		
0	0.03	0.01	4	0.07	0.06	4	0.04	0.00	3	0.04	0.02	4
10	0.04	0.02	4	0.06	0.05	4	0.04	0.01	3	0.04	0.02	4
20	0.04	0.01	4	0.07	0.05	4	0.04	0.00	3	0.06	0.01	4

Station CP2 (Phosphate (µM) standard deviation number of data)												
Depth	Winter			Spring			Summer			Autumn		
50	0.05	0.01	4	0.08	0.05	4	0.03	0.00	3	0.16	0.09	4
75	0.04	0.02	3	0.11	0.05	4	0.04	0.01	3	0.17	0.08	4

Station CP2 (Silicate (µM) standard deviation number of data)												
Depth	Winter			Spring			Summer			Autumn		
0	1.10	0.20	4	0.79	0.22	4	0.59	0.02	3	0.62	0.22	4
10	1.11	0.25	4	0.76	0.18	4	0.60	0.02	3	0.76	0.43	4
20	1.11	0.25	4	0.76	0.33	4	0.68	0.09	3	0.98	0.52	4
50	1.40	0.09	4	1.55	0.41	4	0.92	0.39	3	1.93	0.63	4
75	1.57	0.25	3	2.34	0.23	4	2.07	0.20	3	2.13	0.32	4

Table 4.12. The same as in table 4.11, but for station CP4

Station CP4 (Chlorophyll-a (mg/m ³) standard deviation number of data)												
Depth	Winter			Spring			Summer			Autumn		
0	0.41	0.20	10	0.10	0.04	7	0.09	0.05	9	0.22	0.13	10
10	0.43	0.23	10	0.12	0.07	7	0.10	0.03	9	0.27	0.23	10
20	0.40	0.17	10	0.14	0.08	7	0.12	0.05	9	0.78	1.12	10
50	0.32	0.14	10	0.34	0.09	7	0.26	0.06	9	0.46	0.42	9
75	0.33	0.55	10	0.26	0.10	7	0.40	0.18	9	0.17	0.20	9
100	0.18	0.22	8	0.15	0.11	5	0.08	0.04	6	0.03	0.02	5

Station CP4 (Oxygen (ml/l) standard deviation number of data)												
Depth	Winter			Spring			Summer			Autumn		
0	5.64	0.19	8	5.39	0.23	8	4.62	0.43	7	5.28	0.39	8
10	5.56	0.27	9	5.45	0.28	8	4.67	0.42	7	5.23	0.38	9
20	5.47	0.34	9	5.53	0.42	8	5.05	0.59	7	5.23	0.39	9
50	5.39	0.31	9	5.42	0.49	8	5.49	0.66	7	5.23	0.54	9
75	5.02	0.32	9	5.27	0.41	8	4.99	0.59	7	5.02	0.41	9
100	4.92	0.30	6	5.05	0.42	6	4.48	0.53	4	4.87	0.33	7
200	4.48	0.33	6	4.60	0.55	6	4.09	0.56	4	4.52	0.27	7
300	4.26	0.27	6	4.17	0.22	6	3.81	0.53	4	4.21	0.36	7
500	4.00	0.22	6	4.07	0.16	6	3.82	0.47	4	4.22	0.38	7
700	4.08	0.20	6	4.13	0.18	6	3.89	0.48	4	4.34	0.40	7
1000	4.16	0.20	6	4.26	0.18	6	4.00	0.50	4	4.46	0.40	7
2100				4.44		1				4.97	0.65	2

Station CP4 (Nitrate (µM) standard deviation number of data)												
Depth	Winter			Spring			Summer			Autumn		
0	0.31	0.26	6	0.21	0.32	4	0.12	0.04	5	0.13	0.12	8
10	0.49	0.66	6	0.37	0.52	4	0.11	0.05	5	0.10	0.07	8
20	1.22	1.57	6	0.54	0.70	4	0.17	0.20	5	0.15	0.16	8
50	1.88	1.47	6	0.81	0.78	4	0.55	0.80	5	2.55	2.12	8
75	2.95	1.49	6	1.95	1.30	4	1.62	1.61	5	3.34	2.30	8
100	3.58	1.20	4	4.69	2.83	3	3.96	0.80	3	4.55	1.46	5
200	5.53	1.06	4	6.15	3.29	3	8.50		1	6.88	2.45	5
300	8.02	1.46	3	7.95	1.63	3	9.77		1	7.93	2.58	5
500	8.22	1.21	3	9.56	2.58	3	10.21		1	7.85	2.50	5
700	8.26	1.21	3	9.63	2.86	3	10.09		1	7.77	2.51	5
1000	8.12	1.14	3	9.21	2.50	3	9.92		1	7.56	2.51	5
2100	7.94	1.22	3	10.52	1.76	2	9.48		1	7.45	2.52	5

Station CP4 (Nitrite (µM) standard deviation number of data)												
Depth	Winter			Spring			Summer			Autumn		
0	0.08	0.06	6	0.02	0.02	4	0.08	0.08	5	0.03	0.03	8
10	0.12	0.13	6	0.02	0.01	4	0.06	0.04	5	0.03	0.03	8
20	0.07	0.04	6	0.03	0.01	4	0.03	0.02	5	0.03	0.04	8
50	0.15	0.08	6	0.08	0.04	4	0.08	0.07	5	0.18	0.16	8
75	0.10	0.05	6	0.14	0.09	4	0.23	0.13	5	0.08	0.07	8
100	0.12	0.07	4	0.04	0.01	3	0.08	0.01	3	0.14	0.16	5
200	0.03	0.01	4	0.03	0.01	3	0.05		1	0.04	0.03	5
300	0.03	0.02	2	0.03	0.01	3	0.05		1	0.03	0.02	5
500	0.02	0.02	2	0.03	0.02	3	0.07		1	0.03	0.02	5
700	0.02	0.01	2	0.02	0.01	3	0.05		1	0.03	0.02	5
1000	0.02	0.02	2	0.02	0.01	3	0.02		1	0.03	0.02	5
2100	0.02	0.01	2	0.03	0.01	2	0.02		1	0.03	0.02	5

Station CP4 (Phosphate (µM) standard deviation number of data)												
Depth	Winter			Spring			Summer			Autumn		
0	0.04	0.01	6	0.06	0.05	4	0.03	0.01	5	0.03	0.01	8
10	0.04	0.03	6	0.06	0.05	4	0.04	0.01	5	0.03	0.02	8
20	0.06	0.05	6	0.06	0.06	4	0.03	0.01	5	0.06	0.08	8
50	0.05	0.03	6	0.06	0.05	4	0.04	0.01	5	0.14	0.10	8
75	0.08	0.04	6	0.09	0.06	4	0.06	0.03	5	0.15	0.07	8
100	0.13	0.05	4	0.21	0.14	3	0.14	0.01	3	0.17	0.07	5
200	0.23	0.09	4	0.30	0.17	3	0.37		1	0.31	0.05	5
300	0.41	0.04	3	0.43	0.05	3	0.67		1	0.39	0.05	5

Station CP4 (Phosphate (μM) standard deviation number of data)												
Depth	Winter			Spring			Summer			Autumn		
500	0.43	0.05	3	0.51	0.09	3	0.63	1	0.41	0.07	5	
700	0.45	0.07	3	0.54	0.10	3	0.68	1	0.40	0.09	5	
1000	0.46	0.08	3	0.53	0.10	3	0.75	1	0.41	0.04	5	
2100	0.43	0.06	3	0.49	0.09	2	0.48	1	0.39	0.07	5	

Station CP4 (Silicate (μM) standard deviation number of data)												
Depth	Winter			Spring			Summer			Autumn		
0	0.98	0.14	6	0.74	0.07	4	0.48	0.13	5	0.63	0.15	8
10	0.99	0.20	6	0.87	0.12	4	0.52	0.15	5	0.64	0.17	8
20	1.20	0.40	6	1.01	0.23	4	0.61	0.16	5	0.69	0.21	8
50	1.42	0.46	6	1.31	0.32	4	0.88	0.46	5	1.61	0.77	8
75	1.75	0.36	6	1.79	0.65	4	1.42	0.70	5	1.93	0.75	8
100	2.13	0.35	4	2.70	0.97	3	2.16	0.06	3	2.24	0.51	5
200	3.42	0.64	4	4.01	1.66	3	3.78	1	4.11	0.54	5	
300	6.32	0.96	3	5.39	0.34	3	5.15	1	5.70	0.51	5	
500	7.31	0.48	3	8.34	1.52	3	6.76	1	7.37	0.68	5	
700	8.05	0.41	3	8.96	1.19	3	7.14	1	7.97	0.49	5	
1000	8.25	0.48	3	9.33	1.11	3	7.71	1	8.41	0.36	5	
2100	8.55	0.49	3	10.15	1.06	2	7.54	1	8.62	0.57	5	

Table 4.13. Seasonally averaged Secchi disk depths for the Cape Palos transect. Three columns with mean values, standard deviations and number of data, are presented for each season.

Secchi disk depth (m) standard deviation number of data)												
	Winter			Spring			Summer			Autumn		
CP2	18.6	2.6	7	19.8	7.2	8	25.3	3.1	6	20.4	10.1	5
CP4	15.8	3.0	6	24.0	4.6	6	29.8	4.9	6	24.2	6.3	6

Table 4.14. Seasonal mean values for chlorophyll-a, dissolved oxygen, nitrate, nitrite, phosphate and silicate concentrations along the water column for the station C20. Three columns with mean values, standard deviations and number of data are presented for each season and depth level.

Station C20 (Chlorophyll-a (mg/m^3) standard deviation number of data)												
Depth	Winter			Spring			Summer			Autumn		
0	0.41	0.12	8	0.18	0.06	7	0.09	0.03	3	0.22	0.02	4
25	0.43	0.11	8	0.18	0.08	7	0.10	0.01	3	0.20	0.05	4
50	0.36	0.12	8	0.46	0.35	7	0.19	0.04	3	0.23	0.04	4

Station C20 (Chlorophyll-a (mg/m ³) standard deviation number of data)												
Depth	Winter			Spring			Summer			Autumn		
75	0.30	0.16	8	0.28	0.15	7	0.32	0.09	3	0.18	0.05	4
95	0.33	0.17	8	0.27	0.11	6	0.17	0.10	2	0.18	0.05	4

Station C20 (Oxygen (ml/l) standard deviation number of data)												
Depth	Winter			Spring			Summer			Autumn		
0	5.80	0.27	5	5.22	0.44	7	4.48	0.58	4	5.34	0.42	4
25	5.79	0.26	5	5.55	0.51	7	5.37	0.55	4	5.37	0.38	5
50	5.68	0.15	5	5.31	0.48	7	5.34	0.61	4	5.73	0.76	4
75	5.63	0.14	5	5.10	0.56	7	4.81	0.50	4	5.40	0.64	4
95	5.77	0.05	2	4.80		1				5.10		1

Station C20 (Nitrate (µM) standard deviation number of data)												
Depth	Winter			Spring			Summer			Autumn		
0	0.38	0.35	5	0.29	0.31	6	0.08	0.04	3	0.08	0.08	6
25	0.55	0.38	5	0.23	0.19	6	0.15	0.01	3	0.33	0.35	6
50	1.00	0.46	4	1.25	0.65	6	0.20	0.15	3	0.67	0.68	6
75	1.22	0.50	4	2.55	0.82	6	1.63	1.38	3	1.29	0.87	6
95	1.38	0.44	4	2.68	1.21	6	4.72		1	1.82	1.17	5

Station C20 (Nitrite (µM) standard deviation number of data)												
Depth	Winter			Spring			Summer			Autumn		
0	0.19	0.18	5	0.08	0.07	6	0.05	0.03	3	0.05	0.04	6
25	0.25	0.12	5	0.08	0.06	6	0.10	0.08	3	0.05	0.03	6
50	0.26	0.11	4	0.21	0.13	6	0.18	0.12	3	0.10	0.06	6
75	0.30	0.12	4	0.35	0.21	6	0.21	0.07	3	0.13	0.07	6
95	0.38	0.12	4	0.32	0.15	6	0.62	NaN	1	0.10	0.02	5

Station C20 (Phosphate (µM) standard deviation number of data)												
Depth	Winter			Spring			Summer			Autumn		
0	0.07	0.05	5	0.08	0.07	6	0.03	0.01	3	0.05	0.05	6
25	0.05	0.03	5	0.06	0.05	6	0.03	0.01	3	0.03	0.02	6
50	0.05	0.02	4	0.06	0.05	6	0.03	0.01	3	0.03	0.03	6
75	0.08	0.03	4	0.10	0.05	6	0.06	0.02	3	0.05	0.03	6
95	0.08	0.03	4	0.10	0.04	5	0.14		1	0.08	0.04	5

Station C20. Silicate (μM), standard deviation y number of data												
Depth	Winter			Spring			Summer			Autumn		
0	0.56	0.29	5	0.56	0.28	6	0.51	0.04	3	0.68	0.22	6
25	0.60	0.29	5	0.83	0.51	6	0.66	0.10	3	0.97	0.39	6
50	0.92	0.39	4	1.60	0.43	6	1.40	0.36	3	1.43	0.60	6
75	1.09	0.43	4	2.53	0.45	6	2.70	0.78	3	2.41	0.78	6
95	1.12	0.39	4	2.76	0.39	5	3.45		1	2.79	1.11	5

Table 4.15. The same as in table 4.14, but for station C18.

Station C18 (Chlorophyll-a (mg/m^3) standard deviation number of data)												
Depth	Winter			Spring			Summer			Autumn		
0	0.34	0.07	7	0.13	0.08	8	0.09	0.02	3	0.18	0.06	4
25	0.39	0.10	7	0.22	0.17	8	0.11	0.02	3	0.20	0.06	4
50	0.33	0.08	7	0.48	0.23	8	0.29	0.10	3	0.26	0.05	4
75	0.18	0.08	7	0.22	0.09	8	0.34	0.07	3	0.21	0.10	4
100	0.10	0.06	7	0.09	0.12	8	0.11	0.04	3	0.13	0.06	4

Station C18 (Oxygen (ml/l) standard deviation number of data)												
Depth	Winter			Spring			Summer			Autumn		
0	5.81	0.27	5	5.16	0.43	7	4.43	0.52	4	5.12	0.26	5
25	5.71	0.27	6	5.52	0.48	7	5.57	0.61	4	5.38	0.39	5
50	5.61	0.18	6	5.32	0.43	7	5.39	0.64	4	5.86	0.63	5
75	5.53	0.25	6	5.09	0.50	7	4.88	0.66	4	5.33	0.38	5
100	5.49	0.24	6	5.04	0.40	7	4.76	0.61	4	5.11	0.30	5
200	5.15	0.31	6	4.83	0.42	7	4.72	0.67	4	4.95	0.46	5
300	4.73	0.37	6	4.29	0.38	5	4.64	0.17	2	4.62	0.44	5

Station C18 (Nitrate (μM) standard deviation number of data)												
Depth	Winter			Spring			Summer			Autumn		
0	0.40	0.35	5	0.41	0.77	9	0.07	0.04	3	0.10	0.08	6
25	0.60	0.60	5	0.16	0.23	9	0.17	0.02	3	0.24	0.20	6
50	1.00	0.72	5	1.06	0.69	10	0.11	0.03	3	0.55	0.51	6
75	2.17	0.53	5	2.14	0.94	11	1.30	1.07	3	1.27	0.77	6
100	2.72	0.81	5	3.60	1.87	11	3.27	0.25	3	2.26	1.08	6
200	3.85	1.36	5	4.42	1.27	10	4.64	0.34	2	4.15	1.70	6
300	6.40	0.96	3	6.73	1.77	8	7.29		1	6.20	2.05	6

Station C18 (Nitrite (μM) standard deviation number of data)												
Depth	Winter			Spring			Summer			Autumn		
0	0.12	0.10	5	0.16	0.33	9	0.04	0.02	3	0.02	0.01	6
25	0.19	0.16	5	0.11	0.20	9	0.11	0.11	3	0.03	0.02	6
50	0.14	0.11	5	0.20	0.15	10	0.07	0.02	3	0.04	0.03	6
75	0.13	0.06	5	0.19	0.13	11	0.12	0.04	3	0.08	0.05	6
100	0.10	0.06	5	0.12	0.10	11	0.17	0.15	3	0.05	0.03	6
200	0.08	0.08	5	0.10	0.12	10	0.17	0.16	2	0.04	0.02	6
300	0.02	0.02	3	0.11	0.09	8	0.54		1	0.05	0.05	6

Station C18 (Phosphate (μM) standard deviation number of data)												
Depth	Winter			Spring			Summer			Autumn		
0	0.06	0.04	5	0.07	0.06	9	0.18	0.22	3	0.05	0.05	6
25	0.04	0.02	5	0.05	0.06	9	0.02	0.00	3	0.03	0.02	6
50	0.05	0.03	5	0.07	0.04	10	0.02	0.01	3	0.02	0.01	6
75	0.08	0.04	5	0.08	0.05	11	0.04	0.01	3	0.03	0.01	6
100	0.08	0.03	5	0.11	0.08	11	0.07	0.02	3	0.03	0.01	6
200	0.13	0.07	5	0.18	0.09	10	0.07	0.00	2	0.14	0.07	6
300	0.27	0.16	3	0.30	0.09	8	0.22		1	0.24	0.11	6

Station C18 (Silicate (μM) standard deviation number of data)												
Depth	Winter			Spring			Summer			Autumn		
0	1.09	0.16	5	0.96	0.36	9	0.43	0.28	3	0.66	0.16	6
25	1.15	0.19	5	0.96	0.36	9	0.63	0.12	3	0.73	0.19	6
50	1.17	0.32	5	1.16	0.69	10	0.84	0.17	3	1.06	0.32	6
75	1.55	0.12	5	1.59	0.46	11	1.25	0.51	3	1.49	0.67	6
100	1.74	0.25	5	2.18	0.75	11	2.10	0.25	3	2.16	0.73	6
200	2.39	0.81	5	2.72	0.73	10	2.44	0.16	2	2.85	0.50	6
300	4.02	0.37	3	4.42	1.23	8	4.22		1	4.65	1.03	6

Table 4.16. Seasonally averaged Secchi disk depths for the Ibiza Channel transect. Three columns with mean values, standard deviations and number of data, are presented for each season.

Secchi disk depth (m) standard deviation number of data												
	Winter			Spring			Summer			Autumn		
C20	14.9	2.2	7	18.6	4.1	9	21.3	3.5	3	20.4	4.7	5
C18	18.9	4.1	7	24.0	4.5	9	24.0	2.3	4	21.5	5.6	6

Table 4.17. Seasonal mean values for chlorophyll-a, dissolved oxygen, nitrate, nitrite, phosphate and silicate concentrations along the water column for the station B1. Three columns with mean values,

standard deviations and number of data are presented for each season and depth level.

Station B1 (Chlorophyll-a (mg/m ³) standard deviation number of data)												
Depth	Winter			Spring			Summer			Autumn		
0	0.49	0.38	9	0.14	0.08	11	0.09	0.05	5	0.16	0.06	8
25	0.48	0.36	9	0.17	0.19	11	0.12	0.11	5	0.16	0.05	8
50	0.39	0.25	9	0.35	0.22	11	0.18	0.06	5	0.26	0.10	8
75	0.39	0.36	9	0.49	0.37	11	0.43	0.21	5	0.15	0.08	8

Station B1 (Oxygen (ml/l) standard deviation number of data)												
Depth	Winter			Spring			Summer			Autumn		
0	5.71	0.09	4	5.25	0.21	7	4.42	0.56	4	5.36	0.41	5
25	5.60	0.04	4	5.47	0.30	7	5.04	0.40	4	5.38	0.45	5
50	5.41	0.17	4	5.53	0.40	7	5.32	0.82	4	5.73	0.89	5
75	5.51	0.14	2	5.11	0.47	2	5.63		1	6.96		1

Station B1 (Nitrate (µM) standard deviation number of data)												
Depth	Winter			Spring			Summer			Autumn		
0	0.43	0.47	5	0.05	0.06	8	0.03	0.05	5	0.05	0.07	9
25	0.06	0.10	5	0.20	0.34	8	0.25	0.38	5	0.06	0.08	9
50	0.36	0.37	5	0.67	1.04	8	0.24	0.38	5	0.18	0.31	9
75	1.89	1.46	5	1.71	1.10	8	0.54	0.38	5	1.10	0.75	9

Station B1 (Nitrite (µM) standard deviation number of data)												
Depth	Winter			Spring			Summer			Autumn		
0	0.01	0.01	5	0.02	0.02	8	0.03	0.05	5	0.02	0.03	9
25	0.03	0.04	5	0.04	0.05	8	0.06	0.10	5	0.03	0.04	9
50	0.04	0.05	5	0.08	0.10	8	0.05	0.08	5	0.06	0.06	9
75	0.03	0.03	5	0.15	0.14	8	0.19	0.18	5	0.12	0.09	9

Station B1 (Phosphate (µM) standard deviation number of data)												
Depth	Winter			Spring			Summer			Autumn		
0	0.01	0.01	5	0.02	0.02	8	0.02	0.01	5	0.01	0.01	9
25	0.02	0.02	5	0.02	0.02	8	0.02	0.02	5	0.04	0.07	9
50	0.01	0.02	5	0.02	0.03	8	0.13	0.23	5	0.02	0.01	9
75	0.02	0.02	5	0.06	0.08	8	0.03	0.03	5	0.03	0.03	9

Station B1 (Silicate (μM) standard deviation number of data)												
Depth	Winter			Spring			Summer			Autumn		
0	0.97	0.09	5	0.90	0.42	8	0.69	0.35	5	0.62	0.31	9
25	0.98	0.05	5	1.06	0.35	8	0.68	0.35	5	0.56	0.36	9
50	1.23	0.39	5	1.02	0.63	8	0.63	0.73	5	0.93	0.16	9
75	1.76	0.80	5	1.50	0.87	8	1.38	0.51	5	1.46	0.45	9

Table 4.18. The same as in table 4.17, but for station B2.

Station B2 (Chlorophyll-a (mg/m^3) standard deviation number of data)												
Depth	Winter			Spring			Summer			Autumn		
0	0.31	0.20	9	0.10	0.07	11	0.06	0.03	5	0.09	0.03	7
25	0.39	0.27	9	0.18	0.20	11	0.09	0.05	5	0.12	0.04	7
50	0.33	0.16	9	0.23	0.12	11	0.14	0.04	5	0.25	0.10	7
75	0.30	0.22	9	0.45	0.63	11	0.21	0.10	5	0.14	0.07	7
100	0.14	0.07	9	0.20	0.14	10	0.23	0.13	5	0.06	0.04	7

Station B2 (Oxygen (ml/l) standard deviation number of data)												
Depth	Winter			Spring			Summer			Autumn		
0	5.73	0.08	4	5.20	0.18	7	4.44	0.56	4	5.32	0.42	6
25	5.67	0.06	4	5.43	0.27	7	5.09	0.37	4	5.36	0.41	6
50	5.46	0.24	4	5.64	0.45	7	5.36	0.78	4	5.71	0.80	6
75	5.39	0.30	4	5.06	0.32	7	4.72	0.70	4	5.41	0.66	6
100	4.99	0.17	2	4.75	0.33	4	5.14		1	4.81	0.33	4

Station B2 (Nitrate (μM) standard deviation number of data)												
Depth	Winter			Spring			Summer			Autumn		
0	0.02	0.03	5	0.28	0.46	8	0.05	0.05	5	0.18	0.35	8
25	0.22	0.39	5	0.13	0.26	8	0.44	0.78	5	0.05	0.04	8
50	0.48	0.44	5	0.54	0.83	8	0.47	0.77	5	0.23	0.37	8
75	1.92	1.08	5	1.81	1.14	8	1.31	1.06	5	1.18	0.85	8
100	3.32	0.77	5	4.09	2.47	7	3.10	0.12	5	2.08	1.12	8

Station B2 (Nitrite (μM) standard deviation number of data)												
Depth	Winter			Spring			Summer			Autumn		
0	0.02	0.02	5	0.06	0.11	8	0.02	0.03	5	0.06	0.12	8
25	0.01	0.01	5	0.02	0.02	8	0.03	0.04	5	0.05	0.10	8
50	0.05	0.08	5	0.09	0.12	8	0.05	0.08	5	0.07	0.09	8
75	0.02	0.02	5	0.13	0.15	8	0.14	0.18	5	0.08	0.05	8

Station B2 (Nitrite (μM) standard deviation number of data)												
Depth	Winter			Spring			Summer			Autumn		
100	0.03	0.05	5	0.09	0.11	7	0.15	0.17	5	0.09	0.07	8

Station B2 (Phosphate (μM) standard deviation number of data)												
Depth	Winter			Spring			Summer			Autumn		
0	0.01	0.02	5	0.04	0.05	8	0.03	0.03	5	0.02	0.01	8
25	0.01	0.01	5	0.01	0.01	8	0.02	0.02	5	0.06	0.11	8
50	0.01	0.02	5	0.02	0.02	8	0.02	0.02	5	0.02	0.02	8
75	0.02	0.02	5	0.05	0.05	8	0.03	0.03	5	0.03	0.04	8
100	0.04	0.06	5	0.09	0.08	7	0.07	0.06	5	0.04	0.04	8

Station B2 (Silicate (μM) standard deviation number of data)												
Depth	Winter			Spring			Summer			Autumn		
0	0.95	0.11	5	1.03	0.22	8	0.67	0.35	5	0.66	0.23	8
25	0.99	0.03	5	1.08	0.34	8	0.67	0.34	5	0.56	0.29	8
50	1.19	0.41	5	0.89	0.65	8	0.76	0.67	5	0.88	0.24	8
75	1.52	0.59	5	1.47	0.54	8	1.41	0.56	5	1.27	0.38	8
100	2.09	0.11	5	2.17	0.67	7	2.13	0.49	5	1.77	0.51	8

Table 4.19. The same as in table 4.17, but for station B3.

Station B3 (Chlorophyll-a (mg/m^3) standard deviation number of data)												
Depth	Winter			Spring			Summer			Autumn		
0	0.35	0.20	7	0.10	0.06	11	0.06	0.03	5	0.10	0.03	6
25	0.32	0.25	7	0.11	0.05	10	0.11	0.08	5	0.13	0.04	6
50	0.29	0.13	7	0.18	0.08	11	0.13	0.09	5	0.29	0.11	6
75	0.32	0.21	7	0.30	0.17	11	0.22	0.08	5	0.16	0.08	6
100	0.13	0.13	7	0.14	0.11	11	0.10	0.05	5	0.05	0.02	6

Station B3 (Oxygen (ml/l) standard deviation number of data)												
Depth	Winter			Spring			Summer			Autumn		
0	5.71	0.09	3	5.20	0.19	7	4.44	0.56	4	5.32	0.40	6
25	5.68	0.09	4	5.46	0.28	7	5.15	0.43	4	5.37	0.41	6
50	5.55	0.14	4	5.59	0.46	7	5.41	0.72	4	5.55	0.75	6
75	5.33	0.20	4	5.19	0.40	7	4.71	0.57	4	5.31	0.71	6
100	4.80	0.09	4	4.91	0.29	7	4.51	0.60	4	5.06	0.51	6
200	4.35	0.18	3	4.32	0.23	6	4.16	0.58	4	4.68	0.33	6

Station B3 (Nitrate (µM) standard deviation number of data)												
Depth	Winter			Spring			Summer			Autumn		
0	0.01	0.02	5	0.73	1.79	8	0.07	0.08	5	0.20	0.39	8
25	0.03	0.05	5	0.06	0.06	8	0.64	1.18	5	0.04	0.03	8
50	0.64	0.75	5	0.64	1.43	8	0.86	1.57	5	0.32	0.30	8
75	1.95	0.97	5	1.99	1.48	8	2.11	1.74	5	1.33	0.83	8
100	3.79	1.38	5	3.39	1.28	8	4.11	1.29	5	2.38	1.41	8
200	6.96	1.63	5	7.03	1.37	7	6.35	1.27	3	5.59	1.47	8

Station B3 (Nitrite (µM) standard deviation number of data)												
Depth	Winter			Spring			Summer			Autumn		
0	0.00	0.01	5	0.02	0.02	8	0.02	0.03	5	0.08	0.13	8
25	0.01	0.01	5	0.02	0.02	8	0.02	0.02	5	0.01	0.01	8
50	0.05	0.06	5	0.03	0.03	8	0.02	0.02	5	0.08	0.05	8
75	0.02	0.03	5	0.07	0.07	8	0.13	0.13	5	0.16	0.13	8
100	0.01	0.01	5	0.04	0.05	8	0.08	0.10	5	0.15	0.17	8
200	0.01	0.01	5	0.03	0.03	7	0.01	0.01	3	0.08	0.16	8

Station B3 (Phosphate (µM) standard deviation number of data)												
Depth	Winter			Spring			Summer			Autumn		
0	0.01	0.02	5	0.01	0.02	8	0.02	0.02	5	0.02	0.02	8
25	0.01	0.01	5	0.01	0.01	8	0.02	0.02	5	0.01	0.01	8
50	0.01	0.01	5	0.03	0.04	8	0.14	0.25	5	0.02	0.02	8
75	0.02	0.02	5	0.05	0.05	8	0.03	0.03	5	0.04	0.05	8
100	0.05	0.07	5	0.08	0.07	8	0.12	0.12	5	0.05	0.06	8
200	0.12	0.15	5	0.17	0.15	7	0.12	0.17	3	0.14	0.12	8

Station B3 Silicate (µM) standard deviation number of data)												
Depth	Winter			Spring			Summer			Autumn		
0	0.94	0.13	5	0.85	0.55	8	0.67	0.35	5	0.70	0.20	8
25	0.92	0.14	5	0.91	0.44	8	0.88	0.64	5	0.59	0.28	8
50	1.24	0.39	5	1.09	0.61	8	1.04	1.03	5	0.81	0.16	8
75	1.57	0.50	5	1.66	0.59	8	1.74	1.18	5	1.01	0.25	8
100	2.39	0.48	5	2.26	0.44	8	2.38	0.96	5	1.56	0.50	8
200	4.41	0.82	5	4.32	0.70	7	4.12	0.17	3	3.74	0.39	8

Table 4.20. Seasonally averaged Secchi disk depths for the Mallorca transect. Three columns with mean values, standard deviations and number of data, are presented for each season.

Secchi disk depth (m) standard deviation number of data												
	Winter			Spring			Summer			Autumn		
B1	23.0	5.2	27	25.6	6.8	29	31.4	6.3	18	26.1	5.9	22
B2	22.6	4.8	27	27.7	6.8	30	32.8	5.1	19	27.4	5.6	21
B3	22.0	4.8	27	28.2	6.2	26	31.7	5.7	18	27.0	3.9	20

Table 4.21. Seasonal mean values for chlorophyll-a, dissolved oxygen, nitrate, nitrite, phosphate and silicate concentrations along the water column for the station MH2. Three columns with mean values, standard deviations and number of data are presented for each season and depth level.

Station MH2 (Chlorophyll-a (mg/m ³) standard deviation number of data)												
Depth	Winter			Spring			Summer			Autumn		
0	0.60	0.44	7	0.16	0.13	6	0.05	0.01	2	0.14		1
25	0.42	0.22	7	0.25	0.29	6	0.05	0.01	2	0.15		1
50	0.28	0.17	7	0.35	0.26	6	0.11	0.01	2	0.26		1
75	0.21	0.14	7	0.19	0.11	6	0.35	0.23	2	0.09		1
100	0.25	0.19	7	0.10	0.06	6	0.18	0.08	2	0.01		1

Station MH2 (Oxygen (ml/l) standard deviation number of data)												
Depth	Winter			Spring			Summer			Autumn		
0	5.77	0.10	3	5.37	0.45	6	4.59	0.55	3	4.96	0.07	3
25	5.65	0.19	4	5.53	0.43	6	5.32	0.34	3	4.97	0.09	3
50	5.53	0.23	4	5.59	0.48	6	5.67	0.76	3	5.20	0.34	3
75	5.42	0.27	4	5.29	0.44	6	5.24	0.83	3	5.16	0.16	3
100	5.43	0.19	4	5.16	0.42	6	4.89	0.54	3	4.82	0.20	3

Station MH2 (Nitrate (µM) standard deviation number of data)												
Depth	Winter			Spring			Summer			Autumn		
0	0.57	0.24	2	0.07	0.07	3	0.08	0.01	2	0.14		1
25	0.89	0.41	2	0.28	0.37	3	0.11	0.05	2	0.02		1
50	1.02	0.47	2	0.35	0.40	3	0.06	0.01	2	0.07		1
75	1.14	0.45	2	2.37	1.76	3	0.78	0.73	2	0.63		1
100	1.23	0.38	2	3.06	1.35	3	3.18	0.78	2	1.13		1
180	1.91	0.39	2	3.13	0.38	2	5.35		1			

Station MH2 (Nitrite (µM) standard deviation number of data)												
Depth	Winter			Spring			Summer			Autumn		
0	0.13	0.06	2	0.02	0.01	3	0.02	0.01	2	0.01		1
25	0.20	0.08	2	0.05	0.05	3	0.02	0.01	2	0.00		1
50	0.30	0.16	2	0.06	0.06	3	0.02	0.01	2	0.05		1

Station MH2 (Nitrite (µM) standard deviation number of data)											
Depth	Winter			Spring			Summer			Autumn	
75	0.27	0.09	2	0.08	0.03	3	0.13	0.03	2	0.12	1
100	0.27	0.07	2	0.05	0.01	3	0.06	0.02	2	0.12	1
180	0.27	0.09	2	0.04	0.00	2	0.05		1		

Station MH2 (Phosphate (µM) standard deviation number of data)											
Depth	Winter			Spring			Summer			Autumn	
0	0.04	0.01	2	0.02	0.00	3	0.02	0.01	2	0.01	1
25	0.03	0.00	2	0.01	0.00	3	0.02	0.00	2	0.01	1
50	0.04	0.01	2	0.04	0.02	3	0.02	0.00	2	0.01	1
75	0.04	0.00	2	0.08	0.05	3	0.03	0.02	2	0.02	1
100	0.04	0.00	2	0.11	0.04	3	0.09	0.02	2	0.04	1
180	0.06	0.00	2	0.14	0.04	2	0.30		1		

Station MH2 (Silicate (µM) standard deviation number of data)											
Depth	Winter			Spring			Summer			Autumn	
0	1.40	0.10	2	1.13	0.13	3	0.88	0.01	2	0.64	1
25	1.50	0.18	2	1.41	0.29	3	0.88	0.03	2	0.55	1
50	1.53	0.19	2	1.37	0.31	3	0.59	0.09	2	0.75	1
75	1.59	0.21	2	1.99	0.92	3	1.14	0.39	2	0.89	1
100	1.61	0.16	2	2.24	0.75	3	2.02	0.04	2	1.01	1
180	1.85	0.16	2	2.46	0.08	2	2.88		1		

Table 4.22. The same as in table 4.21, but for the station MH4.

Station MH4 (Chlorophyll-a (mg/m ³) standard deviation number of data)												
Depth	Winter			Spring			Summer			Autumn		
0	0.60	0.46	7	0.12	0.08	6	0.05	0.01	2			
25	0.44	0.24	7	0.35	0.35	6	0.06	0.01	2	0.17	0.02	2
50	0.31	0.17	7	0.41	0.26	6	0.13	0.01	2	0.19	0.06	2
75	0.17	0.07	7	0.21	0.11	6	0.52	0.18	2	0.14	0.03	2
100	0.11	0.15	7	0.11	0.04	5	0.09	0.00	2	0.04	0.01	2

Station MH4 (Oxygen (ml/l) standard deviation number of data)												
Depth	Winter			Spring			Summer			Autumn		
0	5.75	0.26	3	5.14	0.28	4	4.58	0.58	3	5.10	0.26	4
25	5.47	0.21	3	5.50	0.41	5	5.01	0.44	3	5.09	0.26	4
50	5.43	0.20	3	5.57	0.52	5	5.72	0.64	3	5.24	0.30	4

Station MH4 (Oxygen (ml/l) standard deviation number of data)												
Depth	Winter			Spring			Summer			Autumn		
75	5.38	0.20	3	5.14	0.34	5	5.04	0.80	3	5.31	0.36	4
100	5.31	0.32	3	4.94	0.30	5	4.80	0.64	3	5.06	0.49	4
200	4.43	0.22	3	4.42	0.13	5	4.48	0.68	3	4.51	0.33	4
300	4.09	0.08	3	4.27	0.11	5	4.17	0.55	3	4.32	0.25	4
500	3.99	0.02	3	4.18	0.17	5	4.02	0.50	3	4.17	0.23	4
700	4.17	0.09	3	4.24	0.14	5	4.10	0.53	3	4.27	0.25	4
1000	4.19	0.06	3	4.32	0.09	5	4.24	0.56	3	4.37	0.24	4
1500	4.33	0.09	3	4.40	0.06	4	4.33	0.58	3	4.47	0.25	4

Station MH4 (Nitrate (µM) standard deviation number of data)												
Depth	Winter			Spring			Summer			Autumn		
0	1.06	0.41	2	0.39	0.60	4	0.10	0.08	2	0.05	NaN	1
25	1.15	0.44	2	0.25	0.21	4	0.11	0.02	2	0.03	0.03	2
50	1.27	0.32	2	0.57	0.43	4	0.13	0.07	2	0.33	0.23	2
75	1.39	0.38	2	2.94	0.75	4	1.24	0.72	2	1.03	0.62	2
100	4.11	3.25	2	3.87	1.45	4	3.68	0.28	2	1.64	0.74	2
200	6.79	0.59	2	6.27	2.04	4	6.50		1	6.06	0.42	2
300	7.77	0.32	2	6.73	1.99	4	7.50		1	7.78	0.08	2
500	8.84	0.34	2	7.11	1.78	4	9.51		1	8.83	0.64	2
700	8.76	0.23	2	7.07	1.82	4	9.75		1	8.63	0.63	2
1000	8.94	0.03	2	7.01	1.86	4	8.91		1	8.49	0.64	2
1500	8.85	0.03	2	6.94	1.79	4	9.02		1	8.08	0.30	2
2500	8.77	0.01	2	6.24	1.72	3	8.25		1	8.30	0.65	2

Station MH4 (Nitrite (µM) standard deviation number of data)												
Depth	Winter			Spring			Summer			Autumn		
0	0.11	0.01	2	0.02	0.00	4	0.08	0.07	2	0.00		1
25	0.12	0.01	2	0.07	0.04	4	0.18	0.17	2	0.02	0.02	2
50	0.14	0.03	2	0.10	0.08	4	0.06	0.04	2	0.14	0.10	2
75	0.15	0.04	2	0.21	0.12	4	0.48	0.32	2	0.14	0.07	2
100	0.09	0.08	2	0.11	0.04	4	0.45	0.41	2	0.04	0.02	2
200	0.02	0.00	2	0.03	0.01	4	0.89		1	0.03	0.01	2
300	0.01	0.00	2	0.04	0.01	4	0.73		1	0.02	0.02	2
500	0.00	0.00	2	0.04	0.02	4	0.40		1	0.06	0.03	2
700	0.01	0.01	2	0.02	0.01	4	0.25		1	0.04	0.04	2
1000	0.00	0.00	2	0.03	0.01	4	0.75		1	0.02	0.02	2
1500	0.00	0.00	2	0.04	0.03	4	0.77		1	0.10	0.06	2
2500	0.00	0.00	2	0.02	0.01	3	0.55		1	0.03	0.02	2

Station MH4. Phosphate (μM), standard deviation y number of data												
Depth	Winter			Spring			Summer			Autumn		
0	0.04	0.01	2	0.05	0.03	4	0.04	0.02	2	0.01		1
25	0.03	0.00	2	0.03	0.00	4	0.05	0.04	2	0.02	0.02	2
50	0.04	0.00	2	0.03	0.01	4	0.06	0.03	2	0.03	0.01	2
75	0.04	0.00	2	0.08	0.01	4	0.05	0.03	2	0.03	0.00	2
100	0.16	0.13	2	0.17	0.06	4	0.13	0.03	2	0.04	0.02	2
200	0.26	0.03	2	0.37	0.03	4	0.25		1	0.18	0.14	2
300	0.32	0.01	2	0.41	0.03	4	0.31		1	0.26	0.18	2
500	0.39	0.03	2	0.46	0.06	4	0.42		1	0.36	0.14	2
700	0.38	0.02	2	0.46	0.06	4	0.44		1	0.34	0.19	2
1000	0.40	0.01	2	0.45	0.05	4	0.43		1	0.36	0.13	2
1500	0.39	0.01	2	0.44	0.05	4	0.41		1	0.40	0.08	2
2500	0.39	0.01	2	0.45	0.05	3	0.41		1	0.32	0.14	2

Station MH4 (Silicate (μM) standard deviation number of data)												
Depth	Winter			Spring			Summer			Autumn		
0	1.39	0.07	2	1.30	0.31	4	0.84	0.07	2	0.56		1
25	1.39	0.08	2	1.50	0.17	4	0.92	0.21	2	0.64	0.07	2
50	1.47	0.00	2	1.55	0.56	4	1.33	0.15	2	0.76	0.10	2
75	1.50	0.05	2	2.54	0.53	4	1.63	0.20	2	1.05	0.16	2
100	2.89	1.49	2	3.01	0.60	4	2.34	0.16	2	1.40	0.10	2
200	3.93	0.46	2	5.13	0.66	4	3.59		1	3.49	0.48	2
300	5.25	0.24	2	6.22	0.68	4	4.72		1	5.22	0.45	2
500	7.37	0.41	2	7.60	0.40	4	6.99		1	7.34	0.20	2
700	7.67	0.71	2	8.14	0.47	4	7.82		1	7.71	0.31	2
1000	8.58	0.22	2	8.41	0.36	4	7.35		1	8.18	0.39	2
1500	8.69	0.30	2	8.28	0.43	4	7.50		1	8.05	0.01	2
2500	8.82	0.44	2	8.39	0.49	3	7.50		1	8.79	0.61	2

Table 4.23. Seasonally averaged Secchi disk depths for the Mahon transect. Three columns with mean values, standard deviations and number of data are presented for each season.

Secchi disk depth (m) standard deviation number of data												
	Winter			Spring			Summer			Autumn		
MH2	16.5	5.3	8	24.4	8.2	7	29.0		1	23.0	5.2	3
MH4	14.9	4.7	8	24.9	8.2	8	32.0		1	25.8	5.6	4

Table 4.24. Average abundances expressed as cells per milliliter (cel./ml), along the water column for the station CP2 for the following micro-phytoplanktonic groups: diatoms, dinoflagellates and small flagellates. For each season five columns are presented: Seasonal mean value, standard deviation, number of data used, minimum and maximum values recorded for each group along the complete time series.

		Station CP2. Diatoms (cells/ml)																			
		Winter					Spring					Summer					Autumn				
Depth		mean	σ	n	Min.	Max.	mean	σ	n	Min.	Max.	mean	σ	n	Min.	Max.	mean	σ	n	Min.	Max.
0		62	153	8	0	465	16	23	7	0	69	1	1	7	0	4	28	38	6	1	105
10		35	72	8	0	224	22	25	7	0	56	2	3	7	0	9	40	55	6	0	145
20		4	5	8	0	13	35	52	7	0	141	4	5	7	0	12	30	46	5	1	121
50		4	3	8	0	10	57	123	7	0	358	8	16	7	0	48	13	11	6	2	32
75		3	3	7	0	11	23	36	7	0	107	13	28	7	0	83	1	0	4	1	2

		Station CP2. Dinoflagellates (cells/ml)																			
		Winter					Spring					Summer					Autumn				
Depth		mean	σ	n	Min.	Max.	mean	σ	n	Min.	Max.	mean	σ	n	Min.	Max.	mean	σ	n	Min.	Max.
0		6	8	8	0	21	7	6	7	0	16	5	9	7	0	27	18	15	6	0	42
10		6	7	8	0	21	6	6	7	0	15	3	3	7	0	8	17	10	6	0	31
20		5	6	8	0	19	7	9	7	0	25	6	7	7	0	20	8	6	5	0	16
50		2	1	8	0	4	10	11	7	0	30	8	12	7	0	35	10	11	6	1	27
75		3	3	7	0	10	2	3	7	0	7	4	7	7	0	22	1	0	2	1	1

		Station CP2. Small flagellates (cells/ml)																			
		Winter					Spring					Summer					Autumn				
Depth		mean	σ	n	Min.	Max.	mean	σ	n	Min.	Max.	mean	σ	n	Min.	Max.	mean	σ	n	Min.	Max.
0		49	40	7	0	123	42	43	7	0	122	19	19	7	0	52	81	126	6	4	358
10		50	58	8	0	145	45	37	7	0	88	53	64	7	0	190	54	49	6	1	134
20		32	29	7	0	83	26	25	7	0	73	37	32	7	0	73	23	17	5	9	54
50		16	13	7	0	38	32	52	7	0	157	26	30	7	0	85	52	63	6	5	175
75		14	22	7	0	66	12	15	7	0	47	9	8	7	0	21	3	3	5	1	8

Table 4.25. The same as in table 4.24, but for station C20.

Station C20. Diatoms (cells/ml)																				
Depth	Winter				Spring				Summer				Autumn							
	mean	σ	n	Min.	Max.	mean	σ	n	Min.	Max.	mean	σ	n	Min.	Max.	mean	σ	n	Min.	Max.
0	16	17	8	0	54	41	54	8	0	165	1	1	5	0	4	11	15	6	1	44
25	16	20	8	0	65	34	59	8	0	183	1	2	5	0	5	8	9	6	2	29
50	10	11	8	0	35	5	5	7	0	14	3	3	5	0	6	5	4	6	1	12
75	13	14	8	0	44	7	8	8	0	21	7	7	5	0	19	3	1	3	2	4
95	13	18	8	0	53	4	5	7	0	13	3	3	4	0	8	4	2	6	1	6

Station C20. Dinoflagellates (cells/ml)																				
Depth	Winter				Spring				Summer				Autumn							
	mean	σ	n	Min.	Max.	mean	σ	n	Min.	Max.	mean	σ	n	Min.	Max.	mean	σ	n	Min.	Max.
0	11	11	9	0	30	8	9	8	0	25	10	14	5	0	37	5	5	6	1	15
25	5	5	8	0	18	6	6	8	0	20	8	10	5	0	26	9	9	6	1	27
50	5	6	9	0	15	5	7	7	0	18	7	9	5	0	23	4	5	6	0	15
75	3	3	9	0	8	7	14	8	0	44	3	4	5	0	9	3	3	6	0	8
95	2	3	8	0	9	3	3	7	0	8	4	4	4	0	10	1	1	6	0	2

Station C20. Small flagellates (cells/ml)																				
Depth	Winter				Spring				Summer				Autumn							
	mean	σ	n	Min.	Max.	mean	σ	n	Min.	Max.	mean	σ	n	Min.	Max.	mean	σ	n	Min.	Max.
0	67	62	8	0	208	27	21	7	0	52	15	14	5	0	37	44	36	6	0	117
25	52	31	8	0	103	46	50	8	0	146	34	30	5	0	75	33	18	6	4	60
50	27	23	8	0	61	33	33	7	0	88	21	22	5	0	58	35	27	6	4	78
75	21	15	9	0	43	14	14	8	0	43	10	11	5	0	28	23	23	6	7	73
95	15	18	8	0	58	11	11	7	0	29	5	8	4	0	19	24	37	6	0	105

Table 4.26. The same as in table 4.24, but for station B1.

Station B1. Diatoms (cells/ml)																										
		Winter						Spring						Summer						Autumn						
Depth	mean	σ	n	Min.	Max.	mean	σ	n	Min.	Max.	mean	σ	n	Min.	Max.	mean	σ	n	Min.	Max.	mean	σ	n	Min.	Max.	
0	7	15	15	0	51	3	4	14	0	15	3	3	7	0	9	4	6	10	0	20						
25	4	6	12	0	24	2	2	14	0	5	1	1	9	0	2	2	2	10	0	7						
50	4	4	12	0	15	4	10	15	0	38	1	1	9	0	4	4	3	11	0	9						
75	3	3	12	0	9	9	16	13	0	61	2	3	8	0	8	2	2	9	0	6						

Station B1. Dinoflagellates (cells/ml)																										
		Winter						Spring						Summer						Autumn						
Depth	mean	σ	n	Min.	Max.	mean	σ	n	Min.	Max.	mean	σ	n	Min.	Max.	mean	σ	n	Min.	Max.	mean	σ	n	Min.	Max.	
0	4	3	15	1	11	8	7	14	1	29	12	14	7	3	46	4	2	10	1	7						
25	3	2	12	0	8	9	6	14	3	19	6	3	9	0	10	7	7	10	1	23						
50	4	3	12	1	13	5	5	15	0	19	6	4	9	0	15	4	3	10	1	8						
75	3	3	12	0	10	4	4	13	1	17	4	3	8	0	9	4	4	10	0	11						

Station B1. Small flagellates (cells/ml)																										
		Winter						Spring						Summer						Autumn						
Depth	mean	σ	n	Min.	Max.	mean	σ	n	Min.	Max.	mean	σ	n	Min.	Max.	mean	σ	n	Min.	Max.	mean	σ	n	Min.	Max.	
0	13	23	15	0	83	28	43	14	0	150	17	16	7	1	42	46	53	10	0	146						
25	51	78	13	0	232	15	36	14	0	129	9	12	10	0	38	19	23	11	0	59						
50	24	29	13	0	80	7	9	15	0	31	4	3	9	0	7	34	36	11	0	101						
75	13	23	12	0	66	5	9	13	0	33	7	10	9	0	26	9	11	10	0	34						

Table 4.27. The same as in table 4.24, but for station B2.

Station B2. Diatoms.(cells/ml)															
Depth	Winter			Spring			Summer			Autumn					
	mean	σ	n	Min.	Max.	mean	σ	n	Min.	Max.	mean	σ	n	Min.	Max.
0	5	4	6	0	13	2	3	6	0	7	1	1	3	0	2
25	5	3	6	1	10	16	28	6	0	77	3	2	3	1	5
50	6	7	6	1	20	16	32	6	0	88	1	1	3	0	2
75	10	11	6	0	32	20	35	6	1	99	3	4	3	0	8
100	4	3	6	0	9	5	6	5	0	15	16	12	3	5	32

Station B2. Dinoflagellates (cells/ml)															
Depth	Winter			Spring			Summer			Autumn					
	mean	σ	n	Min.	Max.	mean	σ	n	Min.	Max.	mean	σ	n	Min.	Max.
0	2	2	6	0	7	13	16	6	1	46	18	13	3	1	33
25	3	3	6	0	8	8	5	6	1	15	21	21	3	3	51
50	3	3	6	1	8	16	20	6	1	59	11	6	3	2	16
75	2	1	6	0	4	15	19	6	1	52	9	10	3	1	24
100	4	4	6	1	12	25	40	5	1	103	8	9	3	1	21

Station B2. Small flagellates (cells/ml)															
Depth	Winter			Spring			Summer			Autumn					
	mean	σ	n	Min.	Max.	mean	σ	n	Min.	Max.	mean	σ	n	Min.	Max.
0	49	44	6	3	138	71	91	6	0	254	22	19	3	1	47
25	79	84	6	13	259	42	39	6	4	114	41	28	3	12	79
50	47	56	6	1	166	38	16	5	18	62	26	15	3	12	46
75	11	6	5	4	22	15	9	6	6	27	18	20	7	0	56
100	17	10	5	3	32	12	7	5	2	18	10	4	3	5	15

Table 4.28. The same as in table 4.24, but for station B3.

Station B3. Diatoms (cells/ml)																							
Depth	Winter						Spring						Summer						Autumn				
	mean	σ	n	Min.	Max.	mean	σ	n	Min.	Max.	mean	σ	n	Min.	Max.	mean	σ	n	Min.	Max.			
0	7	6	6	2	19	3	4	6	0	9	1	1	3	0	1	3	2	7	0	7			
25	9	11	6	0	32	4	5	6	0	16	1	1	3	0	2	2	3	7	0	8			
50	5	7	6	0	21	6	6	6	1	17	7	5	3	0	13	5	8	7	0	24			
75	10	16	5	0	41	9	14	5	0	37	13	10	3	4	27	8	15	5	0	37			
100	5	6	6	0	16	8	7	6	0	17	10	4	3	4	15	2	1	5	0	3			

Station B3. Dinoflagellates (cells/ml)																							
Depth	Winter						Spring						Summer						Autumn				
	mean	σ	n	Min.	Max.	mean	σ	n	Min.	Max.	mean	σ	n	Min.	Max.	mean	σ	n	Min.	Max.			
0	4	4	6	0	13	31	54	6	1	151	27	22	3	0	55	7	6	7	0	19			
25	4	5	6	0	11	15	16	6	3	49	16	10	3	2	23	20	40	7	0	118			
50	4	4	6	0	10	7	5	6	2	15	19	15	3	2	39	3	2	6	1	5			
75	5	5	5	0	14	20	17	5	2	49	10	9	3	0	22	3	2	5	0	6			
100	1	1	6	0	4	83	175	6	0	474	6	8	3	0	17	2	2	6	1	7			

Station B3. Small flagellates (cells/ml)																							
Depth	Winter						Spring						Summer						Autumn				
	mean	σ	n	Min.	Max.	mean	σ	n	Min.	Max.	mean	σ	n	Min.	Max.	mean	σ	n	Min.	Max.			
0	82	62	6	0	184	79	71	6	8	180	24	8	2	15	32	58	37	6	24	122			
25	76	57	6	17	175	94	111	6	6	317	24	1	1	13	86	32	35	7	2	92			
50	36	19	5	16	61	58	46	6	1	128	46	30	3	13	86	28	21	7	0	63			
75	37	42	5	5	113	12	5	4	5	17	12	7	3	4	20	19	20	5	0	58			
100	11	10	6	0	26	25	33	6	1	92	7	6	3	3	16	11	18	6	0	51			

Table 4.29. The same as in table 4.24, but for station MH2.

Station MH2. Diatoms (cells/ml)															
Depth	Winter			Spring			Summer			Autumn					
	mean	σ	n	Min.	Max.	mean	σ	n	Min.	Max.	mean	σ	n	Min.	Max.
0	3	5	7	0	15	1	1	6	0	3	0	0	3	0	0
25	1	1	6	0	3	1	1	6	0	2	1	1	3	0	2
50	1	1	7	0	2	1	1	6	0	3	9	12	3	0	26
75	27	60	7	0	174	8	15	6	0	41	24	34	3	0	71
100	22	35	7	0	93	1	2	6	0	5	4	5	3	0	12

Station MH2. Dinoflagellates (cells/ml)															
Depth	Winter			Spring			Summer			Autumn					
	mean	σ	n	Min.	Max.	mean	σ	n	Min.	Max.	mean	σ	n	Min.	Max.
0	4	5	7	0	12	4	8	6	0	23	1	2	3	0	4
25	9	12	6	1	36	3	4	6	0	10	5	7	3	0	16
50	4	5	7	0	16	3	4	6	0	10	2	3	3	0	6
75	6	10	7	0	31	4	6	6	0	15	1	2	3	0	4
100	13	25	7	0	74	2	2	6	0	6	1	2	3	0	3

Station MH2. Small flagellates (cells/ml)															
Depth	Winter			Spring			Summer			Autumn					
	mean	σ	n	Min.	Max.	mean	σ	n	Min.	Max.	mean	σ	n	Min.	Max.
0	101	83	7	0	226	73	100	6	0	290	11	15	3	0	32
25	97	70	6	20	221	69	77	6	0	227	15	21	3	0	45
50	52	63	7	0	195	50	39	6	0	108	10	15	3	0	31
75	30	32	7	0	94	30	42	6	0	121	0	1	3	0	1
100	18	17	7	0	42	12	14	6	0	38	1	1	3	0	3

Table 4.30. Average abundances expressed in cells per milliliter (cel./ml), along the water column for the station CP2 for the nanoeukaryote and picoeukaryote cells and for the photoautotroph bacteria of the genera Prochlorococcus and Synechococcus. For each season and depth level, five columns are presented: seasonal mean value, standard deviation, number of data used and minimum and maximum values recorded along the complete time series.

Station CP2. Nanoeukaryotes (cells/ml)																					
		Winter					Spring					Summer					Autumn				
Depth		mean	σ	n	Min.	Max.	mean	σ	n	Min.	Max.	mean	σ	n	Min.	Max.	mean	σ	n	Min.	Max.
0		1699	1075	7	775	3410	906	531	5	3	1591	464	249	7	3	898	1247	753	4	560	2521
10		1755	1009	7	811	3455	811	531	5	0	1659	439	217	7	0	731	1394	1235	4	445	3511
20		1172	813	7	93	2840	1015	721	5	0	2156	515	229	7	0	701	1170	581	4	669	2159
50		797	380	7	165	1291	643	460	5	0	1074	10604	18993	7	0	55327	732	357	4	246	1224
75		394	293	6	62	772	281	125	5	84	458	453	198	7	174	810	220	196	3	66	497

Station CP2. Picoeukaryotes (cells/ml)																					
		Winter					Spring					Summer					Autumn				
Depth		mean	σ	n	Min.	Max.	mean	σ	n	Min.	Max.	mean	σ	n	Min.	Max.	mean	σ	n	Min.	Max.
0		4734	3182	7	2090	11755	1314	733	5	0	2132	640	324	7	0	1157	7157	11569	4	286	27193
10		3862	1869	7	1407	6934	1349	736	5	0	2006	694	381	7	0	1145	8080	13385	4	314	31263
20		3173	1925	7	90	5620	1435	915	5	0	2856	741	443	7	6	1492	3811	5693	4	352	13670
50		2954	1968	7	416	5591	2233	2473	5	3	6446	2704	3062	7	3	9479	2046	1947	4	439	5243
75		1580	1327	6	252	4090	1419	909	5	93	2758	2002	1122	7	710	3926	732	679	3	114	1677

Station CP2. Prochlorococcus (cells/ml)																					
		Winter					Spring					Summer					Autumn				
Depth		mean	σ	n	Min.	Max.	mean	σ	n	Min.	Max.	mean	σ	n	Min.	Max.	mean	σ	n	Min.	Max.
0		5000	8177	7	263	24890	2177	2955	5	0	7590	6528	12470	7	0	36441	32485	28956	4	1023	79782
10		5449	8000	7	314	24739	3756	5465	5	0	14165	6159	9414	7	209	26137	24665	17066	4	1190	47886
20		5975	8916	7	0	27370	7109	6792	5	0	18839	6487	9449	7	62	23706	24106	13082	4	1791	34523
50		4448	4819	7	356	14848	3811	1821	5	1371	6150	25457	11981	7	6150	43729	22964	19595	4	5859	56108
75		1806	1324	6	3	3895	3932	5966	5	293	15773	10961	6923	7	2264	21123	5152	4115	3	2048	10967

Station CP2, <i>Synechococcus</i> (cells/ml)																				
Depth	Winter					Spring					Summer					Autumn				
	mean	σ	n	Min.	Max.	mean	σ	n	Min.	Max.	mean	σ	n	Min.	Max.	mean	σ	n	Min.	Max.
0	25881	10808	7	12800	41387	8796	8388	5	30	22419	17631	14588	7	30	39986	24916	6845	4	16672	35329
10	24785	11902	7	12422	47176	11320	10011	5	37	24737	16186	15041	7	67	40659	25375	9924	4	10547	38235
20	33774	29970	7	11886	105140	17164	22882	5	0	59184	19796	17234	7	482	48106	26326	14008	4	13496	48873
50	16884	13270	7	368	35247	34586	35493	5	123	81432	28526	20853	7	123	55279	8504	6949	4	2856	20407
75	9815	6410	6	850	17213	5402	5057	5	144	14428	10171	10004	7	1252	26160	797	741	3	237	1844

Table 4.31. The same as in table 4.30, but for station CP4.

Station CP4, <i>Nanoeukaryotes</i> (cells/ml)																				
Depth	Winter					Spring					Summer					Autumn				
	mean	σ	n	Min.	Max.	mean	σ	n	Min.	Max.	mean	σ	n	Min.	Max.	mean	σ	n	Min.	Max.
0	1705	851	7	889	3535	522	282	4	66	790	430	178	7	66	686	735	312	5	355	1294
10	1534	294	5	1111	1983	647	419	4	165	1319	444	160	6	165	628	786	507	4	239	1606
20	1912	897	7	798	3713	548	341	4	78	1038	516	206	7	78	765	822	462	5	295	1683
50	1573	1028	7	547	3839	579	346	4	149	1062	674	502	7	149	1556	660	146	5	407	809
75	557	546	7	96	1490	435	148	4	278	638	992	490	7	377	1796	171	110	5	72	333
100	221	173	7	21	512	143	86	4	39	246	172	96	7	60	377	89	68	5	9	198

CP4, <i>Picoeukaryotes</i> (cells/ml)																				
Depth	Winter					Spring					Summer					Autumn				
	mean	σ	n	Min.	Max.	mean	σ	n	Min.	Max.	mean	σ	n	Min.	Max.	mean	σ	n	Min.	Max.
0	6378	4458	7	937	14537	1234	547	4	329	1752	679	314	7	329	1359	1354	1055	5	322	3129
10	7462	4182	5	940	13677	1103	476	4	365	1659	670	218	6	365	1025	1418	864	4	333	2695
20	6538	4643	7	901	15030	1749	1317	4	305	3892	695	245	7	305	1065	1645	1402	5	382	4245
50	5326	2458	7	1757	10000	3045	2074	4	281	5340	523	268	7	46	878	2451	2216	5	166	6515
75	1820	1429	7	75	4195	1548	734	4	914	2780	1946	1805	7	569	6114	434	204	5	260	817
100	733	520	7	21	1380	465	279	4	39	763	416	259	7	120	784	572	511	5	114	1449

Station CP4. Prochlorococcus (cells/ml)																				
Depth	Winter					Spring					Summer					Autumn				
	mean	σ	n	Min.	Max.	mean	σ	n	Min.	Max.	mean	σ	n	Min.	Max.	mean	σ	n	Min.	Max.
0	5953	6164	7	218	18922	425	398	4	0	994	4606	8990	7	0	26515	23757	14596	5	0	37571
10	9750	11682	5	186	31955	698	599	4	3	1446	5961	7956	6	411	22788	31639	18286	4	0	43447
20	11810	14057	7	308	36408	26610	43707	4	0	102266	5523	8826	7	413	26872	36220	25255	5	0	67057
50	9462	10728	7	1388	34832	12423	11489	4	1901	31104	15697	9322	7	3042	26042	19156	18968	5	1347	50835
75	4269	4043	7	695	11064	10582	13120	4	1530	33224	18790	11231	7	4780	36266	10622	14427	5	341	38126
100	1257	979	7	263	3273	2253	3476	4	120	8267	5963	6466	7	383	18168	4822	5952	5	704	16611

Station CP4. Synechococcus (cells/ml)																				
Depth	Winter					Spring					Summer					Autumn				
	mean	σ	n	Min.	Max.	mean	σ	n	Min.	Max.	mean	σ	n	Min.	Max.	mean	σ	n	Min.	Max.
0	34677	22431	7	10093	85215	15653	5149	4	10294	24102	20017	12312	7	4030	36508	30049	7674	5	16776	38121
10	35530	23918	5	13243	77329	27497	22097	4	11710	65620	17537	13551	6	943	40370	35795	7489	4	24231	43192
20	34595	15884	7	15390	58235	42881	37890	4	5680	102040	17305	16127	7	247	43153	31829	9058	5	15728	43663
50	23149	10681	7	13458	46169	41179	17849	4	11865	55584	31526	15858	7	11536	55584	5456	3936	5	431	9810
75	6571	6994	7	60	20496	10708	11025	4	2532	29686	7281	3162	7	3428	12501	1017	1085	5	129	3105
100	1861	1660	7	45	4485	1601	841	4	231	2515	621	602	7	159	1755	342	205	5	108	638

Table 4.32. The same as in table 4.30, but for station C20.

C20. Nanoeukaryotes (cells/ml)																				
Depth	Winter					Spring					Summer					Autumn				
	mean	σ	n	Min.	Max.	mean	σ	n	Min.	Max.	mean	σ	n	Min.	Max.	mean	σ	n	Min.	Max.
0	1517	885	7	512	3413	1064	600	5	138	1892	767	533	5	250	1760	519	148	4	365	753
25	1098	426	7	563	1881	815	375	5	171	1290	612	164	5	410	913	637	188	4	424	933
50	629	223	7	398	1013	1012	710	5	288	2234	660	147	5	481	898	681	143	4	493	836
75	368	185	7	33	659	718	962	5	81	2632	653	294	5	243	1088	294	146	3	99	452

Station C20. Picoeukaryotes (cells/ml)																				
Depth	Winter					Spring					Summer					Autumn				
	mean	σ	n	Min.	Max.	mean	σ	n	Min.	Max.	mean	σ	n	Min.	Max.	mean	σ	n	Min.	Max.
0	4346	4749	7	766	15113	1120	556	5	180	1728	842	268	5	530	1188	788	117	4	596	889
25	3544	3432	7	853	11482	1121	798	5	332	2386	800	175	5	480	967	656	122	4	485	824
50	2492	1769	7	572	6230	3782	4339	5	595	12259	703	294	5	467	1225	1913	770	4	857	2818
75	1210	1029	7	36	3547	1397	931	5	383	2650	2512	1819	5	663	5791	2897	1235	3	1377	4401

Station C20. Prochlorococcus (cells/ml)																				
Depth	Winter					Spring					Summer					Autumn				
	mean	σ	n	Min.	Max.	mean	σ	n	Min.	Max.	mean	σ	n	Min.	Max.	mean	σ	n	Min.	Max.
0	4712	6920	7	464	20607	620	458	5	144	1425	4961	9805	5	0	24570	7658	1276	4	6318	9703
25	7187	11679	7	473	35151	1471	1354	5	171	3913	5596	8612	5	199	22622	10610	3031	4	7668	15672
50	2562	3102	7	0	9485	5807	8920	5	491	23587	12733	7838	5	2328	21269	41759	17252	4	23902	60721
75	913	799	7	133	2305	2219	2962	5	132	8047	14185	10859	5	4638	33054	16016	12849	3	2365	33229

Station C20. Synechococcus (cells/ml)																				
Depth	Winter					Spring					Summer					Autumn				
	mean	σ	n	Min.	Max.	mean	σ	n	Min.	Max.	mean	σ	n	Min.	Max.	mean	σ	n	Min.	Max.
0	33275	16737	7	15397	62845	6430	510	5	346	13261	30609	19922	5	10681	68156	35138	6170	4	27633	44775
25	32478	12825	7	14382	50656	9301	6431	5	1427	15869	31570	22982	5	8149	66417	34701	5699	4	28401	43535
50	15804	11297	7	2698	40564	20074	13857	5	7069	41817	28043	9321	5	13578	41848	10319	2269	4	7549	13831
75	6228	5063	7	45	17066	4872	2742	5	680	8718	23248	21419	5	2111	59018	1854	287	3	1500	2203

Table 4.33. The same as in table 4.30, but for station C18.

Station C18. Nanoeukaryotes (cells/ml)																				
Depth	Winter					Spring					Summer					Autumn				
	mean	σ	n	Min.	Max.	mean	σ	n	Min.	Max.	mean	σ	n	Min.	Max.	mean	σ	n	Min.	Max.
0	1347	803	7	443	2848	1077	665	5	177	2007	688	163	5	417	902	545	225	4	223	757
25	1119	576	7	395	2120	1045	648	5	34	1677	620	65	5	573	749	483	162	4	271	663
50	1197	938	7	350	3302	1492	956	5	281	2923	884	306	5	399	1255	384	117	4	238	555
75	398	166	7	24	530	368	121	5	198	554	1162	1082	5	356	3276	205	57	4	132	282
100	200	126	7	6	374	152	61	5	72	249	168	101	5	48	308	90	19	4	69	120

Station C18. Picoeukaryotes (cells/ml)																				
Depth	Winter					Spring					Summer					Autumn				
	mean	σ	n	Min.	Max.	mean	σ	n	Min.	Max.	mean	σ	n	Min.	Max.	mean	σ	n	Min.	Max.
0	4868	3999	7	1091	13126	800	293	5	341	1239	783	233	5	434	1051	819	316	4	529	1352
25	4192	3052	7	1136	10520	960	792	5	25	2398	1034	355	5	617	1645	806	288	4	432	1234
50	2749	1708	7	1387	6530	2803	1872	5	147	5489	1195	682	5	463	2334	1245	696	4	411	1997
75	1772	1178	7	192	3527	1301	477	5	662	1904	1292	583	5	375	2048	1401	294	4	895	1627
100	986	965	7	15	2868	440	355	5	18	1033	792	577	5	254	1886	716	102	4	593	853

Station C18. Prochlorococcus (cells/ml)																				
Depth	Winter					Spring					Summer					Autumn				
	mean	σ	n	Min.	Max.	mean	σ	n	Min.	Max.	mean	σ	n	Min.	Max.	mean	σ	n	Min.	Max.
0	7069	9256	7	344	26421	226	404	5	0	1029	8509	10558	5	0	25033	8087	3321	4	4360	13457
25	8419	10485	7	203	26722	662	986	5	0	2593	4273	7790	5	0	19842	14572	5682	4	8007	21960
50	7518	8253	7	404	20995	8067	6564	5	2607	17444	28683	11622	5	16054	50292	59413	25547	4	15634	80066
75	2594	3685	7	186	11348	2814	2362	5	266	6069	12883	11147	5	1153	33246	22645	13853	4	392	34954
100	621	521	7	0	1467	349	258	5	75	668	4127	4901	5	0	12827	6000	3437	4	410	9782

Station C18. <i>Synechococcus</i> (cells/ml)																				
Depth	Winter					Spring					Summer					Autumn				
	mean	σ	n	Min.	Max.	mean	σ	n	Min.	Max.	mean	σ	n	Min.	Max.	mean	σ	n	Min.	Max.
0	31525	23895	7	3156	84939	14316	6955	5	6713	27428	13405	14406	5	72	40005	30023	5541	4	23872	36816
25	34341	27132	7	3545	91006	27425	23129	5	10605	73120	15934	12606	5	1567	38906	31011	6537	4	21729	38996
50	26193	27209	7	3773	90139	49793	29060	5	19601	105334	28300	2970	5	24223	32542	8506	2977	4	4083	12478
75	6573	3063	7	683	10506	7187	4374	5	1698	11955	10260	7001	5	2257	23114	1272	958	4	467	2881
100	2889	2688	7	150	8312	1833	1096	5	257	3261	1392	935	5	473	3063	245	58	4	177	329

Table 4.34. The same as in table 4.30, but for station B2.

Station B2. Nanoeukaryotes (cells/ml)																				
Depth	Winter					Spring					Summer					Autumn				
	mean	σ	n	Min.	Max.	mean	σ	n	Min.	Max.	mean	σ	n	Min.	Max.	mean	σ	n	Min.	Max.
0	1841	1123	3	838	3409	838	418	5	159	1255	536	82	3	425	620	901	655	4	329	1998
25	1448	569	3	1009	2251	1120	407	5	506	1737	652	89	3	533	746	766	672	4	207	1914
50	634	112	3	483	750	564	235	5	219	933	658	19	3	633	680	909	476	4	300	1603
75	742	651	3	126	1643	431	220	5	193	772	537	263	3	210	855	493	463	4	42	1179
100	534	480	3	90	1201	386	339	4	51	949	379	299	3	96	793	166	178	4	18	461

Station B2. Picoeukaryotes (cells/ml)																				
Depth	Winter					Spring					Summer					Autumn				
	mean	σ	n	Min.	Max.	mean	σ	n	Min.	Max.	mean	σ	n	Min.	Max.	mean	σ	n	Min.	Max.
0	1696	294	3	1281	1909	949	418	5	314	1597	754	206	3	464	916	1213	1059	4	308	3003
25	3295	2241	3	934	6306	1256	564	5	560	2246	826	309	3	470	1223	1168	550	4	561	2011
50	2149	1385	3	683	4006	1428	762	5	389	2464	2902	3028	3	602	7180	2042	1005	4	563	3357
75	2648	2351	3	719	5958	1341	750	5	316	2466	4975	3409	3	2242	9781	929	511	4	254	1691
100	704	419	3	380	1296	819	555	4	254	1662	2870	1946	3	832	5490	589	346	4	174	1129

Station B2. <i>Prochlorococcus</i> (cells/ml)																				
Depth	Winter					Spring					Summer					Autumn				
	mean	σ	n	Min.	Max.	mean	σ	n	Min.	Max.	mean	σ	n	Min.	Max.	mean	σ	n	Min.	Max.
0	6242	8539	3	183	18318	1479	1910	5	0	5168	155	219	3	0	464	16339	12246	4	2802	36190
25	18941	22779	3	237	51007	777	616	5	0	1683	2806	3613	3	0	7907	23840	12011	4	10692	43183
50	15859	10593	3	1030	25117	9283	15566	5	272	40358	14549	16554	3	1060	37864	29076	8776	4	17719	42163
75	6833	5768	3	799	14604	8299	10140	5	132	25017	24644	18680	3	3159	48698	7930	6287	4	1363	16602
100	4960	4824	3	401	11635	5047	4904	4	0	11365	11941	8229	3	596	19861	7557	3997	4	1425	12566

Station B2. <i>Synechococcus</i> (cells/ml)																				
Depth	Winter					Spring					Summer					Autumn				
	mean	σ	n	Min.	Max.	mean	σ	n	Min.	Max.	mean	σ	n	Min.	Max.	mean	σ	n	Min.	Max.
0	42188	35292	3	11327	91588	16770	17002	5	464	49359	16083	7200	3	10833	26264	20974	5899	4	11204	26755
25	42616	24163	3	14243	73295	23670	16815	5	12701	57037	16995	10071	3	8500	31143	22471	8214	4	10680	32326
50	11479	1074	3	10086	12700	13632	11175	5	386	32960	8391	3720	3	3647	12732	7805	4289	4	1920	13870
75	6528	5759	3	772	14396	7017	3041	5	2222	10891	8424	5428	3	2310	15500	1125	945	4	314	2651
100	1825	1785	3	464	4347	2459	1748	4	189	5081	1647	488	3	1024	2215	266	168	4	108	518

Table 4.35. The same as in table 4.30, but for station MH2.

Station MH2. <i>Nanoeukaryotes</i> (Cells/ml)																				
Depth	Winter					Spring					Summer					Autumn				
	mean	σ	n	Min.	Max.	mean	σ	n	Min.	Max.	mean	σ	n	Min.	Max.	mean	σ	n	Min.	Max.
0	5045	5087	6	1288	15344	1263	978	5	171	3027	508	127	3	395	686	359	126	2	233	485
25	2545	2504	4	548	6838	1111	974	5	123	2912	675	91	3	584	799	8780	8482	2	298	17261
50	867	522	5	219	1519	766	356	5	159	1222	888	57	3	835	967	479	67	2	412	545
75	705	329	5	266	1039	634	639	5	162	1889	760	247	3	413	968	431	105	2	326	536
100	410	295	5	141	970	349	347	5	78	985	633	361	3	123	922	298	220	2	78	518

Station MH2. Picoeukaryotes (cells/ml)																				
Depth	Winter				Spring				Summer				Autumn							
	mean	σ	n	Min.	Max.	mean	σ	n	Min.	Max.	mean	σ	n	Min.	Max.	mean	σ	n	Min.	Max.
0	7151	7550	6	569	19222	1174	631	5	320	1842	633	67	3	539	689	1113	601	2	512	1714
25	4438	5056	4	755	13061	1331	978	5	314	2596	614	7	3	605	623	1017	523	2	494	1540
50	1112	608	5	386	2017	2097	2085	5	575	6135	688	84	3	570	752	736	458	2	278	1193
75	1327	855	5	614	2973	1888	1474	5	234	4429	2618	1591	3	808	4680	876	62	2	814	937
100	1051	570	5	608	2099	716	847	5	90	2395	639	58	3	587	720	740	423	2	317	1162

Station MH2. Prochlorococcus (cells/ml)																				
Depth	Winter				Spring				Summer				Autumn							
	mean	σ	n	Min.	Max.	mean	σ	n	Min.	Max.	mean	σ	n	Min.	Max.	mean	σ	n	Min.	Max.
0	6900	7258	6	527	21911	709	380	5	75	1081	144	159	3	0	365	18060	350	2	17710	18410
25	6204	2206	4	2751	8788	2003	2433	5	108	6794	50	46	3	0	111	23721	2645	2	21076	26365
50	16382	12836	5	746	31046	10087	11560	5	446	30894	6302	2648	3	3593	9895	17852	248	2	17604	18099
75	11096	13692	5	281	37366	9552	10906	5	111	26154	70919	51969	3	6072	133289	14247	1169	2	13078	15416
100	2228	1562	5	455	4371	2082	2787	5	21	7590	13514	9335	3	335	20765	10674	4330	2	6344	15003

Station MH2. Synechococcus (cells/ml)																				
Depth	Winter				Spring				Summer				Autumn							
	mean	σ	n	Min.	Max.	mean	σ	n	Min.	Max.	mean	σ	n	Min.	Max.	mean	σ	n	Min.	Max.
0	34871	30567	6	7237	100496	28070	23884	5	8084	66732	10793	4774	3	6692	17488	14332	3242	2	11090	17574
25	23777	14345	4	877	37402	18776	17596	5	1925	52711	7233	3476	3	2820	11315	17317	712	2	16605	18028
50	18509	19575	5	1545	56167	15548	4207	5	7317	18478	14250	7619	3	7353	24867	13246	1018	2	12228	14263
75	9382	7572	5	2015	22422	6376	3090	5	1746	10477	12110	3160	3	8075	15790	5256	4798	2	458	10054
100	3949	1630	5	2410	6632	2426	1574	5	575	4859	1362	1066	3	503	2864	5737	5674	2	63	11410

Table 4.36. The same as in table 4.30, but for station MH4.

Station MH4. Nanoeukaryotes (cells/ml)																				
Depth	Winter					Spring					Summer					Autumn				
	mean	σ	n	Min.	Max.	mean	σ	n	Min.	Max.	mean	σ	n	Min.	Max.	mean	σ	n	Min.	Max.
0	5344	5590	6	587	15329	1092	533	6	213	1777	351	105	3	219	476	581	215	2	366	795
25	3417	3582	5	620	10494	1720	1929	5	171	5527	647	89	3	521	719	509	296	2	213	805
50	1668	1126	5	683	3631	1079	708	6	176	2350	894	316	3	494	1268	456	123	2	333	578
75	1181	1320	5	228	3754	291	175	6	111	641	1078	114	3	932	1209	796	9	2	787	805
100	759	619	6	45	1618	223	189	5	42	497	329	166	3	120	525	147	24	2	123	171

Station MH4. Picoeukaryotes (cells/ml)																				
Depth	Winter					Spring					Summer					Autumn				
	mean	σ	n	Min.	Max.	mean	σ	n	Min.	Max.	mean	σ	n	Min.	Max.	mean	σ	n	Min.	Max.
0	7579	5818	6	614	15025	1693	1087	6	431	3832	603	160	3	377	722	806	302	2	504	1107
25	4257	5472	5	252	15018	1558	777	5	491	2702	815	130	3	632	919	975	577	2	398	1551
50	3350	2087	5	998	6313	2483	2072	6	428	5557	981	259	3	620	1217	1165	650	2	515	1815
75	2789	1852	5	554	6054	988	485	6	159	1796	4165	3266	3	446	8396	875	135	2	740	1009
100	3005	4141	6	69	12051	507	329	5	129	952	739	210	3	449	942	306	189	2	117	494

Station MH4. Prochlorococcus (cells/ml)																				
Depth	Winter					Spring					Summer					Autumn				
	mean	σ	n	Min.	Max.	mean	σ	n	Min.	Max.	mean	σ	n	Min.	Max.	mean	σ	n	Min.	Max.
0	8716	7573	6	150	17217	307	357	6	0	878	153	127	3	0	311	26403	11446	2	14957	37849
25	8375	7045	5	542	19581	606	882	5	0	2342	83	67	3	0	165	26456	5718	2	20758	32173
50	7678	4443	5	743	14464	4809	8618	6	0	23979	16920	15957	3	192	38402	25146	2572	2	22574	27718
75	7516	10127	5	500	27534	3526	5595	6	51	15855	24743	14277	3	11312	44514	15838	647	2	15191	16485
100	4769	5727	6	341	16237	207	207	5	54	596	4793	3322	3	171	7831	4310	4280	2	30	8590

Station MH4. <i>Synechococcus</i> (cells/ml)																				
Depth	Winter					Spring					Summer					Autumn				
	mean	σ	n	Min.	Max.	mean	σ	n	Min.	Max.	mean	σ	n	Min.	Max.	mean	σ	n	Min.	Max.
0	39313	32289	6	6704	106274	24413	3114	6	1486	92606	11513	5271	3	4446	17099	20101	4008	2	16093	24109
25	23063	13219	5	10207	44472	27994	14273	5	9213	45287	14119	7353	3	4530	22399	17047	1848	2	15199	18895
50	18650	16127	5	6386	50262	28717	29419	6	2311	89337	14655	3658	3	9692	18400	15548	146	2	15402	15693
75	6774	4767	5	1677	13156	4411	4158	6	689	13096	21346	14708	3	7622	41744	4505	3939	2	566	8443
100	6192	8049	6	153	23549	2055	2045	5	225	5713	7592	9657	3	746	21249	181	79	2	102	260

Table 4.37. Table constructed using the information available in Fernández de Puellas et al., 2007. Average abundances, expressed as individuals per cubic meter, for the main meso-zooplanktonic groups for station B1. For each season three columns are presented: mean seasonal value, standard deviation and number of data used.

Mallorca transect. B1. Meso-zooplanktonic abundance (individuals/m ³). Modified from table 1 in Fernández de Puellas et al. (2007).																				
Group	Winter					Spring					Summer					Autumn				
	mean	σ	n	Min.	Max.	mean	σ	n	Min.	Max.	mean	σ	n	Min.	Max.	mean	σ	n	Min.	Max.
Copepods	624	237	10			637	254	10			473	151	10			404	131	10		
Appendicularians	170	67	10			181	76	10			147	60	10			134	72	10		
Cladocerans	23	16	10			144	118	10			177	168	10			34	25	10		
Doliolids	47	46	10			55	51	10			54	66	10			36	32	10		
Chaetognaths	17	14	10			20	14	10			21	12	10			21	11	10		
Siphonophores	31	19	10			41	32	10			17	10	10			13	7	10		
Ostracods	13	9	10			4	3	10			5	4	10			13	7	10		
Scyphozoans																				
Biomass (mg/m ³)																				

According to Fernández de Puellas et al. (2007), the mean annual zooplanktonic biomass is 5.4 mg/m³, with a maximum in April of 6.4 mg/m³ and a minimum in August of 4 mg/m³.

5. TARRAGONA AND BARCELONA.

The two northernmost transects in the RADMED project are located at the continental shelf and slope of Catalonia. One of them is in front of the mouth of river Ebro, in the Tarragona province (T transect), and the other one is in front of Barcelona (BNA transect). Figure 5.1 shows the position of both transects and the position of stations T2 and T4, in the Tarragona transect, and BNA2 and BNA4, in Barcelona transect. These stations will be used in the present chapter to illustrate the environmental conditions over the continental shelf (stations labeled with number 2) and over the continental slope (stations labeled as 4).

This region is characterized by the southward extension of the Northern Current along the continental slope of Catalonia. A frontal system is formed over the shelf break, receiving the name of Catalan Front (Salat et al., 2002; Font et al., 1988; Salat and Font, 1987). The scheme in figure 5.1 shows that the area between the Catalan Front and the northern coast of the Balearic Islands has a cyclonic circulation, that is, counter clockwise. This kind of circulation produces the divergence of surface waters in the central part of the cyclonic cell, the upwelling of sub-surface waters and its sinking in the periphery of the gyre. Therefore, the inner part of this cyclonic gyre shows higher salinity values and a colder temperature, because of the upward movement of the Levantine Intermediate Water. On the contrary, surface Atlantic waters, with lower salinity values, accumulate at the periphery, that is, at the Catalan coast and over the northern continental shelf of the Balearic Islands. In the case of the Catalan waters, the effect of continental waters from the runoff of rivers such as Ebro, must also be considered (Salat and Font, 1987). All these effects produce the formation of a frontal zone where there is a transition from the low salinity shelf waters, to the open sea waters (Catalan Front). In a similar way, the transition from the salty open sea waters to the waters to the north of the Balearic Islands, with a larger influence of the Atlantic Water, is called the Balearic Front (Ruiz et al., 2009; Pinot and Ganachaud, 1999; Pinot et al., 1995).

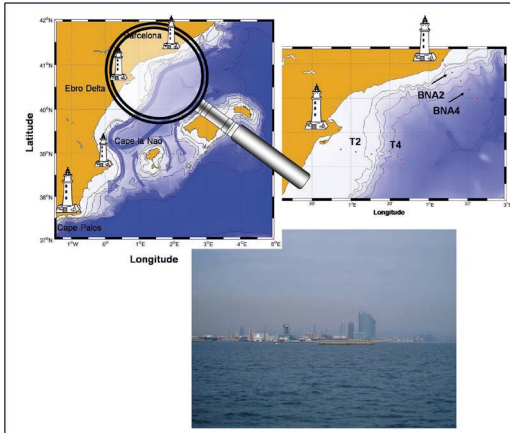


Figure 5.1. Map of the RADMED stations in the Tarragona and Barcelona transects. Picture of Barcelona during a RADMED campaign.

Another characteristic of this geographical area is the persistence of cold and dry winds from the continent during winter. Such winds produce an important decrease of the temperature of the continental shelf waters. Continental shelf waters have a lower salinity than those at the open sea, as explained in the preceding paragraph. Finally, a very cold ($< 13\text{ }^{\circ}\text{C}$) water mass with a salinity range between 37.7 and 38.3 psu is formed. This new water mass sinks below the AW and above the LIW (between 100 and 200 m) and is named as Western Intermediate Water (WIW, Juza et al., 2019; Vargas-Yáñez et al., 2012a; Pinot and Ganachaud, 1999; López-Jurado et al., 1995; López-Jurado, 1990; Salat and Font, 1987).

One of the consequences of the intermediate water formation process and the intense winter mixing, is the homogenization of the properties of the water column during winter and an intense supply of nutrients to the photic layer. This nutrient supply is also favored by the runoff of rivers. This process is even more intense to the north, in front of the Gulf of Lions, where convective processes can affect the whole water column, producing the formation of deep waters. The deep water formation produces a larger nutrient supply to the upper layer of the water column (Saiz et al., 2014), the oxygenation of the Western Mediterranean deep layer and a significant increase of the primary production in these waters. All these changes could also affect the Catalan continental slope waters, because of the advection of the Northern Current. Because of this fertilizing mechanism, at the end of winter or early spring, there is an intense phytoplanktonic bloom, with the prevalence of large cells such as diatoms and an important increase of the primary production if compared with the values observed

at other Mediterranean locations (Estrada, 1996). As spring advances, and mainly during summer, the stratification of the water column is reestablished, the nutrients at the surface layer are depleted and a Deep Chlorophyll Maximum is developed (DCM). The DCM in the Catalan waters can be located between 50 and 75 m depth (Arin et al., 2005; Estrada, 1985).

5.1 Meteorological conditions.

Figure 5.2 shows the seasonal wind charts for the daily winds at the meteorological stations of Sant Jaume, close to the mouth of river Ebro, and Barcelona. This figure shows the frequency for the direction of origin of the wind. The color scale indicates the wind intensity in km/h. Figure 5.2 also includes the monthly averaged values for the daily minimum, mean and maximum temperatures at the two mentioned meteorological stations.

In the case of Barcelona, winds are mainly from the west and southwest. The frequency of easterly winds slightly increases in spring and summer. The wind intensities are generally low, being below 10 km/h. At Sant Jaume, the wind intensity is high during winter and autumn when the wind blows from the northwest. On the contrary, in spring and summer there is a shift in the wind direction, with the prevalence of the southeast winds and the decrease of the intensity.

The lowest temperatures, as for the rest of the Spanish coast, are observed in January, and the maximum ones in August. At Barcelona, the average January daily minimum, mean and maximum temperatures are 8.0, 10.4 and 13.7 °C respectively. The average daily minimum, mean and maximum temperatures for August are 22.6, 25.5 and 28.7 °C. At Sant Jaume, the temperatures for January and August are slightly lower than those observed in Barcelona. Average daily minimum, mean and maximum temperatures are 7.3, 10.1 and 13.3 °C in January and 21.9, 24.7 and 27.9 °C in August.

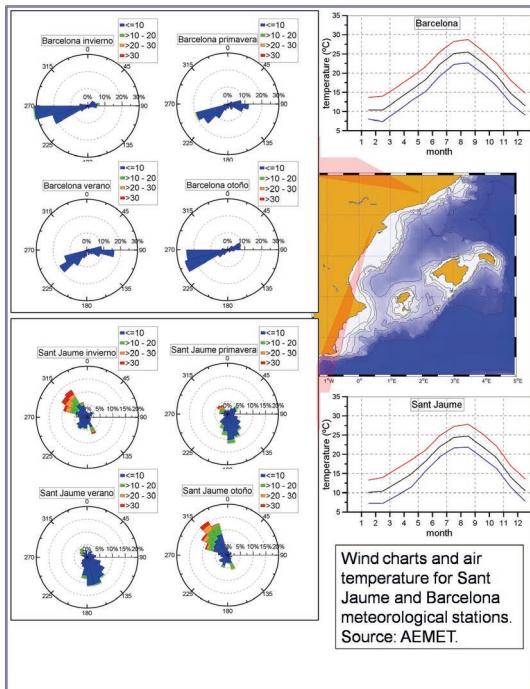


Figure 5.2. Wind charts and air temperature at the meteorological stations of Sant Jaume (Tarragona) and Barcelona. The direction of origin of the wind is expressed as percentages and the color scale indicates the intensity: lower than 10 km/h (blue), between 10 and 20 km/h (green), between 20 and 30 km/h (orange) and higher than 30 km/h (red). The wind chart in the upper left corner corresponds to winter, upper right corner to spring, lower left corner to summer and lower right corner to autumn. Average daily minimum (blue), mean (black) and maximum (red) air temperatures are presented for each month.

5.2 Water masses.

Figures 5.3 and 5.4 show the average TS diagrams for the Tarragona (T2 and T4) and Barcelona (BNA2 and BNA4) transects.

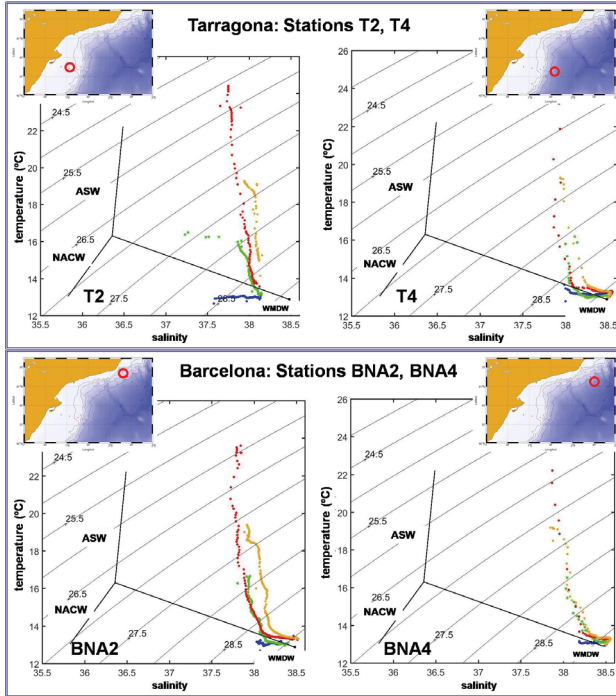


Figure 5.3. Average TS diagrams for winter (blue), spring (green), summer (red) and autumn (light brown) obtained from all the available potential temperature and salinity profiles from RADMED project in stations T2 and T4 from Tarragona transect.

Figure 5.4. The same as in figure 5.3, but for stations BNA2 and BNA4 in the Barcelona transect.

In winter, potential temperatures below 13 °C are observed at stations T2 and BNA2 over the continental shelf. In the case of the Tarragona shelf, such temperatures are observed along the whole water column (75 m of depth) with salinity values ranging between 37.63 psu at the sea surface and 38.13 psu at 75 m depth. These TS values and the intense cooling of the whole water column suggest the existence of processes of WIW formation

in front of the river Ebro mouth. This explanation would be supported by the strong northwest winds observed in figure 5.2. The low salinity values observed at the surface layer at station T2 are caused by the river Ebro runoff, close to this station.

At station BNA2, the surface temperature is slightly higher than at T2, with values around 13 °C. These values decrease below 13 °C at 150 m depth where the salinity is close to 38.12 psu. Once again it can be hypothesized that the Barcelona continental shelf is a place where WIW is frequently formed. On the contrary, this water mass is not observed during winter at the continental slope stations T4 and BNA4. In spring, WIW is observed at 200 m depth only at station BNA4 (12.98 °C, 38.24 psu). This suggests that this WIW is formed to the north, probably in front of the Gulf of Lions during the previous winter. This water mass would be advected by the Northern Current reaching Barcelona transect during the following spring.

The surface salinity reaches minimum values during winter and spring at station T2. This behavior is opposite to that observed in all the oceanographic stations that cover the Spanish Mediterranean (see chapters 3 and 4). This fact is probably caused by a higher water discharge from the river Ebro during these months. The surface salinity at station T4 does not show a clear seasonal cycle, and therefore there is not any indication of which seasons have a larger AW influence. We also speculate that this lack of seasonality is caused by the influence of the river Ebro runoff, although such influence would be weaker than at T2. At Barcelona transect, the seasonal cycle of salinity is similar to that already described for the other areas of the Spanish Mediterranean. Maximum salinity values are observed in winter at BNA2 and BNA4, (38.08 and 38.19 psu respectively) and minimum ones in summer at BNA2 (37.8 psu) and autumn at BNA4 (37.85 psu). This cycle, with a higher influence of AW during summer and autumn could be linked to the lower intensity of the winds and the higher frequency of winds from the east during these months (Fig. 5.2).

The LIW can be clearly observed at stations T4 and BNA4, because of their greater depths. If the salinity maximum associated to this water mass is considered as the position of its core, it would be located between 400 and 600 m at station T4 with TS values that change along the year, and which can reach 13.29 °C and 38.54 psu. At station BNA4, the LIW core is between 300 and 600 m and can reach potential temperature and salinity values of 13.3 °C and 38.55 psu. The maximum depth at station BNA4 is 1200 m. The water masses which occupy this depth level would be a mixing between LIW and Western Mediterranean Deep Water (WMDW) with values around 12.92-12.94 °C and 38.49 psu.

As in the previous chapters, mean values, standard deviations and the number of data used are presented in tables 5.1 to 5.4.

5.3 Dissolved oxygen, nutrient and chlorophyll-a distributions.

Figures 5.5 and 5.6 show the seasonally averaged vertical profiles for the concentrations of chlorophyll-a, dissolved oxygen, nitrate and nitrite for the stations T2 and T4 in the Tarragona transect.

Surface nitrate concentrations are high in winter, with values around 1.5 μM . Consequently, the surface chlorophyll concentration is also relatively high (0.7 mg/m^3) and the chlorophyll maximum is at 10 m depth with a value of 0.75 mg/m^3 . These values are high if compared with those observed at those transects located further south: Cape Palos, Ibiza Channel and Mallorca transects. They are also higher than the values corresponding to the Mahon transect. The maximum value of dissolved oxygen concentration is observed at the sea surface as could be expected for a shallow chlorophyll maximum. A Primary Nitrite Maximum (PNM) is observed at 20 m depth, just below the chlorophyll maximum. It should be noted that nitrate decreases with depth until 50 m depth, where it reaches a concentration of 1 μM . This fact suggests that besides the fertilizing effect of mixing caused by the northwest winds (see Fig. 5.2), the high surface nitrate concentrations could be enhanced by the river Ebro discharges. This effect would be weaker seawards as indicated by the lower surface nitrate concentrations at station T4 (0.49 μM) and by the lower chlorophyll concentrations at the position of the chlorophyll maximum and at the sea surface (0.49 and 0.36 mg/m^3 respectively). The depth of the chlorophyll maximum at station T4, over the continental slope, is 20 m, close to the surface, reflecting the winter fertilization of the upper layers. Chlorophyll concentrations at the position of its maximum and at the sea surface decrease in spring with values around 0.3 mg/m^3 . While maximum chlorophyll concentrations remain close to the surface (10 m) at the continental shelf (T2), there is a Deep Chlorophyll Maximum (DCM) at 50 m at the continental slope (T4). This differences between both stations is coherent with the fact that at station T4, surface nitrate are depleted in spring (0.04 μM), whereas concentrations are higher over the shelf (0.16 μM). Chlorophyll concentrations are very low during summer at stations T2 and T4. The highest values are reached at the DCM which is at 75 m depth at both stations. During autumn, nitrate concentrations remain at low values and so do chlorophyll concentrations at the surface and at the DCM.

The PNM is not observed during spring, summer and autumn at station T2, whereas this trait is present, below the chlorophyll maximum, throughout the whole year at station T4. The statistics corresponding to the concentrations of chlorophyll, dissolved oxygen, nitrate, nitrite, phosphate and silicate for the stations T2 and T4 are presented in tables 5.5 and 5.6.

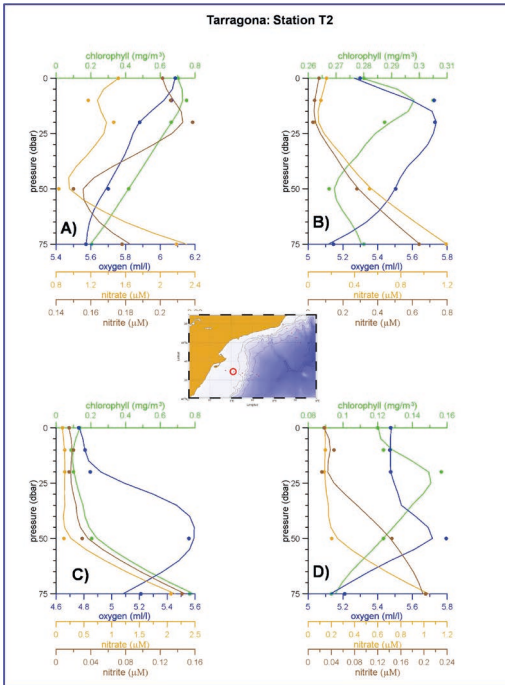


Figure 5.5. Average vertical profiles for the station T2 obtained using all the available profiles from RADMED Project. Green line corresponds to chlorophyll-a, blue line to dissolved oxygen, light brown line to nitrate and dark brown line to nitrite. Figure 5.5A corresponds to winter, B to spring, C to summer and D to autumn.

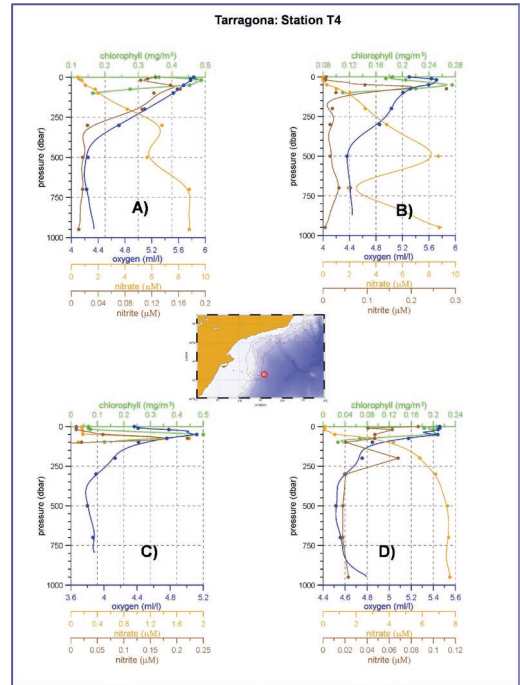


Figure 5.6. The same as in figure 5.5, but for station T4.

Figures 5.7 and 5.8 show the seasonally averaged vertical profiles for the concentrations of chlorophyll-a, dissolved oxygen, nitrate and nitrite for the stations BNA2 and BNA4 from the Barcelona transect. As in the case of Tarragona transect, the highest values of nitrate and chlorophyll at the sea surface and the shallowest position of the chlorophyll maximum are observed in winter as a consequence of winter mixing. During spring and summer, the DCM deepens to 50 m depth at BNA2 and the surface nitrates are depleted. At BNA4, nitrates are depleted at 10 m depth, but show high concentrations at the sea surface, where chlorophyll concentrations also reach high values (see table 5.8). These facts could indicate the influence of continental waters at the sea surface, but it is surprising that this influence is observed at the slope station and not at the continental shelf one. It also should be noted that spring and summer mean values at Barcelona transect are based on just three or two data. An unusual spring or summer would produce a mean value quite different from the real one that represents the most frequent conditions. As the RADMED time series become longer, we will be able to discern whether this result is an anomaly (outlier) or a recurrent situation.

Finally, the DCM is located close to the sea surface during autumn (20 m depth) at both stations. The upper 20 m of the water column are homogenized with a slight increase of the nitrate concentrations (0.25 μM), suggesting the beginning of the stormy season.

Anyway, it seems to be clear that the concentrations of nutrients and chlorophyll at the upper part of the water column are higher in the continental shelf and slope of the Catalan waters than at those stations located to the south, between Cape Palos and the south of the Balearic Islands. Those values recorded to the north of the islands (Mahon transect) would be closer to the values at the Catalan waters than to those observed to the south of the Islands. The reason could be the higher intensity of winter winds at this location.

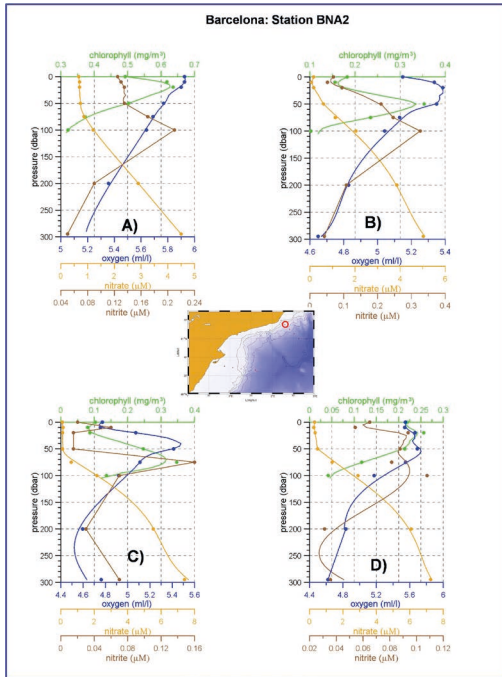


Figure 5.7. The same as in figure 5.5, but for station BNA2.

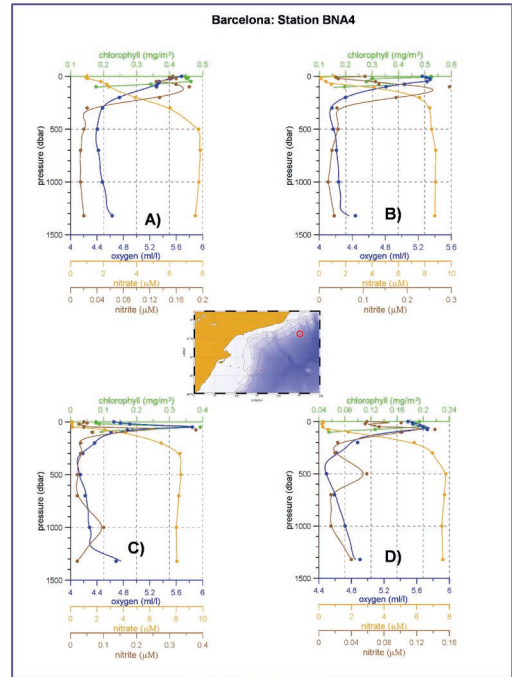


Figure 5.8. The same as in figure 5.5, but for station BNA4.

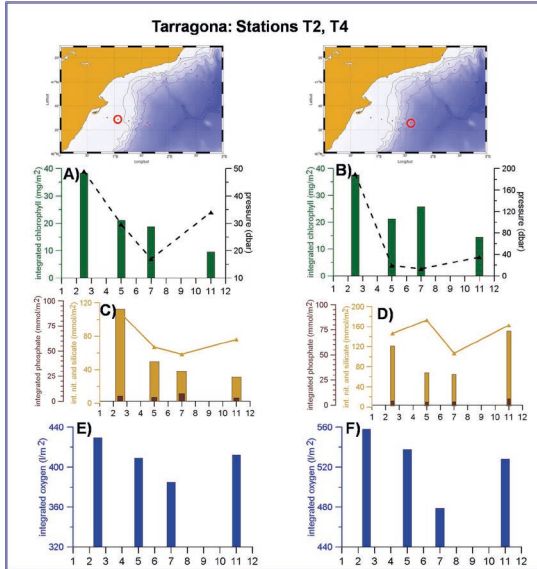
The statistics corresponding to the seasonal mean values for chlorophyll, dissolved oxygen and nutrients at the stations BNA2 and BNA4 are presented in tables 5.7 and 5.8. Table 5.9 shows the seasonally averaged Secchi disk depths for the Tarragona and Barcelona transects.

In order to get some insight of the productivity of the whole water column, figures 5.9 and 5.10 show the chlorophyll, nitrate, phosphate, silicate and oxygen concentrations integrated for the upper 100 m of the water column.

The mixed layer at the Tarragona transect follows the same behavior already described for other regions, with a maximum depth in winter, a minimum one in summer and a slight deepening in autumn. It should be noted that the depth of the mixed layer in winter reaches 200 m at station T4. At both stations T2 and T4, the integrated chlorophyll has a maximum value in winter with values close to 40 mg/m². These values decrease along the year reaching a minimum value in autumn, with integrated concentrations around 10 mg/m². Integrated nitrate concentrations reflect the chlorophyll evolution whereas silicates have a behavior similar to that of the mixed layer at station T2. Integrated nitrate concentrations at station T4 reach the highest values in winter and autumn, and the lowest ones in spring and summer. The highest integrated nitrate concentrations are higher than 120 mmol/m², whereas the lowest ones are close to 50 mmol/m². Phosphate shows the same behavior than the one observed at Cape Palos and Balearic Islands, with values quite homogeneous and around 5 mmol/m² along the whole year. Integrated dissolved oxygen concentrations follow the evolution of the mixed layer and the seasonal cycle of temperature. The nutricline depth, estimated from the vertical profiles in figures 5.5 to 5.8, reaches a minimum value in winter at station T2, when it is located at the sea surface. Then, it deepens progressively during the rest of the year until 65 and 75 m depth, coinciding with the decrease of the integrated chlorophyll and nitrate concentrations from spring to autumn. It is surprising that, despite the deep position of the mixed layer in winter at station T4 (if compared with other values within the presents work), the nutricline remained always around 50 m depth.

The main features observed at Barcelona transect are similar to those described for Tarragona transect. Integrated chlorophyll concentrations reach maximum values in winter, decreasing throughout the rest of the year. Winter values at BNA2 are slightly higher than those corresponding to Tarragona, with

values around 50 mg/m². The most interesting result from this transect is the high value of the winter mixed layer depth at BNA4 which reaches 900 m. This simply indicates that this area is not far from the areas of deep water formation in the Northwestern Mediterranean Sea. This observation would also support that the chlorophyll concentrations found at this area are higher than those observed at the Balearic Islands and Cape Palos transects. The next section will also show that these results are coincident with an increase of micro-phytoplanktonic cells towards the north.



Figures 5.9A and B. Integrated chlorophyll-a concentrations for the upper 100 m of the water column expressed in mg/m² (green bars), mixed layer depth (black dashed line). Figure A corresponds to station T2, and figure B to station T4. Figures C (station T2) and D (station T4) are the integrated nitrate plus nitrite concentrations for the upper 100 m of the water column, expressed in mmol/m² (light brown bars). Dark brown bars show the integrated phosphate concentrations, also in mmol/m². The light brown lines are the silicate integrated concentrations. Figures E (station T2) and F (station T4) show the integrated dissolved oxygen concentrations for the upper 100 m of the water column, expressed in l/m².

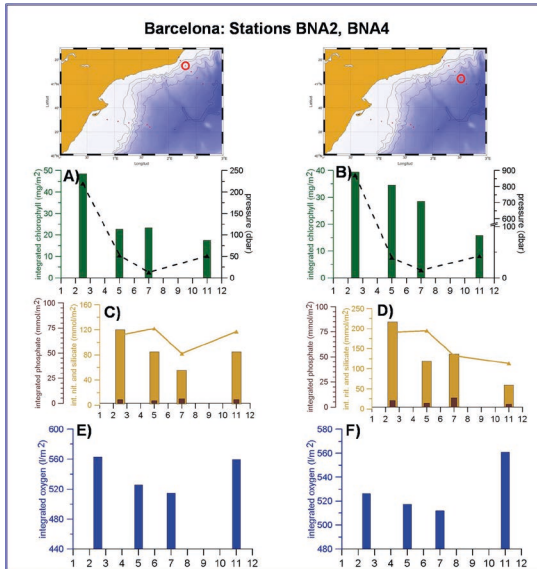


Figure 5.10. The same as in figure 5.9, but for stations BNA2 and BNA4.

5.4 Phytoplankton distribution.

5.4.1 Micro-phytoplankton.

Figures 5.11 and 5.12 show the average vertical distributions of micro-phytoplankton (Figures 5.11 and 5.12A, C, E and G) and of nano and picoplankton (Figures 5.11 and 5.12 B, D, F and H). Nevertheless, as in previous chapters, this section is devoted to the analysis of the largest size fraction (micro-phytoplankton >20 μm Equivalent Spherical Diameter, ESD), and the next section will deal with the nanoplankton and picoplankton, both eukaryote and prokaryote. The statistics corresponding to the abundances of micro-phytoplankton at stations T2 and BNA2 are presented in tables 5.10 and 5.11 at the end of this chapter, while statistics corresponding to the abundances of the nanoplankton and picoplankton are presented in tables 5.12 to 5.15.

Figures 5.11 A, C, E and G show the abundances of diatoms (green), dinoflagellates (red) and small flagellates (light brown) at station T2, over the continental shelf.

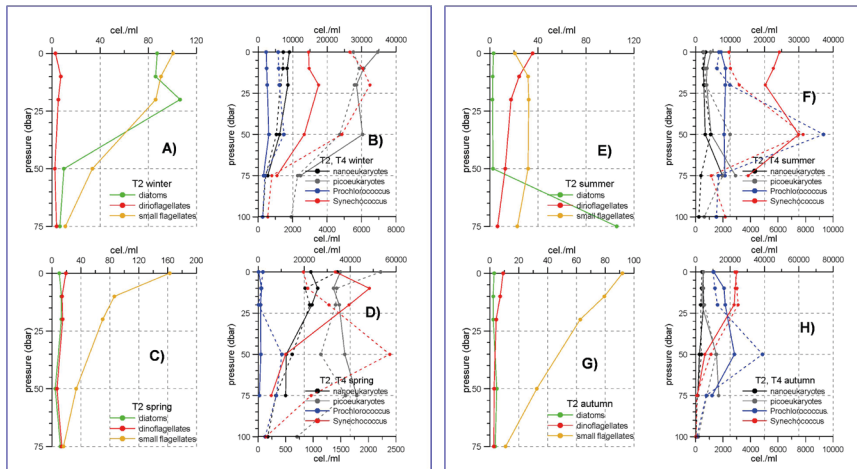


Figure 5.11A shows the winter average profiles for the abundances of diatoms (green), dinoflagellates (red) and small flagellates (light brown) obtained using all the available profiles from RADMED Project at station T2. Figure 5.11B shows the winter average profiles for the abundance of nanoplanktonic cells (continuous black line), picoplanktonic eukaryote cells (continuous grey line), and bacteria from the genera *Prochlorococcus* (continuous blue line) and *Synechococcus* (continuous red line) at station T2. Dashed lines correspond to station T4. All the abundances are expressed in cells per milliliter (cel./ml). Figures C, D are the same, but for spring, figures E, F correspond to summer and figures G, H to autumn. The upper axis in figures B, D, F and H corresponds to *Prochlorococcus* and *Synechococcus*, and the lower axis to pico and nano eukaryotes.

In winter, the highest diatom abundances, with values around 100 cel./ml, are concentrated in the upper 20 m of the water column, and this is coincident with the highest chlorophyll and nitrate concentrations at the sea surface. Small flagellates have similar abundances which also decrease from the surface towards the bottom. Dinoflagellates have low abundances (< 5 cel./ml) along the whole water column. In spring there is an important decrease of diatoms, with abundances close to 10 cel./ml at all the depth levels, being these values quite similar to those of dinoflagellates. Small flagellates are the most abundant group for this season, with values around 160 cel./ml at the sea surface that decrease with increasing depth. During summer, the water column stratification is stronger and diatoms are almost absent, with the only exception of the sea bottom. Only abundances of dinoflagellates and small flagellates have detectable levels, between 10 and 20 cel./ml. It should be noticed the increase of dinoflagellates abundances with respect to winter and spring values. Finally, the abundance of small flagellates increases again in autumn, with higher values at the surface and lower ones towards the bottom. Diatoms and dinoflagellates are very scarce at all the depth levels during this season.

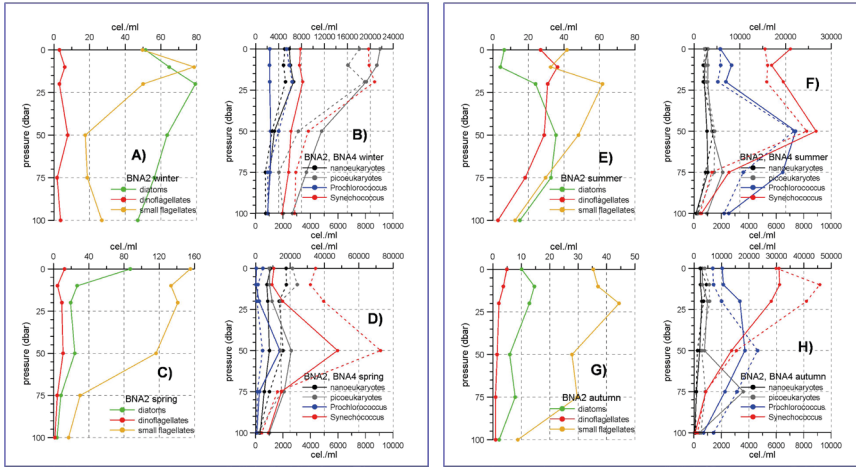


Figure 5.12. The same as in figure 5.11, but for the stations BNA2 and BNA4 from Barcelona transect.

The vertical distribution of micro-phytoplanktonic abundances at station BNA2 is very similar to the one described for T2. The main difference is that the diatom group is more abundant than at T2. Diatoms are the most abundant group in winter, with abundances higher than those of small flagellates. In spring, as in the case of T2, diatoms decrease and small flagellates become the most abundant group. Nevertheless, on the contrary to what was observed at T2, diatoms still have significant abundances, mainly at the sea surface (80 cel./ml). The most important feature of the summer distributions is the important increase of the dinoflagellate abundances which become more abundant than diatoms at the upper 25 m of the water column. Small flagellates remain being the most abundant group with their typical vertical distribution, with abundances decreasing with depth from the sea surface. This situation stands for autumn. The only important difference is the decrease of dinoflagellates.

Figures 5.13 to 5.16 show the relative abundances, integrated for the upper 100 m of the water column, for diatoms, dinoflagellates and small flagellates for the four seasons.

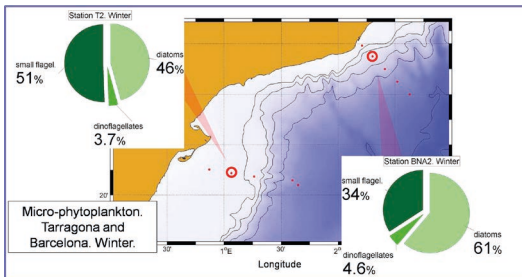


Figure 5.13. Winter relative abundances for the following micro-phytoplankton groups: diatoms (light green), dinoflagellates (green) and small flagellates (dark green) for the continental shelf of Tarragona and Barcelona: stations T2 and BNA2.

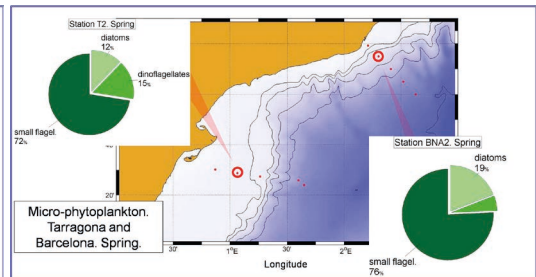


Figure 5.14. The same as in figure 5.13, but for spring.

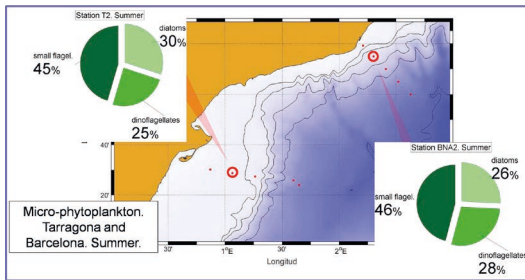


Figure 5.15. The same as in figure 5.13, but for summer.

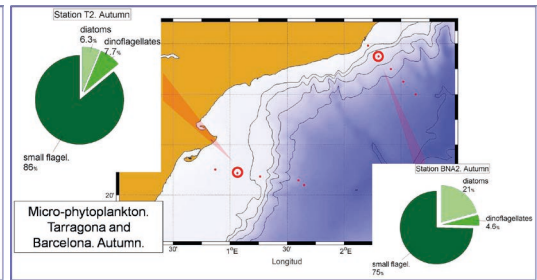


Figure 5.16. The same as in figure 5.13, but for autumn.

When abundances are integrated along the water column, small flagellates become the most abundant group throughout most of the year at both stations T2 and BNA2. These integrated abundances also confirm the increase of diatoms during winter and the increase of dinoflagellates in summer. It is also interesting to note that the integrated abundances of diatoms during summer are relatively high for this season, when conditions of strong stratification prevail and the nutrient supply to the photic layer is very low. In the case of station T2, such high diatom abundance is associated to a very high value at 75 m depth, at the bottom of the shelf. This high average value was caused by very elevated diatom abundances during one of the summer campaigns. The total number of summer campaigns used to estimate this mean value was four. The data scarcity does not allow us to discern whether this is an isolated phenomenon or if it is a recurrent feature in this particular region of the Spanish Mediterranean. As time series become longer and statistical analyses are updated this question will be solved. This diatom increase during summer is also observed at BNA2, but in this latter case it is associated to relatively high values along the whole water column (Fig. 5.12 E).

Besides the changes in the relative composition of the micro-phytoplanktonic community, there are also changes in the total abundances. At T2 and BNA2, the minimum abundances (after integrating vertically and adding the three groups) are observed in summer and autumn with values of 174 and 252 cel./ml, whereas maximum abundances are observed in winter at T2 and in spring at BNA2, with values of 476 and 667 cel./ml respectively. Mean annual values are 337 cel./ml at T2 and 404 cel./ml at BNA2. It is interesting to note that the abundances at Barcelona are higher than in Tarragona, which presents higher abundances than those recorded at Cape Palos and Balearic Islands (chapter 4, section 4.4.1). On the other hand, the abundances at this northern sector of the RADMED project are lower than those reported for the Alboran Sea, (chapter 3, section 3.4.1) showing a possible regionalization of the Spanish Mediterranean waters.

5.4.2 Nano and picoplankton.

Figures 5.11B and 5.12B show that the vertical distributions of nano and picoplankton assemblages in Tarragona and Barcelona are similar during winter. *Synechococcus* abundances are higher (30000 cel./ml) than *Prochlorococcus* ones (< 5000 cel./ml), and the former decrease with depth from the sea surface. *Prochlorococcus* abundances are quite homogeneous along the water column. Nano-eukaryote cells are the least abundant group with abundances lower than 2 000 cel./ml, whereas eukaryote picoplanktonic cells can reach abundances higher than 6 000 cel./ml. It should be noticed the different scales for the eukaryote plankton (lower axis) and the prokaryote one (upper axis). For the rest of the year, eukaryote nano and picoplankton show vertically homogeneous distributions with low abundances that hardly exceed 2 000 cel./ml. It is difficult to establish a clear pattern for the prokaryote picoplankton, probably because of the high temporal variability of these organisms and the short length of the current time series. Nevertheless, as in the cases of the Cape Palos and Balearic Islands transects, *Synechococcus* tend to be more abundant at the upper part of the water column, and *Prochlorococcus* tend to develop a deep maximum, mainly during autumn.

5.5 Tables. Seasonal statistics for Tarragona and Barcelona.

Table 5.1. Seasonal mean values for the potential temperature and salinity along the water column at station T2. Three columns with mean values, standard deviations and number of data are presented for each season and depth level.

Station T2 Potential temperature standard deviation number of data												
Depth	Winter			Spring			Summer			Autumn		
5	12.95	0.86	6	16.26	2.21	5	24.29	1.48	4	19.28	1.28	3
10	12.96	0.84	6	15.86	2.10	5	23.95	1.15	4	19.22	1.23	3
15	13.02	0.79	6	15.51	1.77	5	22.99	0.74	4	19.21	1.22	3
20	13.00	0.76	6	15.29	1.64	5	22.50	1.01	4	19.13	1.29	3
25	13.07	0.64	6	14.90	1.37	5	20.69	1.44	4	19.07	1.36	3
30	13.00	0.62	6	14.30	1.10	5	19.10	1.49	4	18.91	1.36	3
35	12.97	0.61	6	13.95	0.95	5	17.30	0.74	4	18.70	1.32	3
40	12.98	0.60	6	13.71	0.85	5	16.57	0.74	4	18.64	1.35	3
45	12.99	0.59	6	13.60	0.76	5	16.06	0.74	4	18.18	1.47	3
50	13.03	0.58	6	13.47	0.63	5	15.45	0.53	4	17.09	0.98	3
75	12.94	0.52	5	13.25	0.30	4	13.77	0.13	3	15.02	0.99	3

Station T2 Salinity standard deviation number of data												
Depth	Winter			Spring			Summer			Autumn		
5	37.63	0.38	6	37.48	0.76	5	37.75	0.20	4	37.94	0.21	3
10	37.69	0.33	6	37.87	0.23	5	37.74	0.19	4	37.95	0.21	3
15	37.78	0.24	6	37.90	0.19	5	37.79	0.14	4	37.95	0.21	3
20	37.86	0.18	6	37.95	0.16	5	37.79	0.13	4	37.96	0.22	3
25	37.94	0.09	6	37.99	0.15	5	37.79	0.10	4	37.97	0.23	3
30	37.96	0.07	6	38.00	0.14	5	37.86	0.03	4	38.01	0.20	3
35	38.00	0.05	6	38.02	0.13	5	37.92	0.06	4	38.06	0.13	3
40	38.02	0.04	6	38.04	0.13	5	37.96	0.03	4	38.06	0.13	3
45	38.04	0.03	6	38.06	0.12	5	37.99	0.05	4	38.08	0.11	3
50	38.07	0.04	6	38.07	0.12	5	38.02	0.05	4	38.09	0.07	3
75	38.13	0.04	5	38.14	0.15	4	38.06	0.03	3	38.12	0.06	3

Table 5.2. The same as in table 5.1, but for station T4.

Station T4 Potential temperature standard deviation number of data												
Depth	Winter			Spring			Summer			Autumn		
5	13.65	0.53	5	16.21	2.61	4	24.35	1.25	3	19.29	1.52	3
10	13.46	0.56	6	15.81	2.16	5	23.22	0.22	3	19.28	1.52	3
15	13.43	0.55	6	15.16	1.74	5	21.87	0.69	3	19.27	1.51	3

Station T4 Potential temperature standard deviation number of data												
Depth	Winter			Spring			Summer			Autumn		
20	13.43	0.55	6	14.78	1.40	5	20.27	0.36	3	19.26	1.51	3
25	13.41	0.55	6	14.50	1.18	5	19.04	1.08	3	19.22	1.53	3
30	13.36	0.50	6	14.28	1.03	5	18.15	0.97	3	18.96	1.81	3
35	13.27	0.47	6	14.00	0.82	5	17.27	0.84	3	18.71	2.01	3
40	13.25	0.48	6	13.87	0.66	5	16.68	0.86	3	18.07	2.21	3
45	13.25	0.48	6	13.76	0.58	5	16.25	0.75	3	16.67	2.23	3
50	13.25	0.48	6	13.71	0.54	5	15.67	0.42	3	15.84	1.96	3
75	13.20	0.44	6	13.41	0.36	5	13.88	0.20	3	13.79	0.31	3
100	13.20	0.38	6	13.18	0.26	5	13.50	0.08	3	13.52	0.12	3
150	13.17	0.33	6	13.10	0.20	5	13.34	0.16	3	13.41	0.08	3
200	13.14	0.32	6	12.98	0.14	5	13.28	0.14	3	13.31	0.09	3
300	13.15	0.28	6	13.04	0.15	5	13.31	0.13	3	13.27	0.01	3
400	13.28	0.16	6	13.10	0.13	5	13.29	0.09	3	13.19	0.07	3
500	13.25	0.11	6	13.07	0.11	5	13.23	0.08	3	13.15	0.03	3
600	13.22	0.06	6	13.01	0.08	5	13.14	0.06	3	13.10	0.04	3
700	13.14	0.06	6	12.98	0.06	5	13.09	0.04	3	13.06	0.04	3
800	13.08	0.08	6	12.95	0.03	5	13.04	0.04	3	13.02	0.04	3
900	13.04	0.09	6	12.94	0.02	5	13.00	0.03	2	13.00	NaN	1

Station T4 Salinity standard deviation number of data												
Depth	Winter			Spring			Summer			Autumn		
5	37.99	0.11	5	38.11	0.13	4	37.94	0.14	3	37.94	0.21	3
10	38.00	0.10	6	38.00	0.25	5	37.92	0.12	3	37.94	0.21	3
15	38.02	0.06	6	38.02	0.25	5	37.93	0.11	3	37.94	0.20	3
20	38.02	0.05	6	38.04	0.24	5	37.86	0.17	3	37.95	0.20	3
25	38.03	0.04	6	38.04	0.23	5	37.94	0.13	3	37.97	0.21	3
30	38.04	0.02	6	38.04	0.23	5	37.88	0.06	3	37.98	0.21	3
35	38.05	0.03	6	38.04	0.23	5	37.87	0.07	3	37.98	0.20	3
40	38.05	0.03	6	38.04	0.23	5	37.87	0.04	3	37.98	0.20	3
45	38.06	0.04	6	38.05	0.21	5	37.92	0.02	3	38.04	0.20	3
50	38.06	0.03	6	38.07	0.19	5	37.93	0.02	3	38.09	0.17	3
75	38.09	0.04	6	38.14	0.12	5	38.06	0.03	3	38.23	0.07	3
100	38.12	0.03	6	38.15	0.14	5	38.12	0.03	3	38.31	0.07	3
150	38.20	0.08	6	38.21	0.13	5	38.35	0.05	3	38.38	0.06	3
200	38.27	0.11	6	38.24	0.13	5	38.42	0.02	3	38.44	0.04	3
300	38.40	0.14	6	38.40	0.06	5	38.52	0.02	3	38.52	0.01	3
400	38.52	0.04	6	38.48	0.03	5	38.54	0.02	3	38.53	0.02	3

Station T4 Salinity standard deviation number of data												
Depth	Winter			Spring			Summer			Autumn		
500	38.54	0.03	6	38.50	0.03	5	38.54	0.02	3	38.53	0.01	3
600	38.54	0.02	6	38.50	0.02	5	38.53	0.02	3	38.52	0.01	3
700	38.53	0.01	6	38.50	0.02	5	38.52	0.01	3	38.51	0.02	3
800	38.52	0.02	6	38.49	0.01	5	38.51	0.01	3	38.50	0.02	3
900	38.51	0.02	6	38.49	0.01	5	38.50	0.01	2	38.51	NaN	1

Table 5.3. The same as in table 5.1, but for station BNA2.

Station BNA2 Potential temperature standard deviation number of data												
Depth	Winter			Spring			Summer			Autumn		
5	13.24	0.49	6	16.51	2.46	7	23.45	0.65	4	19.01	2.34	4
10	13.13	0.51	7	15.97	2.06	7	22.79	1.39	4	19.39	2.24	5
15	13.10	0.53	7	15.44	1.67	7	20.78	1.51	4	19.23	2.04	5
20	13.09	0.54	7	15.04	1.43	7	19.79	1.33	4	18.93	1.76	5
25	13.09	0.53	7	14.77	1.25	7	18.87	0.86	4	18.60	1.64	5
30	13.09	0.52	7	14.54	1.18	7	18.23	0.82	4	18.57	1.62	5
35	13.09	0.51	7	14.42	1.14	7	17.39	0.71	4	18.50	1.60	5
40	13.09	0.51	7	14.29	1.09	7	16.44	1.04	4	18.44	1.58	5
45	13.09	0.50	7	14.09	0.91	7	15.73	1.33	4	18.40	1.58	5
50	13.11	0.50	7	13.91	0.74	7	15.40	1.35	4	18.09	1.65	5
75	13.12	0.45	7	13.57	0.63	7	13.85	0.29	4	16.15	1.71	5
100	13.04	0.38	7	13.34	0.38	7	13.56	0.11	4	14.46	0.58	5
150	12.96	0.32	7	13.16	0.24	7	13.44	0.09	4	13.60	0.18	5
200	13.11	0.38	7	13.10	0.25	7	13.39	0.10	4	13.44	0.09	5

Station BNA2 Salinity standard deviation number of data												
Depth	Winter			Spring			Summer			Autumn		
5	38.08	0.06	6	37.93	0.19	7	37.80	0.10	4	37.89	0.12	4
10	38.05	0.09	7	37.93	0.20	7	37.80	0.10	4	37.92	0.13	5
15	38.05	0.08	7	37.96	0.16	7	37.72	0.11	4	37.93	0.11	5
20	38.05	0.08	7	37.96	0.17	7	37.78	0.08	4	37.94	0.12	5
25	38.05	0.07	7	37.97	0.16	7	37.80	0.13	4	37.91	0.19	5
30	38.06	0.06	7	38.00	0.14	7	37.82	0.12	4	37.94	0.17	5
35	38.06	0.06	7	38.04	0.12	7	37.81	0.12	4	37.96	0.16	5
40	38.06	0.06	7	38.07	0.11	7	37.89	0.12	4	37.97	0.15	5
45	38.07	0.06	7	38.09	0.10	7	37.91	0.11	4	38.02	0.09	5
50	38.08	0.06	7	38.08	0.11	7	37.93	0.10	4	38.06	0.03	5

Station BNA2 Salinity standard deviation number of data												
Depth	Winter			Spring			Summer			Autumn		
75	38.10	0.05	7	38.11	0.09	7	38.08	0.04	4	38.12	0.05	5
100	38.10	0.05	7	38.14	0.09	7	38.15	0.02	4	38.17	0.08	5
150	38.12	0.07	7	38.19	0.10	7	38.24	0.01	4	38.29	0.05	5
200	38.20	0.05	7	38.26	0.09	7	38.35	0.03	4	38.38	0.06	5

Table 5.4. The same as in table 5.1, but for station BNA4.

Station BNA4 Potential temperature standard deviation number of data												
Depth	Winter			Spring			Summer			Autumn		
5	13.16	0.10	5	16.54	2.47	7	24.04	1.29	4	19.20	2.37	5
10	13.11	0.15	6	15.96	2.03	7	23.66	1.18	4	19.19	2.36	5
15	13.11	0.15	6	15.47	1.80	7	22.23	0.60	4	19.16	2.34	5
20	13.08	0.13	6	15.26	1.65	7	21.56	0.80	4	19.14	2.37	5
25	13.07	0.12	6	15.06	1.54	7	20.40	0.67	4	19.11	2.38	5
30	13.06	0.12	6	14.66	1.25	7	19.57	1.40	4	18.50	1.59	5
35	13.06	0.12	6	14.52	1.13	7	18.87	1.57	4	18.58	1.72	5
40	13.07	0.12	6	14.32	0.98	7	16.99	1.31	4	18.34	1.49	5
45	13.07	0.13	6	14.21	0.92	7	15.90	0.84	4	18.16	1.38	5
50	13.08	0.15	6	14.08	0.84	7	14.99	0.35	4	17.80	1.28	5
75	13.10	0.20	6	13.58	0.67	7	13.55	0.20	4	15.55	1.21	5
100	13.07	0.13	6	13.26	0.23	7	13.41	0.11	4	14.38	0.96	5
150	13.08	0.24	6	13.13	0.09	7	13.33	0.14	4	13.49	0.11	5
200	13.09	0.21	6	13.15	0.12	7	13.28	0.16	4	13.34	0.10	5
300	13.12	0.21	6	13.12	0.11	7	13.29	0.16	4	13.38	0.11	5
400	13.14	0.21	6	13.07	0.14	7	13.23	0.12	4	13.31	0.09	5
500	13.13	0.18	6	13.02	0.11	7	13.14	0.10	4	13.25	0.07	5
600	13.09	0.16	6	12.98	0.08	7	13.07	0.07	4	13.17	0.06	5
700	13.05	0.12	6	12.96	0.06	7	13.01	0.05	4	13.11	0.06	5
800	13.02	0.10	6	12.95	0.04	7	12.98	0.05	4	13.06	0.06	5
900	12.99	0.08	6	12.93	0.02	7	12.96	0.04	4	13.02	0.05	5
1000	12.96	0.05	6	12.92	0.01	7	12.95	0.03	4	12.99	0.04	5
1200	12.92	0.01	6	12.91	0.01	7	12.94	0.02	4	12.94	0.02	5

Station BNA4 Salinity standard deviation number of data												
Depth	Winter			Spring			Summer			Autumn		
5	38.19	0.10	5	38.05	0.13	7	37.96	0.09	4	37.85	0.26	5
10	38.19	0.09	6	38.03	0.14	7	37.91	0.07	4	37.88	0.29	5
15	38.19	0.09	6	38.05	0.15	7	37.87	0.05	4	37.88	0.29	5

Station BNA4 Salinity standard deviation number of data												
Depth	Winter			Spring			Summer			Autumn		
20	38.20	0.10	6	38.12	0.10	7	37.87	0.09	4	37.89	0.28	5
25	38.20	0.09	6	38.14	0.10	7	37.90	0.16	4	37.93	0.22	5
30	38.21	0.09	6	38.12	0.14	7	37.95	0.14	4	37.88	0.30	5
35	38.22	0.09	6	38.16	0.13	7	37.95	0.10	4	38.01	0.14	5
40	38.23	0.09	6	38.18	0.10	7	38.04	0.11	4	38.03	0.12	5
45	38.23	0.09	6	38.22	0.08	7	38.06	0.11	4	38.05	0.12	5
50	38.24	0.08	6	38.24	0.07	7	38.15	0.08	4	38.05	0.12	5
75	38.27	0.07	6	38.31	0.07	7	38.26	0.02	4	38.08	0.05	5
100	38.29	0.07	6	38.37	0.05	7	38.34	0.03	4	38.25	0.06	5
150	38.35	0.07	6	38.44	0.02	7	38.44	0.02	4	38.35	0.09	5
200	38.40	0.06	6	38.49	0.00	7	38.49	0.02	4	38.42	0.08	5
300	38.47	0.05	6	38.51	0.01	7	38.54	0.03	4	38.53	0.04	5
400	38.51	0.05	6	38.51	0.03	7	38.54	0.03	4	38.55	0.02	5
500	38.52	0.04	6	38.50	0.02	7	38.53	0.02	4	38.55	0.02	5
600	38.52	0.04	6	38.50	0.02	7	38.51	0.02	4	38.54	0.02	5
700	38.51	0.03	6	38.49	0.01	7	38.50	0.01	4	38.52	0.02	5
800	38.51	0.02	6	38.49	0.01	7	38.50	0.01	4	38.51	0.02	5
900	38.50	0.02	6	38.49	0.01	7	38.49	0.01	4	38.50	0.01	5
1000	38.49	0.01	6	38.49	0.01	7	38.49	0.01	4	38.50	0.01	5
1200	38.49	0.00	6	38.49	0.01	7	38.49	0.01	4	38.49	0.01	5

Table 5.5. Seasonal mean values for chlorophyll-a, dissolved oxygen, nitrate, nitrite, phosphate and silicate concentrations along the water column for the station T2. Three columns with mean values, standard deviations and number of data are presented for each season and depth level.

Station T2 (Chlorophyll-a (mg/m ³) standard deviation number of data)												
Depth	Winter			Spring			Summer			Autumn		
0	0.70	0.42	7	0.28	0.13	4	0.14	0.11	4	0.12	0.06	3
10	0.75	0.60	7	0.31	0.16	4	0.09	0.01	4	0.12	0.06	3
20	0.66	0.50	7	0.29	0.09	4	0.10	0.02	4	0.16	0.08	3
50	0.42	0.20	7	0.27	0.04	4	0.21	0.10	4	0.12	0.06	3
75	0.20	0.12	7	0.28	0.06	4	0.77	0.23	4	0.09	0.04	3

Station T2 (Oxygen (ml/l) standard deviation number of data)												
Depth	Winter			Spring			Summer			Autumn		
0	6.09	0.35	6	5.30	0.40	5	4.76	0.59	3	5.47	0.02	2
10	6.07	0.35	6	5.72	0.33	5	4.81	0.59	3	5.47	0.01	2
20	5.88	0.32	6	5.73	0.41	5	4.85	0.60	3	5.48	0.01	2

Station T2 (Oxygen (ml/l) standard deviation number of data)												
Depth	Winter			Spring			Summer			Autumn		
50	5.70	0.17	6	5.50	0.51	5	5.56	0.56	3	5.79	0.41	2
75	5.57	0.33	5	5.14	0.56	4	5.21	0.68	2	5.21	0.09	2

Station T2 (Nitrate (μM) standard deviation number of data)												
Depth	Winter			Spring			Summer			Autumn		
0	1.52	1.48	3	0.16	0.07	2	0.12	0.10	2	0.15	0.12	4
10	1.17	0.98	3	0.11	0.04	2	0.16	0.13	2	0.15	0.12	4
20	1.46	0.59	3	0.06	0.03	2	0.16	0.14	2	0.14	0.12	4
50	0.83	0.46	3	0.53	0.42	2	0.14	0.10	2	0.20	0.12	4
75	2.19	1.43	3	1.19	0.32	2	2.07	0.92	2	1.01	0.90	4

Station T2 (Nitrite (μM) standard deviation number of data)												
Depth	Winter			Spring			Summer			Autumn		
0	0.20	0.14	3	0.06	0.02	2	0.02	0.01	2	0.03	0.02	4
10	0.21	0.14	3	0.04	0.01	2	0.02	0.01	2	0.04	0.03	4
20	0.22	0.14	3	0.03	0.00	2	0.02	0.01	2	0.02	0.02	4
50	0.15	0.05	3	0.28	0.13	2	0.03	0.01	2	0.14	0.05	4
75	0.18	0.09	3	0.64	0.30	2	0.15	0.01	2	0.20	0.09	4

Station T2 (Phosphate (μM) standard deviation number of data)												
Depth	Winter			Spring			Summer			Autumn		
0	0.06	0.05	3	0.05	0.00	2	0.02	0.00	2	0.02	0.02	4
10	0.03	0.02	3	0.03	0.01	2	0.03	0.01	2	0.02	0.01	4
20	0.11	0.09	3	0.04	0.01	2	0.30	0.30	2	0.03	0.02	4
50	0.04	0.00	3	0.07	0.04	2	0.02	0.01	2	0.05	0.04	4
75	0.11	0.06	3	0.06	0.02	2	0.05	0.03	2	0.08	0.06	4

Station T2 (Silicate (μM) standard deviation number of data)												
Depth	Winter			Spring			Summer			Autumn		
0	1.24	0.66	3	0.19	0.05	2	0.57	0.05	2	0.71	0.19	4
10	1.09	0.48	3	0.22	0.09	2	0.60	0.02	2	0.69	0.19	4
20	1.21	0.43	3	0.21	0.06	2	0.29	0.27	2	0.74	0.21	4
50	1.44	0.30	3	1.31	0.55	2	0.54	0.14	2	0.97	0.23	4
75	2.17	0.63	3	1.88	1.17	2	2.33	0.65	2	1.94	1.03	4

Table 5.6. The same as in table 5.5, but for station T4.

Station T4 (Chlorophyll-a (mg/m ³) standard deviation number of data)												
Depth	Winter			Spring			Summer			Autumn		
0	0.36	0.16	6	0.19	0.12	2	0.07	0.01	3	0.21	0.07	3
10	0.47	0.13	6	0.18	0.11	2	0.07	0.01	3	0.18	0.04	3
20	0.49	0.13	6	0.21	0.14	2	0.07	0.02	3	0.20	0.04	3
50	0.45	0.11	6	0.28	0.05	2	0.50	0.49	3	0.20	0.11	3
75	0.28	0.16	6	0.22	0.05	2	0.33	0.11	3	0.07	0.04	3
100	0.16	0.11	6	0.11	0.01	2	0.13	0.04	3	0.03	0.01	3

Station T4 (Oxygen (ml/l) standard deviation number of data)												
Depth	Winter			Spring			Summer			Autumn		
0	5.83	0.24	5	5.30	0.32	4	4.37	0.49	2	5.46	0.01	2
10	5.78	0.29	6	5.64	0.44	5	4.41	0.53	2	5.46	0.01	2
20	5.78	0.28	6	5.71	0.54	5	4.78	0.50	2	5.44	0.02	2
50	5.68	0.22	6	5.59	0.54	5	5.12	0.66	2	5.44	0.50	2
75	5.59	0.27	6	5.32	0.51	5	4.76	0.65	2	5.17	0.46	2
100	5.52	0.30	6	5.21	0.54	5	4.41	0.53	2	4.85	0.24	2
200	5.09	0.51	6	5.03	0.46	5	4.13	0.42	2	4.75	0.16	2
300	4.71	0.57	6	4.85	0.35	5	3.90	0.38	2	4.60	0.07	2
500	4.25	0.27	6	4.36	0.23	5	3.80	0.44	2	4.52	0.07	2
700	4.23	0.25	6	4.41	0.22	5	3.86	0.44	2	4.56	0.11	2

Station T4 (Nitrate (µM) standard deviation number of data)												
Depth	Winter			Spring			Summer			Autumn		
0	0.49	0.18	4	0.04		1	0.17		1	0.11	0.09	4
10	0.58	0.33	4	0.00		1	0.17		1	0.10	0.07	4
20	0.78	0.81	4	0.00		1	0.17		1	0.10	0.06	4
50	1.04	0.58	4	0.28		1	0.18		1	0.70	0.97	4
75	1.79	0.57	4	0.99		1	1.79		1	2.79	1.27	4
100	2.00	0.84	3	2.03		1	0.11		1	4.26	0.61	4
200	4.18	2.81	3	3.18		1				5.85	0.78	4
300	6.77	3.37	3	4.81		1				6.79	1.19	4
500	5.67	4.60	3	8.70		1				7.52	1.47	4
700	8.80	2.13	3	1.91		1				7.59	1.51	4
950	8.81	2.14	3	8.77		1				7.67	1.56	4

Station T4 (Nitrite (µM) standard deviation number of data)										
Depth	Winter			Spring		Summer		Autumn		
0	0.13	0.09	4	0.01	1	0.01	1	0.09	0.13	4
10	0.11	0.07	4	0.01	1	0.01	1	0.04	0.03	4
20	0.10	0.07	4	0.01	1	0.01	1	0.06	0.08	4
50	0.15	0.06	4	0.10	1	0.06	1	0.05	0.01	4
75	0.16	0.06	4	0.28	1	0.22	1	0.05	0.01	4
100	0.12	0.10	3	0.03	1	0.02	1	0.02	0.01	4
200	0.11	0.09	3	0.02	1			0.07	0.07	4
300	0.02	0.01	3	0.02	1			0.02	0.01	4
500	0.02	0.01	3	0.02	1			0.02	0.01	4
700	0.02	0.01	3	0.04	1			0.02	0.01	4
950	0.01	0.01	3	0.01	1			0.02	0.01	4

Station T4 (Phosphate (µM) standard deviation number of data)										
Depth	Winter			Spring		Summer		Autumn		
0	0.03	0.01	4	0.02	1	0.03	1	0.03	0.02	4
10	0.04	0.00	4	0.02	1	0.03	1	0.02	0.02	4
20	0.05	0.02	4	0.02	1	0.02	1	0.02	0.01	4
50	0.04	0.02	4	0.03	1	0.03	1	0.04	0.02	4
75	0.05	0.03	4	0.03	1	0.05	1	0.10	0.06	4
100	0.05	0.02	3	0.06	1	0.02	1	0.15	0.07	4
200	0.10	0.02	3	0.11	1			0.27	0.12	4
300	0.20	0.11	3	0.18	1			0.36	0.15	4
500	0.25	0.20	3	0.40	1			0.42	0.10	4
700	0.41	0.09	3	0.08	1			0.40	0.13	4
950	0.40	0.13	3	0.41	1			0.43	0.13	4

Station T4 (Silicate (µM) standard deviation number of data)										
Depth	Winter			Spring		Summer		Autumn		
0	1.38	0.30	4	1.65	1	0.85	1	0.68	0.21	4
10	1.45	0.23	4	1.68	1	0.86	1	0.69	0.21	4
20	1.52	0.29	4	1.71	1	0.89	1	0.69	0.17	4
50	1.53	0.26	4	1.73	1	0.77	1	1.24	0.62	4
75	1.71	0.29	4	1.70	1	1.84	1	2.53	0.98	4
100	1.70	0.21	3	1.89	1	0.72	1	3.29	0.49	4
200	2.47	0.67	3	2.28	1			3.90	0.54	4
300	4.03	1.30	3	3.31	1			5.34	0.92	4
500	4.38	3.11	3	7.82	1			6.92	0.18	4
700	7.95	0.11	3	2.37	1			7.64	0.21	4

Station T4 (Silicate (μM) standard deviation number of data)												
Depth	Winter			Spring			Summer			Autumn		
950	8.43	0.05	3	9.01		1				8.47	0.56	4

Table 5.7. The same as in table 5.5, but for station BNA2.

Station BNA2 (Chlorophyll-a (mg/m^3) standard deviation number of data)												
Depth	Winter			Spring			Summer			Autumn		
0	0.49	0.33	7	0.18	0.06	6	0.11	0.02	4	0.22	0.11	5
10	0.62	0.44	7	0.16	0.06	6	0.09	0.04	4	0.21	0.13	5
20	0.64	0.47	7	0.17	0.06	6	0.11	0.04	4	0.26	0.11	5
50	0.50	0.18	7	0.35	0.17	6	0.29	0.10	4	0.21	0.10	5
75	0.37	0.22	7	0.23	0.17	6	0.38	0.14	4	0.12	0.06	5
100	0.32	0.22	7	0.10	0.07	6	0.18	0.07	4	0.04	0.01	5

Station BNA2 (Oxygen (ml/l) standard deviation number of data)												
Depth	Winter			Spring			Summer			Autumn		
0	5.93	0.26	3	5.15	0.74	7	4.77	0.57	3	5.55	0.36	4
10	5.93	0.23	4	5.34	0.52	7	4.75	0.77	3	5.54	0.35	4
20	5.90	0.24	4	5.39	0.53	7	5.07	0.62	3	5.66	0.52	4
50	5.77	0.34	4	5.35	0.53	7	5.41	0.57	3	5.69	0.52	4
75	5.69	0.34	4	5.13	0.47	7	5.11	0.62	3	5.55	0.40	4
100	5.64	0.28	4	5.04	0.51	7	4.92	0.58	3	5.17	0.35	4
200	5.36	0.36	4	4.83	0.51	7	4.59	0.57	3	4.83	0.39	4
295				4.65	0.05	2	4.76		1	4.62		1

Station BNA2 (Nitrate (μM) standard deviation number of data)												
Depth	Winter			Spring			Summer			Autumn		
0	0.81	0.30	3	0.12	0.18	4	0.08	0.01	2	0.25	0.26	5
10	0.82	0.30	3	0.05	0.05	4	0.14	0.05	2	0.21	0.22	5
20	0.84	0.31	3	0.12	0.11	4	0.10	0.01	2	0.28	0.23	5
50	0.96	0.41	3	0.45	0.41	4	0.11	0.01	2	0.39	0.47	5
75	1.20	0.51	3	1.10	0.51	4	0.62	0.45	2	1.09	0.89	5
100	1.41	0.28	3	2.05	0.56	4	2.16	0.65	2	2.44	1.64	5
200	2.80	1.08	3	3.66	1.68	4	5.53		1	5.81	1.42	5
295	4.30	1.34	3	5.11	1.42	4	7.40		1	7.20	1.39	5

Station BNA2 (Nitrite (μM) standard deviation number of data)												
Depth	Winter			Spring			Summer			Autumn		
0	0.14	0.03	3	0.06	0.05	4	0.02	0.01	2	0.06	0.03	5
10	0.15	0.02	3	0.04	0.02	4	0.06	0.04	2	0.04	0.04	5
20	0.15	0.02	3	0.07	0.07	4	0.02	0.01	2	0.08	0.08	5
50	0.17	0.05	3	0.16	0.18	4	0.02	0.01	2	0.07	0.05	5
75	0.18	0.02	3	0.21	0.11	4	0.16	0.08	2	0.07	0.05	5
100	0.22	0.06	3	0.26	0.27	4	0.07	0.02	2	0.12	0.07	5
200	0.12	0.04	3	0.09	0.09	4	0.03		1	0.05	0.04	5
295	0.07	0.03	3	0.04	0.01	4	0.07		1	0.03	0.02	5

Station BNA2 (Phosphate (μM) standard deviation number of data)												
Depth	Winter			Spring			Summer			Autumn		
0	0.04	0.01	3	0.03	0.01	4	0.06	0.03	2	0.03	0.02	5
10	0.03	0.01	3	0.02	0.00	4	0.05	0.02	2	0.02	0.01	5
20	0.05	0.00	3	0.02	0.00	4	0.05	0.03	2	0.02	0.02	5
50	0.03	0.02	3	0.02	0.01	4	0.03	0.01	2	0.02	0.01	5
75	0.04	0.02	3	0.03	0.01	4	0.04	0.01	2	0.04	0.04	5
100	0.04	0.02	3	0.05	0.02	4	0.07	0.03	2	0.09	0.07	5
200	0.07	0.02	3	0.13	0.10	4	0.22		1	0.22	0.09	5
295	0.14	0.04	3	0.20	0.08	4	0.33		1	0.32	0.09	5

Station BNA2 (Silicate (μM) standard deviation number of data)												
Depth	Winter			Spring			Summer			Autumn		
0	0.91	0.49	3	0.68	0.44	4	0.50	0.12	2	0.82	0.14	5
10	0.96	0.45	3	0.84	0.45	4	0.65	0.26	2	0.79	0.11	5
20	1.00	0.40	3	0.89	0.38	4	0.47	0.10	2	0.81	0.09	5
50	1.03	0.41	3	1.22	0.31	4	0.44	0.33	2	0.92	0.19	5
75	1.26	0.31	3	1.44	0.18	4	1.12	0.09	2	1.44	0.56	5
100	1.39	0.26	3	1.83	0.39	4	1.90	0.05	2	2.22	0.78	5
200	2.13	0.08	3	2.77	1.07	4	3.15		1	3.84	0.75	5
295	2.91	0.15	3	3.86	0.85	4	5.38		1	5.11	1.10	5

Table 5.8. The same as in table 5.5, but for station BNA4.

Station BNA4 (Chlorophyll-a (mg/m^3) standard deviation number of data)												
Depth	Winter			Spring			Summer			Autumn		
0	0.45	0.21	6	0.52	0.74	5	0.09	0.02	4	0.19	0.03	5
10	0.46	0.20	6	0.52	0.78	5	0.09	0.02	4	0.19	0.04	5
20	0.45	0.17	6	0.30	0.29	5	0.10	0.02	4	0.19	0.04	5

Station BNA4 (Chlorophyll-a (mg/m ³) standard deviation number of data)												
Depth	Winter			Spring			Summer			Autumn		
50	0.47	0.27	6	0.28	0.14	5	0.64	0.44	4	0.20	0.05	5
75	0.34	0.29	6	0.42	0.20	5	0.27	0.16	4	0.13	0.07	5
100	0.18	0.16	6	0.20	0.12	5	0.08	0.02	4	0.06	0.03	5

Station BNA4 (Oxygen (ml/l) standard deviation number of data)												
Depth	Winter			Spring			Summer			Autumn		
0	5.68	0.29	3	5.25	0.54	7	4.66	0.68	3	5.49	0.29	4
10	5.54	0.34	4	5.29	0.49	7	4.76	0.57	3	5.55	0.35	4
20	5.52	0.36	4	5.34	0.51	7	4.90	0.57	3	5.55	0.38	4
50	5.34	0.40	4	5.31	0.53	7	5.84	0.68	3	5.67	0.57	4
75	5.31	0.40	4	5.04	0.50	7	4.86	0.77	3	5.73	0.78	4
100	5.30	0.41	4	4.81	0.45	7	4.61	0.63	3	5.42	0.61	4
200	4.74	0.35	4	4.32	0.45	7	4.37	0.57	3	4.87	0.50	4
300	4.48	0.30	4	4.16	0.36	7	4.18	0.56	3	4.62	0.50	4
500	4.41	0.31	4	4.17	0.36	7	4.15	0.55	3	4.49	0.39	4
700	4.42	0.27	4	4.21	0.35	7	4.22	0.55	3	4.59	0.43	4
1000	4.48	0.24	4	4.23	0.35	7	4.29	0.55	3	4.72	0.50	4
1320	4.63	0.27	3	4.44	0.07	3	4.69	0.25	2	4.91	0.54	3

Station BNA4 (Nitrate (µM) standard deviation number of data)												
Depth	Winter			Spring			Summer			Autumn		
0	1.36	0.49	3	2.16	1.70	3	0.11	0.10	2	0.21	0.25	5
10	1.35	0.58	3	0.09	0.10	3	0.08	0.04	2	0.21	0.29	5
20	1.44	0.60	3	0.08	0.05	3	0.12	0.05	2	0.16	0.23	5
50	2.10	0.45	3	0.40	0.43	3	0.14	0.07	2	0.19	0.24	5
75	2.49	0.58	3	1.40	0.87	3	2.60	0.89	2	0.54	0.45	5
100	2.52	0.53	3	3.99	0.86	3	4.16	0.20	2	2.02	1.02	5
200	4.96	1.60	3	7.37	0.39	3	6.87		1	6.04	1.15	5
300	6.63	1.35	3	8.18	0.28	3	8.28		1	7.36	1.37	5
500	8.16	2.08	3	8.58	0.21	3	8.36		1	7.96	1.46	5
700	8.24	2.08	3	8.82	0.13	3	8.20		1	8.03	1.50	5
1000	8.17	2.07	3	8.80	0.14	3	8.01		1	7.85	1.52	5
1320	7.99	1.94	3	8.73	0.05	3	8.05		1	7.99	1.62	5

Station BNA4. Nitrite (µM) standard deviation number of data)												
Depth	Winter			Spring			Summer			Autumn		
0	0.17	0.05	3	0.09	0.07	3	0.04	0.02	2	0.05	0.06	5
10	0.16	0.04	3	0.03	0.02	3	0.05	0.00	2	0.08	0.13	5

Station BNA4. Nitrite (μM) standard deviation number of data)												
Depth	Winter			Spring			Summer			Autumn		
20	0.16	0.03	3	0.03	0.03	3	0.03	0.01	2	0.05	0.05	5
50	0.15	0.02	3	0.09	0.08	3	0.04	0.02	2	0.06	0.05	5
75	0.17	0.03	3	0.13	0.02	3	0.38	0.05	2	0.14	0.03	5
100	0.20	0.05	3	0.21	0.18	3	0.07	0.03	2	0.08	0.05	5
200	0.10	0.10	3	0.12	0.14	3	0.03		1	0.03	0.02	5
300	0.03	0.01	3	0.03	0.02	3	0.03		1	0.02	0.01	5
500	0.02	0.01	3	0.03	0.03	3	0.02		1	0.05	0.08	5
700	0.01	0.00	3	0.03	0.01	3	0.02		1	0.01	0.01	5
1000	0.01	0.01	3	0.02	0.00	3	0.10		1	0.01	0.01	5
1320	0.02	0.01	3	0.03	0.01	3	0.02		1	0.03	0.04	5

Station BNA4 (Phosphate (μM) standard deviation number of data)												
Depth	Winter			Spring			Summer			Autumn		
0	0.04	0.03	3	0.06	0.04	3	0.08	0.01	2	0.02	0.01	5
10	0.05	0.02	3	0.02	0.01	3	0.08	0.01	2	0.02	0.01	5
20	0.05	0.03	3	0.02	0.00	3	0.07	0.01	2	0.02	0.02	5
50	0.06	0.02	3	0.02	0.01	3	0.08	0.03	2	0.03	0.02	5
75	0.08	0.03	3	0.03	0.01	3	0.10	0.03	2	0.03	0.02	5
100	0.08	0.02	3	0.12	0.05	3	0.16	0.05	2	0.04	0.02	5
200	0.19	0.08	3	0.29	0.03	3	0.28		1	0.25	0.08	5
300	0.31	0.10	3	0.35	0.02	3	0.38		1	0.36	0.05	5
500	0.42	0.08	3	0.37	0.03	3	0.52		1	0.56	0.31	5
700	0.42	0.09	3	0.32	0.11	3	0.40		1	0.49	0.16	5
1000	0.42	0.07	3	0.32	0.10	3	0.38		1	0.44	0.07	5
1320	0.40	0.08	3	0.33	0.10	3	0.45		1	0.46	0.14	5

Station BNA4 (Silicate (μM) standard deviation number of data)												
Depth	Winter			Spring			Summer			Autumn		
0	1.55	0.32	3	1.88	0.77	3	0.58	0.01	2	0.84	0.15	5
10	1.59	0.32	3	1.59	0.35	3	0.64	0.07	2	0.85	0.16	5
20	1.62	0.37	3	1.55	0.18	3	0.62	0.08	2	0.83	0.21	5
50	1.93	0.27	3	1.72	0.07	3	1.14	0.13	2	0.95	0.24	5
75	2.17	0.24	3	2.08	0.23	3	1.92	0.27	2	1.27	0.32	5
100	2.16	0.16	3	3.11	0.61	3	2.54	0.58	2	2.09	0.50	5
200	3.42	0.72	3	5.48	0.52	3	4.24		1	4.00	0.78	5
300	5.03	0.74	3	6.51	0.55	3	5.81		1	5.39	0.54	5
500	7.43	0.17	3	7.56	0.32	3	6.84		1	6.97	0.38	5
700	8.04	0.14	3	8.15	0.15	3	7.04		1	7.78	0.37	5

Station BNA4 (Silicate (μM) standard deviation number of data)											
Depth	Winter			Spring			Summer		Autumn		
1000	8.33	0.41	3	8.45	0.36	3	7.16	1	8.17	0.44	5
1320	8.46	0.69	3	8.70	0.31	3	7.80	1	8.78	0.66	5

Table 5.9. Seasonally averaged Secchi disk depths for the Tarragona and Barcelona transects. Three columns with mean values, standard deviations and number of data, are presented for each season.

Secchi disk depth (m) standard deviation number of data												
	Winter			Spring			Summer			Autumn		
T2	15.7	6.5	9	22.0	7.6	5	22.2	5.6	5	23.5	2.6	4
T4	18.4	5.9	9	18.8	3.7	5	25.5	4.0	4	21.8	2.5	4
BNA2	16.0	7.3	9	23.0	5.3	7	25.0	5.4	5	17.4	2.5	5
BNA4	17.9	2.9	10	20.2	5.0	6	23.4	1.5	5	21.4	3.8	5

Table 5.10. Average abundances expressed as cells per milliliter (cel./ml), along the water column for the station T2 for the following micro-phytoplanktonic groups: diatoms, dinoflagellates and small flagellates. For each season five columns are presented: Seasonal mean value, standard deviation, number of data used, minimum and maximum values recorded for each group along the complete time series.

Station T2. Diatoms (cells/ml)																				
Depth	Winter					Spring					Summer					Autumn				
	Mean	σ	n	Min.	Max.	Mean	σ	n	Min.	Max.	Mean	σ	n	Min.	Max.	Mean	σ	n	Min.	Max.
0	66	79	8	0	198	8	8	5	0	19	1	2	4	0	5	3	2	3	1	6
10	65	100	8	0	279	9	9	5	0	24	1	2	4	0	5	2	2	1		5
20	80	120	8	0	340	10	12	5	0	29	1	1	4	0	3	2	2	3	1	5
50	6	4	7	0	11	4	3	5	0	9	1	2	4	0	5					
75	3	3	7	0	8	9	11	5	0	29	53	84	4	0	198	4	3	3	0	8

Station T2. Dinoflagellates (cells/ml)																				
Depth	Winter					Spring					Summer					Autumn				
	Mean	σ	n	Min.	Max.	Mean	σ	n	Min.	Max.	Mean	σ	n	Min.	Max.	Mean	σ	n	Min.	Max.
0	2	4	8	0	13	15	22	5	0	59	18	29	4	0	68	9	6	3	2	15
10	5	9	8	0	27	11	11	5	0	32	12	20	4	0	46	7	5	3	3	15
20	4	6	8	0	15	12	11	5	0	31	9	13	4	0	30	3	3	1		5
50	2	2	8	0	5	5	4	5	0	10	6	8	4	0	19	3	2	3	1	5
75	3	4	8	0	11	11	6	5	0	17	3	3	4	0	7	3	4	3	0	8

Station T2. Small flagellates (cells/ml)																				
Depth	Winter					Spring					Summer					Autumn				
	Mean	σ	n	Min.	Max.	Mean	σ	n	Min.	Max.	Mean	σ	n	Min.	Max.	Mean	σ	n	Min.	Max.
0	75	78	8	0	223	130	99	5	0	286	10	18	4	0	41	92	42	3	60	151
10	68	69	8	0	186	69	37	5	0	98	16	19	4	0	47	79	53	3	37	154
20	65	97	8	0	252	56	37	5	0	97	16	20	4	0	49	63	56	3	15	142
50	25	33	8	0	90	27	26	5	0	75	16	17	4	0	40	26	5	2	21	30
75	8	9	8	0	24	13	10	5	0	25	11	12	4	0	25	11	10	3	0	25

Table 5.11. The same as in table 5.10, but for station BNA2.

Station BNA2. Diatoms (cells/ml)																				
Depth	Winter					Spring					Summer					Autumn				
	Mean	σ	n	Min.	Max.	Mean	σ	n	Min.	Max.	Mean	σ	n	Min.	Max.	Mean	σ	n	Min.	Max.
0	38	60	8	0	167	73	116	6	0	325	3	4	4	0	10	10	12	5	1	33
10	48	76	8	0	195	22	23	5	0	62	2	3	4	0	7	15	14	5	2	39
20	60	104	8	0	295	16	18	6	0	51	12	13	4	0	31	13	11	5	2	29
50	48	79	8	0	187	20	37	6	0	102	18	19	4	0	44	6	4	5	1	10
75	42	65	8	0	194	7	5	6	0	13	16	18	4	0	43	8	7	5	0	17
100	35	61	8	0	176	3	3	6	0	9	8	8	4	0	17	2	2	5	0	7

Station BNA2. Dinoflagellates (cells/ml)																				
Depth	Winter					Spring					Summer					Autumn				
	Mean	σ	n	Min.	Max.	Mean	σ	n	Min.	Max.	Mean	σ	n	Min.	Max.	Mean	σ	n	Min.	Max.
0	2	3	8	0	10	10	8	6	0	19	13	19	4	0	45	5	4	5	0	10
10	5	8	8	0	26	4	5	5	0	13	18	31	4	0	71	4	3	5	1	7
20	2	3	8	0	9	8	7	6	0	16	15	26	4	0	60	2	2	5	0	6
50	6	7	8	0	24	9	10	6	0	27	14	22	4	0	53	2	2	5	0	5
75	1	2	8	0	7	4	4	6	0	10	9	9	4	0	22	1	1	5	0	2
100	3	5	8	0	15	1	1	6	0	3	1	2	4	0	4	1	1	5	0	2

Station BNA2. Small flagellates (cells/ml)																				
Depth	Winter					Spring					Summer					Autumn				
	Mean	σ	n	Min.	Max.	Mean	σ	n	Min.	Max.	Mean	σ	n	Min.	Max.	Mean	σ	n	Min.	Max.
0	37	56	8	0	168	129	107	6	0	295	21	22	4	0	52	35	19	5	0	57
10	22	15	7	0	41	107	90	5	0	262	16	19	4	0	46	37	30	5	9	92
20	38	33	8	0	91	118	92	6	0	293	31	31	4	0	65	44	48	5	0	136
50	13	14	8	0	42	97	68	6	0	196	24	28	4	0	68	28	30	5	0	86

Station BNA2. Small flagellates (cells/ml)																									
Depth	Winter					Spring					Summer					Autumn									
	Mean	σ	n	Min.	Max.	Mean	σ	n	Min.	Max.	Mean	σ	n	Min.	Max.	Mean	σ	n	Min.	Max.	Mean	σ	n	Min.	Max.
75	14	11	8	0	32	25	20	6	0	63	15	23	4	0	54	30	25	5	2	67					
100	20	24	8	0	75	14	14	6	0	39	6	6	4	0	15	9	10	5	0	27					

Table 5.12. Average abundances expressed in cells per milliliter (cel./ml), along the water column for the station T2 for the nanoeukaryote and picoeukaryote cells and for the photoautotroph bacteria of the genera Prochlorococcus and Synechococcus. For each season and depth level, five columns are presented: seasonal mean value, standard deviation, number of data used and minimum and maximum values recorded along the complete time series.

Station T2. Nanoeukaryotes (cells/ml)																									
Depth	Winter					Spring					Summer					Autumn									
	Mean	σ	n	Min.	Max.	Mean	σ	n	Min.	Max.	Mean	σ	n	Min.	Max.	Mean	σ	n	Min.	Max.	Mean	σ	n	Min.	Max.
0	1812	723	7	1120	3338	957	785	5	0	2096	733	159	4	487	930	551	42	2	509	592					
10	1680	652	7	1093	3144	1081	568	5	296	2071	568	281	4	325	1033	563	152	2	411	714					
20	1725	1185	6	608	4274	974	617	5	249	2030	598	319	3	322	1045	585	13	2	572	597					
50	1247	971	7	237	3464	510	168	5	264	767	705	198	4	425	903	282	20	2	262	301					
75	557	465	7	54	1419	499	287	5	93	832	1954	1993	4	547	5374	161	23	2	138	183					

Station T2. Picoeukaryotes (cells/ml)																									
Depth	Winter					Spring					Summer					Autumn									
	Mean	σ	n	Min.	Max.	Mean	σ	n	Min.	Max.	Mean	σ	n	Min.	Max.	Mean	σ	n	Min.	Max.	Mean	σ	n	Min.	Max.
0	6946	7320	7	1365	21974	1491	1113	5	132	3043	1105	414	4	718	1752	582	120	2	462	701					
10	6125	5948	7	1392	15746	1366	1005	5	257	2814	826	58	4	769	922	505	87	2	418	592					
20	5702	7634	6	1359	22600	1469	1029	5	263	3153	802	150	3	648	1006	455	193	2	262	647					
50	6066	6733	7	647	21204	1572	1141	5	192	3231	1138	504	4	380	1643	1521	143	2	1378	1663					
75	2454	2518	7	114	6919	1789	1070	5	482	3458	2901	1669	4	851	5263	1689	566	2	1123	2255					

Station T2. Prochlorococcus (cells/ml)																								
Depth	Winter					Spring					Summer					Autumn								
	Mean	σ	n	Min.	Max.	Mean	σ	n	Min.	Max.	Mean	σ	n	Min.	Max.	Mean	σ	n	Min.	Max.	Mean	σ	n	Min.

Station T2. *Prochlorococcus* (cells/ml)

	Winter							Spring							Summer							Autumn																																																														
	2296	1546	7	368	4530	150	237	5	0	611	7342	12529	4	0	29042	10532	10532	2	0	21064	21064	2296	1546	7	368	4530	150	237	5	0	611	7342	12529	4	0	29042	10532	10532	2	0	21064	21064	2296	1546	7	368	4530	150	237	5	0	611	7342	12529	4	0	29042	10532	10532	2	0	21064	21064																					
0	2296	1546	7	368	4530	150	237	5	0	611	7342	12529	4	0	29042	10532	10532	2	0	21064	21064	2296	1546	7	368	4530	150	237	5	0	611	7342	12529	4	0	29042	10532	10532	2	0	21064	21064	2296	1546	7	368	4530	150	237	5	0	611	7342	12529	4	0	29042	10532	10532	2	0	21064	21064	2296	1546	7	368	4530	150	237	5	0	611	7342	12529	4	0	29042	10532	10532	2	0	21064	21064
10	2434	1638	7	368	4722	1434	1456	5	0	3985	8674	14705	4	108	34143	16509	6131	2	10378	22639	2434	1638	7	368	4722	1434	1456	5	0	3985	8674	14705	4	108	34143	16509	6131	2	10378	22639	2434	1638	7	368	4722	1434	1456	5	0	3985	8674	14705	4	108	34143	16509	6131	2	10378	22639	2434	1638	7	368	4722	1434	1456	5	0	3985	8674	14705	4	108	34143	16509	6131	2	10378	22639				
20	2591	2003	6	257	5024	999	1188	5	0	2677	8628	11643	3	83	25090	17183	5237	2	11946	22420	2591	2003	6	257	5024	999	1188	5	0	2677	8628	11643	3	83	25090	17183	5237	2	11946	22420	2591	2003	6	257	5024	999	1188	5	0	2677	8628	11643	3	83	25090	17183	5237	2	11946	22420	2591	2003	6	257	5024	999	1188	5	0	2677	8628	11643	3	83	25090	17183	5237	2	11946	22420				
50	3055	1875	7	386	6434	1090	1396	5	87	3842	8278	8241	4	1204	22292	22558	13439	2	9119	35996	3055	1875	7	386	6434	1090	1396	5	87	3842	8278	8241	4	1204	22292	22558	13439	2	9119	35996	3055	1875	7	386	6434	1090	1396	5	87	3842	8278	8241	4	1204	22292	22558	13439	2	9119	35996	3055	1875	7	386	6434	1090	1396	5	87	3842	8278	8241	4	1204	22292	22558	13439	2	9119	35996				
75	1519	1549	7	293	4773	513	313	5	159	919	8494	9175	4	683	24121	9532	1685	2	7847	11216	1519	1549	7	293	4773	513	313	5	159	919	8494	9175	4	683	24121	9532	1685	2	7847	11216	1519	1549	7	293	4773	513	313	5	159	919	8494	9175	4	683	24121	9532	1685	2	7847	11216	1519	1549	7	293	4773	513	313	5	159	919	8494	9175	4	683	24121	9532	1685	2	7847	11216				

Station T2. <i>Synechococcus</i> (cells/ml)																				
Depth	Winter					Spring					Summer					Autumn				
	Mean	σ	n	Min.	Max.	Mean	σ	n	Min.	Max.	Mean	σ	n	Min.	Max.	Mean	σ	n	Min.	Max.
0	14591	5979	7	8443	24940	33558	48623	5	1143	129303	24374	9743	4	13201	37969	23782	1695	2	22087	25476
10	14736	6154	7	8153	26529	48375	51353	5	2835	138565	22613	6684	4	12494	28965	22998	2546	2	20452	25543
20	17502	11533	6	3195	38161	39550	52158	5	6123	143121	20252	4880	3	14306	26259	22317	2779	2	19538	25095
50	13349	12212	7	2773	42199	11867	7616	5	5243	26505	29953	9355	4	20213	40657	5328	895	2	4433	6222
75	5400	4360	7	404	14066	5680	2265	5	2829	9572	15281	3754	4	10452	19766	939	41	2	898	979

Table 5.13. The same as in table 5.12, but for station T4.

Station T4. Nanoeukaryotes (cells/ml)																				
Depth	Winter					Spring					Summer					Autumn				
	Mean	σ	n	Min.	Max.	Mean	σ	n	Min.	Max.	Mean	σ	n	Min.	Max.	Mean	σ	n	Min.	Max.
0	1455	505	6	665	1998	1437	1387	3	220	3377	556	117	3	395	668	471	71	2	400	542
10	1440	548	6	680	2322	853	653	3	180	1737	553	153	3	416	766	437	119	2	318	556
20	1282	416	6	761	1919	937	648	3	243	1802	665	30	3	626	699	370	7	2	363	377
50	1056	454	6	482	1803	618	335	3	266	1068	1088	341	3	800	1567	424	134	2	290	557
75	435	129	6	269	617	323	124	3	150	438	398	198	3	183	661	128	41	2	87	168
100	265	117	4	93	401	174	37	3	141	225	239	187	3	105	503	32	20	2	12	51

Station T4. Picoeukaryotes (cells/ml)																				
Depth	Winter					Spring					Summer					Autumn				
	Mean	σ	n	Min.	Max.	Mean	σ	n	Min.	Max.	Mean	σ	n	Min.	Max.	Mean	σ	n	Min.	Max.
0	5527	4777	6	1631	13859	2223	2154	3	455	5255	598	172	3	470	841	586	114	2	472	699
10	5875	4894	6	1506	14973	1424	899	3	482	2635	686	257	3	434	1039	531	52	2	479	583
20	5600	4451	6	1464	13785	1404	957	3	234	2578	766	161	3	542	910	638	162	2	476	799
50	4744	2265	6	1515	7800	1138	997	3	361	2545	2511	1896	3	745	5141	1495	377	2	118	1871
75	2289	1977	6	569	6105	1585	806	3	611	2585	1974	1009	3	889	3319	821	306	2	515	1126
100	1928	1611	4	237	4350	707	320	3	284	1057	637	193	3	377	841	204	72	2	132	275

Station T4. <i>Prochlorococcus</i> (cells/ml)																				
Depth	Winter					Spring					Summer				Autumn					
	Mean	σ	n	Min.	Max.	Mean	σ	n	Min.	Max.	Mean	σ	n	Min.	Max.	Mean	σ	n	Min.	Max.
0	5739	9001	6	0	25324	1968	2484	3	110	5479	6775	9316	3	168	19949	10207	3862	2	6345	14068
10	5918	9087	6	543	25841	1196	1396	3	187	3171	6161	8507	3	117	18192	11143	4622	2	6521	15765
20	6101	9012	6	449	25765	189	104	3	81	329	9961	13489	3	147	29034	12642	3959	2	8683	16601
50	7449	9108	6	455	26033	10286	7362	3	314	17866	37171	12853	3	19229	48666	38857	10479	2	28378	49336
75	1904	1480	6	572	4871	7836	5432	3	368	13129	6617	5836	3	1105	14693	6152	601	2	5551	6752
100	1294	1234	4	449	3413	3004	3255	3	243	7575	6050	7570	3	464	16752	704	210	2	494	913

Station T4. <i>Synechococcus</i> (cells/ml)																				
Depth	Winter					Spring					Summer				Autumn					
	Mean	σ	n	Min.	Max.	Mean	σ	n	Min.	Max.	Mean	σ	n	Min.	Max.	Mean	σ	n	Min.	Max.
0	26623	24085	6	3620	73378	19676	11472	3	11201	35894	9696	9759	3	2063	23470	22876	3069	2	19807	25944
10	30269	27355	6	3653	83553	21507	18511	3	7503	47664	10116	9729	3	1623	23737	23993	3672	2	20321	27664
20	32437	28965	6	3371	84506	30710	27016	3	6386	68388	12641	12306	3	3728	30043	24627	2687	2	21940	27313
50	24232	24112	6	3856	71442	57201	63858	3	4704	147088	31259	15598	3	14362	51988	8803	1252	2	7551	10055
75	3924	1178	6	2021	5332	23026	22866	3	4515	55244	4474	3088	3	677	8241	584	246	2	338	829
100	2721	1057	4	991	3602	3314	1886	3	1581	5937	8620	10926	3	263	24054	234	84	2	150	317

Table 5.14. The same as in table 5.12, but for station BNA2.

Station BNA2. <i>Nanoeukaryotes</i> (cells/ml)																				
Depth	Winter					Spring					Summer				Autumn					
	Mean	σ	n	Min.	Max.	Mean	σ	n	Min.	Max.	Mean	σ	n	Min.	Max.	Mean	σ	n	Min.	Max.
0	2449	2050	7	668	6579	1090	327	6	500	1527	1020	708	4	402	2180	460	87	3	389	582
10	2530	2599	7	713	8215	820	327	5	234	1153	784	653	4	338	1913	478	80	3	383	578
20	2766	2782	6	823	8455	893	230	6	600	1293	758	494	4	398	1608	574	111	3	421	679
50	1370	620	7	835	2758	1010	440	6	495	1645	945	124	4	794	1132	414	62	3	357	500
75	1031	239	7	713	1452	635	396	6	293	1272	1014	830	4	284	2317	185	98	3	84	317
100	880	383	7	249	1407	335	233	5	78	692	150	89	4	45	260	63	18	2	45	81

Station BNA2. Picoeukaryotes (cells/ml)																				
Depth	Winter					Spring					Summer				Autumn					
	Mean	σ	n	Min.	Max.	Mean	σ	n	Min.	Max.	Mean	σ	n	Min.	Max.	Mean	σ	n	Min.	Max.
0	9061	7785	7	781	22785	998	359	6	503	1572	984	202	4	763	1281	613	323	3	162	905
10	8834	7807	7	599	23413	1012	413	5	431	1566	1015	313	4	581	1428	627	355	3	126	907
20	8052	8094	6	623	23080	1203	472	6	639	2126	1000	220	4	691	1313	985	591	3	198	1622
50	4795	3169	7	575	11093	2600	2476	6	557	7653	1299	762	4	460	2290	763	420	3	174	1122
75	3700	1933	7	970	7258	2078	2724	6	320	8071	2096	926	4	1180	3533	3606	4416	3	407	9850
100	2680	1518	7	584	5132	1003	1307	5	93	3602	959	686	4	254	2045	398	30	2	368	428

Station BNA2. Prochlorococcus (cells/ml)																				
Depth	Winter					Spring					Summer				Autumn					
	Mean	σ	n	Min.	Max.	Mean	σ	n	Min.	Max.	Mean	σ	n	Min.	Max.	Mean	σ	n	Min.	Max.
0	2477	2126	7	392	7093	348	373	6	0	1039	5760	9234	4	0	21738	10234	4982	3	4559	16687
10	2427	1891	7	386	6240	190	158	5	0	464	8166	13817	4	0	32097	10670	4942	3	5070	17091
20	2434	2147	6	371	6865	1954	3913	6	0	10693	6929	11238	4	0	26380	16725	3615	3	11940	20676
50	2626	2208	7	413	6961	14104	16320	6	114	43765	22210	13573	4	0	34019	18508	8748	3	10398	30654
75	2526	1898	7	710	6413	2146	2204	6	78	6602	19364	13459	4	2329	40010	11213	3184	3	7294	15093
100	2075	1452	7	814	5464	656	447	5	201	1231	7555	7624	4	153	18653	3415	1143	2	2272	4557

Station BNA2. Synechococcus (cells/ml)																				
Depth	Winter					Spring					Summer				Autumn					
	Mean	σ	n	Min.	Max.	Mean	σ	n	Min.	Max.	Mean	σ	n	Min.	Max.	Mean	σ	n	Min.	Max.
0	7791	4211	7	2473	14025	10558	5978	6	401	18602	21067	11049	4	13319	40103	30971	11439	3	15731	43292
10	7647	4605	7	2368	15615	9519	7487	5	323	22005	16949	3373	4	12986	21655	31198	10352	3	17530	42574
20	8211	5463	6	2374	18303	15687	9288	6	452	26073	19516	9870	4	5548	33019	28100	8278	3	18571	38754
50	6163	2790	7	2749	12198	47619	29461	6	1805	80163	26669	8858	4	12993	34889	13639	4373	3	7861	18437
75	5736	2160	7	3829	9111	14992	20854	6	1084	60600	7625	5136	4	1155	13528	4317	5005	3	766	11395
100	4621	1933	7	1192	7386	7403	7670	5	668	21102	1616	1324	4	171	3749	375	132	2	243	506

Table 5.15. The same as in table 5.12, but for station BNA4.

Station BNA4. Nanoeukaryotes (cells/ml)																				
Depth	Winter					Spring					Summer					Autumn				
	Mean	σ	n	Min.	Max.	Mean	σ	n	Min.	Max.	Mean	σ	n	Min.	Max.	Mean	σ	n	Min.	Max.
0	2125	734	7	1069	3360	2211	2387	5	137	6777	851	301	4	519	1204	497	212	3	277	784
10	2035	609	7	1186	3076	2250	2552	5	269	7207	687	244	4	369	949	917	822	3	246	2075
20	2177	334	7	1710	2878	1727	1092	5	299	2834	674	184	4	453	868	695	507	3	226	1399
50	1202	734	7	281	2339	2001	1851	5	560	5313	1421	508	4	644	2063	254	89	3	132	341
75	712	660	6	117	2094	1021	1235	5	314	3486	845	664	4	111	1910	150	75	3	60	244
100	735	755	7	120	2206	276	318	5	60	907	268	239	4	48	671	126	55	3	63	198

Station BNA4. Picoeukaryotes (cells/ml)																				
Depth	Winter					Spring					Summer					Autumn				
	Mean	σ	n	Min.	Max.	Mean	σ	n	Min.	Max.	Mean	σ	n	Min.	Max.	Mean	σ	n	Min.	Max.
0	7546	4245	7	2996	16111	2689	3205	5	280	8924	763	277	4	491	1195	779	341	3	421	1238
10	6723	2632	7	2911	10967	3033	3875	5	317	10627	874	349	4	497	1410	1111	451	3	587	1688
20	7941	5003	7	2902	19678	1820	1884	5	452	5467	886	319	4	467	1258	1136	230	3	904	1450
50	3115	2258	7	240	6639	1834	1837	5	638	5485	1510	624	4	823	2384	568	177	3	419	817
75	1690	1807	6	30	5510	1885	1356	5	464	4240	1461	684	4	467	2138	830	311	3	458	1219
100	2016	2236	7	45	6393	215	101	5	36	332	302	89	4	171	389	508	279	3	278	901

Station BNA4. Prochlorococcus (cells/ml)																				
Depth	Winter					Spring					Summer					Autumn				
	Mean	σ	n	Min.	Max.	Mean	σ	n	Min.	Max.	Mean	σ	n	Min.	Max.	Mean	σ	n	Min.	Max.
0	5407	3856	7	1720	12095	4118	5705	5	0	15314	5689	9518	4	0	22171	6830	6185	3	0	14977
10	5870	3756	7	2263	12983	1308	1388	5	0	3506	5819	9811	4	0	22810	7047	5995	3	0	14653
20	6380	3925	7	1863	14189	749	790	5	0	2231	5168	8102	4	269	19197	9984	7157	3	0	16417
50	3998	4424	7	290	13998	3943	3819	5	189	9389	21882	13441	4	4419	42056	23132	20684	3	5737	52196
75	2100	1885	6	90	5704	977	930	5	0	2461	10770	7872	4	2317	18857	15642	11905	3	4820	32223

Station BNA4. <i>Prochlorococcus</i> (cells/ml)																				
		Winter			Spring			Summer			Autumn									
Depth	Mean	σ	n	Min.	Max.	Mean	σ	n	Min.	Max.	Mean	σ	n	Min.	Max.					
100	2149	2058	7	114	6503	468	623	5	0	1677	6573	10392	4	111	24566	7127	4397	3	2293	12931
Station BNA4. <i>Synechococcus</i> (cells/ml)																				
		Winter			Spring			Summer			Autumn									
Depth	Mean	σ	n	Min.	Max.	Mean	σ	n	Min.	Max.	Mean	σ	n	Min.	Max.					
0	19681	12631	7	4096	40671	34813	27040	5	16955	88399	15477	5092	4	9156	21830	29931	2916	3	26417	33558
10	19779	14383	7	4503	47106	31839	12822	5	15422	52898	16087	6592	4	9918	27017	45808	22404	3	27776	77386
20	20744	15971	7	5419	50766	39598	18130	5	15997	58724	15858	9993	4	2875	30976	40993	14129	3	27676	60553
50	9188	10506	7	1383	33636	72663	68455	5	2500	16013	24631	11314	4	16918	44079	15427	9941	3	5036	28824
75	6989	10174	6	569	29507	12653	10562	5	1296	26292	3856	3113	4	868	8177	4150	2425	3	1045	6964
100	6809	10031	7	473	30899	3506	4674	5	832	12842	1291	1197	4	278	3267	1217	236	3	931	1509

6. CLIMATE CHANGE. TRENDS.

This book has been focused on the analysis of mean values and variability ranges for certain physical, chemical and biological variables that could help to characterize the different areas of the Spanish Mediterranean waters. As already explained in previous chapters, the goal was to establish the current environmental state of the sea, by means of statistical analyses presented in figures and tables. These statistics could be used as a reference for future works and could help to detect future alterations and changes that the Mediterranean Sea could suffer.

The maintenance of a monitoring system such as the RADMED one is expensive and has to face many difficulties such as, instrument failures, lack of personnel or vessel availability. Therefore, the generated time series have frequent gaps. Furthermore, RADMED Project was launched in 2007 and the length of the time series is not appropriate for the study of long-term changes as those associated to climate change. Nevertheless, in some cases the oceanographic stations were already sampled under the umbrella of previous monitoring programs and time series are available for certain variables and geographical areas since 1992, 1994 or 1996, depending on the cases. In the case of variables such as the temperature and salinity, alternative data sources are available. These sources are other monitoring programs funded by other institutions, such as l'Estartit Oceanographic station (Institut de Ciències del Mar, ICM/CSIC), international data bases that have compiled oceanographic data along the twentieth century, or data obtained by means of radiometers operated from satellites. These series are analyzed in this last chapter with the objective of establishing the current long-term trends and the changes that the Western Mediterranean could be suffering at present. This chapter can be considered as an update of previous reports published by the Instituto Español de Oceanografía dealing with Climate Change in the Spanish Mediterranean waters (Vargas-Yáñez et al., 2010a, 2008).

6.1 Description of the time series.

MEDAR/MEDATLAS data base (Mediterranean Data Archeology and Rescue, MEDAR Group, 2002) has compiled most of the oceanographic cruises carried out in the Mediterranean Sea during the twentieth century, whereas the temperature and salinity time series collected in the frame of the IEO monitoring programs were initiated during the 1990s. For this reason, all the available temperature and salinity profiles from the sea surface to 2500 m from MEDAR data base were collected for extending RADMED data backwards in time. MEDAR data base has information from the beginning of the twentieth century and some previous works have used it to estimate long-term trends for a period of more than a century (Vargas-Yáñez et al., 2010b). Nevertheless, the available data for the first half of the century is scarce and in the present work only those data from 1945 are considered. Temperature and salinity data from MEDAR/MEDATLAS have been merged with those from RADMED for constructing time series that extend from 1945 to 2016 (García-Martínez et al., 2018b, Vargas-Yáñez et al., 2017). This process has been used in four geographical areas where RADMED project has oceanographic stations. Such areas have been marked with rectangles in figure 6.1. Hereafter these areas will be referred to as Alboran, Murcia, Balearic Islands and Catalonia. It has to be noticed that, in the case of Catalan waters, there exist sea temperature data from l'Estartit oceanographic station as well as sea level data from the tide gauge located at this site (green triangle in figure 6.1, Salat and Pascual, 2006; Pascual et al., 1995). Daily sea temperature in the Fuengirola Beach (Alboran Sea) are obtained by the IEO (green triangle in figure 6.1).

Besides the "in situ" temperature data (from research vessels), sea surface temperature measured from satellites were obtained from the Earth System Research Laboratory, Physical Science Division of NOAA (National Oceanic and Atmospheric Administration, www.esrl.noaa.gov/psd/data/gridded/data.noaa.oisst.v2.html, Reynolds et al., 2002). The areas where satellite data were obtained are the same where in situ temperature and salinity time series were constructed. These areas are marked as red rectangles in figure 6.1. Satellite time series extend from 1982 to 2017.

Monthly sea level data at Algeciras, Malaga and Palma de Mallorca were obtained from the IEO tide gauge network (blue triangles in figure 6.1). Sea level data from l'Estartit oceanographic station were also used (green triangle in figure 6.1).

Finally, time series of nutrient concentrations, nutricline depth, integrated chlorophyll concentration, chlorophyll concentration at the Deep Chlorophyll Maximum (DCM), integrated dissolved oxygen and oxygen concentration at the oxygen minimum and maximum, were analyzed. Meso-zooplanktonic biomass time series were also considered. The estimation of trends for these chemical and biological time series was accomplished only in the case of the longest time series which are those initiated during the 1990s. The analysis of those time series initiated in 2007, when RADMED Project was launched, will be addressed in future updates of the present work.

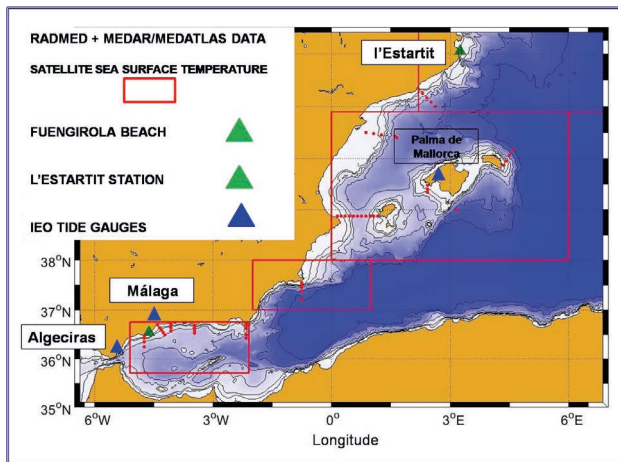


Figure 6.1. Red rectangles are the geographical areas where temperature and salinity data have been compiled using RADMED Project data and MEDAR/MEDATLAS data base. Sea surface temperature data from the ESRL/NOAA satellites have been collected at the same areas. The green triangle at the upper part of the figure shows the position of l'Estartit Oceanographic Station (ICM/CSIC) and the green triangle at the lower part of the figure corresponds to the Fuengirola Beach where IEO measures the sea temperature at a daily basis. Blue triangles show the positions of the IEO tide gauges. There is another tide gauge at l'Estartit Oceanographic station.

6.2 Analysis of trends for temperature, salinity and mean sea level.

All available temperature and salinity data from RADMED project and from MEDAR/MEDATLAS data base were collected for the four selected areas: Alboran, Murcia, Balearic Islands and Catalonia. Hereafter potential temperature will always be used, although for brevity temperature will be written. Data were analyzed from the sea surface to a maximum depth of 2500 m. Data from the same year were grouped and seasonally averaged. Then, the four annual data were averaged to obtain a single annual value for each depth level from the sea surface to 2500 m depth. As already explained, the Mediterranean Sea can be considered as divided into three main layers. The surface layer is filled by the Atlantic Water (AW) that flows into the Mediterranean Sea through the Strait of Gibraltar. This water mass is more or less modified depending on the geographical region considered and its residence time within the Mediterranean Sea. This layer extends from the sea surface to approximately 150 m depth. The intermediate layer is mainly occupied by Levantine Intermediate Water (LIW) and by Western Intermediate Water (WIW), although the presence of this second water mass is somehow intermittent and elusive. The intermediate layer extends from 150 to 600 m depth approximately. The deep layer extends below the intermediate layer, from 600 m depth to the sea bottom and is occupied by Western Mediterranean Deep Water (WMDW). Temperature and salinity data were averaged for these three layers. Finally, three annual time series of temperature (surface, intermediate and deep layers) and three annual time series of salinity were obtained for each of the four geographical areas.

Nevertheless, the construction of time series is not a direct process, as could be thought according to the brief description presented in the preceding paragraph. Data are not available for every season and for every year. Therefore, the time series have frequent gaps. On the other hand, some works have evidenced that some instruments such as expendable bathythermographs introduce biases in temperature measurements (Ishii and Kimoto, 2009; Domingues et al., 2008; Wijffels et al., 2008; Gouretski and Koltermann, 2007). Vargas-Yáñez et al. (2012b, 2010c, 2009) have shown that the resulting time series in the Mediterranean Sea could be different, depending on the inclusion of these data type, or depending on the way in which the temporal and spatial gaps were filled. According to these limitations, the uncertainty associated to the estimation of the annual values for each layer

and region is twofold. On one hand, it has to be considered the uncertainty linked to the estimation of the mean value (standard deviation). On the other hand, it has to be considered the uncertainty associated to the election of the data processing methodology. Details concerning methodological problems will not be described here, but can be consulted in Vargas-Yáñez et al. (2017) and García-Martínez et al. (2018b). These works reveal that the sensitivity of the results to the methodology used is caused by the oceanographic data scarcity (Llasses et al., 2015; Jordà and Gomis, 2013).

Anyway, the present work considers the uncertainty caused by the election of the data processing methodology. For each year a mean value is estimated for the temperature and salinity using different methodologies. All the results are averaged and the result is considered as the annual mean value (red lines in figures 6.2 to 6.13). The minimum and maximum values obtained using the different methodologies are considered as an estimation of the error or uncertainty (grey shaded areas in figures 6.2 to 6.13).

Figures 6.2, 6.3, 6.4 and 6.5 show the evolution of the potential temperature at the intermediate and deep layers of the four regions: Alboran, Murcia, Balearic Islands and Catalan waters. For each figure, it has been included the value of the estimated linear trend expressed in degrees per 100 years, and the 95 % confidence interval.

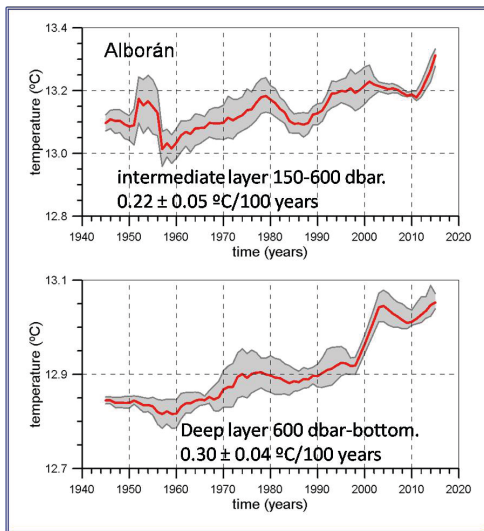


Figure 6.2. Upper plot is the evolution of the potential temperature for the intermediate layer (150-600 dbar) in the Alboran Sea. Several time series were obtained using different data types and methodologies for the data processing. Red line is the average value from the different time series and shaded grey areas show the difference between the minimum and maximum values obtained using the different methodologies, and represent an estimation of the time series uncertainty. The lower plot is the same, but for the deep layer, from 600 m depth to the sea bottom.

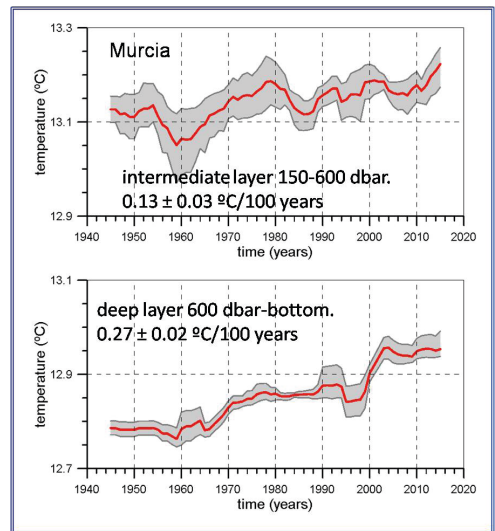


Figure 6.3. The same as in figure 6.2, but for the Murcia region.

Only those time series with significant trends at the 95 % confidence level in all the four selected regions are presented in figures 6.2 and followings (see table 6.1). Consequently, these results could be considered as robust ones. On the contrary, estimated trends for the surface layer are positive in some cases and negative in others, and require further analyses.

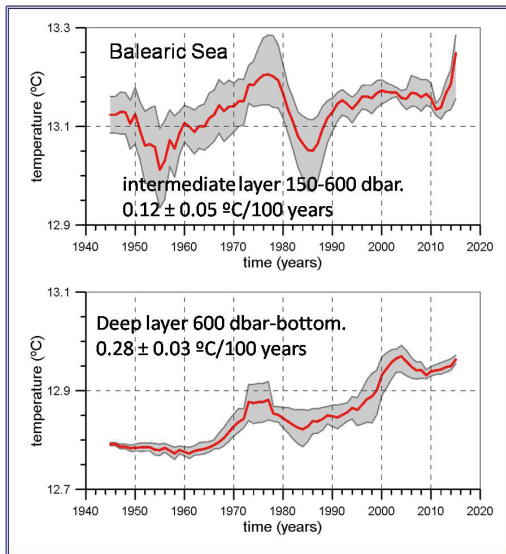


Figure 6.4. The same as in figure 6.2, but for the Balearic Islands region. *region.*

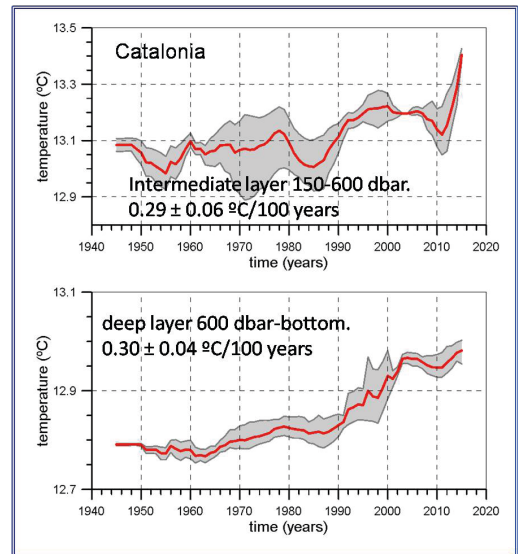


Figure 6.5. The same as in figure 6.2, but for the Catalonia region.

Intermediate and deep waters have warmed since mid twentieth century at a rate that ranges between 0.13 and 0.3 °C/100 year. It should be noted that an increase of 0.3 °C throughout a century could look like a small change, but it has to be considered that it corresponds to a large amount of absorbed heat. This warming and the associated absorbed heat are in accordance with previous observations and works (Rhein et al., 2013; Levitus et al., 2012, 2009).

The lack of significant trends at the surface layers is a surprising result, as the world oceans have stored at their upper 700 m most of the heat absorbed by the Earth because of the global warming process (Levitus et al., 2012, 2009). Furthermore, this result could be considered as contradictory. The intermediate waters are the result of the sinking of surface waters (AW) after suffering winter convection in the Eastern Mediterranean (see the introduction chapter). It is difficult to explain the warming of the intermediate layer without the participation of a warmer AW. Similarly, the WMDW is the result of the mixing between AW and LIW. Once again, the warming of WMDW requires the warming of AW, or LIW, or both.

A plausible explanation is that surface waters have a very large variability because of the exchanges with the atmosphere. Besides the seasonal temperature cycle that affects the upper layer, these waters experience strong changes over shorter periods of time. As a consequence, the sampling of these waters should be periodic, not being this the case for the MEDAR/MEDATLAS data. The data scarcity for the twentieth century makes it difficult the detection of long-term trends for time series with such a strong short-term variability. Even the periodic sampling carried out in the frame of RADMED project could not be adequate, and new data sources would be needed. To relieve this deficiency, sea surface temperature time series from satellite data were analyzed at the Alboran Sea, Murcia region, Balearic Sea and Catalonia region. These time series and those obtained from MEDAR/MEDATLAS and RADMED data are presented in figures 6.6 and 6.7.

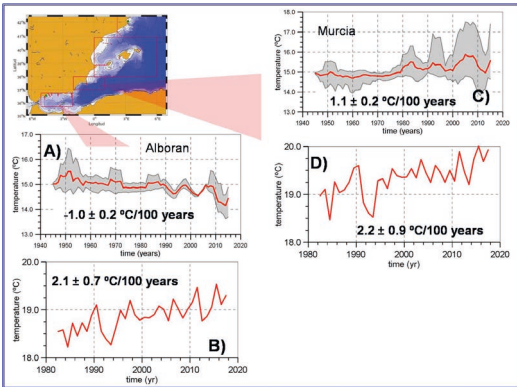


Figure 6.6. Figure 6.6A shows the evolution of the temperature at the surface layer in the Alboran Sea (0-150 dbar) from 1945, using MEDAR/MEDATLAS and RADMED data. The red line shows the time series averaged from different methodologies. Grey shaded areas are the uncertainty associated to the election of the data processing method. Figure B corresponds to the sea surface temperature measured from satellites. Figures C and D are the same, but for the Murcia region.

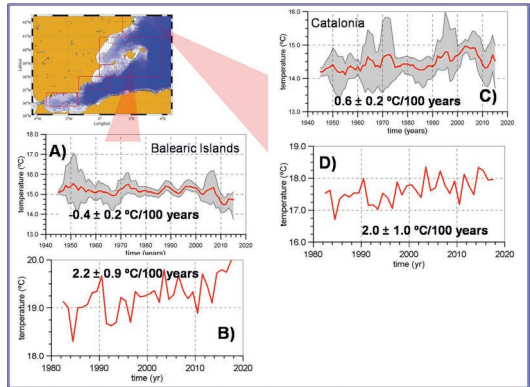


Figure 6.7. The same as in figure 6.6, but for the Balearic Islands and the Catalonia region.

Other data sources that could contribute to clarify the behavior of the upper layer are those obtained in Fuengirola Beach and those from the continental shelf in l'Estartit coast. Figure 6.8 shows the mean seasonal cycle for the sea temperature in Fuengirola Beach and the temperature evolution since 1986. In this case, time series are sampled on a daily basis and can capture the complete time variability of the surface waters, being data gaps very scarce. This series has a clear warming trend. Considering the estimated uncertainty, this trend would be between 1 and 3 °C/100 years.

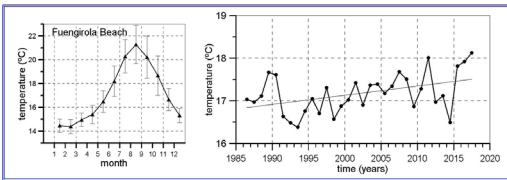


Figure 6.8. Mean seasonal cycle for the sea temperature in Fuengirola Beach and temperature evolution since 1986.

Figure 6.9. Figure A shows the mean seasonal cycle for the air daily minimum (blue), mean (black) and maximum (red) temperatures at l'Estartit station. Figure B shows the evolution of the air daily minimum, mean and maximum temperatures. Figure C shows the average temperature profiles in winter (blue), spring (green), summer (red) and autumn (light brown). The sampled depth levels at l'Estartit oceanographic station are 0, 20, 50 and 80 m. Figure D shows the time evolution of the sea temperature at the same depths. Trends and 95 % confidence intervals have been included.

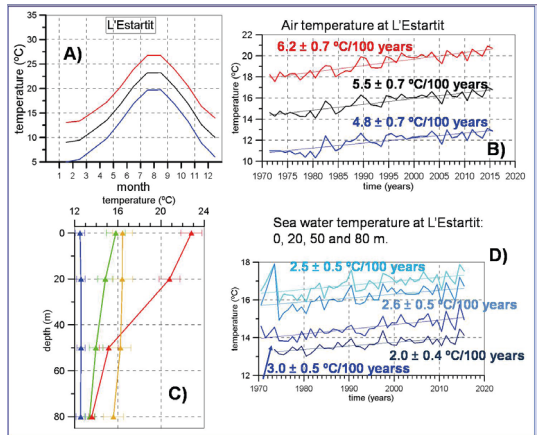


Figure 6.9 shows the mean seasonal cycle for the air temperature (daily minimum, mean and maximum) at l'Estartit station (Fig. 6.9A), and their temporal evolution since 1971. These figures show very strong positive trends, very likely caused by some sort of decadal variability. The sea water temperature at 0, 20, 50 and 80 m depth (Fig. 6.9D) also shows a significant increase since 1970, with trends that range between 2 and 3 °C/100 years.

Both satellite data and those data from Fuengirola Beach and l'Estartit oceanographic station confirm that the warming of the intermediate and deep waters is not possible without the warming of surface waters. These time series confirm that such a warming is occurring at a very high rate, at least since 1970. It could be considered the possibility that the surface water temperature had remained stable from 1945 to 1970 and that the warming trends had initiated or intensified at this latter date. This would explain the discrepancy between the MEDAR/MEDATLAS and RADMED time series on one hand, and the Fuengirola and l'Estartit series on the other. Nevertheless, previous works show the warming of

the upper part of the water column since mid twentieth century. Furthermore, there are contradictions between the results obtained at the four analyzed regions, when MEDAR/MEDATLAS data are used, with a warming of Murcia and Catalan waters, and the cooling of the waters in the Alboran Sea and the Balearic Islands. All these facts make us hypothesize that the lack of warming trends in the surface layer of the RADMED area is a methodological problem caused by the data scarcity.

Figures 6.10, 6.11, 6.12 and 6.13 show the evolution of salinity for the four analyzed regions and for the upper, intermediate and deep layers. The color criterion for the salinity figures is the same used for the temperature ones, with the red lines corresponding to the annual time series estimated averaging the series obtained using different methodologies, and the shaded areas corresponding to the uncertainty associated to the election of the data processing method.

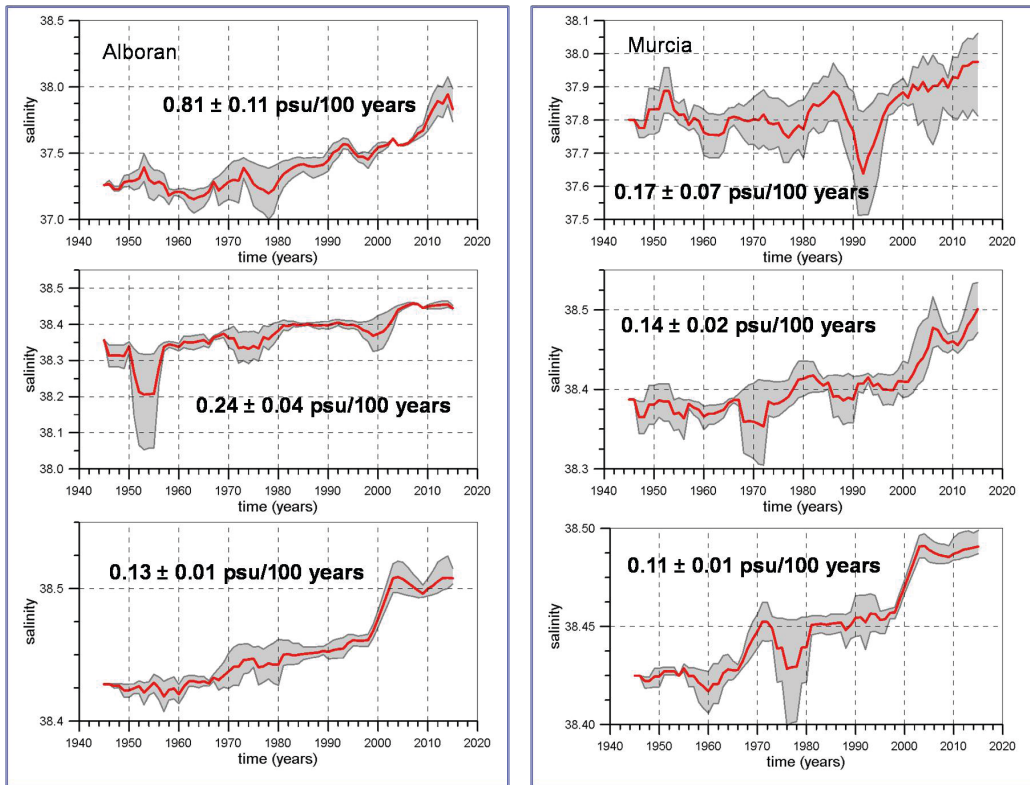


Figure 6.10. Evolution of the salinity for the Alboran Sea for the surface layer (0-150 dbar), intermediate layer (150-600 dbar) and deep layer (600 dbar-sea bottom).

Figure 6.11. The same as in figure 6.10, but for the Murcia region.

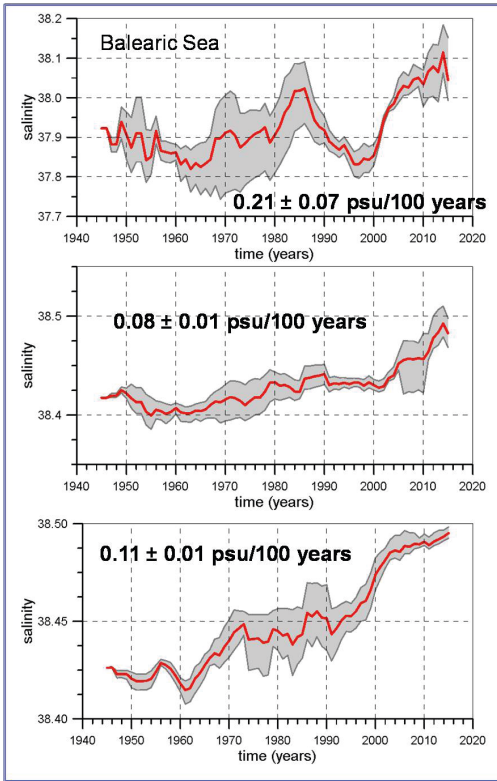


Figure 6.12. The same as in figure 6.10, but for the Balearic Islands.

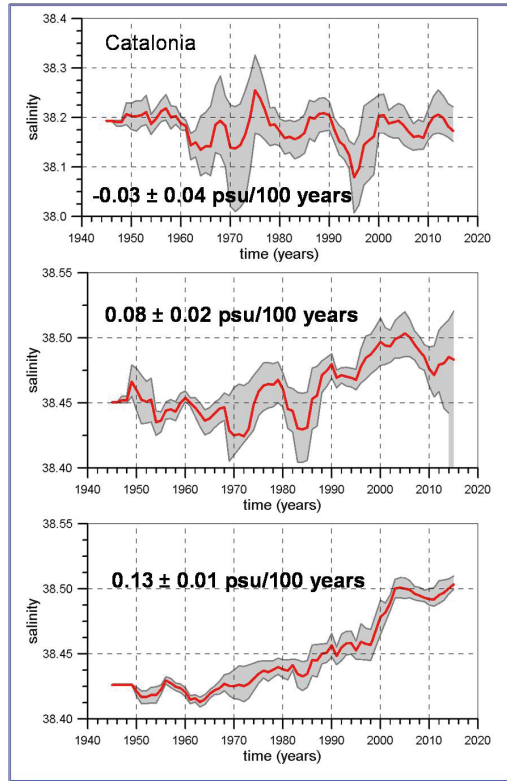


Figure 6.13. The same as in figure 6.10, but for the Catalonia region.

The salinity in the RADMED area has increased with the only exception of the upper layer of the waters at the northernmost sector. This salinity increase indicates a possible increase of the evaporation, a decrease of precipitations, or a combination of both. It should also be considered the construction of dams in the main rivers that drain into the Mediterranean Sea since the mid twentieth century. These constructions have affected rivers such as Nile, Ebro, and those rivers draining into the Black Sea, that finally is connected to the Mediterranean through the Dardanelles and Bosphorus Straits. Several works have shown that this anthropogenic factor has contributed to the salinity increase of the Mediterranean waters (García-Martínez et al., 2018b, Rohling and Bryden, 1992, Krahnmann and Schott, 1998).

To complete this review about the main changes observed for the physical properties of the Mediterranean waters, figure 6.14 presents the evolution of the mean sea level at Algeciras, Malaga and Palma de Mallorca, from the IEO tide gauge network. The sea level time series from l'Estartit oceanographic station (ICM/CSIC) is also included.

The main causes for the sea level rise are the increment of the total mass produced by the melting of continental ice, and the increment of the water volume (density decrease) caused by the sea warming (thermsteric sea level). Obviously, if continental ice would increase or density would increase, the effect would be the opposite, that is, a sea level decrease. To separate these two effects is not an easy task. Tectonic land movements and the effect of the atmospheric pressure and wind can affect sea level at a more local scale. An extensive review of all these factors and their influence on sea level can be consulted in Gomis et al. (2012) or Salat et al. (2017). Other authors have compared sea level measurements from altimeters and from tide gauges (Bonaduce et al., 2016).

Summarizing the main results, the Mediterranean mean sea level did not rise or rose at a very low rate from mid twentieth century to mid 1990s. For the same period, the global mean sea level rose at a rate of 1.6 ± 0.2 mm/yr. The reason seems to be the increase of atmospheric pressure during this period, associated to the variability of one of the main atmospheric circulation patterns in the North Atlantic (NAO, North Atlantic Oscillation). A positive phase of the NAO since 1960 to the beginning of the 1990s induced the sea level decrease (Tsimplis et al., 2005).

Sea level time series from Algeciras and Málaga extend from 1943 to 2002 and from 1944 to 2013 respectively (Fig. 6.14). Linear trends estimated for these time series show positive trends of 0.3 ± 0.4 mm/yr for Algeciras and 0.7 ± 0.6 mm/yr for Malaga. These values are low if compared with those observed at a global scale. As already explained, the reason seems to be the strong influence of the NAO from mid twentieth century to the beginning of the 1990s. If the Malaga sea level time series is considered from 1990 to 2013, once the high atmospheric pressure period had already ended, the trend is 5.8 ± 2.0 mm/yr. The sea level time series at Palma shows a positive trend from 1997 to 2017 of 2.1 ± 3.3 mm/yr, and the series at l'Estartit, from 1990 to 2017, of 3.1 ± 1.1 mm/yr. These values are in agreement with those observe on a global scale since the beginning of the 1990s, which are around 3.1 mm/yr (Cazenave et al., 2014), and with those estimated from altimetry data which show a sea level rise in the Mediterranean Sea from 1993 to 2015 of 2.6 ± 0.2 mm/yr (Marcos et al., 2016).

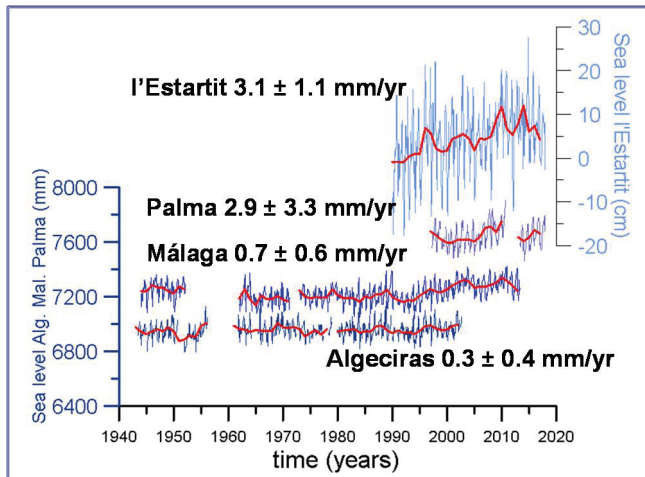


Figure 6.14. From the bottom to the top, monthly mean sea level time series (blue) at Algeciras, Malaga and Palma. Annual times series have also been included (read lines). These time series are expressed in millimeters (mm). Offsets of 300 mm with respect to the previous series have been introduced in the series of Malaga and Palma for the clarity of the plot. The curve at the upper part of the plot shows the mean sea level (monthly, blue and annual, red) at l'Estartit. These latter time series is expressed in centimeters (cm).

6.3 Analyses of trends for chemical and biological variables.

As already explained throughout the present work, the physical, chemical and biological properties of sea water, can change on very different time scales. There exist high frequency variations over periods of days or weeks. Inter-annual variability is responsible for the difference between consecutive years. On a longer time scale, there can be alterations (positive or negative anomalies) that persist over several years or decades. Finally, the average values of these properties can change slowly towards new ones. These latter changes can produce a shift in the conditions of the environmental state of the marine ecosystems. The detection of long-term trends, requires the analysis of long time series, typically longer than 30 years. Only in this way, long-term changes and decadal variability can be distinguished. This analysis and the trend detection are more difficult when time series are affected by a strong high frequency variability.

The length of the chemical and biological time series collected under the umbrella of IEO monitoring programs have, in the best cases, a length of 25 years (the oldest ones correspond to 1992). Furthermore, the high variance of the time series of nutrients, chlorophyll or the abundance of the different groups in the phyto and zooplanktonic communities, makes it difficult to infer the existence of any trend

from the analysis of such time series. For these reasons, these estimations have been carried out only for the longest time series, those corresponding to the former projects ECOMALAGA (P, M, V), ECOMURCIA (CP) and ECOBALEARES (B) which were initiated in the mid 1990s. Nevertheless, these results must be taken with caution. The goal of this analysis is simply to have some initial indications of the possible changes that the Spanish Mediterranean ecosystems could be suffering, and to show the potentiality of the RADMED monitoring program, in the case it was kept in time.

Since 2007, the sampling protocols for all the geographical areas and transects monitored in RADMED Project were unified. Stations labeled as 4, over the continental slope, were included at this date. For this reason, the length of the time series from these stations is not appropriate for the trend analysis. Therefore, the strategy of presenting results systematically for stations 2 and 4, will not be followed in this section. Only those oceanographic stations with the longest time series will be analyzed.

For each time series, the average seasonal cycle was subtracted to obtain a series of residuals. Figures 6.15, 6.16 and 6.17 show the time series of residuals for the integrated concentrations of nitrate, phosphate, chlorophyll-a and the depth of the nutricline, the Deep Chlorophyll Maximum (DCM) and the chlorophyll concentration at the position of the DCM for the oceanographic stations of the former ECOMALAGA Project. Figure 6.15 corresponds to the stations P2 and P3 from Cape Pino transect, figure 6.16 corresponds to stations M2 and M3 from Malaga transect, and figure 6.17 to stations V2 and V3 from Velez transect.

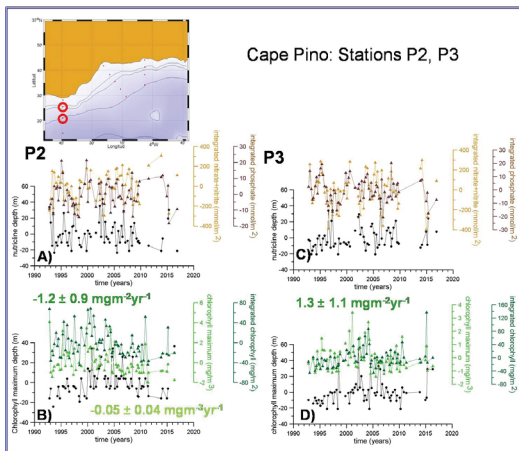


Figure 6.15. Figure 6.15A: Station P2. Time series of residuals for the integrated concentration of nitrate (light brown line) and phosphate (dark brown line). Time series of residuals for the nutricline depth (black line). Residuals have been calculated extracting the average seasonal cycle to the original time series. Figure 6.15 B: Station P2. Time series of residuals for the integrated chlorophyll-a concentration (dark green line), chlorophyll concentration at the position of the DCM (light green line), and depth of the DCM (black line). Figures 6.15C and D are the same as figures 6.15A and B, but for station P3.

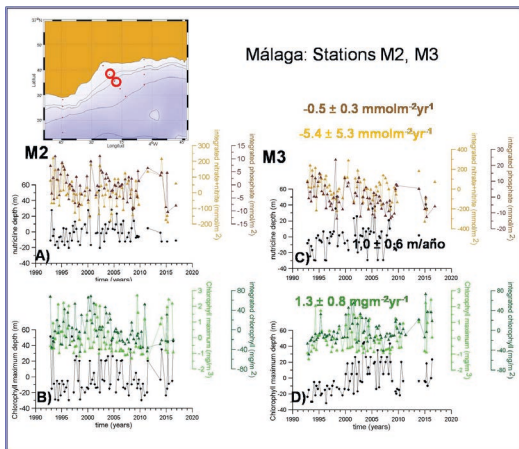


Figure 6.16. The same as in figure 6.15, but for stations M2 and M3 from the Malaga transect

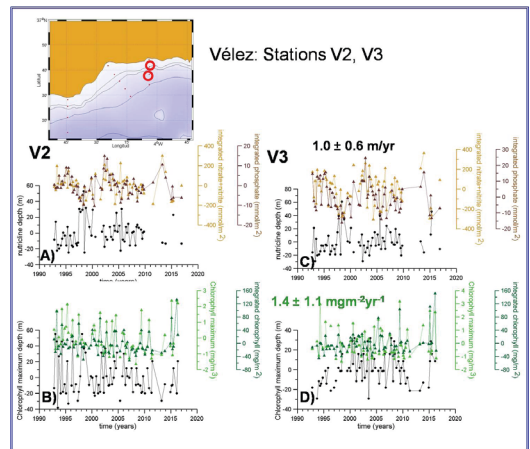


Figure 6.17. The same as in figure 6.15, but for stations V2 and V3 from the Velez transect.



In all the cases, figures A) and C) show the time series of residuals for the concentrations of integrated nitrate (light Brown line), integrated phosphate (dark Brown line) and depth of the nutricline (black line). Figures B) and D) show the time series of residuals for the integrated concentration of chlorophyll-a (dark green line), the chlorophyll concentration at the DCM (light green line), and for the depth of the DCM (black line). Linear trends have been inserted in the figures when they were significant at the 95 % confidence level.

No significant trends were observed at the P2 and P3 stations at the Cape Pino transect for the nitrate and phosphate concentrations integrated over the upper 100 m of the water column. Neither the nutricline depth, the depth of the DCM or the chlorophyll concentration at the DCM showed any change. The only significant trends were obtained for the case of the chlorophyll-a integrated concentration. Nevertheless, this variable decreased for the observed period at station P2 and increased at P3.

In a similar way, the time evolution of biochemical variables did not show a clear pattern at the Malaga transect (M2 and M3). Nitrate and phosphate decreased in a significant way at station M3. They also decreased at station M2, but in this case the trends were not significant. The chlorophyll integrated concentration has a positive significant trend at station M3, and did not change at M2. Finally, the depth of the DCM has a positive trend (increasing depth) at station M3.

At Velez transect (V2 and V3), the only variables with a positive and significant trend were the integrated chlorophyll and the nutricline depth at V3. All the other variables analyzed and presented in figures 6.17A, B, C and D did not show any significant trend.

Linear trends were also estimated for the oxygen integrated concentration and for the oxygen concentration at the minimum level (associated to the nutrient maximum) and maximum levels (associated to the DCM). The corresponding figures are not shown for brevity. The results were contradictory, with positive trends in some cases, and negative ones or absence of trends in others.

Figures 6.18 and 6.19 show the time series of residuals at stations CP1 and CP3 in Cape Palos transect and at the stations B1 and B2 in the Mallorca transect. The integrated concentrations of nitrate, phosphate, and chlorophyll-a, decreased at station CP1. The depth of the DCM and the nutricline increased. In this case, the changes are consistent: The nutrient decrease produces the deepening of the nutricline and the decrease of the primary production which, in turn, produces a decrease of the chlorophyll concentration and the deepening of the DCM. Nevertheless, all these trends were not significant at the 95 % confidence level. Integrated concentrations of silicate and dissolved oxygen showed negative and significant trends. Nevertheless, changes observed at CP3, very close to CP1, were not significant and, in some cases, had opposite signs to those observed at CP1. The only coincidence was the significant trend of integrated dissolved oxygen.

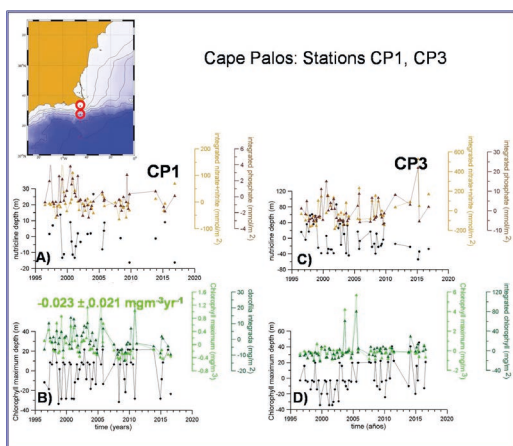


Figure 6.18. The same as in figure 6.15, but for stations CP1 and CP3 in the Cape Palos transect.

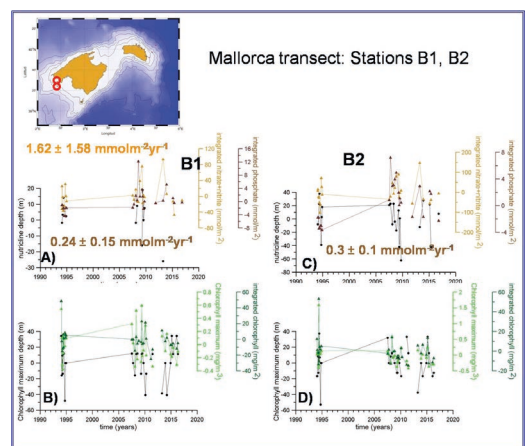
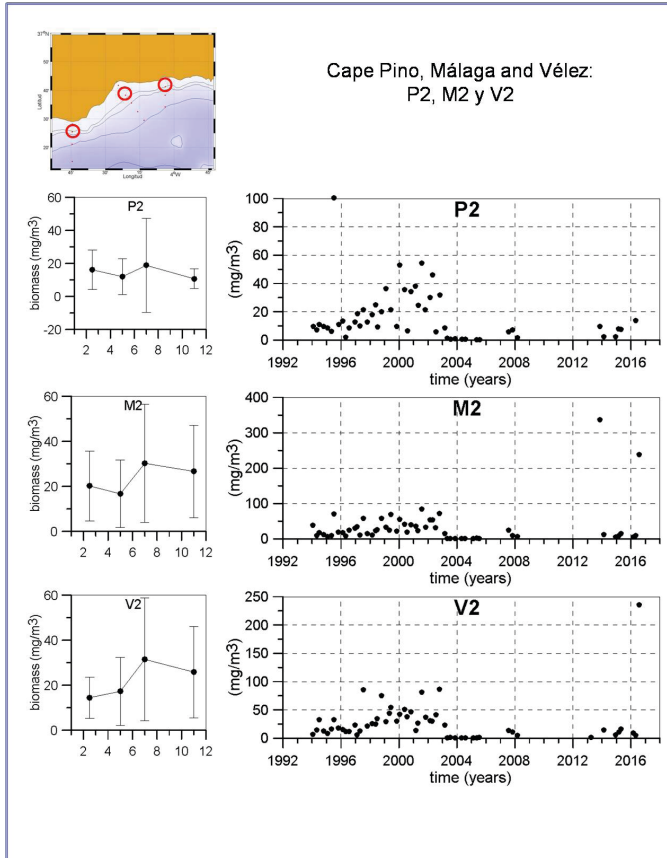


Figure 6.19. The same as in figure 6.15, but for stations B1 and B2 in Mallorca transect.

Figure 6.19 shows the time series for stations B1 and B2 in the Mallorca transect. In this transect, the systematic sampling of biochemical variables was initiated in 2007. Nevertheless, data from 1994 are

also available. These data correspond to the former Project ECOBALEARES and have been included in figure 6.19 for comparison with the data from the current Project RADMED. The only significant result is the increase of nitrate and phosphate concentrations in both stations. However, these results should be taken with caution because of the data scarcity.



The analysis of the mixed layer depth, estimated from temperature data, showed a significant negative trend at station V3 (shallower position and stronger stratification) and a positive and significant trend at station M2 (deeper position and weaker stratification). For the rest of the stations, trends were both positive and negative, but none of them were significant.

In summary, the available time series have a strong high-frequency variability. Such variability and the length of the current time series does not allow us to detect robust trends for the nutrient and chlorophyll concentrations or the depth of the nutricline and the mixed layer.

The time series of meso-zooplanktonic biomass at P2, M2 and V2, at the Malaga continental shelf, have been analyzed. Neither these time series show significant trends (Fig. 6.20). the most interesting feature in this figure is the strong decadal variability, with very high values between years 1996 and 2004.

Figure 6.20. The left column shows the average seasonal values for the meso-zooplanktonic biomass at stations P2, M2 and V2. Vertical bars represent the standard deviation. The right column shows the time evolution of meso-zooplanktonic biomass at the stations P2, M2 and V2.



Trends in °C/100 years; psu/100 years; kgm-3/100 years				
	Alboran	Murcia	Baleares	Cataluña
θ_S	-1.0 ± 0.2	1.1 ± 0.2	-0.4 ± 0.2	0.6 ± 0.2
θ_I	0.2 ± 0.1	0.1 ± 0.0	0.1 ± 0.0	0.3 ± 0.1
θ_D	0.3 ± 0.0	0.3 ± 0.0	0.3 ± 0.0	0.3 ± 0.0
SS	0.8 ± 0.1	0.2 ± 0.1	0.2 ± 0.1	-0.0 ± 0.0
SI	0.2 ± 0.0	0.1 ± 0.0	0.1 ± 0.0	0.1 ± 0.0
SD	0.1 ± 0.0	0.1 ± 0.0	0.1 ± 0.0	0.1 ± 0.0
σ_S	0.8 ± 0.1	-0.1 ± 0.1	0.3 ± 0.1	-0.2 ± 0.1
σ_I	0.1 ± 0.0	0.1 ± 0.0	0.0 ± 0.0	0.0 ± 0.0
σ_D	0.0 ± 0.0	0.0 ± 0.0	0.0 ± 0.0	0.0 ± 0.0
SST	2.1 ± 0.7	2.2 ± 0.9	2.2 ± 1.0	2.0 ± 1.0
$\theta_{\text{Fuengirola}}$			1.9 ± 1.2	
$\theta_{\text{l'Estartit}}$	2.5 ± 0.5 (0 m)	2.6 ± 0.5 (20 m)	2.0 ± 0.4 (50 m)	3.0 ± 0.5 (80 m)
MSL Algeciras			0.3 ± 0.4	
MSL Malaga			0.7 ± 0.6	
MSL Palma			2.1 ± 3.3	
MSL l'Estartit			3.1 ± 1.1	

Table 6.1. Trends for potential temperature (°C/100 years), salinity (psu/100 years) and potential density (kgm⁻³/100 years) for the surface layer (S), Intermediate layer (I) and deep layer (D) in the Alboran Sea, Murcia, Balearic Islands and Catalonia (see red rectangles in figure 6.1). Trends for sea surface temperature, obtained from satellite data at the same regions (SST). Trends for sea temperature at Fuengirola Beach (°C/100 years) and at l'Estartit Oceanographic Station at 0, 20, 50 and 80 m depth. Trends for the mean sea level (MSL) at Algeciras, Malaga, Palma de Mallorca and l'Estartit tide gauges (mm/yr).



REFERENCES

- Anati, D. H., Stommel, 1970. The initial phase of deep water formation in the northwest Mediterranean during MEDOC '69 on the basis of observations made by Atlantis II. January 25-February 12, 1969. *Cahiers Oceanographiques*, 4, 343-351.
- Arín, L., M. Estrada, J. Salat, A. Cruzado, 2005. Spatio-temporal variability of size fractionated phytoplankton on the shelf adjacent to the Ebro river (NW Mediterranean). *Cont. Shelf. Res.*, 25, 1081-1095, doi: 10.1016/j.csr.2004.12.011.
- Armstrong, F., C. Stearns, J. Strickland, 1967. The measurement of upwelling and subsequent biological process by means of the Technicon Autoanalyzer® and associated equipment, in: *Deep-Sea Res. II*, 14 (3), 381-389, Elsevier. [https://doi.org/10.1016/0011-7471\(67\)90082-4](https://doi.org/10.1016/0011-7471(67)90082-4)
- Balbín, R., J.L. López-Jurado, A. Aparicio-González, M. Serra, 2014. Seasonal and interannual variability of dissolved oxygen around the Balearic Islands from hydrographic data. *J. Mar. Syst.*, 138, 51-62.
- Bethoux, J. P., P. Morin, D. P., Ruiz-Pino, 2002. Temporal trends in nutrient ratios: chemical evidence of Mediterranean ecosystem changes driven by human activity, *Deep-Sea Res. II*, 49 (11), 2007-2015. [https://doi.org/10.1016/S0967-0645\(02\)00024-3](https://doi.org/10.1016/S0967-0645(02)00024-3)
- Bethoux, J. P., B. Gentili, P. Morin, E. Nicolas, C. Pierre, R. P. Diana, 1999. The Mediterranean Sea: A miniature ocean for climatic and environmental studies and a key for the climatic functioning of the North Atlantic. *Progress in Oceanography*. 44. 131-146. [10.1016/S0079-6611\(99\)00023-3](https://doi.org/10.1016/S0079-6611(99)00023-3).
- Bethoux, J.P., P. Morin, C. Chaumery, O. Connan, B. Gentili, D. Ruiz-Pino, 1998. Nutrients in the Mediterranean Sea, mass balance and statistical analysis of concentrations with respect to environmental change. *Marine Chemistry*, 63, 155-169.
- Bethoux, J.P., 1979. Budgets of the Mediterranean Sea. Their dependence on the local climate and on the characteristics of the Atlantic Waters. *Oceanol. Acta*, Vol. 2, nº 2, 157-163.
- Bonaduce, A., N. Pinardi, P. Oddo, G. Spada, G. Larnicol, 2016. Sea-level variability in the Mediterranean Sea from altimetry and tide gauges. Volume 47, Issue 9-10, 2851-2866, doi.org/10.1007/s00382-016-3001-2.
- Boukthir, M., B. Bernier, 2000. Seasonal and inter-annual variations in the surface freshwater flux in the Mediterranean Sea from the ECMWF re-analysis Project. *J. Mar. Syst.*, 24, 343-354.
- Cano, N., J. Gil, 1984. Campaña hidrológica "Albrán 78". *Bol. Inst. Esp. Oceanogr.* 1(2), 114-125.
- Cano, N., 1978. Hidrología del Mar de Alborán en primavera-verano. *Bol. Inst. Esp. Oceanogr.*, 248 (4), 51-66.
- Cazenave, A., H.-B. Dieng, B. Meyssignac, K. Von Schuckmann, B. Decharme, E. Berthier, 2014. The rate of sea-level rise. *Nature Climate Change*, 4, 358-361.
- Criado-Aldeanueva, F., F.J. Soto-Navarro, J. García-Lafuente, 2012. Seasonal and interannual variability of surface heat and freshwater fluxes in the Mediterranean Sea: budgets and Exchange through the Strait of Gibraltar. *Int. J. Climatol.*, 32, 286-302.
- De Boyer Montégut, C., G. Madec, A. S. Fischer, A. Lazar, D. Iudicone, 2004. Mixed layer depth over the global ocean: An examination of profile data and a profile-based climatology. *Journal of Geophys. Res.* 109. C12003, doi:10.1029/2004JC002378
- Domingues, C. M., J. A. Church, N. J. White, P. J. Gleckler, S. E. Wijffels, P. M. Barker, and J. Dunn, 2008. Improved estimates of upper-ocean warming and multi-decadal sea level rise, *Nature*, 453, 1090 - 1093, doi:10.1038/nature07080.
- D'Ortenzio, F., R. d'Alcala, 2009. On the trophic regimes of the Mediterranean Sea: a satellite analysis. *Biogeosciences*, 139-148. <https://doi.org/10.5194/bg-6-139-2009>
- Estrada, M., M. Latasa, M. Emelianov, A. Gutiérrez-Rodríguez, B. Fernández-Castro, J. Isern-Fontanet, B. Mouriño-Carballido, J. Salat, M. Vidal, 2014. Seasonal and mesoscale variability of primary production in the deep winter-mixing region of the NW Mediterranean. *Deep-Sea Res. I*, 94, 45-61.

- Estrada, M., 1996. Primary production in the northwestern Mediterranean. *Sci. Mar.*, 60 (Supl. 2): 55-64.
- Estrada, M., 1985. Deep phytoplankton and chlorophyll máxima in the Western Mediterranean. En "Mediterranean Marine Ecosystems", editado por M. Moraitou-Apostolopoulou y V. Kiortsis. NATO Conference Series (I Ecology), vol 8. Springer, Boston, 247-277.
- Fernández de Puellas, M. L., F. Alemany, J. Jansá, 2007. Zooplankton time series in the Balearic Sea (Western Mediterranean): Variability during the decade 1994-2003. *Prog. In Oceanogr.*, 74, 329-354, doi: 10.106/j.pocean.2007.04.009.
- Font, J., J. Salat, J. Tintoré, 1988. Permanent features of the circulation in the Catalan Sea. *Oceanol. Acta*, 9, 51-57.
- García-Lafuente J., C. Naranjo, S. Sammartino, J.C. Sánchez-Garrido, J. Delgado, 2017. The Mediterranean outflow in the Strait of Gibraltar and its connection with upstream conditions in the Alborán Sea. *OceanSci.* 13: 195-207, doi: 10.5194/os-13-195-2017
- García Lafuente, J., N. Cano, M. Vargas, J.P. Rubín, A. Hernández-Guerra, 1998. Evolution of the Alboran Sea hydrographic structures during July 1993. *Deep-Sea Res.* I (45), 39-65.
- García-Martínez, M.C., M. Vargas-Yáñez, F. Moya, R. Santiago, A. Reul, M. Muñoz, J.L. López-Jurado, R. Balbín, 2019. Spatial and temporal long term patterns of phyto and zooplankton in the W-Mediterranean: RADMED project. *Water*, 11(3), 534, <https://doi.org/10.33901/w11030534>.
- García-Martínez, M.C., M. Vargas-Yáñez, F. Moya, R. Santiago, M. Muñoz, A. Reul, T. Ramírez, R. Balbín, 2018a. Average nutrient and chlorophyll distributions in the Western Mediterranean: RADMED project. *Oceanologia*. 10.1016/j.oceano.2018.08.003.
- García-Martínez, M.C., M. Vargas-Yañez, F. Moya, P. Zunino, B. Bautista, 2018b. The Effects of Climate Change and Rivers Damming in the Mediterranean Sea during the Twentieth Century. *International journal of environmental sciences and natural resources*, 8(4). 10.19080/IJESNR.2018.08.555741.
- Gasol J.M., 1999. How to count picoalgae and bacteria with the FACScalibur flowcytometer. www.marbef.org/training/FlowCytometry/Lectures/Gasol2.pdf
- Gomis, D., M. Tsimplis, M. Marcos, L. Fenoglio-Marc, B. Pérez, F. Raicich, I. Vilibic, G. Wöppelmann, S. Monserrat, 2012. Mediterranean Sea-Level Variability and trends. En *The Climate of the Mediterranean Region*. Editor: P. Lionello, Elsevier, 257-300, doi: 10.1016/B978-0-12-416042-2.00004-5.
- Gomis, D., S. Ruiz, M. A. Pedder, 2001. Diagnostic analysis of the 3-D ageostrophic circulation from a multivariate spatial interpolation of CTD and ADCP. *Deep-Sea Res.* I, 269-295.
- Gouretski, V., K. P. Koltermann, 2007. How much is the ocean really warming?, *Geophys. Res. Lett.*, 34, L01610, doi:10.1029/2006GL027834.
- Grasshof, K., 1969. On an Apparatus for Simultaneous Determination of 6 Chemical Compounds in Sea Water with Digital and Analogue Output, vol. 20, Verlag Paul Parey, Hamburg.
- Harris, R., P. Wiebe, J. Lenz, H. R. Skjoldal, M. Huntley, 2000. ICES zooplankton methodology manual. Academic Press, UK, pp 684. ISBN: 9780123276452.
- Holm-Hansen, O., C. J. Lorenzen, R. W. Holmes, J. D. Strickland, 1965. Fluorometric determination of chlorophyll, *J. Conseil*, 30, 3-15. <https://doi.org/10.1093/icesjms/30.1.3>
- Ishii, M., M. Kimoto, 2009. Reevaluation of historical ocean heat content variations with time-varying XBT and MBT bias, *J. Oceanogr.*, 65, 287- 299.
- Jordà G., K. Von Schuckmann, S. A. Josey, G. Caniaux, J. García-Lafuente, S. Sammartino, E. Özsoy, J. Polcher, G. Notarstefano, P.M. Poulain, F. Adloff, J. Salat, C. Naranjo, K. Schroeder, J. Chiggiato, G. Sannino, D. Macías, 2017. The Mediterranean Sea heat and mass budget: Estimates, uncertainties and perspectives. *Prog. In Oceanogr.* 156: 174-208.
- Jordá, G., D. Gomis, 2013. Reliability of the steric and mass components of the Mediterranean sea level es

- estimated from hydrographic gridded products. *Geophys. Res. Lett.*, 40, 3655-3660, doi: 10.1002/grl.50718.
- Juza M., R. Escudier R., M Vargas-Yañez, B. Mourre, E. Heslop, J. Allen and J. Tintoré, 2019. Characterization of changes in Western Intermediate Water properties enabled by an innovative geometry-based detection approach, *Journal of Marine Systems*, 191, 1-12, doi: 10.1016/j.jmarsys.2018.11.003.
 - Krahnmann, G., F. Schott, 1998. Long-term increases in Western Mediterranean salinities and temperatures: anthropogenic and climatic sources. *Geophys. Res. Lett.* Vol. 25, No. 22, 4209-4212.
 - Lacombe, H., P. Tchernia, 1972. Le problem de la formation des eaux marines profondes. Déroulement du phenomene en Méditerranéenord-occidentale par hiver très froid (Janvier-Mars 1963). *Annales de l'Institut Oceanographique*, XLVIII, 1, 75-110.
 - Latasa, M., A. Gutiérrez-Rodríguez, A.M. Cabello, R. Scharek, 2016. Influence of light and nutrients on the vertical distribution of marine phytoplankton groups in the deep chlorophyll maximum. *Sci. Mar.*, 80, 57-62. Doi: 10.3989/scimar.04316.01A.
 - Latasa, M., R. Scharek, M. Vidal, G. Vila-Reixach, A. Gutiérrez-Rodríguez, M. Emelianov, J. M. Gasol, 2010. Preferences of phytoplankton groups for waters of different trophic status in the northwestern Mediterranean Sea. *Marine Ecology Progress Series*, 407, 27-42. Doi: 10.3354/meps08559.
 - Lavigne, H., F. D'Ortenzio, M. Ribera D'Alcalá, H. Claustre, R. Sauzède, M. Gacic, 2015. On the vertical distribution of the chlorophyll a concentration in the Mediterranean Sea: a basin-scale and seasonal approach. *Biogeosciences*, 12, 5021-5039. Doi: 10.5194/bg-12-5021-2015.
 - Leaman, K.D., F. Schott, 1991. Hydrographic structure of the convection regime in the Gulf of Lions: Winter 1987. *J. Phys. Oceanogr.*, Vol. 21, 575-598.
 - Léger F., C. Lebeaupin-Brossier, H. Giordani, T. Arsouze, J. Beuvier, M. N. Bouin, E. Bresson, V. Ducrocq, N. Fourrié, M. Nuret, 2017. Dense water formation in the north-western Mediterranean area during HyMeX-SOP2 in 1/36° ocean simulations: Sensitivity to initial conditions. *J. Geophys. Res.* 122(7): 5749-5773, doi: 10.1002/2015JC011542.
 - Levitus S., J.I. Antonov, T.P. Boyer, O.K. Baranova, H. E. García, R. A. Locarnini, A. V. Mishonov, J. R. Reagan, D. Seidov, E. S. Yarosh, M. M. Zweng, 2012. World ocean heat content and thermosteric sea level change (0-2000 m), 1955-2010. *Geophys. Res. Lett.*, Vol. 39, L10603, doi: 10.1029/2012GL051106.
 - Levitus, S., J.I. Antonov, T.P. Boyer, R.A. Locarnini, H.E. García, A.V. Mishonov, 2009. Global ocean heat content 1955-2008 in light of recently revealed instrumentation problems. *Geophys. Res. Lett.*, 36, L07608, doi: 10.1029/2008GL037155.
 - L'Helguen, S., P. Le Corre, C. Madec, P. Morin, 2002. New and regenerated production in the Almería-Orán front area, eastern Alboran Sea. *Deep-Sea Res. I*, 49, 83-99.
 - Llasses, J., G. Jordá, D. Gomis, 2015. Skills of different hydrographic networks in capturing changes in the Mediterranean Sea at climate scales. *Climate Research*, 63, 1-18.
 - Lomas, M. W., F. Lipschultz, 2006. Forming the primary nitrite maximum: Nitrifiers or phytoplankton?. *Limnol. Oceanogr.*, 5(15), 2453-2467.
 - López-Jurado, J.L., R. Balbín, B. Amengual, A. Aparicio-González, M.L. Fernández de Puelles, M.C. García-Martínez, M. Gaza, J. Jansá, A. Morillas-Kieffer, F. Moya, R. Santiago, M. Serra, M. Vargas-Yañez, L. Vicente, 2015. The RADMED monitoring program: towards an ecosystem approach. *Ocean Sci. Discuss.*, 12, 645-671. <https://doi.org/10.5194/osd-12-645-2015>
 - López-Jurado, J.L., J. García-Lafuente, N. Cano, 1995. Hydrographic conditions of the Ibiza Channel during November 1990, March 1991 and July 1992. *Oceanol. Acta*, 18(2), 235-243.
 - López-Jurado, J.L., 1990. Masas de agua alrededor de las Islas Baleares. *Bol. Inst. Esp. Oceanogr.*, 6(2), 3-20.
 - Lovegrove, T., 1966. The determination of dry weight of Plankton and the effect of various factors on the values obtained, in: *Some Contemporary Studies in Marine Science*, edited by: Barnes, H., George Allen and Undwin Ltd., London, 429-467.

- Ludwig, W., E. Dumont, M. Meybeck, S. Heussner, 2009. River discharges of water and nutrients to the Mediterranean and Black Sea: Major drivers for ecosystem changes during past and future decades. *Prog. In Oceanogr.*, 80, 199-217.
- Malanotte-Rizzoli, P., B. Manca, S. Marullo, M. Ribera d'Alcala, W. Roether, A. Theocharis, A. Bergamasco, G. Budillon, E. Sansone, G. Civitarese, F. Conversano, I. Gertman, B. Hernt, N. Kress, S. Kioroglou, H. Kontoyiannis, K. Nittis, B. Klein, A. Lascaratos, V. Kovacevic, 2003. The Levantine Intermediate Water Experiment (LIWEX) Group: Levantine basin—A laboratory for multiple water mass formation processes. *Journal of Geophysical Research*.108. 8101. 10.1029/2002JC001643.
- Macías, D., E. García-Gorriz, A. Stips, 2018. Major fertilization mechanisms for Mediterranean Sea coastal ecosystems. *Limnology and Oceanography*, 63, 897-914.
- Macías, D., E. García-Gorriz, C. Piroddi, A. Stips, 2014. Biogeochemical control of marine productivity in the Mediterranean Sea during the last 50 years. *Global Biogeochem. Cy.*, 28, 897-907. <https://doi.org/10.1002/2014GB004846>
- Macias, D., M. Bruno, F. Echevarria, A. Vazquez, C.M. Garcia, 2008. Meteorologically-induced mesoscale variability of the North-western Alboran Sea (southern Spain) and related biological patterns. *Estuarine, coastal and shelf science*, 78, 250-266. Doi: doi:10.1016/j.ecss.2007.12.008
- Marcos, M., G. Jordà, G. Le Cozannet, 2016. Sea level rise and its impacts on the Mediterranean, in AllEnvi (ed) *The Mediterranean region under climate change. A scientific update* (coordinated by S. Thiébaud and J-P Moatti). 22nd Conference of the Parties to the United Nations Framework Convention on Climate Change (COP22, Marrakech, 2016).
- MEDAR Group, 2002. Mediterranean and Black Sea Database of temperature, salinity and biogeochemical parameters and climatological atlas (4 CD-ROMs). Ifremer Ed., Plouzane, France (<http://www.ifremer.fr/sismer/program/medar>).
- MEDOC Group, 1970. Observation of the formation of Deep Water in the Mediterranean Sea, 1969. *Nature*, Vol., 227, No. 5262, 1037-1040.
- Mihanovic H., I. Janekovic, I. Viblic, V. Kovacevic, M. Bensi, 2018. Modelling interannual changes in dense water formation on the Northern Adriatic shelf. *Pure Appl. Geophys.* 175: 4065-4081. <https://doi.org/10.1007/s00024-018-1935-5>
- Millot, C., 1999. Circulation in the Western Mediterranean Sea. *J. Mar. Syst.*, 20, 423-442.
- Minas, H.J., B. Coste, P. Le Corre, M. Minas, P. Raimbault, 1991. Biological and geochemical signatures associated with the water circulation through the Strait of Gibraltar and the Western Alboran Sea. *J. Geophys. Res.*, Vol. 96, No. C5, 8755-8771.
- Moore, L. R., R. Goericke, S. W. Chisholm, 1995. Comparative physiology of *Synechococcus* and *Prochlorococcus*: influence of light and temperature on growth, pigments, fluorescence and absorptive properties. *Mar. Ecol. Prog. Ser.*, 116, 259-275.
- Naranjo C., S. Sammartino, J. García-Lafuente, M. J. Bellanco, I. Taupier-Letage, 2015. Mediterranean waters along and across the Strait of Gibraltar, characterization and zonal modification. *Deep-Sea Res. I* 105, 41-52.
- Nittis K., A. Lascaratos, 1999. Intermediate Water Formation in the Levantine Sea: The Response to Interannual Variability of Atmospheric Forcing. In: Malanotte-Rizzoli P., Eremeev V.N. (eds) *The Eastern Mediterranean as a Laboratory Basin for the Assessment of Contrasting Ecosystems*. NATO Science Series (Series 2: Environmental Security), vol 51. Springer, Dordrecht.
- Parrilla, G., T. H. Kinder, 1987. Oceanografía física del Mar de Alborán. *Bol. Inst. Esp. Oceanogr.*, 4(1), 133-166.
- Parrilla, G., 1984. Situación del giro anticiclónico en el Mar de Alborán en abril de 1980. *Bol. Inst. Esp. Oceanogr.* 1(2), 106-113.
- Pascual, J., J. Salat, M. Palau, 1995. Evolución de la temperatura del mar entre 1973 y 1994, cerca de la costa catalana, en *Int. Coll. Okeanos*, 23-28, Montpellier.

- Pinot, J.M., A. Ganachaud, 1999. The role of Winter intermediate waters in spring-summer circulation of the Balearic Sea I. Hydrography and inverse modeling. *J. Geophys. Res.*, 104, No. C12, 29843-29864.
- Pinot, J.M., J. Tintoré, D. Gomis, 1995. Multivariate analysis of the surface circulation in the Balearic Sea. *Prog. Oceanogr.*, 36, 343-376.
- Powley, H.R., P.V. Cappellen, M.D. Krom, 2017. Nutrient cycling in the Mediterranean Sea: The key to understanding how the unique marine ecosystem functions and responds to anthropogenic pressures. *Mediterranean Identities-Environment, Society, Culture*, chapter 3, 47-77, InTech, <http://dx.doi.org/10.5772/intechopen.70878>
- Ramírez, T., D. Cortés, J.M. Mercado, M. Vargas-Yáñez, M. Sebastián, E. Liger, 2005. Seasonal dynamics of inorganic nutrients and phytoplankton biomass in the NW Alboran Sea. *Estuarine, Coastal and Shelf Science*, 65, 654-670.
- Renault L., T. Oguz, A. Pascual, G. Vizoso, J. Tintoré, 2012. Surface circulation in the Alboran Sea (western Mediterranean) inferred from remotely sensed data. *J. Geophys. Res.* 117, C08009, doi: 10.1029/2011JC007659.
- Reul, A., V. Rodríguez, F. Jiménez-Gómez, J.M. Blanco, B. Bautista, T. Sarhan, F. Guerrero, J. Ruiz, J. García-Lafuente, 2005. Variability in the spatio-temporal distribution and size-structure of phytoplankton across an upwelling area in the NW-Alboran Sea (W-Mediterranean). *Cont. Shelf Res.*, 25, 589-608.
- Reynolds, R.W., N.A. Rayner, T.M. Smith, D.C. Stokes, and W. Wang, 2002. An improved in situ and satellite SST analysis for climate. *J. Climate*, 15, 1609-1625.
- Rhein, M., S.R. Rintoul, S. Aoki, E. Campos, D. Chambers, R.A. Feely, S. Gulev, G.C. Johnson, S.A. Josey, A. Kostianoy, C. Mauritzen, D. Roemmich, L.D. Talley and F. Wang, 2013: Observations: Ocean. In: *Climate Change 2013: The Physical Science Basis. Contribution of Working Group I to the Fifth Assessment Report of the Intergovernmental Panel on Climate Change* [Stocker, T.F., D. Qin, G.-K. Plattner, M. Tignor, S.K. Allen, J. Boschung, A. Nauels, Y. Xia, V. Bex and P.M. Midgley (eds.)]. Cambridge University Press, Cambridge, United Kingdom and New York, NY, USA.
- Rodríguez, J., J. M. Blanco, F. Jiménez-Gómez, F. Echevarría, J. Gil, V. Rodríguez, J. Ruiz, B. Bautista, F. Guerrero, 1998. Patterns in the size structure of the phytoplankton community in the deep fluorescence maximum of the Alboran Sea (Southwestern Mediterranean). *Deep-Sea Res. I* (45), 1577-1593.
- Rodríguez, J., 1982. Estudio de una comunidad nerítica en el Mar de Alborán. I. Ciclo de los factores ambientales y fitoplanctónicos. *Bol. Inst. Esp. Oceanogr.*, 7(1), 97-113.
- Rohling, E.J., H.L. Bryden, 1992. Man-induced salinity and temperature increase in Western Mediterranean Deep Water. *J. Geophys. Res.*, Vol. 97, No. C7, 11191-11198.
- Ruiz, S., A. Pascual, B. Garau, Y. Faugère, A. Alvarez, J. Tintoré, 2009. Mesoscale dynamics of the Balearic front, integrating glider, ship and satellite data. *J. Mar. Syst.*, 78, s3-s16, doi: 10.1016/j.jmarsys.2009.01.007.
- Ruíz, S., D. Gomis, M.G. Sotillo, S.A. Josey, 2008. Characterization of surface heat fluxes in the Mediterranean Sea from a 44-year high-resolution atmospheric data set. *Global and Planetary Change*, 63, 258-274.
- Saiz, E., A. Sabatés, J.M. Gili, 2014. The zooplankton, en *The Mediterranean Sea, its history and present challenges*. Editores: S. Goffredo y Z. Dubinsky. Springer Dordrecht, Heidelberg, doi: 10.1007/978-94-007-6704-1.
- Salat, J., A. Lavín, C. González-Pola, P. Vélez-Belchí, R. Sánchez, M. Vargas-Yáñez, J. García-Lafuente, M. Marcos, D. Gomis, 2017. Oceanic variability and sea level changes around the Iberian Peninsula, Balearic and Canary Islands. In *CLIVAR Exchanges*, No 73. Special Issue on climate over the Iberian Peninsula: An overview of CLIVAR-Spain coordinated science.
- Salat, J., J. Pascual, 2006. Principales tendencias climatológicas en el Mediterráneo Noroccidental a partir de más de 30 años de observaciones oceanográficas en la costa catalana. En *Clima, Sociedad y Medio Ambiente*. J.M. Cuadrat Prats, M.A. Sánchez, S.M. Vicente Serrano, S. Lanjeri, N. De Luis Arrillaga, J.C. González-Hidalgo (Editores). Publicaciones de la Asociación Española de Climatología (AEC), serie A, nº 5, 284-290.
- Salat, J., M. A. García, A. Cruzado, A. Palanques, L. Arín, D. Gomis, J. Guillen, A. de León, J. Puigdefábregas, J. Sospedra, Z. R. Velásquez, 2002. Seasonal changes of wáter mass structure and shelf slope exchanges at

the Ebro Shelf (NW Mediterranean). *Cont. Shelf Res.*, 22, 327-348.

- Salat, J., J. Font, 1987. Water mass structure near and offshore the Catalan coast during the winters of 1982 and 1983. *Annales Geophysicae*, 5B (1), 49-54.
- Schroeder, K., J. Garcia-Lafuente, S. A. Josey, V. Artale, B. Buongiorno Nardelli, A. Carrillo, M. Gacic, G. P. Gasparini, M. Herrmann, P. Lionello, W. Ludwig, C. Millot, E. Ozsoy, G. Pisacane, J. C. Sanchez-Garrido, G. Sannino, R. Santoleri, S. Somot, M. Struglia, E. Stanev, I. Taupier-Letage, M. N. Tsimplis, M. Vargas-Yanez, V. Zervakis, G. Zodiatis, 2012. *EnCirculation of the Mediterranean Sea and its Variability* (Editor P. Lionello). 187-238. ISBN 978-0-12-416042-2, Amsterdam.
- Schroeder, K., G.P. Gasparini, M. Borghini, G. Cerrati, R. Delfanti, 2010. Biogeochemical tracers and fluxes in the Western Mediterranean Sea, spring 2005. *J. Mar. Syst.*, 80, 8-24. <https://doi.org/10.1016/j.jmarsys.2009.08.002>
- Segura-Noguera, M., A. Cruzado, D. Blasco, 2016. The biogeochemistry of nutrients, Dissolved Oxygen and chlorophyll-a in the Catalan Sea (NW Mediterranean Sea). *Sci. Mar.*, 80, 39-56. <https://doi.org/10.3989/scimar.04309.20A>
- Siokou-Frangou, I., U. Christaki, M. G. Mazocchi, M. Montesor, M. Ribera d'Alcalá, D. Vaqué, A. Zignone, 2010. *Biogeosciences*, 7, 1543-1586, doi: 10.5194/bg-7-1543-2010.
- Skliris N, J.D. Zika, L. Herold, S.A. Josey, R. Marsh, 2018. Mediterranean sea water budget long-term trend inferred from salinity observations. *Climate Dynamics* 51: 2857-2876.
- Smith, R.O., H.L. Bryden, K. Stansfield, 2008. Observations of new western Mediterranean deep water formation using Argo floats 2004-2006. *Ocean Sci.*, 4, 133-149.
- Sournia, A., 1978. *Phytoplankton Manual*. Edited by A. Sournia. Monographs on oceanographic methodology 6. With 54 figs., 16 tab., 337 pp. Paris: Unesco 1978. ISBN 92 3 101572 9.
- Sournia, A., 1973. La production primaire planctonique en Méditerranée: Essai de mise à jour. *Bulletin de l'Etude en commun de la Méditerranée*, 5-128.
- Stommel, H., 1972. Deep winter-time convection in the Western Mediterranean Sea. In *Studies in Physical Oceanography, a tribute to G. Wüst on his 80th birthday*, 207-210, Vol. 2. Gordon and Breach Science, New York.
- Strickland, J., T. Parsons, 1972. A practical handbook of seawater analysis, B. Fish. Res. Board Can., Bulletin 167, 310 pp. <https://doi.org/10.1002/iroh.19700550118>
- Struglia, M.V., A. Mariotti, A. Filogrosso, 2004. River discharge into the Mediterranean Sea: Climatology and aspects of the observed variability. *J. Clim.*, 17, 4740-4751.
- Thomas, C. R., 1997. *Identifying Marine Phytoplankton*. Academic Press, San Diego, 858 pp.
- Tintoré, J., D. Gomis, S. Alonso, G. Parrilla, 1991. Mesoscale dynamics and vertical motion in the Alborán Sea. *J. Phys. Oceanogr.*, 21(6), 811-823.
- Tintoré, J., P.E. La Violette, I. Blade, A. Cruzado, 1988. A study of an intense front in the Eastern Alboran Sea: The Almería-Orán Front. *J. Phys. Oceanogr.*, 18, 1384-1397.
- Tixeront, J., 1970. Le bilan hydrologique de la Mer Noire et de la Mer Méditerranée. *Cah. Océanogr.*, 22, 227-237.
- Treguer, P., P. Le Corre, 1975. *Manuel d'analyse des sels nutritifs dans l'eau de mer, Utilisation de l'AutoAnalyser II Technicon*, Occidentale, Univ. Bretagne, Laboratoire de Chimie marine, 5 Brest, France. 110 pp.
- Tsimplis, M.N., E. Álvarez-Fanjul, D. Gomis, L. Fenoglio-Marc, B. Pérez, 2005. Mediterranean Sea level trends: Atmospheric pressure and wind contribution. *Geophys. Res. Lett.*, VOL. 32, L20602, doi:10.1029/2005GL023867
- Utermöhl, H., 1958. Zur Vervollkommnung der quantitativen Phytoplankton-Methodik: Mit 1 Tabelle und 15 abbildungen im Text und auf 1 Tafel. *SIL Communications*, 1953-1996. 9. 1-38. 10.1080/05384680.1958.11904091.

- Vargas-Yáñez, M., M.C. García-Martínez, F. Moya, R. Balbín, J.L. López-Jurado, M. Serra, P. Zunino, J. Pascual, J. Salat, 2017. Updating temperature and salinity mean values and trends in the Western Mediterranean: The RADMED Project. *Progress in Oceanography*, 157, 27–46.
- Vargas-Yáñez, M., P. Zunino, K. Schroeder, J.L. López-Jurado, F. Plaza, M. Serra, C. Castro, M.C. García-Martínez, F. Moya, J. Salat, 2012a. Extreme Western Intermediate Water formation in Winter 2012. *J. Mar. Syst.* 105-108, 52-59.
- Vargas-Yáñez, M., E. Mallard, M. Rixen, P. Zunino, M.C. García-Martínez, F. Moya, 2012b. The effect of interpolation methods in temperature and salinity trends in the Western Mediterranean Mediterranean. *Mar. Sci.*, 13/1, 118-125.
- Vargas-Yáñez, M., M^a Carmen García Martínez, Francina Moya, Elena Tel, Gregorio Parrilla, Francisco Plaza, Alicia Lavín, M^a Jesús García, Jordi Salat, José Luis López-Jurado, Josep Pascual, Jesús García Lafuente, DamiáGomis, Enrique Álvarez, Marcos García Sotillo, César González Pola, Fausto Polvorinos, Eugenio Fraile Nuez, M^a Luz Fernández de Puellas, Patricia Zunino, 2010a. Cambio Climático en el Mediterráneo español. Segunda edición actualizada. Editado por Instituto Español de Oceanografía, ISBN: 978-84-95877-48-2, 176 pp., Madrid.
- Vargas-Yáñez, M., F. Moya, M.C. García-Martínez, E. Tel, P. Zunino, F. Plaza, J. Salat, J. Pascual, J.L. López-Jurado, M. Serra, 2010b. Climate change in the Western Mediterranean Sea 1900-2008, *J. Mar. Syst.*, 82, 171-176.
- Vargas-Yáñez, M., P. Zunino, A. Benali, M. Delpy, F. Pastre, F. Moya, M. C. García-Martínez, E. Tel, 2010c. How much is the Western Mediterranean really warming and salting?. *J. Geophys. Res.*, 115, C04001, doi: 10.1029/2009JC005816.
- Vargas-Yáñez, M., F. Moya, E. Tel, M.C. García-Martínez, E. Guerber, M. Bourgeon, 2009. Warming and salting in the Western Mediterranean during the second half of the 20th century: Inconsistencies, unknowns and the effect of data processing. *Sci. Mar.* 73(1), doi: 10.3989/scimar.2009.73n1007.
- Vargas-Yáñez, M., M. C. García Martínez, F. Moya, E. Tel, G. Parrilla, F. Plaza, A. Lavín, M.J. García, J.Salat, J. Pascual, J. García Lafuente, D.Gomis, E. Álvarez, M. García Sotillo, C. González Pola, F.Polvorinos, E. Fraile Nuez, 2008. Cambio Climático en el Mediterráneo español. Editado por Instituto Español de Oceanografía, ISBN: 84 95877 39 2, 171 pp., Madrid.
- Vargas-Yáñez, M., F. Garivier, O. Pirra, M. García-Martínez, 2005. The use of routine hydrographic stations for the estimation of the parameters needed for optimal statistical interpolation. Application to the northern Alboran Sea. *Sci. Mar.*, 69(4), 435-449.
- Vargas-Yáñez, M., F. Plaza, J. García-Lafuente, T. sarhan, J.M. Vargas, P. Vélez-belchi, 2002. About the seasonal variability of the Alboran Sea circulation. *J. Mar. Syst.*, 35, 229-248.
- Viúdez, A., J. Tintoré, R. L. Haney, 1996. Circulation of the Alboran Sea determined by quasi-synoptic hydrographic observations. Part I: Three-dimensional structure of the two anticyclonic gyres. *J. Phys. Oceanogr.*, 26, 684-705.
- Wijffels, S., J. Willis, C. M. Domingues, P. Barker, N. J. White, A. Gronell, K. Ridgwy, and J. A. Church (2008), Changing eXpendable bathythermograph fall-rates and their impact on estimates of thermosteric sea level rise, *J. Clim.*, 5657- 5672, doi:10.1175/2008JCLI2290.1.
- Wüst G., 1961. On the vertical circulation of the Mediterranean Sea. *Journal of Geophysical Research*, 66, 3261-3271

Editado por:

Tuimagina Editorial
Grupo Mediterráneo de Cambio Climático

DEPÓSITO LEGAL: MA 1023-2019

ISBN: 978-84-09-13597-4



INSTITUTO
ESPAÑOL DE
OCEANOGRAFÍA



Mediterranean Climate Change Group - IEO (Spanish Institute of Oceanography)